

**Expression, subcellular localisation and
regulation of Programmed Cell Death Gene 4
(Pdc4) in human pancreatic cells in response to
hypoxia**

Sandeep Kumar

A thesis submitted in fulfilment of the requirements of the University of Brighton for
the degree of Doctor of Philosophy

October 2014

The University of Brighton

Abstract

Pancreatic ductal adenocarcinoma is one of the most aggressive human malignancies, with a five year survival rate of less than five percent. New targets and more effective therapeutic intervention are required to improve diagnosis and prognosis for all patients with pancreatic cancer. Recent studies have established that the tumour suppressor protein Programmed Cell Death Gene 4 (PDCD4) plays a key role in the control of differentiation and neogenesis within the healthy adult pancreas. Pcd4 was originally identified as a gene up-regulated during the process of apoptosis. However, recent data suggests a function for Pcd4 as a tumour suppressor, making it a promising target for pancreatic cancer therapy. The present study utilised a novel model of tissue hypoxia, mimicking the oxygen-deprived core of cancerous tumours which is often resistant to conventional chemotherapeutic drugs and which is likely to lead to secondary tumour formation or metastases, especially in pancreatic cancer. Understanding how Pcd4 regulates pancreatic cell fate, both in healthy pancreatic cells and in conditions of tissue hypoxia, may well arm us with a new weapon in our fight for more effective therapeutic intervention in the treatment and prevention of pancreatic cancer.

This study was conducted to investigate subcellular localisation, expression and regulation of Pcd4, as well as key hypoxic-response genes hypoxia inducible factor 1 α (HIF-1 α) and nuclear factor kappaB (NF κ B) under the influence of hypoxic conditions in human pancreatic adenocarcinoma (PSN-1) cells, rat pancreatic ductal cells (ARIP) and murine pancreatic beta cells (MIN6). Hypoxic cell culture system has been utilised, western blotting and immunocytochemistry analyses to begin to define the cellular regulation of these key proteins. The subcellular localisation and expression of these key proteins was also evaluated in primary human pancreatic adenocarcinoma tissue (four case studies) and normal mouse pancreatic tissue sections by immunohistochemistry.

Results indicate that hypoxic conditions reduced the cell viability of MIN6 and ARIP cells, however, PSN-1 cell viability was unaffected, as analysed by MTT assay and HPI staining. Phalloidin staining and SEM analyses revealed that the cancer cell morphological characteristics of PSN-1 cells did not alter under hypoxic conditions; however, changes in morphology from normal cell to cancerous were observed in ARIP cells. Western blotting and immunocytochemistry analyses showed loss or reduced expression of Pcd4 in PSN-1 cells under hypoxic conditions; however, hypoxia induced the expression of Pcd4 in ARIP and MIN6 cells. Hypoxic conditions triggered expression of HIF-1 α in ARIP cells; however, in PSN-1 cells it remained unchanged. However, hypoxia efficiently triggered nuclear translocation of NF κ B in PSN-1 cells.

Detailed immunohistochemistry analyses of primary human pancreatic tissue sections revealed loss or reduced expression of Pcd4. Very high expression of HIF-1 α was observed in all four human pancreatic ductal adenocarcinoma tissue samples examined, in addition to differential cytoplasmic expression of NF κ B.

The results presented here indicate that hypoxia may be the factor which triggers expression of Pcd4 in normal pancreatic ductal and beta cells which ultimately induces apoptosis under hypoxic conditions. However, loss or reduction in expression of Pcd4 under hypoxic conditions in pancreatic adenocarcinoma cells promotes cell survival. Levels of Pcd4 expression may ultimately decide the fate of pancreatic cells. This is the first study to begin to define the regulation of Pcd4 under hypoxic conditions in human pancreatic adenocarcinoma. Presented data indicate that Pcd4 expression may be a useful diagnostic tool as well as a potentially exciting target in new and improved therapies for pancreatic cancer.

Table of Contents

Abstract	i
Figures	v
List of tables	xi
List of Abbreviations	xii
Acknowledgments	xvi
Author's Declaration	xvii
Chapter 1. General Introduction	1
1.1. THE PANCREAS	1
1.2. THE FINE STRUCTURE OF THE PANCREAS	4
1.3. PANCREATIC CANCER:	6
1.3.1. Symptoms and risk factors	7
1.3.2. Statistics	7
1.3.3. Early detection and diagnosis	8
1.3.4. Treatments	8
1.3.5. Pancreatic cancer stages and typing	9
1.3.6. Histological classification of pancreatic cancer	11
1.3.7. Molecular mechanisms in pancreatic cancer	15
1.4. PROGRAMMED CELL DEATH GENE 4(PDCD4): A NOVEL TUMOUR SUPPRESSOR	17
1.4.1. Background	17
1.4.2. The Structure of PDCD4	18
1.4.3. Potential role of PDCD4 in the nucleus and cytoplasm	21
1.4.4. Expression and regulation of PDCD4	22
1.4.1. PDCD4 as a tumour suppressor and role in tumour development	26
1.5. HYPOXIA INDUCIBLE FACTOR-1 (HIF-1): MASTER REGULATOR OF OXYGEN HOMEOSTASIS	29
1.5.1. Introduction	29
1.5.2. The structure of HIF-1	30
1.5.3. Regulation of HIF-1 α	30
1.5.4. Role of HIF-1 α in cancer	34
1.6. NUCLEAR FACTOR KAPPA B (NF- κ B)	36
1.6.1. Introduction	36
1.6.2. The structure and signalling pathway of NF- κ B	36
1.6.3. Diverse and complex role of NF- κ B in cancer	40
1.6.1. Activation of NF- κ B and role in pancreatic cancer	41
1.7. AIMS OF STUDY	43
Chapter 2. Material and Methods	45
2.1. MATERIAL	45
2.2. METHODS	46
2.2.1. Cell culture conditions	46
2.2.1. Cell Viability evaluation	49
2.2.2. Morphological analysis	51
2.2.3. Protein extraction and quantification	52

2.2.4.	SDS-PAGE and Western Blotting	54
2.2.5.	Immunocytochemistry.....	57
2.2.6.	Confocal Microscopy	58
2.2.7.	Histology.....	59
2.2.8.	Data and statistical analysis	64
Chapter 3.	Cell Viability in Hypoxia	65
3.1.	INTRODUCTION	65
3.2.	VIABILITY ASSAYS	66
3.2.1.	MTT assay.....	66
3.2.2.	Hoescht Propidium Iodide (HPI) Staining.....	71
3.3.	DISCUSSION	76
Chapter 4.	Cells morphology	80
4.1.	INTRODUCTION	80
4.2.	MORPHOLOGY OF CELL LINES	83
4.2.1.	Cytoskeleton analysis (Actin staining).....	83
4.2.2.	Scanning Electron Microscopy (SEM)	88
4.3.	MORPHOLOGY OF NORMAL AND CANCEROUS PANCREASES.....	93
4.3.1.	Mouse normal pancreas.....	93
4.3.2.	Morphology of human pancreatic cancer tissue.....	101
4.4.	DISCUSSION	118
Chapter 5.	Programmed Cell Death 4 Gene (<i>PDCD4</i>)	125
5.1.	INTRODUCTION	125
5.2.	RESULTS	127
5.2.1.	<i>PDCD4</i> in pancreatic cells	127
5.2.2.	<i>PDCD4</i> expression and subcellular localisation in normal and adenocarcinoma pancreas tissue	139
5.3.	DISCUSSION	159
Chapter 6.	Hypoxia Inducible Factor -1 alpha (<i>HIF-1α</i>)	169
6.1.	INTRODUCTION	169
6.2.	RESULTS	172
6.2.1.	<i>HIF-1α</i> in pancreatic cells.....	172
6.2.2.	<i>HIF-1α</i> expression and subcellular localisation in normal and adenocarcinoma pancreas tissue	182
6.3.	DISCUSSION	201
Chapter 7.	Nuclear Factor kappa B (<i>NFκB</i>)	206
7.1.	INTRODUCTION	206
7.2.	RESULTS	207
7.2.1.	<i>NFκB</i> in pancreatic cells	207

7.2.2. NFκB expression and subcellular localisation in normal and adenocarcinoma pancreas tissue	217
7.3. DISCUSSION	236
Chapter 8. General discussion.....	241
8.1. CELL VIABILITY IN HYPOXIA	242
8.2. CELL MORPHOLOGY	242
8.3. ROLE OF PDCD4 IN PANCREATIC CANCER.....	246
8.4. ROLE OF HIF-1A IN PANCREATIC CANCER.....	248
8.5. ROLE OF NFκB IN PANCREATIC CANCER.....	250
8.6. OVERVIEW OF HYPOTHESIS.....	251
Chapter 9. Conclusions and Future Work.....	257
9.1. AIMS, MAIN FINDINGS AND CONCLUSION.....	257
9.2. FUTURE WORK.....	262
References.....	265
Publications.....	290
Appendix.....	291

Figures

Figure 1-1: Pancreas.....	2
Figure 1-2: Histology of pancreas:.....	5
Figure 1-3: Pancreatic intraepithelial neoplasia (PanIns)	10
Figure 1-4: Ductal adenocarcinoma of pancreas.....	14
Figure 1-5: Structure of PDCD4	19
Figure 1-6: Schematic representation of PDCD4 action in translation inhibition	20
Figure 1-7: Overview of the reported regulatory mechanisms for PDCD4.....	25
Figure 1-8: PDCD4 functions: Overview of known function of programmed cell death gene 4 (PDCD4)	28
Figure 1-9: Schematic representation of domain structure of HIF-1 α and their potential functions in stability and transcriptional activity.	31
Figure 1-10: Regulation of Hypoxia inducible factor 1 α	33
Figure 1-11: Subunits of NF- κ B	37
Figure 1-12: NF- κ B signalling pathways: Canonical and non-canonical	39
Figure 2-1: Hypoxia glove box from coy laboratories.....	48
Figure 2-2: MTT reduction by mitochondria reductase in living cells results in the formation of insoluble formazan dye crystal.	49
Figure 3-1: Viability of PSN-1 cells synchronised and grown in normoxic and hypoxic culture conditions by MTT assay	68
Figure 3-2: Viability of ARIP cells synchronised and grown in normoxic and hypoxic culture conditions by MTT assay	69
Figure 3-3: Viability of MIN6 cells synchronised and grown in normoxic and hypoxic culture conditions by MTT assay.	70
Figure 3-4: Viability of PSN-1 cells synchronised and grown in normoxic and hypoxic culture conditions by HPI staining.....	73
Figure 3-5: Viability of ARIP cells synchronised and grown in normoxic and hypoxic culture conditions by HPI staining	74
Figure 3-6: Viability of MIN6 cells synchronised and grown in normoxic and hypoxic culture conditions by HPI staining.....	75
Figure 4-1: Morphology of PSN-1 cells under hypoxic and normoxic conditions.....	85

Figure 4-2: Morphology of ARIP cells under hypoxic and normoxic conditions.	86
Figure 4-3: Morphology of MIN6 cells under hypoxic and normoxic conditions.....	87
Figure 4-4: Scanning electron microscopy of the surface morphology of human pancreatic adenocarcinoma cells (PSN-1).	90
Figure 4-5: Scanning electron microscopy of the surface morphology of pancreases ductal cell (ARIP).	91
Figure 4-6: Scanning electron microscopy of the surface morphology of mouse pancreases beta cells (MIN6).	92
Figure 4-7: Morphology of normal mouse pancreas (40X magnification).....	95
Figure 4-8: Morphology of normal mouse pancreas (100X magnification).....	96
Figure 4-9: Morphology of normal mouse pancreas stained with H&E staining (5X magnification).	98
Figure 4-10: Morphology of normal mouse pancreas stained with H&E staining (10X magnification).	99
Figure 4-11: Morphology of normal mouse pancreas stained with H&E staining (40X magnification).	100
Figure 4-12: Haematoxylin and Eosin (H&E) staining of human adenocarcinoma pancreas tissue case study 1 (5X magnification).	102
Figure 4-13: Haematoxylin and Eosin (H&E) staining of human adenocarcinoma pancreas tissue case study 1 (10X magnification).	103
Figure 4-14: Haematoxylin and Eosin (H&E) staining of human adenocarcinoma pancreas tissue case study 1 (40X magnification).	104
Figure 4-15: Haematoxylin and Eosin (H&E) staining of human adenocarcinoma pancreas tissue case study 2 (5X magnification).	107
Figure 4-16: Haematoxylin and Eosin (H&E) staining of human adenocarcinoma pancreases tissue case study 2 (10X magnification).	108
Figure 4-17: Haematoxylin and Eosin (H&E) staining of human adenocarcinoma pancreases tissue case study 2 (40X magnification).	109
Figure 4-18: Haematoxylin and Eosin (H&E) staining of human adenocarcinoma pancreases tissue case study 3 (5X magnification).	111
Figure 4-19: Haematoxylin and Eosin (H&E) staining of human adenocarcinoma pancreases tissue case study 3 (10X magnification).	112
Figure 4-20: Haematoxylin and Eosin (H&E) staining of human adenocarcinoma pancreases tissue case study 3 (40X magnification).	113

Figure 4-21: Haematoxylin and Eosin (H&E) staining of human pancreatic cancer tissue case study 4 (5X magnification).	115
Figure 4-22: Haematoxylin and Eosin (H&E) staining of human pancreatic cancer tissue case study 4 (10X magnification).	116
Figure 4-23: Haematoxylin and Eosin (H&E) staining of human pancreatic cancer tissue case study 4 (40X magnification).	117
Figure 5-1: Expression of PDCD4 under hypoxic and normoxic conditions in human pancreatic adenocarcinoma cells.	130
Figure 5-2: Subcellular expression (A) cytoplasm and (B) nucleus of PDCD4 in human pancreatic adenocarcinoma cells.	131
Figure 5-3: Subcellular expression (A) cytoplasm and (B) nucleus of PDCD4 in pancreatic ductal cells.	132
Figure 5-4: Subcellular expression (A) cytoplasm and (B) nucleus of PDCD4 in pancreatic beta cells.	133
Figure 5-5: Sub-cellular localisation and expression of PDCD4 in human pancreatic adenocarcinoma cells.	136
Figure 5-6: Sub-cellular localisation and expression of PDCD4 in pancreatic ductal cells.	137
Figure 5-7: Sub-cellular localisation and expression of PDCD4 in mouse pancreatic beta cells.	138
Figure 5-8: Immunohistochemical analysis of the expression of PDCD4 in mouse pancreas (10X magnification).	140
Figure 5-9: Immunohistochemical expression of PDCD4 in mouse pancreas (40X magnification).	141
Figure 5-10: Immunohistochemical expression analysis of the PDCD4 in human pancreatic adenocarcinoma tissue case study 1 (5X magnification).	143
Figure 5-11: Immunohistochemical expression analysis of the PDCD4 in human pancreatic adenocarcinoma tissue case study 1 (10X magnification).	144
Figure 5-12: Immunohistochemical expression analysis of the PDCD4 in human pancreatic adenocarcinoma tissue case study 1 (40X magnification).	145
Figure 5-13: Immunohistochemical expression analysis of the PDCD4 in human pancreatic adenocarcinoma tissue case study 2 (5X magnification).	148
Figure 5-14: Immunohistochemical expression analysis of the PDCD4 in human pancreatic adenocarcinoma tissue case study 2 (10X magnification).	149
Figure 5-15: Immunohistochemical expression analysis of the PDCD4 in human pancreatic adenocarcinoma tissue case study 2 (40X magnification).	150

Figure 5-16: Immunohistochemical expression analysis of the PDCD4 in human pancreatic adenocarcinoma tissue case study 3 (5X magnification).....	152
Figure 5-17: Immunohistochemical expression analysis of the PDCD4 in human pancreatic adenocarcinoma tissue case study 3 (10X magnification).....	153
Figure 5-18: Immunohistochemical expression analysis of the PDCD4 in human pancreatic adenocarcinoma tissue case study 3 (40X magnification).....	154
Figure 5-19: Immunohistochemical expression analysis of the PDCD4 in human pancreatic adenocarcinoma tissue case study 4 (5X magnification).....	156
Figure 5-20: Immunohistochemical expression analysis of the PDCD4 in human pancreatic adenocarcinoma tissue case study 4 (10X magnification).....	157
Figure 5-21: Immunohistochemical expression analysis of the PDCD4 in human pancreatic adenocarcinoma tissue case study 4 (40X magnification).....	158
Figure 5-22: Schematic representation of the proposed effect of PDCD4 expression on cell survival in the pancreas	162
Figure 6-1: Role of hypoxia in pancreatic tumour development:	170
Figure 6-2: Expression of HIF-1 α under hypoxic and normoxic conditions in human pancreatic adenocarcinoma cells.....	175
Figure 6-3: Subcellular expression (A) cytoplasm and (B) nucleus of HIF-1 α in human pancreatic adenocarcinoma cells.....	176
Figure 6-4: Subcellular expression (A) cytoplasm and (B) nucleus of HIF-1 α in pancreatic ductal cells.	177
Figure 6-5: Sub-cellular localisation and expression of HIF-1 α in human pancreatic adenocarcinoma cells.	180
Figure 6-6: Sub-cellular localisation and expression of HIF-1 α in pancreatic ductal cells.	181
Figure 6-7: Immunohistochemical analysis of the expression of HIF-1 α in mouse pancreas (10X magnification).	183
Figure 6-8: Immunohistochemical analysis of the expression of HIF-1 α in mouse pancreas (40X magnification).	184
Figure 6-9: Immunohistochemical analysis of the expression of HIF-1 α in human pancreatic adenocarcinoma tissue case study 1 (5X magnification).....	186
Figure 6-10: Immunohistochemical analysis of the expression of HIF-1 α in human pancreatic adenocarcinoma tissue case study 1 (10X magnification).....	187
Figure 6-11: Immunohistochemical analysis of the expression of HIF-1 α in human pancreatic adenocarcinoma tissue case study 1 (40X magnification).....	188

Figure 6-12: Immunohistochemical analysis of the expression of HIF-1 α in human pancreatic adenocarcinoma tissue case study 2 (5X magnification).....	190
Figure 6-13: Immunohistochemical analysis of the expression of HIF-1 α in human pancreatic adenocarcinoma tissue case study 2 (10X magnification).....	191
Figure 6-14: Immunohistochemical analysis of the expression of HIF-1 α in human pancreatic adenocarcinoma tissue case study 2 (40X magnification).....	192
Figure 6-15: Immunohistochemical analysis of the expression of HIF-1 α in human pancreatic adenocarcinoma tissue case study 3 (5X magnification).....	194
Figure 6-16: Immunohistochemical analysis of the expression of HIF-1 α in human pancreatic adenocarcinoma tissue case study 3 (10X magnification).....	195
Figure 6-17: Immunohistochemical analysis of the expression of HIF-1 α in human pancreatic adenocarcinoma tissue case study 3 (40X magnification).....	196
Figure 6-18: Immunohistochemical analysis of the expression of HIF-1 α in human pancreatic adenocarcinoma tissue case study 4 (5X magnification).....	198
Figure 6-19: Immunohistochemical analysis of the expression of HIF-1 α in human pancreatic adenocarcinoma tissue case study 4 (10X magnification).....	199
Figure 6-20: Immunohistochemical analysis of the expression of HIF-1 α in human pancreatic adenocarcinoma tissue case study 4 (40X magnification).....	200
Figure 7-1: Expression of NF κ B under hypoxic and normoxic conditions in human pancreatic adenocarcinoma cells.....	210
Figure 7-2: Subcellular expression of NF κ B in human pancreatic adenocarcinoma cells.....	211
Figure 7-3: Subcellular expression (A) cytoplasm and (B) nucleus of NF κ B in pancreatic ductal cells.....	212
Figure 7-4: Sub-cellular localisation and expression of NF κ B in human pancreatic adenocarcinoma cells.....	215
Figure 7-5: Sub-cellular localisation and expression of NF κ B in pancreatic ductal cells.....	216
Figure 7-6: Immunohistochemical analysis of the expression of NF κ B in mouse pancreas (10X magnification).....	218
Figure 7-7: Immunohistochemical analysis of the expression of NF κ B in mouse pancreas (40X magnification).....	219
Figure 7-8: Immunohistochemical analysis of the expression of NF κ B in human pancreatic adenocarcinoma tissue case study 1 (5X magnification).....	221
Figure 7-9: Immunohistochemical analysis of the expression of NF κ B in human pancreatic adenocarcinoma tissue case study 1 (10X magnification).....	222

Figure 7-10: Immunohistochemical analysis of the expression of NFκB in human pancreatic adenocarcinoma tissue case study 1 (40X magnification).....	223
Figure 7-11: Immunohistochemical analysis of the expression of NFκB in human pancreatic adenocarcinoma tissue case study 2 (5X magnification).....	225
Figure 7-12: Immunohistochemical analysis of the expression of NFκB in human pancreatic adenocarcinoma tissue case study 2 (10X magnification).....	226
Figure 7-13: Immunohistochemical analysis of the expression of NFκB in human pancreatic adenocarcinoma tissue case study 2 (40X magnification).....	227
Figure 7-14: Immunohistochemical analysis of the expression of NFκB in human pancreatic adenocarcinoma tissue case study 3 (5X magnification).....	229
Figure 7-15: Immunohistochemical analysis of the expression of NFκB in human pancreatic adenocarcinoma tissue case study 3 (10X magnification).....	230
Figure 7-16: Immunohistochemical analysis of the expression of NFκB in human pancreatic adenocarcinoma tissue case study 3 (40X magnification).....	231
Figure 7-17: Immunohistochemical analysis of the expression of NFκB in human pancreatic adenocarcinoma tissue case study 4 (5X magnification).....	233
Figure 7-18: Immunohistochemical analysis of the expression of NFκB in human pancreatic adenocarcinoma tissue case study 4 (10X magnification).....	234
Figure 7-19: Immunohistochemical analysis of the expression of NFκB in human pancreatic adenocarcinoma tissue case study 4 (40X magnification).....	235
Figure 8-1: Schematic representation of the proposed effect of HIF-1α, NFκB and PDCD4 expression on normal pancreatic cell survival under hypoxic conditions.	253
Figure 8-2: Schematic representation of the proposed effect of HIF-1α, NFκB and PDCD4 expression on pancreatic cancer cell (PSN-1) survival under hypoxic conditions.	254
Figure 8-3: Proposed effect of desmoplastic reaction or fibrous stroma and hypoxia in human pancreatic adenocarcinoma tissue.	255
Figure 8-4: Gradient expression of PDCD4 in human pancreatic ductal adenocarcinoma tissue.	256

List of tables

Table 1-1 Pancreatic islets peptides products and there functions[3]	3
Table 2-1 Reagents used for one gel to make resolving and stacking gel	54
Table 2-2: Example of calculations to determine normalized and relative densitometry values from experimental blot.....	56
Table 2-3: Human pancreatic cancer tissue sections information.....	60
Table 2-4 Tissue dehydration schedule.....	60
Table 4-1: Morphological characteristics of normal and cancer cells.	80

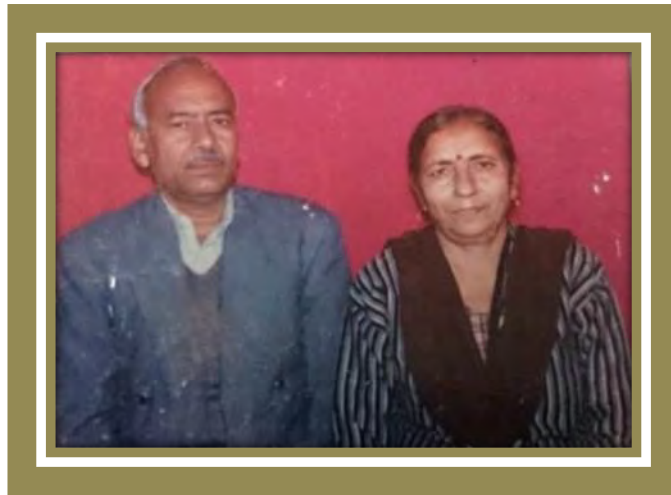
List of Abbreviations

AP-1	Activating Protein -1
APS	Ammonium Persulphate
ATP	Adenosine Triphosphate
bHLH	basic Helix-Loop-Helix
bp	Base Pairs
BSA	Bovine serum Albumin
CAII	Carbonic Anhydrase II
cAMP	cyclic Adenosine Monophosphate
CAP	cAMP- Activator Protein
Cdc2	Cell division cycle 2
CDK1	Cyclin Dependent Kinase 1
cDNA	complementary Deoxyribonucleic Acid
CO ₂	Carbone Dioxide
COX1	Cyclooxygenase 1
COX2	Cyclooxygenase 2
DAB	3,3'-diaminobenzidine
DAP-5	Death Associated Protein – 5
DAPI	4'6 diamidino-2-phenylindole
DMEM	Dulbecco's Modified Eagle's Medium
DMSO	Dimethyl Sulphate
DNA	Deoxyribonucleic Acid
DTT	Dithiothreitol
DUG	Death Up-regulated Gene
ECL	Enhanced Chemi-luminescence
ECM	Extracellular Matrix
EDTA	Ethylene di-amine tetra-acetic Acid
eIF	eukaryotic Initiation factor
EMT	Epithelia Mesenchymal Transition
FBS	Foetal Bovine Serum
FCS	Foetal Calf Serum
FITC	Fluorescein Isothiocyanate

GAPDH	Glyceraldehyde-3-phosphate dehydrogenase
H&E	Haematoxylin and Eosin
H ₂ O ₂	Hydrogen Peroxide
HEPES	4-(2-hydroxyethyl)-1 piperazineethanesulfonic acid
HIF-1 α	Hypoxia Inducible Factor 1 alpha
HIF-1 β	Hypoxia Inducible Factor 1 beta
His	Histidine
HREs	Hypoxia Response Elements
HRP	Horseradish Peroxidase
IAPP	Islet Amyloid Polypeptide
IL	Islet of Langerhans
IPMNs	Intra Papillary Mucinous Neoplasms
I κ B	Inhibitor of kappa B
JNK	Jun NH ₂ -terminal Kinase
kb	kiloase
KCL	Potassium Chloride
KH ₂ PO ₄	Potassium Persulphate
MAPK	Mitogen Activated Protein Kinase Kinase Kinase Kinase
MCNs	Mucinous Cystic Neoplasms
MgSO ₄	Magnesium Sulphate
miRNA	Micro Ribonucleic Acid
mRNA	messenger Ribonucleic Acid
NaCl	Sodium Chloride
NF κ B	Nuclear Factor kappa B
O ₂	Oxygen
ODDD	Oxygen Dependent Degradation Domain
PanINs	Pancreatic Intraepithelial Neoplasia
PBS	Phosphate Buffer Saline
PC	Pancreatic Cancer
PCR	Polymerase Chain Reaction
PDAC	Pancreatic Ductal Adenocarcinoma
PDCD4	Programmed Cell Death 4
PDX1	Pancreatic Duodenal Homeobox 1

PHD1-3	Propyl Hydroxylases 1-3
PP	Pancreatic Polypeptide (cells)
PSC	Pancreatic Satellite Cell
pVHL	von Hippel-Lindau
RAR	Retinoic Acid Receptor
RHD	REL Homology Domain
RNA	Ribonucleic Acid
rpm	Revolution per minute
RPMI-1640	Roswell Park Memorial Institute 1640 Medium
RT-PCR	Reverse transcriptase- Polymerase Chain Reaction
S	Serine
SDS	Sodium Dodecyl Sulphate
SDS-PAGE	Sodium Dodecyl Sulphate Polyacrylamide Gel Electrophoresis
SEM	Scanning Electron Microscopy
TAD	Transactivation Domain
TEMED	Tetramethylethylenediamine
TRITC	Tetramethylrhodamine-5-6-Isothiocyanate
U	Units
UTR	Un-translated Region
UV	Ultra- Violet
v/v	Volume per volume
w/v	Weight per volume

I WOULD LIKE TO DEDICATE
MY PhD THESIS TO
MY PARENTS



My biggest thanks of all go to my mother [Shrimati Tarsem Kumari](#) and my Father [Shri Kewal Krishan](#), for their love, support, encouragement and blessings, without them I could not have succeeded.

Acknowledgments

I would like to express my sincere gratitude toward my supervisors [Dr Wendy MacFarlane](#), [Dr Claire Marriott](#) and [Prof Adrian Bone](#) for their guidance and support throughout my PhD journey. Only with their patient guidance, generous trust, never ending encouragement, and constructive advice could the research be made possible. They are the stars and family to me.



A special thanks to Dr Moira Harrison, for all her help and support and standing behind me in tough times during my PhD. I would also like to thank Dr Carol Howell, for giving me an opportunity for a knowledge transfer visit to IEPOR, Kiev, Ukraine.

I am very grateful to ‘special gems’ (who can only be found in our school) Dr Yishan Zheng, Christine Smith, Dr Howard Dodd, Dr Ganesh Ingavle and other technical staff for encouragement, support and valuable advises.

Thanks to my PhD and post doc colleagues both present and past for encouraging dinner parties, tea breaks, playing games (Carcassonne on every Wednesday), hangovers and for the best memories, which I will never forget in my life.

Finally, I want to thank my brother Kuldeep Kumar, my sister Neeraj Kumari and her husband Naveen Kumar for their day to day encouragement, support and blessings.

Author's Declaration

I declare that the research contained in this thesis, unless otherwise formally indicated within the text, is the original work of the author. The thesis has not been previously submitted to this or any other university for a degree, and does not incorporate any material already submitted for a degree.

Sandeep Kumar

Signed

Date

Chapter 1. General Introduction

1.1. The Pancreas

The pancreas plays a key role in the human digestive system. It is situated deep in the centre of abdomen and located beneath the stomach, near the bottom of the breastbone. The pancreas is a large gland, about 6 inches long, 2 inch wide and with a leaf-like structure, divided into three parts called the head, the thin end called the tail and a middle part called the body of the pancreas. The head of the pancreas is on the right side of belly, the body is located behind the stomach and tail is on the left of the abdomen next to the spleen as shown in Figure 1-1. [1, 2]

The exocrine pancreas accounts for > 85% of pancreatic mass and is comprised of acinar and ductal cells which secrete pancreatic juices. The acinar cells secrete amylase, protease and lipase in response to ingestion of carbohydrates, protein and fat respectively. The acinar cells are pyramid shaped and are surrounded by ductal epithelia; the function of ductal epithelia is to secrete bicarbonate fluid which helps to deliver various enzymes to the duodenum. The exocrine pancreas secretes approximately 500 to 800 mL per day of colourless, odourless, alkaline pancreatic juice. The rest of the pancreas is comprised of 10% extracellular matrix, 4% blood vessels and only 2% of endocrine tissue [3, 4]. This 2% of endocrine tissue or endocrine pancreas consists of nearly 1 million islets of Langerhans. Islets of Langerhans vary in size from 40 to 900 μm diameter and contain 3000 to 4000 cells of four types, the alpha (α), beta (β), delta (δ) and pancreatic polypeptide cell [5]. It has been reported a fifth islet cell type exists, epsilon cells, which secrete ghrelin [6]. Different islet cells secrete different hormones which have different functions as shown in Table 1-1 [3].

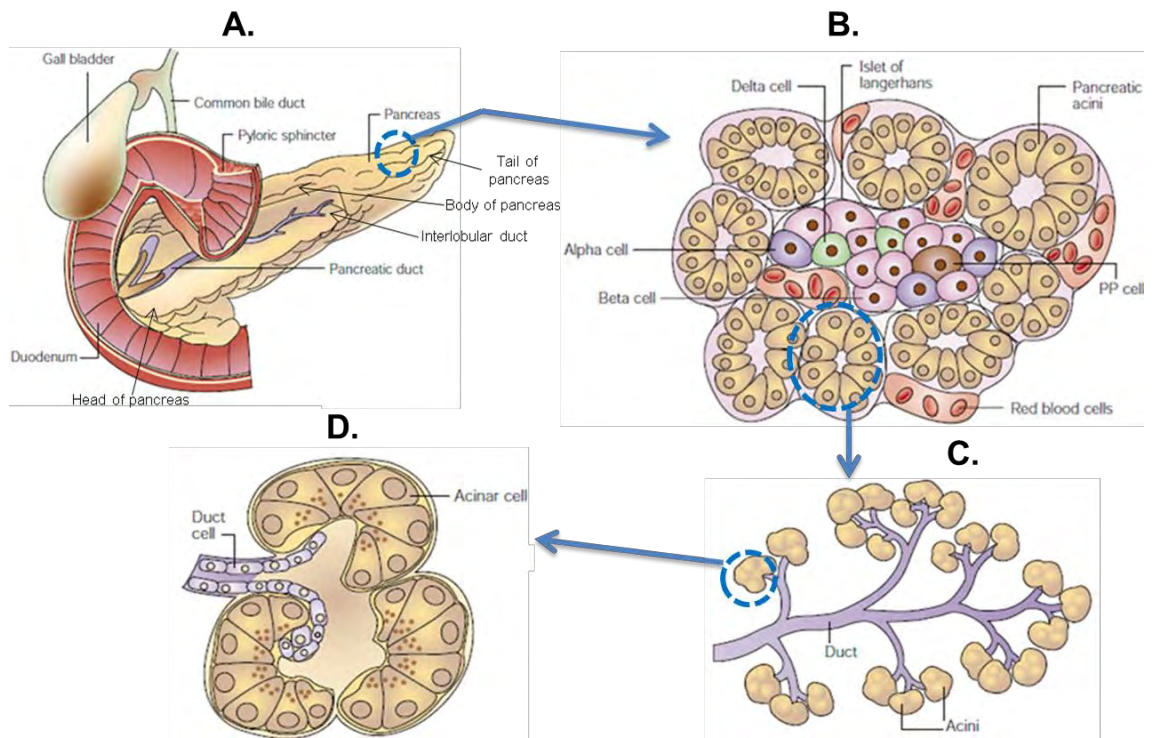


Figure 1-1: Pancreas

(A) Gross examination of the pancreas: The pancreas is divided into three parts; head lies in the C-shaped concavity of the duodenum, body lies behind stomach (in front of aorta, left renal artery and left suprarenal artery) and tail lies closely related to the spleen (in front of left kidney). At a cellular level the pancreas is divided into two : the exocrine and endocrine pancreas. **(B) Islet of Langerhans embedded in exocrine tissue:** Endocrine pancreas consists of four types of specialised cells alpha (α), beta (β), delta (δ), pancreatic polypeptide and epsilon cells and these cells organise into compact islets cells which embedded inside the acinar tissue. The alpha (α) and beta (β) cells produce glucagon and insulin in response to glucose. **(C) The exocrine pancreas & (D) A single acinus:** Exocrine pancreas consists of acinar cells (grape like structure) which produce digestive enzymes and ducts which add mucus and bicarbonate, all of this enzyme mixture is secreted into the duodenum. [1]

Adapted from Bardeesy, N. and R.A. DePinho, Nat Rev Cancer 2: 897-909 (2002).

Table 1-1 Pancreatic islets peptides products and there functions[3]

Hormones	Islet cells	Function
Insulin	Beta (β) cells	Decrease gluconeogenesis, glycogenolysis, fatty acid breakdown and ketogenesis. Increase glycogenesis, protein synthesis. Main effect is increase glucose uptake by muscle and adipose tissue [7].
Glucagon	Alpha (α) cells	Opposite effect of insulin: increase hepatic glycogenolysis and gluconeogenesis [8].
Somatostatin	Delta (δ) cells	Inhibits GI secretions; Inhibits secretion and action of all GI endocrine peptides; Inhibits cell growth [9].
Pancreatic polypeptide (PP)	PP cells	Inhibits pancreatic exocrine secretion and section of insulin [10, 11].
Amylin (islet amyloid polypeptide)	Beta (β) cells	Counter regulates insulin secretion and function [12]
Pancreastatin	Beta (β) cells	Decrease insulin and somatostatin release Increase glucagon release. Decrease pancreatic exocrine secretion. [13]
Ghrelin	Epsilon (ϵ) cells	Decrease insulin release and its action [14].

Adapted from Fisher, W.E., et al., Chapter 33; Pancreas 9th ed. Mc Graw Hill (2009).

Despite the exocrine and endocrine pancreas cells having distinct morphology and function, they share a common embryonic origin [15]. Involvement of different genes in pancreatic development is characterised by various signalling pathways and a network of transcriptional factors from adjacent cells [16, 17]. Pancreatic progenitor cells require expression of PDX1 (Pancreatic and duodenal homeobox 1) transcription factor for proliferation and early branching of pancreatic progenitor cells to develop into pancreatic epithelium cells type. Pancreatic progenitor derived epithelium cells then differentiate into endocrine and exocrine pancreas under the control of various transcription factors [1, 16].

1.2. The fine structure of the pancreas

The pancreas is surrounded by a moderately dense capsule of connective tissue (no fibrous tissue) and the septum from the capsule divides the pancreas into lobules. These lobules are very loosely held together with connective tissue and are visible on gross examination. The large lobules are divided into small lobules by intra-lobular connective tissue. Large blood vessels and nerve bundles run through the septa of connective tissues [18]. As shown in Figure 1-2, within each lobule numerous acini are arranged in ring-like structures composed of serous or zymogen cells. These acini consist of round nuclei within acinar cells at the base of cells, enzyme producing granules in the centre of acini and spindle shaped cells which start forming an intercalated duct system called centro-acinar cells (powerful bicarbonate maker). These intercalated ducts lead into intra-lobular ducts and both these ducts are within the lobule. These intra-lobular ducts join to inter-lobular duct (simple cuboidal epithelium) and finally into large interlobular duct (stratified columnar epithelium). The islets of Langerhans (IL) are scattered throughout the pancreas; however, large size islets of Langerhans are located near major blood supply vessels and small size islets are located deep inside the parenchyma of the pancreas.

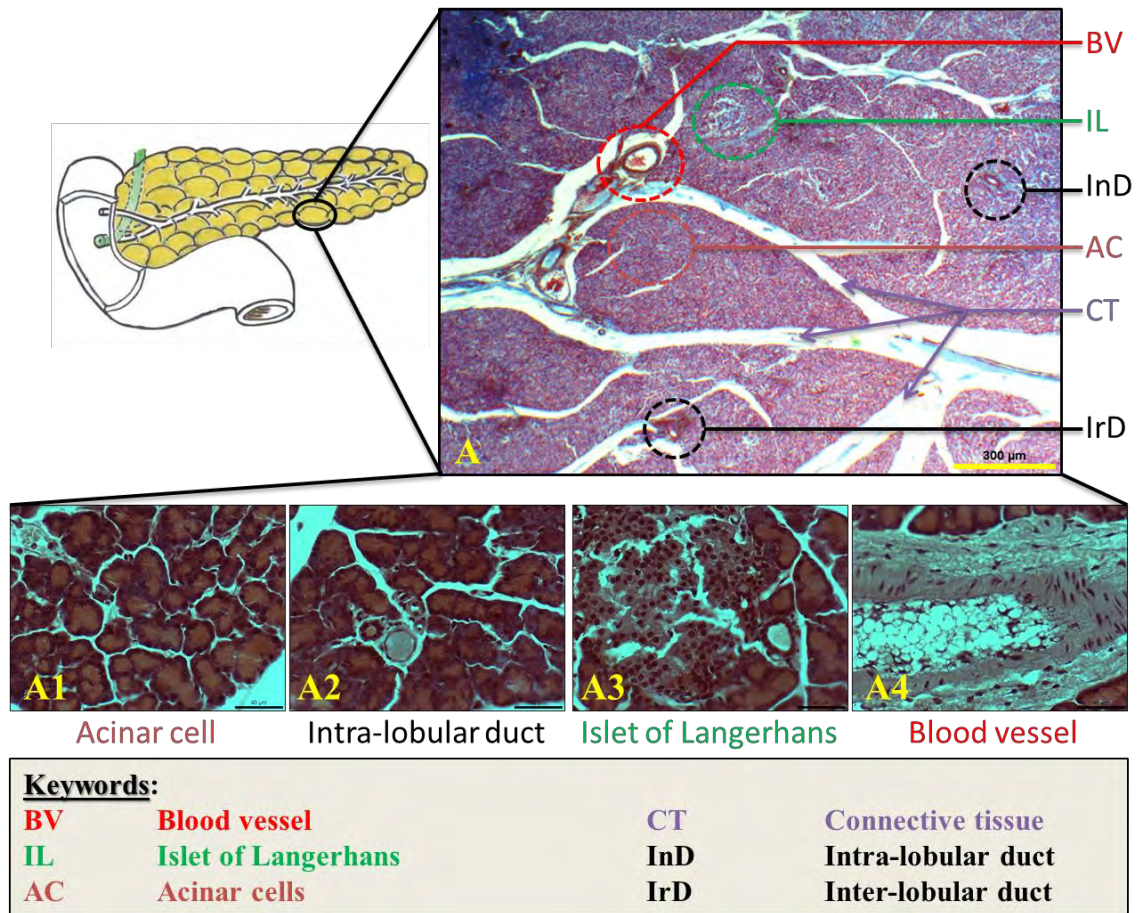


Figure 1-2: Histology of pancreas:

(A) Pancreas surrounded by moderately dense capsule of connective tissue and septa from **connective tissue (CT)** divide pancreas into lobules. (A1) Numerous acini lay within the lobule and a round nuclei cell at the base of acini called **acinar cell (AC)** and spindle shaped cells are centro-acinar which is in the beginning of intercalated duct. (A2) Interlobular duct (IrD) lies in-between lobules, however Intra-lobular ducts (InD) lies within lobule as shown in A3. (A3) very large **Islet of Langerhans (IL)** connected with duct. (A4) Large **blood vessels (BV)** travel in the connective tissue septa and nerves also travel in the septa but they are seen only infrequently.

The islets of Langerhans are more concentrated in the tail region as compared to the head region. Commonly islets are surrounded by acini; however, islets can occur at the periphery of lobules with one side covered with inter-lobular connective tissue and rarely surrounded by connective tissue. On staining with H&E (haematoxylin and eosin) islets are clearly visible with a lighter staining than surrounding cells. Cells within Islets of Langerhans are arranged irregularly and it is not possible to identify different cell types within; however, β -cells are most numerous followed by α -cells. The pancreas is well supplied with blood and blood vessels come from multiple branches of the coeliac and superior mesenteric arteries. Inter-lobular arteries give rise to small branches within the lobule and are further divided into capillaries. A nerve supply passes through the septa of connective tissue as blood vessels in the pancreas. The pancreas is innervated by both the sympathetic as well as the parasympathetic nervous system. The sympathetic nervous system inhibits endocrine and exocrine secretion and the parasympathetic nervous system stimulates secretion [18-20].

1.3. Pancreatic Cancer:

Loss of controlled cell growth, division and apoptosis can lead to cancer development. [21]. In many cases cancer results in tumour formation and migrates to other body parts where they grow. This process when cancer cells migrate from one part of the body to another and replace normal cells with cancer cells is known as metastasis. There are two types of tumour; benign tumours (which do not spread) and malignant tumours (which invade and spread). Although benign tumours do not invade to other organs they can grow very large but usually not life threatening. Pancreatic cancer or carcinoma of the pancreas mostly begins in the ducts carrying digestive juices, or, rarely in insulin making cells (called islet cell cancer or insulinoma)[3].

1.3.1. Symptoms and risk factors

The exact cause of pancreatic cancer is still not known. Pancreatic cancer is one of most deadly cancers and often referred to as a “Silent disease” because of its notorious late presentation. Symptoms rarely present in the early stages and it can become highly aggressive in the late stages with high metastatic potential and a very poor prognosis [22, 23]. Pancreatic cancer symptoms include weight loss, weakness, and pain in upper abdomen or lower back, yellow skin (Jaundice), intense itching in the skin and dark urine.

Identification of various risk factors associated with pancreatic cancer development is of great public health importance. Some people are at higher risk of developing pancreatic cancer than others depending on various risk factors. Some of the risk factors are smoking [24], alcohol [25], people working in radiation industries [26], high consumption of red meat and processed meat [27], age and race [28]. Medical conditions that increase the risk for pancreatic ductal adenocarcinoma are chronic pancreatitis [29], diabetes mellitus [30-32], obesity [33] and familial type.

1.3.2. Statistics

Despite all new technologies and therapeutic efforts, the mortality rate still remains high, as the number of people diagnosed and the death rate are nearly the same for pancreatic cancer. Pancreatic cancer has the worst survival rate, relative survival rate to 5 years is only 4% and these figures have not changed in over 40 years [34, 35]. According to Cancer Research UK figures in 2011, pancreatic cancer was the fifth most common cause of cancer death, around 24 people were diagnosed every day and around 23 died every day in the UK from pancreatic cancer [35] The American Cancer Society’s estimates for 2014 in United States for pancreatic cancer are: about 46,420 people (23,530 men and 22890 women) will be diagnosed and about 39,590 people (20,170

and 19,420) will die of pancreatic cancer. In the past 10 years the rate of pancreatic cancer is slowly increasing [36].

1.3.3. Early detection and diagnosis

One of the major reasons behind a low survival rate is that symptoms do not present in the early stages of pancreatic cancer and in the late stages symptoms are non-specific. Early detection and screening could help to fight this deadly cancer. Currently researchers are working on various methods for early detection of symptoms by combination of imaging modalities. Imaging modalities have been used to detect lesions in the patients with high risk of pancreatic cancer. Imaging modalities include combinations of techniques such as endoscopic retrograde, magnetic resonance imaging, endoscopic ultrasound, computed tomography and exploratory laparotomy [37, 38]. Another approach is the study of disease specific biomarkers for early detection of pancreatic cancer. Biomarkers have been studied as a cost effective and simple detection method. Serum biomarkers include: carbohydrate antigens 19-9 (CA 19-9) [39], macrophage inhibitory cytokine (MIC-1) [40], tumour specific growth factor (TSGF) [39], cell adhesion molecule 17.1 (CAM 17.1) [41], regenerating islet-derived family member 4 (REG4) [42] and carcino-embryonic antigen-related cell adhesion molecule 1 (CEACAM1) [43]. Important tissue markers have been identified such as human trophoblast cell surface antigen TROP2 [44, 45] and recently studied plectin 1 (PLEC1) [46].

1.3.4. Treatments

Due to low survival rates only 10% to 20% of patients with pancreatic cancer are considered for curative resection [47, 48]. Most patients end up with aggressive malignant PC and they have only palliative chemotherapy options for treatment [49]. There are different treatments options such as surgery [50], chemotherapy (5-Flouro

uracil [51], Gemcitabine [52, 53], FOLFIRINOX [54]), targeted molecular therapy (EGFR [55], HER2[56]) and radiotherapy [57]. It has been reported that combination of chemotherapy with radiotherapy improved the survival of patients with locally advanced un-resectable pancreatic cancer [58]. Despite the various treatments and improvements in different therapies pancreatic cancer still poses a big challenge. However, small but promising steps to fight back against pancreatic cancer by improving various therapies provide hope.

1.3.5. Pancreatic cancer stages and typing

The exocrine gland produces enzymes which digest food and endocrine glands produce very important hormones such as insulin, which regulate the level of sugar in blood. Tumours arising from both glands form completely different tumour types with distinct risk factors, symptoms, treatments and rate of survival. Many reports on pancreatic cancer refer to ductal adenocarcinoma, which is the most common malignant type of pancreatic cancer. Different variants of pancreatic cancer have different prognosis and cellular / tissue histology of those described include colloid carcinoma, medullary carcinoma, adeno-squamous carcinoma, undifferentiated carcinoma and undifferentiated carcinoma with osteoclast like giant cell [59]. It has been reported that pancreatic cancer has three distinct precursor lesions: pancreatic intraepithelial neoplasia (PanINs), intra papillary mucinous neoplasms (IPMNs) and mucinous cystic neoplasms (MCNs). PanINs is the most common, well-studied and characterized precursor lesion of pancreatic cancer. On the basis of histology, PanINs have been classified into three lesions: PanIN-1, PanIN-2 and PanIN-3. These different lesions differentiate from each other by the degree of cellular atypia, architectural atypia, varying degrees of loss of polarity and luminal budding. PanIN-3 may harbour mitotic figures and exhibit local invasion, represent as carcinoma *in situ* as shown in Figure 1-3 [60-62].

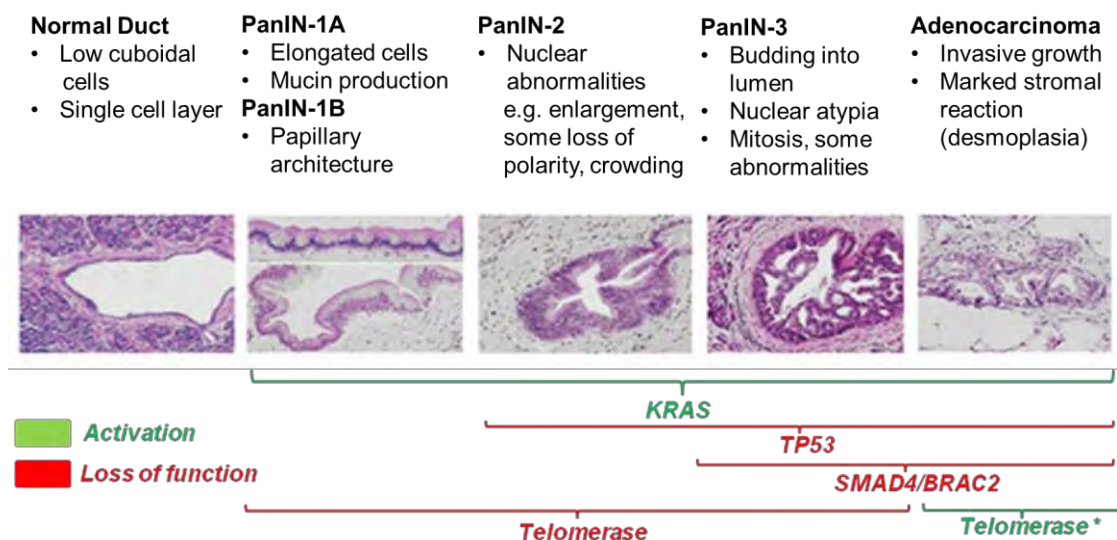


Figure 1-3: Pancreatic intraepithelial neoplasia (PanIns)

Progressive stages of PanINs neoplastic growth from initial stage (PanIN-1A) to the aggressive and invasive carcinoma. The increase in mutations of various genes results in progression of pancreatic lesions from low grade to carcinoma as shown above from left to the right. Lines under the figure from left to right represent onset of mutation of various genes specifically in adenocarcinoma *KRAS*, *TP53*, *SMAD4* and *BRAC2*. Increase in alteration in the number of genes increases with progression PanIN-1 to adenocarcinoma. *KRAS* mutation is the first genetic change that occurs with progression of PanIN-1 to adenocarcinoma and it is found in 100% of adenocarcinomas. Telomerase is eroded as cells proliferate with progression PanIN-1A to PanIN-3 and reactivation of telomerase in adenocarcinoma which is subsequently stabilizes the genome and facilitates immortal growth of the tumour [63].

Adapted from Hruban, et al, Int J Clin Exp Pathol, 1(4): p. 306-16(2008).

Cell proliferation and genetic alteration increase with advancing stages of PanINs from PanIN-1 to PanIN-3 then leading to pancreatic cancer. The genetic progression model of PanIN to pancreatic cancer was proposed by Dr Ralph Hruban in 2008 based on the results from different studies showing that increases in genetic alteration of various genes resulted in more aggressive and higher grades of pancreatic cancer [63]. PanIN lesions are the signs for pancreatic cancer and could potentially be used in early detection of pancreatic cancer. However, PanIN lesions are not associated with clinical signs because current diagnostic techniques have limitations to detect PanIN lesions at an early stage [64]. It has been reported that on follow up with the patients with high-grade lesion (PanIN-3) have progressed to invasive carcinoma [65-68].

1.3.6. Histological classification of pancreatic cancer

Pancreatic adenocarcinoma is the most common form of the pancreatic carcinoma and accounts for over 90% of all cases of pancreatic cancers [69, 70]. The second most common type of pancreatic tumour is mucinous tumour which is another type of exocrine pancreatic cancer, accounting for <10% of all tumours [71]. Cancer of the endocrine pancreas accounts for less than 5% of all pancreatic cancer; tumour from islet cell (α and β cells) [72]. Pancreatic ductal adenocarcinoma is a highly desmoplastic cancer and is characterised by prominent and complex stroma that consists of cancer associated fibroblasts, rudimentary acinar cells, inflammatory cells, pancreatic satellite cells (PSC), aberrant micro-angiogenesis and aberrant ducts [73]. The desmoplastic stromal compartment play an active role in chemotherapy resistance and promotes invasion and growth of pancreatic adenocarcinoma cells [74]. Especially, pancreatic satellite (PSC) cells play a strategic role in stroma formation, involved in tumour growth, invasion and metastasis [75]. It has been reported that upon activation of PSC, production of extracellular matrix (ECM) proteins (fibrosis) occurs, which ultimately results to hypo-vascular and hypoxic stroma [76].

The pancreatic ductal adenocarcinoma glands generally show varying degrees of cytological atypia, produce various amounts of mucin, elicit a desmoplastic reaction, invade the stroma and are often well developed [77]. Hyland *et al.*, (1981) reported three major (nuclear size variation, incomplete ductal lumens and disorganized duct distribution) and five minor (huge, irregular epithelial nucleoli; necrotic glandular debris; glandular mitosis; perineural invasion and glands unaccompanied by connective tissue stroma) criteria for the diagnosis of pancreatic ductal adenocarcinoma established by prospective review of 64 frozen sections of pancreatic carcinoma. These major and minor criteria for diagnosis are especially helpful in cases to differentiate pancreatic ductal adenocarcinoma from chronic pancreatitis [78]. These major and minor criteria were further confirmed in a series of 38 cases of adenocarcinoma and 14 cases of chronic pancreatitis and two additional findings were found single cell infiltration and disorganised desmoplastic stroma [79].

Ductal adenocarcinomas can be divided into well, moderately and poorly differentiated as shown in Figure 1-4. However, variation of differentiation within the same neoplasm is quite common, but well to poor differentiation are uncommon [77, 80].

Characterisation of well differentiated carcinoma (illustrated in Figure 1-4):

- Large duct-like structures with medium sized neoplastic gland.
- Large duct-like structures may have small irregular papillary like projection without distinct fibro-vascular stalk.
- Neoplastic duct-like gland structure imitates normal pancreatic duct, however, can be easily distinguished from normal duct as mostly neoplastic gland may be ruptured or incompletely formed.
- In between neoplastic gland few non-neoplastic ducts as well as remaining acini and islet cells.

- Low mitotic activity and mucin-producing neoplastic cells tend to be in a columnar structure with pale or eosinophilic or even clear cytoplasm. Cytoplasm of neoplastic duct larger than non-neoplastic ducts.
- Large round or ovoid cells which may vary in shape and size with distinct nuclei which are not found in normal cells. Neoplastic duct nucleus tends to be situated at the base of the cells.

Characterisation of moderately differentiated carcinoma (illustrated in Figure 1-4):

- Mixture of high number of medium size duct like structures, embedded in desmo-plastic stroma.
- Greater variation in the size, shape of nucleus with high variation in chromatin structure as well as prominence of nuclei.
- High mitotic figures and mucin producing cells are usually eosinophilic but cells with clear cytoplasm are occasionally abundant.
- Poor and irregular glandular differentiation are often found, particularly where cancer invades at peri-pancreatic tissues.

Characterisation of poorly differentiated carcinoma (illustrated in Figure 1-4):

- Mixture of densely packed small irregular glandular structures.
- Replacement of entire acini with small irregular glandular structures as well as solid tumour sheets and nest.
- Absence of large duct like structure and intra ductal tumour components.
- Abrupt mitotic activity and little or no mucin production.
- At the advancing edge of the carcinoma, the peri-pancreatic tissue and gland are infiltrated small clusters of cancer cells.

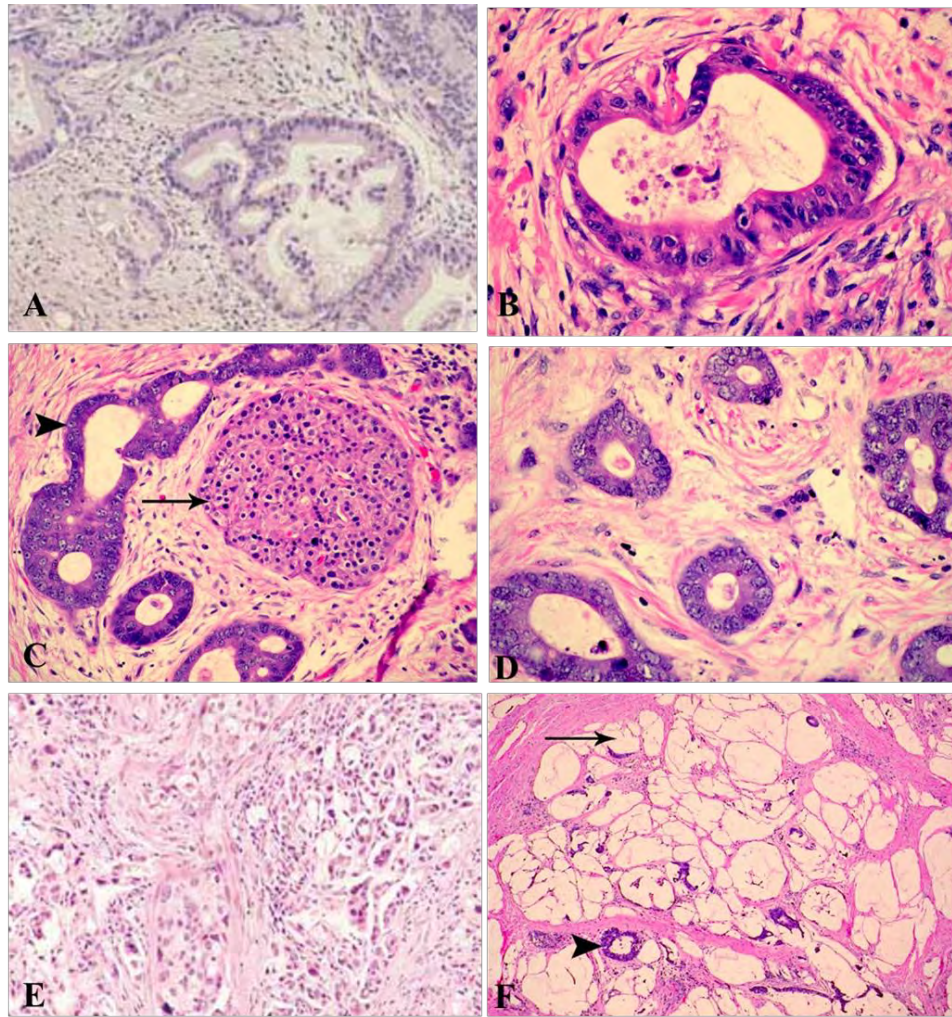


Figure 1-4: Ductal adenocarcinoma of pancreas

(A) Well differentiated tumour with desmoplasia (overproduction of extracellular matrix proteins and extensive proliferation of myo-fibroblast like cells which results into fibrous and dense connective tissue [81]) and irregular gland formation (B) Moderately differentiated invasive adenocarcinoma showing nuclear hyperchromasia, nuclear stratification and prominent nucleoli with desmoplastic stroma. (C) Moderately differentiated adenocarcinoma shows fibrous connective tissue around islet of Langerhans (as pointed by arrow). (D) Small tubular gland and ductal structure with nuclear atypia and desmoplasia. (E) Poorly differentiated ductal adenocarcinoma; No lobular structure, no acini, no large ducts, many small gland-like structures and desmoplasia. (F) Ductal adenocarcinoma of pancreas with abundant mucin with only a small strip of gland floating (as pointed by arrow) [80].

Adapted from Klöppel, et al., (IARC) 220-251, 2000 [80] and Yen, et al., Surgery, 129-34. 2002 [81].

1.3.7. Molecular mechanisms in pancreatic cancer

Pancreatic cancers are often composed of several different cells such as tumour stroma cells, pancreatic cancer stem cells and pancreatic cancer cells. Pancreatic cancer cells are resistant to various therapies and survive because of genetic alterations in various signalling pathways, proto-oncogenes and tumour suppressor genes [82]. In pancreatic cancer, 80% of cases reported activation of the *K-ras* oncogene and more than 60% report inactivation of various tumour suppressor genes such as *p53*, *p16* and *DPC4* [83, 84].

Functional inactivation or mutation of the *p53* gene is a universal sign of most cancers. Different cellular DNA damage signals activate the *p53* gene; subsequent *p53* expression activates apoptosis, senescence and cell cycle arrest. *p53* is involved in cell cycle control at the G1/S interface and has a role in apoptosis [85]. It has been reported that the *p53* gene is inactivated in 55-75% of pancreatic cancer because of various mutations in one of the alleles [86]. Expression of *p53* is suppressed in a great fraction however, mutated *p53* is found in only half of pancreatic ductal adenocarcinoma cases [84].

Tumour suppressor gene *p16* acts as a cyclin dependent kinase (CDK4 and CDK6) inhibitor and the loss of expression of p16 protein or *p16 gene* has been reported in many cases of pancreatic cancer [87-90].

Oncogene *K-ras* was the first to be identified as playing role in pancreatic adenocarcinoma [91]. In pancreatic cancer, it has been found that the *K-ras* gene is highly mutated, especially at codon 12 in pancreatic adenocarcinoma patients [92-94]. *K-ras* mutations are one of the earliest events in the development of pancreatic adenocarcinoma cancer (PDAC) [95].

Breast cancer type 2 susceptibility protein (BRAC2) is found inside the cell just like BRAC1, it is involved in the error free repair of chromosomal aberrations or correction of breaks in double stranded DNA. *BRAC2* plays a very critical role in the repair of any gene aberration in ds DNA and provides gene stability and the loss of this protein usually leads to accumulation of various chromosomal aberrations [96]. Individuals with a mutation on *BRAC2* have a higher risk of developing PDAC and patients with *BRAC2* mutations were reported to account for one fifth of all cases of pancreatic ductal adenocarcinoma [97]. Recently *PALB2*, a complement and localizer of *BRAC2* gene was identified as a pancreatic cancer susceptibility gene [98, 99].

1.4. Programmed cell death gene 4(PDCD4): A novel tumour suppressor

1.4.1. Background

Apoptosis, also called programmed cell death, plays a crucial role in many biological processes from embryonic development and metamorphosis to normal tissue turn over. Unlike in necrosis, where cells die due to insult from stimuli such as injury or toxic agents, apoptosis is a well-controlled and regulated process of cell death that insures tissue integrity [100-103]. Any disruption to the highly regulated process of apoptosis can result in the development of cancer. Consequently, genes that regulate the process of apoptosis can be targeted for cancer treatments. Programmed cell death gene 4 (PDCD4) was first identified during the investigation of genes up-regulated in the process of apoptosis or programmed cell death. Shibahara *et al.*, (1995) used differential display polymerase chain reaction (PCR) to identify a clone named *MA-3* which was highly up-regulated during the process of apoptosis in thymocytes, and named it *PDCD4* [104]. Since then, *PDCD4* has also been termed *H73I*[105], *197/15 α* [106], *A7-1* [106] and in rats the homologous protein is *DUG* (death up-regulated gene)[107]. Homologous counterparts of *PDCD4* have also been identified in distantly related organisms such as the fruit fly *Drosophila melanogaster* (GenBank name CG10990) and marine sponge *Suberites domunculata* [108]. From this it has been suggested that *PDCD4* was highly conserved during evolution. To simplify matters, different mammalian homologues have been termed as *PDCD4* gene, however, in addition to up-regulation of *PDCD4* in apoptotic cells, certain cells which are not programmed to die or healthy cells may also express significant amounts of *PDCD4*. It has been identified in some cell lines including liver, brain, heart, kidney, lung, thymus and spleen [104].

1.4.2. The Structure of PDCD4

The deduced protein sequence of PDCD4 comprises 469 amino acids (aa). PDCD4 comprises two basic domains (at the N-terminal and C-terminal) and two conserved α -helical MA-3 domains as shown in Figure 1-5 [105, 107, 109]. The human *PDCD4* gene has been mapped by *in situ* hybridization to human chromosomal band 10q24 [110]. MA-3 domains have been proposed to be functionally important because of high conservation during evolution and homologs have been found in chicken, human, xenopus and drosophila [104]. The PDCD4 structure has two highly conserved MA-3 domains, MA-3m (164 to 275aa) and MA-3c (327 to 440 aa) [111]. It has been reported that these domains are involved in protein-protein interaction with eukaryotic translation initiation factor 4GI (eIF4GI) and eukaryotic translation initiation factor 4GII (eIF4GII) with eIF4A (ATP-dependent RNA helicase) [112].

PDCD4 inhibits eukaryotic translation by interacting with eIF4A (ATP-dependent RNA helicase) and results in translation inhibition [107, 113]. A schematic representation of the action of PDCD4 in translation inhibition is illustrated in Figure 1-6 [113]. Yang *et al.*, (2003) reported that PDCD4 inhibits helicase activity of eIF4A in a concentration dependent manner which results in the repression of cap-dependent translation [113]. The C-terminal MA-3 domain (MA-3c) of PDCD4 binds to eIF4A by competing with eIF4G leading to inhibition of translation. Suzuki *et al.* (2008) analysed the structure of the second N-terminal MA-3 domain (MA-3m) [114], which has the same function as MA-3c, with which it acts together giving a synergetic effect. Thus both domains are required to form a high affinity bond with eIF4A and displacement of RNA. It has been reported that RNA binding activity and direct interaction of PDCD4 with eIF4G make translation regulation more complex by PDCD4 [109, 115].

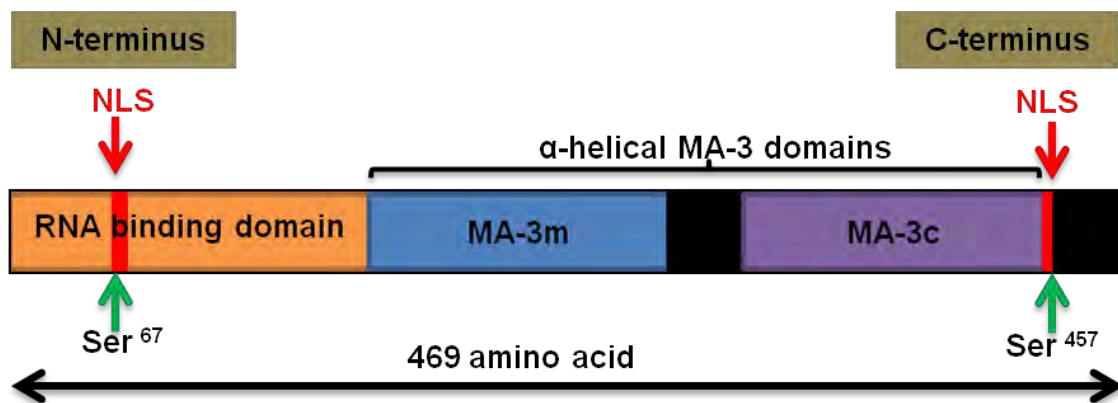


Figure 1-5: Structure of PDCD4

PDCD4 protein comprises 469 amino acids (aa) and is composed of three domains; N-terminal RNA binding domain (residue 1-157aa) and two interacting α -helical conserved MA-3 domains: MA-3m domain (residue 157-305) and MA-3c (319-449) domain. Two putative nuclear localisation sites (NLS) are shown in red and arrows indicate two important phosphorylation sites at Ser⁶⁷ and Ser⁴⁵⁷. Akt/protein kinase B specifically phosphorylates these sites and induces two effects: a nuclear translocation of PDCD4 and a decreased ability of PDCD4 to act as an inhibitor of AP-1 (activator protein-1) mediated transcription [116]. MA-3 domains are involved in protein-protein interactions with eukaryotic translation factors (eIF4G1 and eIF4GII) [112].

Adapted from Waters, et al., J Biol Chem, 286(19): p. 17270-80 (2011) [117]

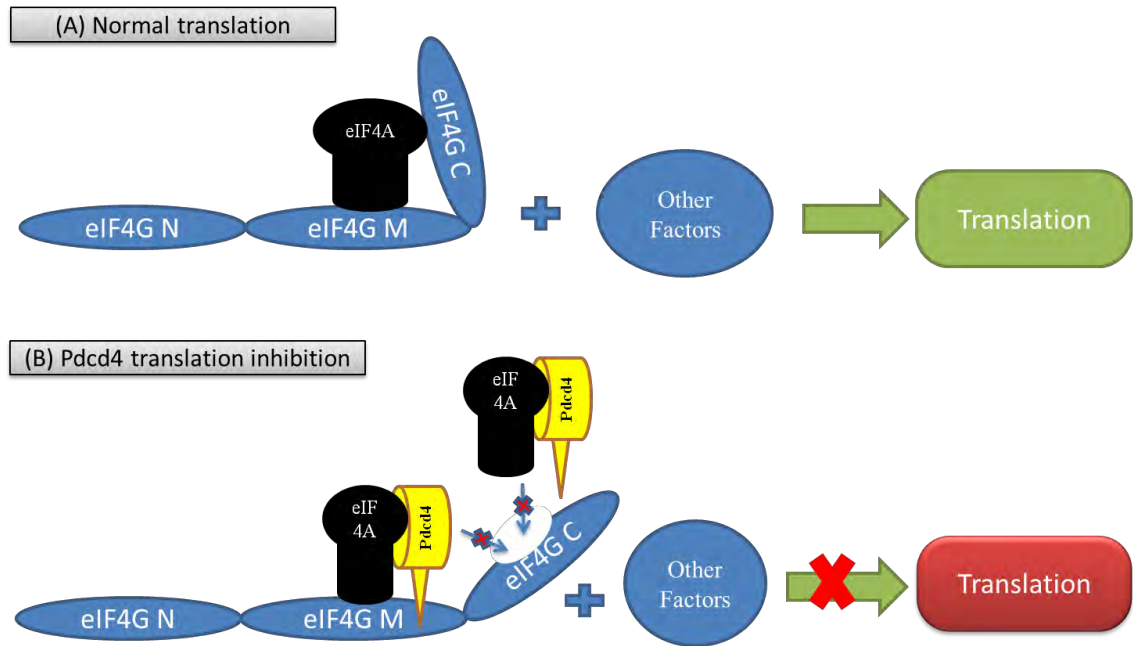


Figure 1-6: Schematic representation of PDCD4 action in translation inhibition

(A) Initiation of translation is the first step in the protein biosynthesis and is mediated by several eukaryotic translation initiation factors (eIFs). Normal translation where eIF4A (ATP-dependent RNA helicase) binds to the 4GM and 4GC terminal of eIF4G [118]; (B) Model of PDCD4 inhibition of translation. PDCD4 inhibit helicase activity of eIF4A. PDCD4 continuously binds to eIF4A and blocks its association-dissociation cycle results into inactivation of eIF4F complex. Also PDCD4 also prevents binding of eIF4A binding to the 4gC of eIF4G which prevent eIF4A from stimulating the activity of eIF4F [113].

Adapted from Yang, et al., Molecular and Cellular Biology, 23(1): p. 26-37(2003).

1.4.3. Potential role of PDCD4 in the nucleus and cytoplasm

Many studies have revealed that PDCD4 is expressed in both the nucleus and cytoplasm depending upon the cell type. Matsushashi *et al.*, (1987) was the first to identify PDCD4 as an antigen which was recognised by a monoclonal antibody Pr-28 directed against a nuclear antigen present only in proliferating cells, however, it was not detected in quiescent cells [119]. In HeLa cells PDCD4 has been described in nuclei [105] and cytoplasmic regions of the cell [120]. However, further studies revealed that PDCD4 localisation was cell cycle dependent after observing nuclear localisation at prophase, cytoplasmic localisation at M-phase and no expression was detected at S-phase of the cell cycle [121]. The putative nuclear export sequences identified in PDCD4 indicate that the protein is capable of shuttling between the nucleus and cytoplasm under certain conditions. In 2003 Bohm *et al.*, reported nuclear localisation of PDCD4 in QT6 fibroblast cells and on serum starvation it exported to the cytoplasm [115]. As discussed earlier, PDCD4 comprises 469 amino acids and has multiple phosphorylation sites although the importance of these sites remained unclear for several years [120]. In 2005, Palamarchuk, *et al.*, reported that Akt/protein kinase B phosphorylates PDCD4 at the specific amino acid sites (Ser⁶⁷ and Ser⁴⁵⁷) and causes nuclear translocation of PDCD4, and inactivates PDCD4 in its function as an inhibitor of AP-1 (activator protein) mediated transcription [116].

Schlichter *et al.*, in 2001 reported that, PDCD4 localized inside the nucleus [122] however, in 2003, Yang *et al.*, reported PDCD4 localised in cytoplasm [113]. Some reports have shown that PDCD4 is localised in the nucleus in normal tissues and in the cytoplasm in cancer tissues [123, 124] whilst others have reported that PDCD4 is localized in the nucleus in cancer tissues and in the cytoplasm in normal tissues [125]. As mentioned earlier, PDCD4 shuttles between nucleus and cytoplasm [115] which might give rise to this conflicting data. Another explanation might be that, sub-cellular

localisation of PDCD4 is cell-type specific [126]. Still more research is needed to find out the exact localisation in different cells under different conditions. One of the aims of the present study is to determine the subcellular localisation of PDCD4 under different conditions (hypoxic and normoxic) in human adenocarcinoma pancreatic cells (PSN-1 cells), Ductal cells (ARIP cells), β -cells (insulin producing cells, Min6 cells), mouse normal pancreas and human pancreatic cancer tissues from pancreatic cancer patients.

1.4.4. Expression and regulation of PDCD4

Although PDCD4 has been identified as up-regulated during apoptosis, a definitive role for this protein still not has been identified in the process of programmed cell death. There is conflicting data between different cell types. PDCD4 is ubiquitously expressed in normal tissues, phosphorylation by S6K1 (S6 kinase 1) marks the protein for degradation by ubiquitin ligase SCF ^{β TrCP} [127] and reaches its highest levels in the liver [111]. *PDCD4* was first identified as an up-regulated gene during the investigation of genes up-regulated during the process of apoptosis [104]. It has been identified that on treating cells with different pro-apoptotic substances (dexamethasone and ionomycin) increased levels of PDCD4 result [104]. However, in some reports on treating cells with UV-radiations or topoisomerase inhibitor, which were inducers of apoptosis, no effect on the level of PDCD4 was observed [128, 129]. Cytokines such as IL-12 (interleukin 12) induced the level of PDCD4 whereas IL-2 and IL-15 down regulated the level of PDCD4 [106]. Recently in 2014, Vikhрева, *et al.*, investigated the expression of PDCD4 in 23 human melanoma cells lines and loss of PDCD4 expression was observed, however, on treating cells with inhibitor of Akt pathway induced the expression of PDCD4 [130]. It has been reported that overexpression of PDCD4 in ovarian cancer cells can inhibit the proliferation, reduction in colony number and cell cycle arrest [131]. In addition it has also been reported that PDCD4 expression can induce apoptosis in

breast cancer [132] and hepatocellular carcinoma [133]. However, in colon carcinoma overexpression of PDCD4 did not induce apoptosis or cell cycle progression [134].

It has been identified that down regulation of PDCD4 protein as well as mRNA were significantly linked to the lung primary carcinoma and grade of the tumour [135]. Loss of PDCD4 expression has been found in different types of cancers such as tongue tumour [136], invasive ductal breast carcinoma [137], melanoma [123, 130], human glioma [138], nasopharyngeal carcinoma [139], lung cancer [135], gastric cancer [140], colon cancer [141] and ovarian cancer [142]. All these data suggest the important role of PDCD4 in tumour development as discussed earlier. Interestingly, treating cancer cells with various anti cancerous drugs such as retinoic acid receptor (RAR) agonists, cyclo-oxygenase-2 inhibitor (COX-2) induced the expression of PDCD4 suggesting a role of PDCD4 in cancer therapies [132, 143]. Treating Huh7 (Hepatocellular carcinoma cells) with transforming growth factor- β (TGF- β) increased the expression of PDCD4 and induced apoptosis of cells [133]. However, Davis *et al.*, in 2008 reported that, TGF- β induces the expression of microRNA-21 (miRNA-21) which down regulates PDCD4 [144]. Other reports identified and reported that miRNA-21 regulates PDCD4 expression [145-148]. Some reports recently also identified and reported that miRNA-21 overexpression inhibits the tumour suppressor effect of PDCD4 in gastric cancer [149], tongue squamous cell carcinoma cells [150], ovarian cancer [151]. Other than miRNA-21 it has been reported that miRNA-182 also regulates PDCD4; Wang *et al.*, 2013 reported that miRNA-182 expression led to an opposite alteration of endogenous PDCD4 protein level in ovarian carcinomas. Down-regulating PDCD4 by miRNA-182 promotes cell growth, invasion and chemo-resistance in ovarian carcinoma cells [152]. Recently in 2014, it has been reported that hypoxia induced miR424 enhanced tumour cell resistance to apoptosis by targeting PDCD4 in human melanoma cells. Overexpression of miR-424 functionally decreases the sensitivity of cancer cells to anti-

cancerous drugs such as doxorubicin and etoposide. Inhibition of miR-424 enhanced apoptosis and increases the sensitivity of cancer cells to anti-cancerous drugs [153].

Akt and S6K1 kinase regulate PDCD4 by phosphorylating PDCD4 protein leading to proteasomal degradation [127, 154]. Woodard *et al.*, in 2008, reported up-regulation of PDCD4 on suppression of Akt and S6K1 by fluvostatin, which results in the induction of apoptosis and repression of proliferation in the case of renal cell carcinoma (RCC) cells [155]. The level of any protein in any cell depends upon transcription as well as translation of the target gene. The transcription factor v-Myb has been found to be an inducer of PDCD4 [156] and it has been identified that, in chicken cells on blocking or knocking out v-Myb results in reduced levels of PDCD4 [157]. In another study it has been reported that, inhibiting DNA methyltransferase 1 resulted in demethylation of DNA which induced the expression of PDCD4 in hepatocellular cancer cells, thus an epigenetic mechanism might also contribute to PDCD4 regulation [158]. From all of these studies it has been confirmed that PDCD4 is regulated by different signalling pathways at different levels. A summary of PDCD4 regulatory mechanisms is shown in Figure 1-7 [111].

Discrepancies in reports of the function of PDCD4 in different types of human cancer might be because of its cell type specific function or regulatory mechanism. In order to clarify these discrepancies further more investigations are needed to elucidate the apoptotic effect of PDCD4, especially in pancreatic cancer.

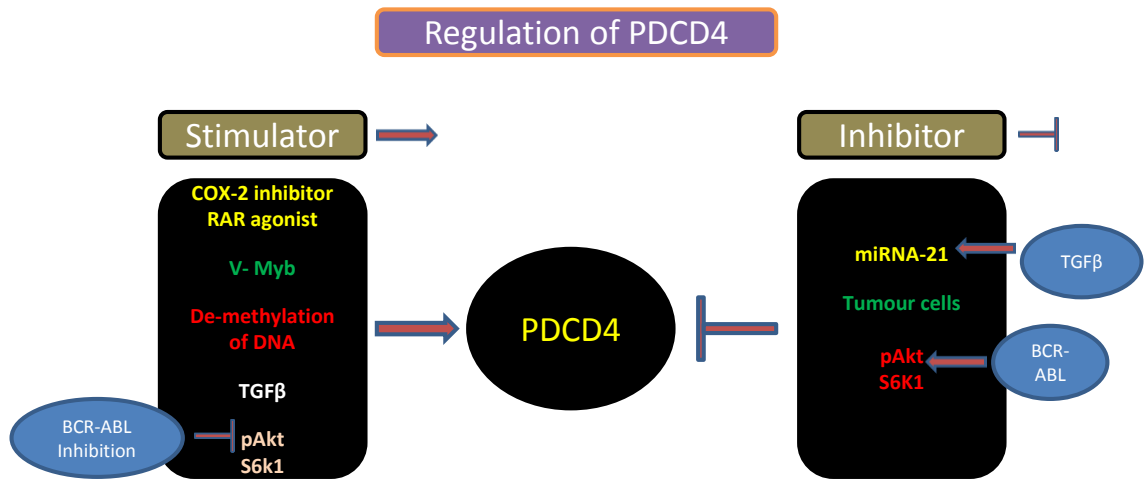


Figure 1-7: Overview of the reported regulatory mechanisms for PDCD4

As PDCD4 has cell type specific mechanisms so it has to be considered that not all regulatory pathways may be active in every cell type. PDCD4 expression induced by drugs with anti-cancerous effects such as COX-2 (cyclo-oxygenase-2) and RAR (retinoic acid receptor) agonists. TGF- β (trans-forming growth factor $-\beta$) and V-Myb induces expression of *PDCD4*. The knockdown of DNA methyl-transferase 1 therefore, de-methylation of DNA induces *PDCD4* expression. Inhibition of pAkt and S6K1 induces and stimulation inhibits the expression of *PDCD4*. TGF- β induces miRNA-21 (micro RNA-21) expression which down regulates the PDCD4. Adapted from Lankat-Buttgereit, B. and R. Goke. *Biol Cell*, 101(6):309-179 (2009) [111].

1.4.1. PDCD4 as a tumour suppressor and role in tumour development

After its original identification, PDCD4 has been shown to regulate many proteins in the cell and is implicated in inhibition of transcription as well as translation of various proteins which are involved in tumour progression, cell cycle and differentiation and has a role as a tumour suppressor. PDCD4 acts as a translation inhibitor via the MA-3 domains which influence the pattern of protein expressed in the cells. The first indication of PDCD4 function as a tumour suppressor was achieved by the experiment on the JB6 mouse epidermal cell line [159]. Yang *et al.*, (2001) showed that the overexpression of PDCD4 was sufficient to inhibit transformation [160] and then in 2003 Yang *et al.*, reported that, overexpression of PDCD4 did lead to transformation inhibition [161]. In 2004, Biotomsky *et al.*, reported that an enhanced level of PDCD4 was generated by reduced phosphorylation of c-jun by Jun N-terminal kinase (JNK) pathway which results in the inhibition AP-1. Results strongly suggested that PDCD4 is directly involved in the regulation of C-Jun activity [162]. Yang *et al.*, in 2006 reported that PDCD4 suppresses neoplastic transformation by blocking C-Jun activation by inhibiting the expression of MAP4K1 (Mitogen-activated protein kinase kinase 1) /HPK1 (Hematopoietic progenitor kinase 1), a kinase upstream of JNK in RKO human colon carcinoma cells [163].

Expression of carbonic anhydrase (CA) I and II correlated with aggressiveness of colorectal cancer [164] and on transfecting human embryonic kidney cells HEK-293 with PDCD4 resulted in down regulation of carbonic anhydrase (CA) II [165].

As discussed above PDCD4 appears to play a role both as tumour suppressor and in the development of tumour. Most of the data are obtained from cell culture studies but also some studies with animal models have been reported yielding surprising results about PDCD4 as a tumour suppressor. Jansen *et al.*, in 2005 reported that, compared to wild-type mice, transgenic mice with over-expression of PDCD4 in the epidermis showed

significant reduction in tumour development in skin [166]. Mice deficient in PDCD4 resulted in increased secretion of IL-4, IL-10 leading to the development of lymphomas [167]. In 2011, Hufbauer *et al.*, reported that skin tumour formation in human papillomavirus 8 (HPV8-CER) transgenic mice was associated with up-regulation of various oncogenic down-regulation of PDCD4 leading to induction of tumour formation [168]. Recently Wang *et al.*, in 2013 demonstrated that PDCD4 knock down increased the expression of mesenchymal specific proteins and decrease in the expression of epithelial specific protein *in vivo* and *in vitro* resulted in epithelial to mesenchymal transition. [169]. These results revealed a mechanism of metastasis promotion by knockdown of PDCD4 and a role for PDCD4 as a tumour suppressor. Recently in 2014 White *et al.*, introduced the miRNA-21/PDCD4/caspase-3/apoptotic molecular axis which when active induces pulmonary arterial endothelial cell apoptosis *in vivo* and *in vitro*. In this study, it has been reported that knock down of miRNA-21 (miR-21^{-/-} mice) resulted in activation of the PDCD4/caspase-3/apoptotic molecular axis and overexpression of miRNA-21 (miR-21 mice) resulted in reduced PDCD4 expression. Furthermore knockout of PDCD4 (PDCD4^{-/-} mice) blocked caspase-3 activation and resulted in development of chronic hypoxia and disease onset [170].

PDCD4 interferes with cap-dependent translation and regulates multiple proteins in cells at both a transcription and translation level. PDCD4 regulates the expression of many proteins inside the cell which play important role in the tumour development and this is why PDCD4 is known as a tumour suppressor.

Various functions and roles of PDCD4, are summarized in Figure 1-8 [111].

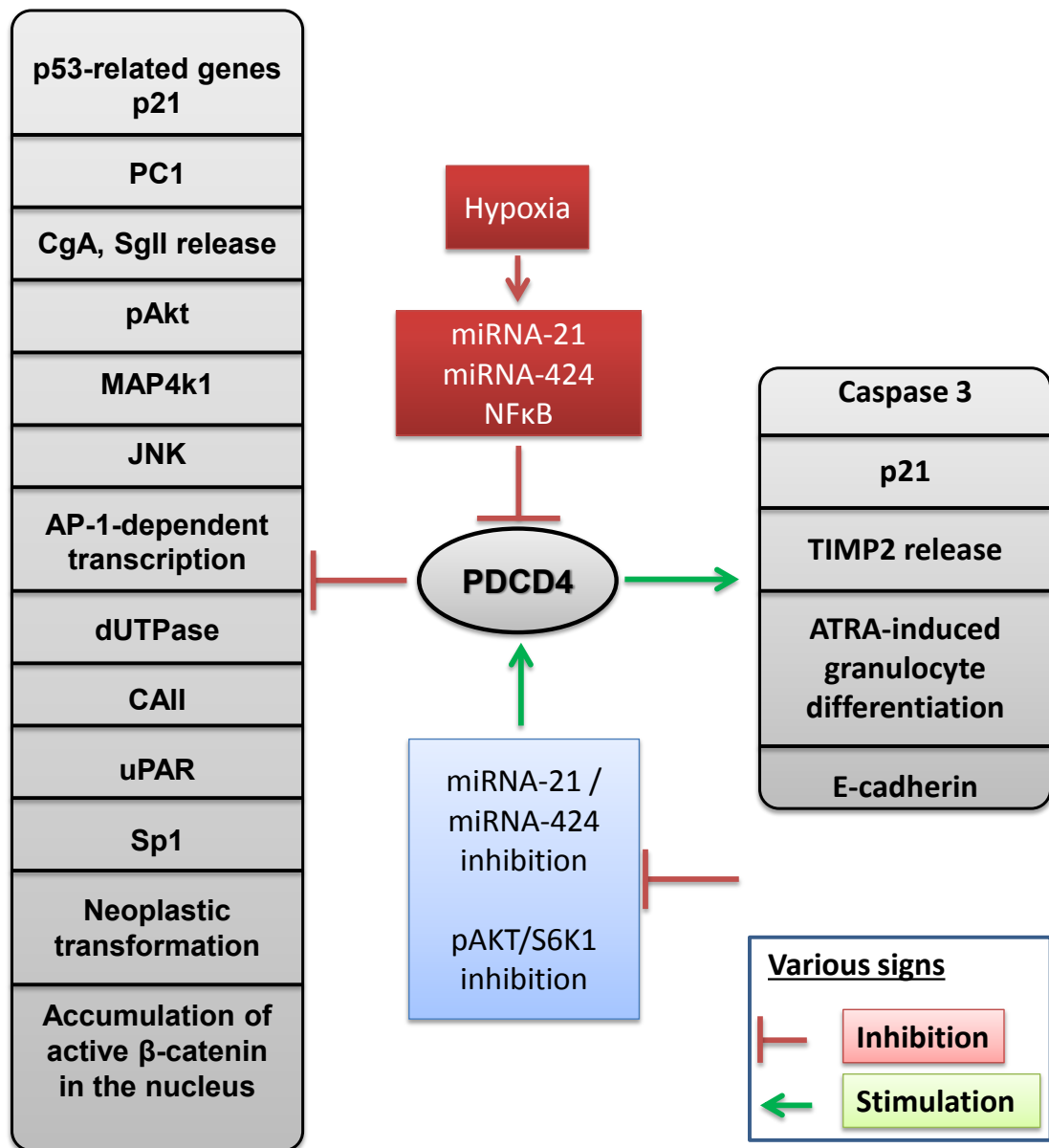


Figure 1-8: PDCD4 functions: Overview of known function of programmed cell death gene 4 (PDCD4).

PDCD4 plays role in neoplastic transformation inhibiting AP-1 dependent transcription in concentration dependent manner. PDCD4 inhibits the expression of kinase upstream of JNK and MAKKKK (MAPK kinase kinase or MAPK4) ultimately AP-1 dependent transcription. PDCD4 plays a role in tumour development by inhibiting CA II (carbonic anhydrase type II) and uPAR (urokinase receptor). High level of PDCD4 influence on the cell cycle and cell type specific action by inhibiting p21 and dUTPase.

Adapted from Lankat-Buttgereit, B. and R. Goke. Biol Cell, 101(6):309-179 (2009) [111].

1.5. Hypoxia inducible factor-1 (HIF-1): Master regulator of oxygen homeostasis

1.5.1. Introduction

Cells require oxygen to survive in order to maintain aerobic metabolism for intracellular bioenergetics. Ambient air is 21% (150 mm Hg); however, the majority of healthy tissues are exposed to 2-9 % of oxygen (40mm Hg). Low oxygen levels (hypoxia) can occur in many pathological conditions and are defined as an oxygen level below $\leq 2\%$, while severe hypoxia can occur when the oxygen level drops below $\leq 0.02\%$ [171]. Hypoxic conditions are common within regions of intense inflammation such as synovial joints and in highly proliferative cancer tumours [172]. Hypoxia is one pathological characteristic of solid tumours which is due to the rapid cell proliferation and low blood supply. Peripheral tumour cells are most likely to have an adequate amount of oxygen; however, cells deep inside the centre of the tumour face decreased levels of oxygen; from hypoxia to anoxia due to poor blood supply. In order to survive in hypoxic conditions cancer cells induce and stabilize the hypoxia inducible factor (HIFs), which partly restores new blood vessels to supply adequate amounts of oxygen to the tumour. Hypoxia inducible factor-1 (HIF-1) is a transcription factor that mediates an adaptive response to decreased oxygen availability by activating the transcription of genes encoding angiogenesis factors (such as vascular endothelial growth factor), energy metabolism, iron transport and vasomotor control [173]. HIF-1 and HIF-2 regulate expression of more than 1000 target genes such as VEGF, NF κ B etc. [174]. Hypoxic conditions trigger the expression of HIF-1 α ; through depression of tumour suppressor genes and activation of oncogenes. Increased expression of HIF-1 in tumours has been correlated to increased angiogenesis, metastasis and poor survival of cancer patients; this makes HIF-1 an important target for anti-cancer drugs [175]. As

reviewed by Xia *et al.* (2012) many anti-cancer agents have been reported to inhibit HIF-1 activity by targeting various mechanisms such as signalling pathways related to HIF-1, HIF-1 α transcription, HIF-1 α translation, HIF-1 α mediated transcription of target genes and HIF-1 α degradation [175].

1.5.2. The structure of HIF-1

The HIFs are heterodimeric proteins consisting of two subunits; constitutively expressing subunit HIF-1 β and the oxygen sensitive or hypoxically inducible subunit HIF-1 α . Both subunits are members of the basic helix-loop-helix-ARNT-Sim (bHLH/PAS) family of transcription factors and are primarily regulated through post-translational modification and stabilization [176]. HIF- α has three subunits: HIF-1 α , HIF-2 α , and HIF-3 α [177-179], both HIF-1 α and HIF-2 α have a common ability to hetero-dimerise to HIF-1 β and also share a high degree of sequence identity [177, 178]. Although HIF-1 α and HIF-2 α have common sequence identity, their tissue specific gene expression and target genes are different. HIF-1 α contains one N-terminal nuclear localisation sequence (N-NLS), one bHLH (basic helix-loop-helix) domain, one PAS (Per-ARNT-Sim homology) domain, oxygen-dependent degradation domain (ODD), two transactivation domains (TAD), one inhibitory domain (ID) and one C-terminal transactivation domain (C-TAD). The bHLH and PAS domains are required for dimerization and DNA binding; C-NLS is responsible for importing HIF-1 α in the nucleus [180, 181]; the schematic structure of HIF-1 α is shown in Figure 1-9 [182].

1.5.3. Regulation of HIF-1 α

Although HIF-1 β is constitutively expressed and maintained at constant levels regardless of oxygen availability [183], HIF-1 α protein has a short half-life ~5 min and is highly regulated by oxygen [184].

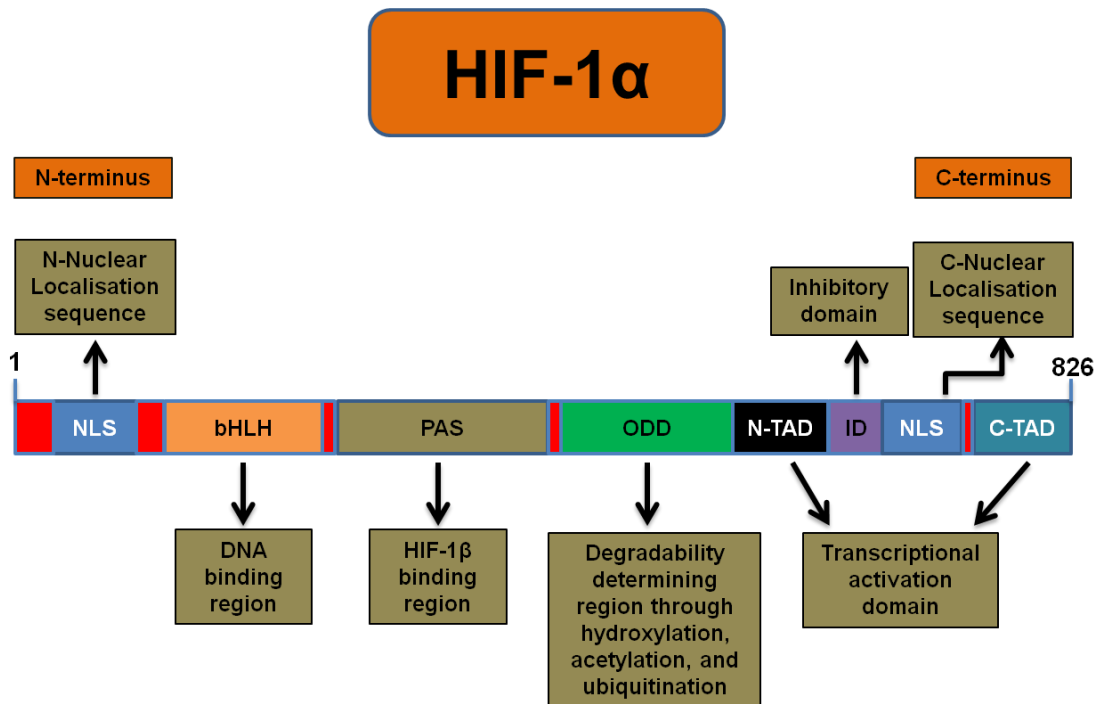


Figure 1-9: Schematic representation of domain structure of HIF-1 α and their potential functions in stability and transcriptional activity.

From N-terminal to C-terminal, HIF-1 α contains nuclear localisation domain (N-NLS), a basic helix-loop-helix (bHLH) domain, Per-ARNT-Sim homology domain (PAS), oxygen-dependent degradation domain (ODD) and two transactivation domain (N-TAD and C-TAD) separated by an inhibitory domain (ID). bHLH and PAS are required for DNA binding and dimerization of HIF-1 β . ODD confers oxygen dependent regulation through hydroxylation, acetylation and ubiquitination. C-terminal NLS is the more crucial in the nuclear localisation of HIF-1 α compared to N-NLS.

Adapted from Hu, Y., et al., J Cell Biochem. 114(3): p. 498-509 (2013) [182].

The transcription and synthesis of HIF-1 α are regulated by an O₂-independent mechanism [183, 185] however, in normoxic conditions the HIF-1 α proteins get degraded by proteasomal degradation [186]. Oxygen dependent and independent regulation of HIF-1 α is guarded by its post translational modification, such as phosphorylation, hydroxylation, acetylation and ubiquitination within several domains [187].

In normoxia, within the oxygen dependent degradation domain (ODDD) of HIF-1 α , it gets hydroxylated by HIF-1-propyl hydroxylases 1-3 (PHD 1-3) at the proline residue P402 and P564, acetylated by the ARD1 acetyltransferase at lysine residue L532. Hydroxylation and acylation is required for the binding of von Hippel-Lindau (pVHL) ubiquitin E3 ligase complex to the HIF-1 α [188, 189]. This pVHL complex tags HIF-1 α with ubiquitin, resulting in the degradation of HIF-1 α by 26S proteasome. In addition hydroxylation of the asparagine residue at 803 in the C-terminal transactivation domain (C-TAD) by the factor inhibiting HIF-1 (FIH-1) enzyme blocks the binding of transcriptional co-activator p300 /CBP to HIF-1 α and thus inhibits its transcriptional activity [190].

In hypoxia, activity of PHD1-3 and FIH-1 are inhibited due to lack of oxygen, therefore no hydroxylation at proline and asparagine residue which results to no binding of von Hippel-Lindau (pVHL) ubiquitin E3 ligase complex to the HIF-1 α and no degradation. HIF-1 α becomes stabilised and translocates to the nucleus from the cytoplasm and dimerises with HIF-1 β (ARNT) [183, 191]. Non-hydroxylated N803 residue within C-TAD domain allows binding of p300/CBP to the target gene. The HIF-1 dimer and transcriptional co-activator binds to the hypoxia response elements (HREs) in the regulatory regions of the target genes results in to gene expression [192].

The mechanism of transactivation of HIF-1 under hypoxic conditions is shown in Figure 1-10 [173].

Regulation of HIF-1 α

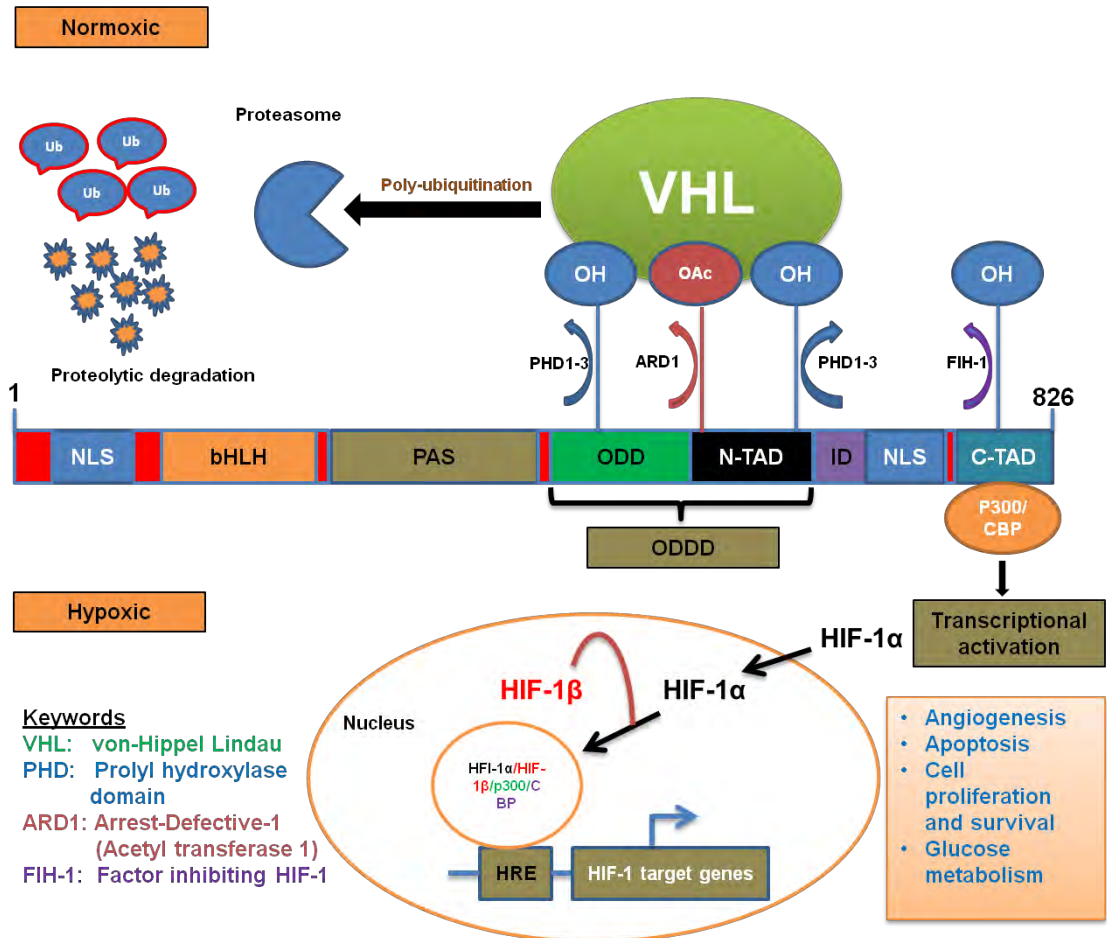


Figure 1-10: Regulation of Hypoxia inducible factor 1 α .

In normoxic conditions, the alpha subunit of HIF1 gets hydroxylated by PHDs at proline residue (402 and 564) and FIH-1 at asparagine residue (803). Hydroxylated HIF-1 α proteins bind to the E3 ubiquitin ligase VHL complex, leading to its degradation by the proteasome. Acetylation of lysine (at 532) by ARD1 favours the interaction of HIF-1 α with VHL. Hydroxylated asparagine residue (803) blocks the recruitment of transcriptional co-activator CBP/p300. In hypoxic conditions, the activities of FIH-1 and PHDs are inhibited due to lack of oxygen which ultimately results in no hydroxylation. Therefore there is no VHL binding and HIF-1 α stabilization and translocate to the nucleus and bind to HIF-1 β . HIF-1 α / β dimer binds to hypoxia response elements and activates transcription of several genes.

Adapted from Semenza, G.L., Nat Rev Cancer, 3(10): p. 721-32(2003)[173].

1.5.4. Role of HIF-1 α in cancer

Intra-tumoral hypoxia is a major factor which contributes to cancer progression, however, the exact mechanism by which hypoxic conditions favours progression still remains poorly understood. The interior tumour mass or centre of the tumour mass becomes progressively hypoxic and nutrient deprived as its size increases until adequate vascularisations are achieved by tumours [193]. Analysis of human cancer biopsies and experimental animal models has identified a crucial role of HIFs in cancer progression. The overexpression of HIF-1 α (the major transcription factor activated under hypoxic conditions) has been observed in a broad spectrum of malignancies [173, 194, 195], especially in pancreatic cancer [196]. Nuclear expression of HIF-1 α has been observed in 80% of human pancreatic ductal adenocarcinoma (PDAC) cases. Even stroma adjacent to the pancreatic ductal carcinoma (43% case) showed positive expression of HIF-1 α [197]. It has been reported HIF-1 α plays a complex but important role in the regulating pathway in tumour development such as apoptosis, proliferation, angiogenesis, extracellular modelling, invasion and metastasis [198]. It is speculated that HIF-1 α expression help pancreatic cancer proliferate, invade and metastasise under hypoxic conditions.

HIF-1 α expression has been analysed in 179 tumour samples (pancreatic adenocarcinoma, lung adenocarcinoma, breast adenocarcinoma, colon adenocarcinoma etc.) and identified that HIF-1 α expression increased with progression of cancer from benign, primary malignant to metastases tumour [199]. It has been reported in many studies that accumulation of HIF-1 α in early stages is associated with poor patient survival in many cancers such as breast cancer [200], cervical cancer [201], ovarian cancer [202], endometrial cancer [203], oligodendroglioma [204] and oropharyngeal carcinoma [205]. There is a remarkable frequency of common genetic alterations, namely loss of tumour suppressors or expression of oncogenes, in cancer cells

associated with increased expression of HIF-1 α . Such as loss of VHL [206], wild type p53 [207] and PTEN [208] have been identified in conjunction with increase in the expression of HIF-1 α .

Pancreatic ductal adenocarcinoma is poorly perfused and poorly vascularized. It has been long suspected that pancreatic tumours contain regions of extremely low oxygen conditions. Pancreatic tumour hypoxia has been confirmed by direct intra-tumour oxygen probes in surgery at the time resection in seven patients with pancreatic cancer [209]. *In vitro* and *in vivo* investigations of pancreatic cancer have revealed the activation of HIF-1 α in response to hypoxia [210]. Also dramatic up-regulation of HIF-1 α mRNA expression has been observed in human pancreatic cancer specimens [211]. Other studies also suggested the correlation between HIF-1 α and hypoxic condition in cancer cells [212-214]. Akakura *et al.*, (2001) reported that HIF-1 α mediates an adaptive cellular response in pancreatic cancer which results in the survival and proliferation of pancreatic cancer cells under hypoxic and low glucose conditions [215]. These results emphasize the importance of HIF-1 α in the growth and metastasis of cancer especially pancreatic cancer. Recently, it has been reported that the hypoxic microenvironment in pancreatic ductal adenocarcinoma might promote invasion and metastasis [216]. Currently, gemcitabine is the only approved chemo-drug for pancreatic cancer [217] which shows some survival benefit for patients [53], however, pancreatic cancer is the most intrinsically resistant tumour to almost all chemo-drugs including gemcitabine [218]. It has been identified that a higher expression of HIF-1 α is involved in gemcitabine resistance in pancreatic cancer [219]. It has been suggested in many studies that disruption of the HIF-1 pathway might be effective in the treatment of pancreatic cancer [220, 221]. Recently, it has also been reported that by knockdown HIF-1 α can induce apoptosis in pancreatic cancer cells [222].

1.6. Nuclear factor kappa B (NF- κ B)

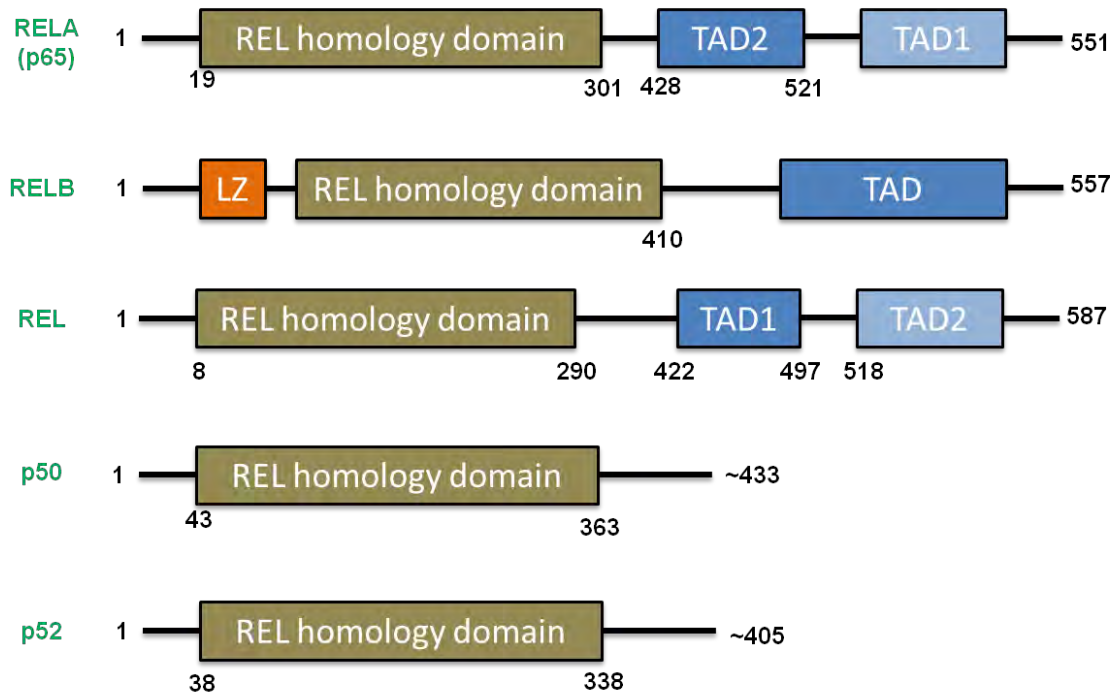
1.6.1. Introduction

NF- κ B was discovered in 1986 as a nuclear factor that binds to the kappa light-chain of activated B cells hence name Nuclear factor kappa B [223] and was thought to be restricted to these cells. However, the functions of nuclear kappa protein widened extraordinarily and at present NF- κ B has been shown to play a key role in the regulation of many cellular responses throughout many tissues particularly in immunity, inflammation and ontogenesis [224, 225]. As NF- κ B plays such a broad role in many cellular responses, dysfunction can lead to severe consequences and diseases. NF- κ B regulates many transcriptional pathways, which are essential to the development and maintenance of the skeleton system [226], immune system [227], epithelium homeostasis and inflammation [228]. The normal function of NF- κ B is to stimulate cell proliferation [229], inhibit apoptosis [230, 231] and promote migratory and invasive cell behaviours which are associated with the progression of cancer [232]. These results suggest that under normal conditions the persistent activation of NF- κ B most likely plays a role in its oncogenic potential. Activation of NF- κ B has been observed in many cancers, such as pancreatic cancer [233-235], breast cancer [236], melanoma [237], lung cancer [238], colon cancer [239], multiple myeloma [240], leukemia [241] and lymphoma [242].

1.6.2. The structure and signalling pathway of NF- κ B

There are five NF- κ B subunit family members in mammals which share a related DNA-binding and dimerization domain known as RHD (REL homology domain). These subunits are RelA/p65 (also known as transcription factor p65), RelB, c-Rel, p50 (NF- κ B1 also known as p105) and p52 (NF- κ B2 also known as p100) as illustrated in Figure 1-11 [225, 243, 244].

NF-κB subunits



Keywords:

REL	v-rel avian reticuloendotheliosis viral oncogene homolog
TAD	Trans activation domain
RHD	REL homology domain
LZ	Leucine zipper

Figure 1-11: Subunits of NF-κB

The mammalian NF-κB (Rel) protein family consists of five subunits RELA, RELB, REL, p50 and p52. All of these subunits share an approximately 300 amino acid long DNA binding and dimerization domain called RHD. RELA (also called as transcription factor p65), RELB and REL (also known as c-Rel) contain transactivation domains (TADs) on C-terminal, which are capable of mediating interactions with transcription factors and cofactors. RELB has a leucine zipper like motif on N-terminal. p50 and p52 are derived from proteolysis of their precursor proteins p105 (also known as NF-κB1) and p100 (also known as NF-κB2) respectively.

Adapted from Perkins, N.D., Nat Rev Cancer, 12(2): p. 121-32 (2012) [225]

NF- κ B binds to target sites (κ B sites) to form dimers (homo or hetero) and can up-regulate or down-regulate the target gene transcription. Crystal structure analysis of the NF- κ B dimer bound to κ B has shown that it is the RHD domain on the N-terminal of NF- κ B which makes contact with DNA and suppresses dimerization. Only RelA/p65, RelB and C-Rel contain C-terminal TAD (transactivation domain) which mediate interaction with cofactors and transcription factors such as TBP (TATA binding protein), p300 (E1A binding protein 300KD) and CBP (CREB binding protein). However, p52 and p50 lack TADs but they positively regulate transcription through interaction with TAD-containing NF- κ B subunits or interact with non-Rel proteins [245]. On the other hand p52 and p50 homodimers negatively regulate transcription through binding to κ B sites by competing with TAD-containing dimers. p52 and p50 are derived from the proteolysis of their precursor proteins p100 and p105 respectively [245].

The NF- κ B signalling pathway can be classified into two types: classical or canonical and non-canonical pathway [245]. The classical pathway represents the pathway through which NF- κ B is generally regulated by activation on binding of ligand to the various receptors. These receptors are such as TNFR (TNF receptor), pattern recognition receptors (PRRs) such as TLR4 (Toll like receptor-4), antigen receptors and IL-1 receptor. In the non-canonical or alternative pathway, activation of NF- κ B needs specific inducers which are members of the TNF cytokine family such as CD40 ligand, lymphotoxin- β and BAFF [246]. The schematic illustration of NF- κ B signalling pathways is illustrated in Figure 1-12 [247]. A hallmark of the NF- κ B pathway is its regulation by inhibitor of NF- κ B (I κ B) protein and I κ B keeps NF- κ B in an inactive state. I κ Bs are the family of inhibitors consist of I κ B α , I κ B β and I κ B ϵ . Activation of NF- κ B is achieved by phosphorylation of I κ Bs, as I κ Bs bind to the NF- κ B complex and keeps it mostly in the cytoplasm form.

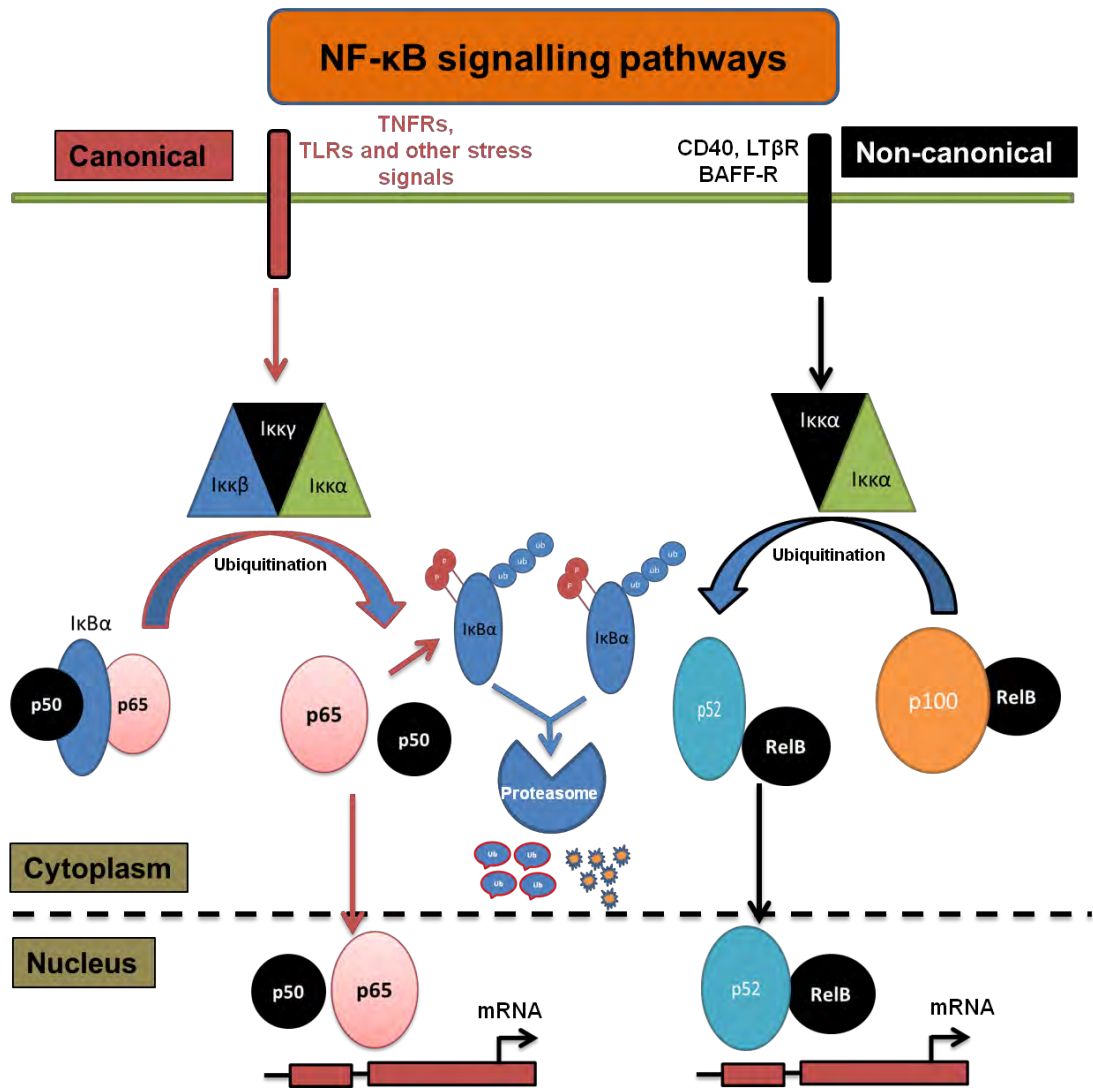


Figure 1-12: NF-κB signalling pathways: Canonical and non-canonical
 The classical (canonical) NF-κB pathway lipopolysaccharides (LPS), tumour necrosis factor α (TNF α) activate toll like receptor (TLRs) and tumour necrosis factor receptor (TNFR). Through a variety of adaptor proteins and signalling kinase this leads to an activation of IκB β in the IκB complex, which can then phosphorylate IκB α followed by poly-ubiquitination and degradation by the 26S proteasome. NF-κB homo or hetero dimer translocate to the nucleus and activate target gene transcription. In non-canonical NF-κB signalling, activation of B-cell activator factor (BAFFR), CD40 or lymphotoxin β -receptor (LT β R), leads to activation of IκB α which phosphorylates p100 for its subsequent poly-ubiquitination and subsequent proteasomal processing to p52. Then this p52-RelB heterodimer translocates to the nucleus and activates target gene transcription.

Adapted from Hoesel, B. and J.A. Schmid, Mol Cancer, 12: p. 86 (2013) [247].

On stimulus the I κ B kinase complex phosphorylates I κ B on conserved serine residues (so called distraction serine residues [DSGXXS]) which promotes their ubiquitination and proteasome-mediated degradation resulting in nuclear localisation of NF- κ B [248]. NF- κ B subunits p100 and p105 contain ankrin repeat motifs in their C-terminal that are also found in I κ Bs. These ankrin repeats mediate interaction between NF- κ B and I κ B so that the presence of ankrin repeats in NF- κ B subunits result in them functioning as I κ B. I κ B α not only localizes in the cytoplasm but also in the nucleus where it binds to the NF- κ B complex and removes it from the promoter region of DNA. I κ B α is the most extensively studied member of the I κ B. It rapidly degrades during the activation of canonical NF- κ B signalling pathway which releases multiple dimers of NF- κ B. Hetero dimer p65:p50 is the primary target of I κ B α and after forming complex of I κ B α :p65:p50 it is constantly shuttled between cytoplasm and nucleus [245].

1.6.3. Diverse and complex role of NF- κ B in cancer

NF- κ B subunits have homology to the viral oncogene *v-Rel*, (avian reticuloendotheliosis) virus. Due to the established association of these oncogenes in the development of cancer, a link has been suggested between NF- κ B and oncogenesis. Consistent with this, structural alteration of subunits of NF- κ B (p52/p100) have been found in certain T-cell lymphomas, chronic lymphocytic leukaemias, myelomas and B-cell lymphomas [249, 250]. Aberrant activation of NF- κ B results in the expression of anti-apoptotic genes enabling cancer cell survival. Induced expression of proto-oncogene and cyclins lead to cell proliferation, while regulation of matrix metalloproteinase and cell adhesion genes promoting metastasis and up-regulation of VEGF, IL-1/6, IL-8 genes promote angiogenesis [251-254]. NF- κ B also induces the expression of glycolytic enzymes and does also help to promote a metabolic switch from oxidation phosphorylation to glycolysis in cancer cells and NF- κ B (RelA subunit) and regulates mitochondrial gene expression which depend upon tumour suppressor p53 [255].

The role of NF- κ B in inflammation has been identified in many cancers [256] and the ability of the IKK-NF- κ B pathway to induce inflammation provides a crucial bridge between chronic inflammation conditions and cancer in mouse models [257]. The response of NF- κ B in a non-disease state is normally self-controlling by induced transcription of inhibitor of NF- κ B (I κ B α and I κ B β) genes which encode a protein that negatively regulates activation of IKK such as TNFAIP3. However, NF- κ B activity becomes deregulated in cancer cells [251, 257, 258]. In many types of solid tumours, leukaemia and lymphomas, aberrant or deregulated activity of NF- κ B has been found [259]. It has been reported that NF- κ B activity can be induced by chemotherapy drugs [251, 254] and its activity potentially regulates survival and malignancy of most, if not all tumours.

1.6.1. Activation of NF- κ B and role in pancreatic cancer

Activation of NF- κ B has been reported in pancreatic cancer, however, it has been found that NF- κ B is not active in normal pancreatic tissues or non-tumorigenic cell lines [260-262]. Fujioka *et al.*, (2003) reported that inhibition of NF- κ B signalling pathways can suppress angiogenesis as well as metastasis in pancreatic cancer, suggesting these signalling pathways may be potential targets for cancer therapy [263]. The mechanism of NF- κ B activation in pancreatic cancer appears to involve various genes such as nuclear glycogen synthase kinase-3 β [264] Vav1 [265] and K-Ras [262]. In pancreatic cancer constitutive activation of PI3K/akt targets and activates transcription factor NF- κ B [266]. Niu *et al.*, (2004) reported that pro-inflammatory cytokine interleukin-1 α (IL-1 α) that induces constitutive NF- κ B activation in metastatic pancreatic cancer cells [267]. In turn NF- κ B can enhance the expression of IL-1 α , which is a positive feedback loop for constitutive NF- κ B activation in pancreatic cancer. IL-1 α additionally enhances the expression of IL-8 and VEGF genes (which are regulated by NF- κ B) in pancreatic cancer cells [268]. These findings suggest the link between inflammation and cancer.

Wang *et al.*, in 2006 reported that down-regulation of notch-1 results in inactivation of NF- κ B as well its target genes such as MMP-9 and VEGF leading to inhibition of invasion and metastasis in pancreatic cancer cells [269]. Since the 1990's gemcitabine is the best known drug available for pancreatic cancer treatment [270] offering very little survival benefit. It has been reported that hypoxia can activate NF- κ B [271] and induce resistance to pancreatic cancer cells against anti-cancer drugs such as gemcitabine through PI3K/Akt/NF κ B pathways [272]. Dihydroartemisinin (DHA) enhances the effect of gemcitabine and induces growth inhibition and apoptosis in pancreatic cancer cells. Thus *in vitro* and *in vivo* studies concluded that DHA significantly increases the apoptosis and decreases the NF- κ B activity and its target gene as well as target gene products which results in significant reduction of pancreatic cancer tumour volume [273]. Kong *et al.*, (2010) identified a synergistic effect of p65 siRNA with gemcitabine on pancreatic cancer cells; finding they inhibit proliferation and induce apoptosis *in vitro* and *in vivo* and suppress cancer growth and angiogenesis in nude mice. p65 siRNA with gemcitabine inhibit NF- κ B activity as well as its target genes Bcl-2, cyclinD1, VEGF and activation of caspase-3 in pancreatic cancer [274].

EMT (Epithelial mesenchymal transition) is the process by which adherent epithelium cell are converted into motile mesenchymal cells [275] and it occurs in the progression of cancer. Hypoxic conditions can trigger the EMT program in many human cancer and results in an increase in the invasiveness of pancreatic cancer [276]. Many studies have been reported that NF- κ B is involved in the progression of EMT [236, 277]. It has been reported that EMT contributes drug resistance in pancreatic cancer [278]. Recently Cheng *et al.* (2011) reported that overexpression of HIF-1 α induces the epithelia to mesenchymal transition (EMT) and is largely dependent on NF- κ B in pancreatic cancer cells [279].

1.7. Aims of study

Recent cancer statistics on the successful treatment and increase in the survival rate of various cancers such as breast cancer and leukaemia are hugely encouraging however, successful outcome for pancreas cancer sufferers remains depressingly low [36]. New targets and more effective therapeutic intervention are required to improve diagnosis and prognosis for all patients with pancreatic cancer. It has been identified that the tumour suppressor gene PDCD4 plays a key role in the birth of new insulin-producing cells in the pancreas, a process that continues throughout the lifetime of an individual [280]. The role of tumour hypoxia has become a major focus in cancer research as it can trigger the invasive and metastatic nature of cancer, a phenomenon noted in pancreatic cancer in particular [281]. PDCD4 has not previously been investigated in pancreas cancer, especially under hypoxic conditions. Utilising a novel model of tissue hypoxia, mimicking the oxygen-deprived core of cancerous tumours which is often resistant to conventional chemotherapeutic drugs and which is likely to lead to secondary tumour formation or metastases, the aims of this study are to:

- Investigate the expression, subcellular localisation and regulation of PDCD4 in human adenocarcinoma pancreatic cell line (PSN-1), mouse β -cell (MIN6) and rat pancreas ductal cell line (ARIP) under normoxic (21% oxygen) and hypoxic (1% oxygen) conditions. Also to investigate expression, subcellular localisation and regulation of HIF-1 α and NF κ B in human adenocarcinoma pancreatic cancer cell line (PSN-1) and rat pancreas ductal cell line (ARIP) under normoxic (21% oxygen) and hypoxic (1% oxygen) conditions.
- Investigate subcellular localisation and expression of PDCD4, HIF-1 α and NF κ B in primary human pancreatic adenocarcinoma tissue and normal mouse pancreatic tissue sections.

It is hoped that a new understanding of how PDCD4 regulates pancreatic cell fate, both in healthy pancreatic cells and in conditions of tissue hypoxia, may well arm us with a new weapon in our fight for more effective therapeutic intervention in the treatment and prevention of pancreatic cancer.

Chapter 2. Material and Methods

2.1. Material

Cell culture materials: RPMI-1640 with L-glutamine, DMEM low glucose with L-glutamine, F-12K with L-glutamine, foetal calf serum (FCS) and trypsin were purchased from PAA laboratory, UK.

Paraffin embedded human (Male and Female) pancreatic cancer tissue sections on slides were provided by Zemskov Centre for Hepato-Pancreato-Biliary Surgery, Kiev, Ukraine.

Protein assay reagents were purchased from Bio-Rad laboratories, UK and Western blotting reagents and nitrocellulose membrane purchased from Amersham, Biosciences UK.

Program Cell Death Gene 4 (PDCD4), Nuclear Factor kappa B (NF- κ B), Glyceraldehyde-3-phosphate dehydrogenase (GAPDH), β -actin, Lamin B1 and α -tubulin were purchased from AbCam, UK. HIF-1 alpha purchased from Novus biology, UK. HRP-conjugated anti rabbit and anti-mouse secondary antibodies were purchased from Sigma, UK. For confocal analysis FITC and TRITC conjugated anti-rabbit and anti-mouse secondary antibodies were purchased from DAKO, UK. DAPI and mounting solution were purchased from Vectashield, UK, Hematoxylin (Sigma, UK), Eosin (Sigma, UK), DPX mount medium (Sigma, UK), Treated glass slides (Fisher Thermo scientific, UK), DAB (3,3'-diaminobenzidine) substrate kit (Vector Laboratories, UK).

Phalloidin, goat serum and all other chemicals and reagents were purchased from Sigma, UK. All other consumables and chemicals were purchased from Fisher scientific, UK unless otherwise stated

2.2. Methods

2.2.1. Cell culture conditions

2.2.1.1. *Cell culture*

All cell lines were grown in T75 tissue culture flasks at 37°C in a humidified atmosphere of 5% CO₂. Cells were passaged when approximately 80% confluent; medium was removed and cells were washed with Phosphate Buffer Saline (PBS, 1 tablet per 100ml of autoclaved distilled water, Sigma, UK). Cells were detached from flask by addition of 1ml 1X trypsin (0.05% W/V trypsin/0.5 EDTA) followed by 5 minutes incubation at 37°C. Once cells were dislodged, trypsin was neutralized by adding 9ml of medium containing 10% FBS. Suspended cells were then centrifuged at 500 g for 5 minutes and medium was removed. Cell pellets were re-suspended in 10ml of medium; cells were counted using a haemocytometer and an appropriate number of cells were seeded for different experiments.

In all analyses; cells were grown to 60% confluence and serum starved overnight in medium without FBS (to synchronise cells to G0) [282, 283]. The following day cells were washed with PBS and stimulated with standard culture medium containing 10% FBS. Cells were grown in different conditions; for hypoxic culture condition cells were grown in hypoxic chamber set at 1% oxygen concentration, 5% CO₂ and 94% nitrogen and for normoxic culture condition cells were grown under 21% of oxygen concentration, 5% CO₂ at 37°C.

2.2.1.2. *Cell lines*

The human adenocarcinoma pancreatic cancer cell line PSN-1 [284] was cultured in RPMI-1640 supplemented with 10% of heat inactivated foetal bovine serum.

The mouse pancreatic β -cell line Min6 [285] was cultured in Dulbecco's Modified Eagle's Medium (DMEM) low glucose supplemented with 10% foetal bovine serum and 100 IU/ml penicillin and streptomycin 100 μ g/ml.

The rat pancreas ductal cell line ARIP was cultured in F-12 medium supplemented with 10% foetal bovine serum and 100 IU/ml penicillin and streptomycin 100 μ g/ml.

2.2.1.3. *Cryo-preservation and Resurrection of cells*

Cells with low passage number were stored in liquid nitrogen for long term storage. To freeze cells; at ~80% confluence cells were detached from flask by addition of 1ml 1X trypsin (0.05% W/V trypsin/0.5 EDTA) followed by 5 minutes incubation at 37°C. Once cells were detached from flask trypsin was neutralized by adding 10ml of medium containing 10% FBS. Suspended cells were then centrifuged at 500 g for 5 minutes. Cells were re-suspended into 10ml of freezing medium (90% RPMI medium (15% FBS) + 10% DMSO for PSN-1 cells) and transferred into cryovials for freezing. Cells were slowly frozen with a decrease in temperature of 1°C per minute. Cells were transferred to liquid nitrogen for long term storage.

Cells were rapidly thawed from liquid nitrogen at 37°C and the cells were re-suspended in fresh medium (as described above) into tissue culture flasks and incubated overnight at 37°C in a humidified atmosphere of 5% CO₂. Freezing medium contains DMSO which is toxic to cells so medium was changed next day to avoid toxicity.

2.2.1.4. *Hypoxic chamber*

The hypoxic chamber was set at 1% oxygen concentration, 5% CO₂ and 94% nitrogen. The outer surfaces of all culture flasks or dishes were cleaned with 70% of ethanol before putting inside the airlock chamber and the nitrogen was purged. Cell culture flasks or dishes were put in or taken out from the hypoxia chamber through the airlock chamber. The hypoxia chamber is shown in Figure 2-1.

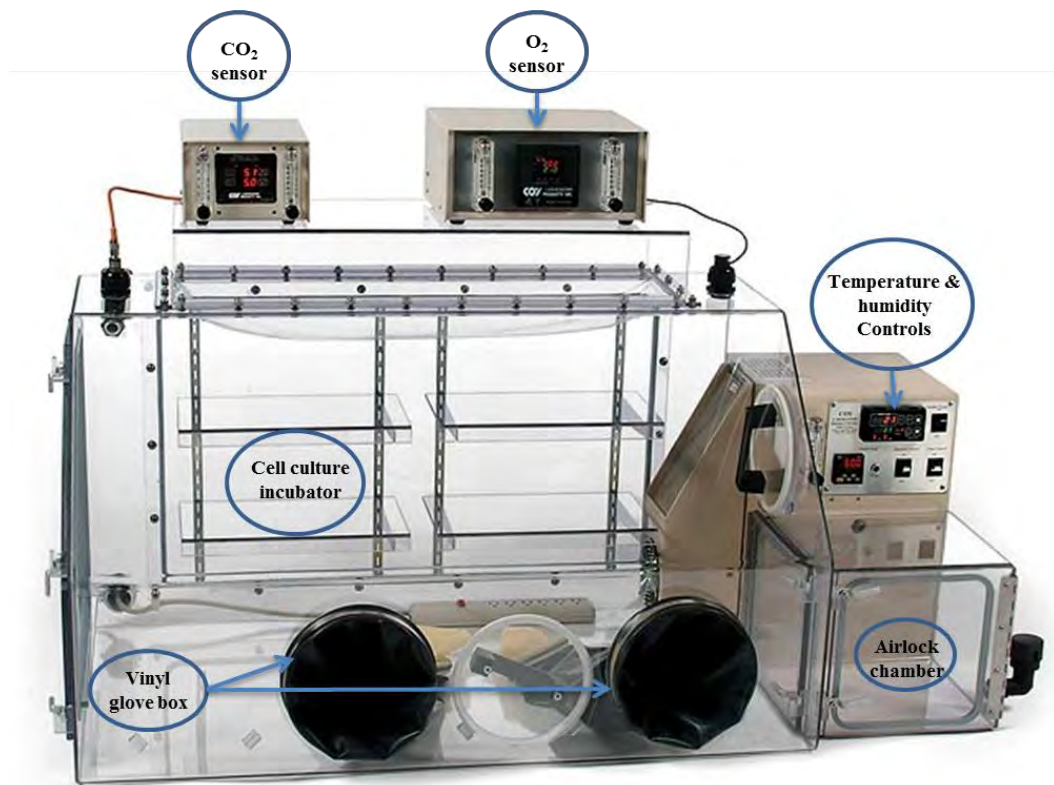


Figure 2-1: Hypoxia glove box from coy laboratories

Hypoxia glove box used in this study has controls for oxygen, carbon dioxide, temperature and humidity options. The hypoxic chamber was set at 1% oxygen, 5% carbon dioxide at 37°C for all experiments.

2.2.1. Cell Viability evaluation

2.2.1.1. *MTT Assay*

The MTT assay is a colorimetric assay developed by Mossman in 1983 to determine cell proliferation and viability [286]. In MTT assay tetrazolium salts, MTT, 3-(4,5-dimethyl-2-thiazol)-2,5-diphenyl-2H-tetrazolium bromide (yellow) is reduced to an insoluble formazan dye crystal product (purple) by mitochondrial dehydrogenase enzymes present only in living cells as showed in Figure 2-2. The purple formazan dye is then dissolved in DMSO and colour change is assessed via spectrophotometry. The rate of MTT reduction is proportional to the cell proliferation and viability.

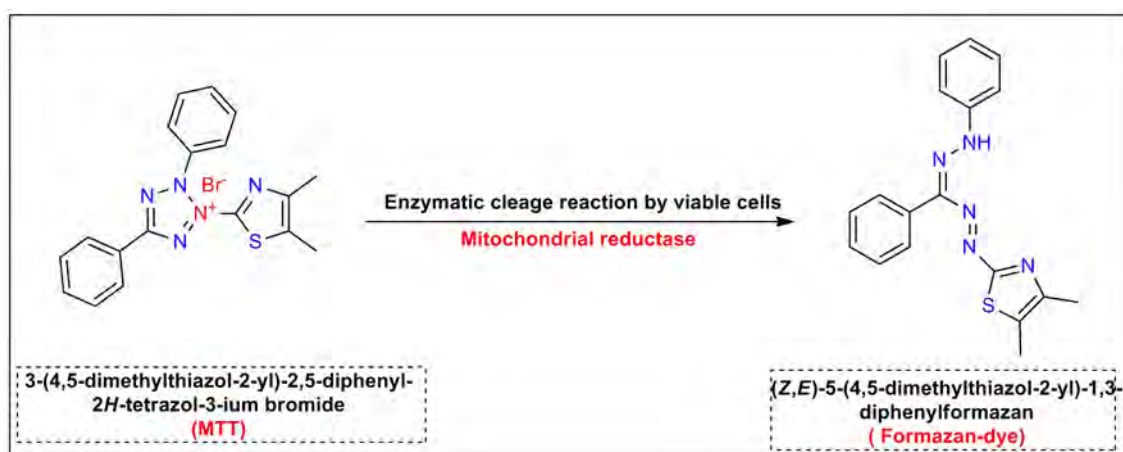


Figure 2-2: MTT reduction by mitochondria reductase in living cells results in the formation of insoluble formazan dye crystal.

To perform MTT assay; cells were cultured in 6-well plates under normoxic and hypoxic conditions as described in section 1.3.1.1. Medium was removed and cells were washed with PBS. Yellow coloured MTT solution (0.5mg/ml in PBS) was added to each well and incubated for 1 hour. MTT solution was aspirated and 1ml of DMSO was added to each well to dissolve the formazan and cells were incubated on an orbital shaker for 5 min. Dissolved formazan solution (200µl) was transferred (triplicate) in to

a 96 well plate and analysed at 540nm wavelength on plate reader. Data was interpreted by measuring absorbance from triplicate samples and then average of absorbance was subtracted from a blank (DMSO was used as blank). Then absorbance on y-axis was plotted versus treatments on X-axis. An absorbance higher than control indicates an increase in cell proliferation and an absorbance lower than control indicates a decrease in cell proliferation.

2.2.1.1. *Hoechst Propidium Iodide (HPI) staining*

HPI staining is a rapid and easy method to find out cell viability based upon fluorescence with visual, colorimetric differentiation of apoptotic, necrotic and viable cells.

Hoechst 333258 belongs to the family of bis-benzimide dyes and on binding to DNA of cell gives blue fluorescence (excitation/emission maxima ~350/461 nm when bound to chromatin). It binds to the minor groove of double stranded AT-rich regions of DNA and can be detected as a blue stain. Hoechst 333258 dye stains the condensed chromatin of apoptotic cells more brightly blue as compared to more relaxed chromatin in normal cells which stains light blue [287, 288].

Propidium iodide (PI) is a large molecule and penetrates only cells without an intact membrane. It binds to the DNA of cells to give red fluorescence (excitation/emission maxima ~535/617 nm when bound to chromatin) therefore necrotic cells are easily identified [289, 290].

HPI staining mixture was prepared by mixing Hoechst (5mg/ml)/ Propidium iodide (1mg/ml) prepared in cell culture medium. Cells were grown in six-well plates and medium was removed. 200µl of HPI staining mixture was added on each well of six well plates and incubated in incubator for 5 minutes under standard conditions. Cells were analysed by fluorescence microscopy (Zeiss, Axiovert 25) using DAPI filter and

images were captured at 10X magnification. Necrotic cells were stained red, bright blue stained the nucleus apoptotic cells and blue for the nucleus of normal cells.

2.2.2. Morphological analysis

2.2.2.1. *Phalloidine staining (Actin staining)*

Sterile cover slips were placed into each well of six well plates and 3×10^5 cells/ml (PSN-1, ARIP and Min6 cells) were seeded. Once cells were 60% confluent; cells were washed with PBS and serum starved overnight. Cells were cultured under normoxic and hypoxic conditions as described in section 2.2.1.1. Cells were fixed with 3.7% of formalin (in PBS) for 30 minutes inside the fume hood at room temperature. Fixative solution was removed and cells were washed three times for 5 minutes with PBS with gentle shaking. Coverslips were transferred onto parafilm and 30 μ l of diluted phalloidin (0.1 μ g/ml in DMSO) in PBS was added on top of cells followed by a layer of another parafilm was placed on top of coverslips. This sandwich of parafilm / coverslip / parafilm was sealed from the sides with tape and incubated for 1 hour at room temperature under dark and humid conditions. After incubation parafilm was carefully removed and coverslips transferred to six well plates containing wash buffer (0.4% Tween 20; 0.7% Glycerol in PBS filtered in 0.45 μ m syringe filter). Cells were washed with wash buffer for 5 minutes three times. Coverslips were mounted on a glass slide and 5 μ l of vectashield mounting medium with 4', 6-diamidino-2-phenylindole (DAPI) added. Cells were incubated for 5 minutes and excess vectashield removed. The edges of coverslips were sealed with nail polish and slides were analysed under confocal microscope. Glass slides were analysed under Leica TCS SP5 confocal microscope and images were taken at X20, X40 and X100. For nuclear staining visualization DAPI settings and for Phalloidin TRITC settings were used. Sequential scans were performed between the two frames: DAPI and TRITC to avoid false signals.

2.2.2.2. *Scanning Electron Microscope (SEM) analysis*

Sterile cover slips were placed into each well of six well plates. Cover slips were washed with sterile distilled water and 3×10^5 cells/ml (PSN-1, ARIP and Min6 cells) were seeded. Once cells were 60% confluent; cells were washed with PBS and serum starved overnight. Cells were cultured under normoxic and hypoxic conditions as described in section 2.2.1.1. Cells were fixed with 2.5% of glutaraldehyde (in 0.1M sodium cacodylate buffer) for 1 hour inside the fume hood at room temperature. Fixative solution was removed and cells were washed three times for 5 minutes with 0.1M sodium cacodylate buffer pH 7.4. The samples were dehydrated by 60 seconds immersion into graded ethanol series (5%, 10%, 20%, 50%, 70%, 90% and 100% v/v). Samples were frozen at -80°C and freeze dried (Christ® Alpha labs) under vacuum (0.42mbar) overnight. For SEM analysis coverslips were mounted on the aluminium stubs with silver conducting paint and let paint to dry for 2 hours. Then stubs were transferred into coater and 4nm thick layer of platinum coating was done using Q150TES Turbo pumped sputter coater (Quorum Technology Ltd, UK). Platinum was used in order to reduce accumulation of charge at the surface which distorts image quality [291]. Samples were examined using Zeiss Sigma field emission gun SEM (Zeiss NTS) at an accelerating voltage (EHT) of 3, 5 and 10 k V. Images were at various magnifications (X1.00K, X5.00K, X10.00K, X20.00K, X30.00K, X50.00K, X70.00K and X100.00K).

2.2.3. **Protein extraction and quantification**

2.2.3.1. *Preparation of whole cell, nuclear and cytoplasmic extract*

Cells were cultured under normoxic and hypoxic conditions as described in section 2.2.1.1. Cells were pelleted and re-suspended in 400 μl of buffer A (10mM HEPES pH

7.9; 10mM KCL; 0.1mM EDTA pH 8; 0.1mM EGTA pH 8; 1mM DTT; 1 x protease inhibitor cocktail,) and incubated on ice for 15 minutes.

For whole cell extracts, 25 μ l of 10% (V/V) triton X-100 was added and samples were incubated on ice for 30 minutes. Then samples were centrifuged for 60 seconds at 13000rpm and the supernatant (the whole cell extract) was removed into a new 1.5ml centrifuge tube. Samples were snap freeze in liquid nitrogen and stored at -20°C.

For nuclear and cytoplasmic extracts; 25 μ l of 10% of NP-40 (v/v) was added and samples were mixed by vortex for 30 seconds followed by centrifugation at 13000rpm for 45 seconds. Supernatant was removed and snap frozen in liquid nitrogen and samples were stored at -20°C. The pellet was re-suspended in 50 μ l of buffer C (20mM HEPES pH 7.9; 400mM NaCl; 1mM EDTA pH 8; 1mM EGTA pH 8; 1mM DTT; 5% glycerol; 1 x protease inhibitor cocktail) and incubated for 1 hour at 4°C with vigorous shaking. After incubation samples were centrifuged at 13000rpm for 30 second. Supernatant was collect into sterile 1.5ml centrifuge tubes and snap frozen in liquid nitrogen; samples were stored at -20°C.

2.2.3.2. **Bradford Assay**

Bradford protein assay (Bio-Rad, UK) was used to estimate the concentration of protein in samples. The dye binds to the protein present in the sample giving a change in colour which is directly proportional to the concentration of protein in the sample. Bio Rad dye contains Coomassie Brilliant Blue G-250 which shows maximum absorbance on 465 nm but on binding with protein it absorbance dye shift to 595 nm [292].

Bio-Rad dye solution mix was prepared by mixing a stock solution of Bio-Rad dye with autoclaved distilled water in ratio of 800 μ l of water and 200 μ l of dye. To calculate protein concentration a standard curve was determined using known concentrations of Bovine Serum Albumin (Sigma, UK) (1mg/ml). To calculate the concentration of

sample 5µl of cell extract was mixed with 1ml of Bradford dye (x1) followed by incubation for 5 minutes at room temperature. Absorbance was determined spectrophotometrically at 595nm.

2.2.4. SDS-PAGE and Western Blotting

2.2.4.1. *SDS-PAGE*

Equal amounts of protein from whole cell extracts, nuclear and cytoplasmic extracts were mixed with 1:1 ratio of SDS sample buffer (20% SDS; 0.1% of bromophenol blue; 1.25M sucrose; 1M Tris-HCl pH 6.8; 10% β-Mercaptoethanol). SDS in sample buffer binds strongly to protein and denatures it; β-Mercaptoethanol reduces any disulphide bridges that are holding the tertiary structure of proteins. All SDS-PAGE, in this study, use a 10% polyacrylamide gel. Protein samples were loaded and separated on stacking gel (30% acrylamide/ Bis- acrylamide Mix, 1M Tris-HCl pH 6.8, 10% SDS, 10% of ammonium per sulphate, TEMED) and resolving gel (30% acrylamide/ Bis- acrylamide Mix, 1.5M Tris-HCl pH 8.8, 10% SDS, 10% of ammonium per sulphate, TEMED) as shown in Table 2-1.

Table 2-1 Reagents used for one gel to make resolving and stacking gel

Reagents	Resolving gel	Stacking gel
Acrylamide/ Bis- acrylamide Mix	30%	30%
Tris-HCl	1.5M (pH 8.8)	1M (6.8)
SDS	10%	10%
Ammonium per sulphate	10%	10%
TEMED	4 µl/gel	5 µl/gel

A full range ECL rainbow molecular weight marker was loaded in the first lane of the gel to assist in identifying the approximate size of the protein. The gel was run for 1 hour at 150V in running buffer (3g/l Tris base; 14.4g/l; 1g/l SDS in distilled water); HIF-1 alpha samples were run for 90 minutes at 150V in SDS running buffer.

2.2.4.1. *Transfer of proteins from PAGE to nitrocellulose membrane*

Proteins were transferred to nitrocellulose membrane using TRANS-BLOT semi-dry blotting apparatus (Bio-Rad, UK). Thick filter papers and a nitrocellulose membrane were soaked in transfer buffer (0.3% Tris-base; 1.44% glycine). Pre-soaked filter paper was placed first onto TRANS-BLOT followed by nitrocellulose membrane; gel and then filter paper on the top again avoiding any air bubbles between each layer of transfer sandwich. Protein transfers were performed for 1 hour at 15V with a current limit of 50mA for one gel transfer (or for 1.5hr if two gels were transferring). Following transfer the nitrocellulose membrane was blocked by incubating the membrane in 10% blocking buffer (10g dried milk without fat in 100ml 1x of wash buffer: 200mM Tris-HCl pH7.6; 29.2g/l NaCl; 500µl Tween 20) for 1 hour on an orbital shaker. Before placing the membrane into appropriate primary antibody, the blot was washed in 1x wash buffer; with two quick washes, followed by three five minutes washes on an orbital shaker at room temperature.

2.2.4.2. *Immunodetection*

For immune detection, all membranes were incubated overnight with primary antibody at 4°C in cold room with rotation and varying concentrations of primary antibodies were used for each protein of interest. Concentrations of primary antibodies used were: PDCD4 (1:1000), NF-κB (p65) (1:1000), HIF-1α (1:1000), GAPDH (1:1000), LAMIN-B1 (1:2000), β-ACTIN (1:1000) and α-TUBULIN (1:1000). The following day the membrane was washed in 1x wash buffer (200mM Tris-HCl pH7.6; 29.2g/l NaCl;

500µl Tween 20), with two quick washes followed by one 15 minute and six 5 minutes washing on orbital shaker at room temperature. Membranes were incubated for 1 hour with rotation at room temperature in HRP linked secondary antibody (1:5000) diluted in 1x wash buffer. Following this, the membrane was washed in 1 x wash buffer; with two quick washes followed by one 15 minute and six five minutes washing on orbital shaker at room temperature. To develop, ECL (Amersham Biosciences, UK) detection mix was used; each membrane was drained of excessive wash buffer on tissue paper and then membrane was placed on plastic membrane. ECL mixture was prepared by mixing 500µl of solution A with 500µl of Solution B just before application on membrane. ECL mixture was applied on membrane for 1 minute and excess of detection mix was drained off. Membrane was wrapped inside saran wrap and placed inside the film cassette followed by exposed to X-ray film (Amersham Biosciences, UK) in dark conditions. The X-ray film was developed using a Konika SRX101A automatic developer.

2.2.4.3. *Densitometry analysis by Image J*

Densitometry analyses were performed by software image J: to normalize the experimental conditions: ratio of densitometry values from experimental blot divided with densitometry values from loading control and then expression was calculated as example as shown in Table 2-2.

Table 2-2: Example of calculations to determine normalized and relative densitometry values from experimental blot.

Experiment blot number (E)	Experimental densitometry values	Loading control values (L)	Normalize $En = E/LC$	Relative expression
E1	100	500	$100/500 = 0.2$	$0.20/0.2$
E2	200	600	$200/600 = 0.33$	$0.33/0.2$
E3	300	800	$300/800 = 0.375$	$0.37/0.2$

2.2.5. Immunocytochemistry

Immunocytochemistry was used to determine the expression and subcellular localisation of protein of interest present inside the cells.

2.2.5.1. *Preparing cover slips, seeding cells and incubation of cells*

Glass cover slips were sterilized by autoclaving and oven dried to remove moisture. In a tissue culture hood, sterile glass cover slips were placed inside each well of a 6-well plate and washed with sterile PBS. Cell suspensions (PSN-1 cells 1×10^5 cells/ml and 4×10^5 cells/ml for Min6) were added to each well and cultured overnight at 37°C in a humidified atmosphere of 5% CO₂; allowing cells to adhere to coverslips.

2.2.5.2. *Cells permeabilisation, fixing and blocking*

Cells grown in six well plates were serum starved overnight and cultured under normoxic and hypoxic conditions as described in section 2.2.1. Cells were washed three times with sterile PBS with gentle shaking on an orbital shaker. To fix cells different fixing solution were used; for PDCD4 chilled (-20°C) methanol: acetone (1:1) was used and cells were incubated at -20°C for 10 minutes; for NFκB 3.7% of formalin (in PBS) was used and cells were incubated for 15 minutes at room temperature. In all cases; following incubation the fixing solution was removed and cells were washed with PBS for 5 minutes with gentle shaking. Cells were permeabilised with 0.1% of triton X-100 in PBS for 10 minutes followed by three times wash in PBS for 5 minutes. To prevent non-specific binding of the antibody, cells were blocked in filtered (0.45 μm syringe filter) blocking buffer (10% Goat serum; 2% BSA; 0.2% Tween 20; 0.7% Glycerol in PBS) for 1 hour with low agitation at room temperature.

2.2.5.3. *Immunostaining*

All primary antibodies were diluted in blocking buffer and different concentrations of primary antibodies were used for different antigens of interest. PDCD4 antibody was used at a concentration of 1:100. NF- κ B and HIF-1 α antibodies were used at a concentration of 1:500. Primary antibody was added on top of cells fixed on cover slip and parafilm lowered on top. The sandwich of parafilm, coverslip and parafilm was sealed from the sides with tape (to stop evaporation of antibodies) and incubated overnight at 4°C. Cells were incubated in blocking buffer for 1 hour. Using the same parafilm method as used for primary antibody application; FITC or TRIC conjugated secondary (1:80) antibody was applied to cells and incubated at room temperature for 1 hour in dark and humid conditions. Parafilm was removed and coverslips placed in six-well plates containing wash buffer. Cells were washed three times for 5 minutes followed by one 30 minute wash in wash buffer on orbital shaker at room temperature.

Coverslips were picked up from six well plates and the back was washed with sterile distilled water (to remove salt from PBS). 5 μ l DAPI was added on to a glass slide and the coverslip carefully lowered onto the DAPI mounting medium at an angle to avoid trapping any air bubble. Cells were incubated for 5 to 10 min and excess vectashield removed. Edges of coverslips were sealed with nail polish and slides were analysed by confocal microscopy.

2.2.6. **Confocal Microscopy**

Cells were analysed by Leica TCS SP5 confocal microscope to find out the expression and sub cellular localisation of various proteins in the cell.

2.2.6.1. *Image Acquisition*

To acquire images from cells by confocal microscopy various parameters were optimized. Cells were visualized under the confocal microscope to find DAPI, FITC

and TRIC staining on cells. The area of interest was selected from samples and images were captured and samples were visualised at different magnifications (20X, 65X and 100X); initially samples were visualised at 20X magnification, and then final images were captured at 65X and 100X magnifications. Specific lasers were selected Diode 405 (DAPI), Argon (FITC), DPSS 561 (TRIC & Alex568) and HeNe 633 (TRIC & Alex568) and set at 25% of laser power. Cells were labelled with two fluorophores (DAPI and FITC) therefore images, were taken into two sequential scans between frames to avoid cross talk (false signal) between two channels. Two sequences were built first for DAPI (UV laser, laser 405 at 20% laser power) and second for FITC (Visible source, laser 488 between 5% to 20% laser power). On the PMT (Photo multiplier tube) detection window the PMT spectra was adjusted by adjusting absorption and emission wavelengths ~350 to ~490nm for DAPI and ~490 to ~525 nm for FITC. Various scanning parameters were selected such as: pixel format 2048×2048, scanning speed 400 Hz, pinhole size 1 AU (airy unit), line average 6 and frame average 8, zoom factor 1. Cells were previewed first on live scan; smart gain and smart offset were adjusted to get low noise and high quality images. After building this method parameters were saved and applied to all experiments. Images were captured and saved as tif (tagged image file) and lif (Leica image file) files.

Leica TCS SP5 confocal microscope software was used to process all images after image acquisition to reduce any background, noise and dye separation (to reduce cross talk) between two fluorophores. Images were exported as tif and lif (Leica image file) files.

2.2.7. Histology

Paraffin embedded tissues were provided by Zemskov Centre for Hepato-Pancreato-Biliary Surgery, Kiev, Ukraine (Table 2-3) and all of histology experiments were

carried in the Institute of Experimental Pathology, Oncology & Radiobiology (IEPOR) in Kiev, Ukraine. This visit was sponsored by FP7 IRSES MEAD-ET project for knowledge transfer visits.

Table 2-3: Human pancreatic cancer tissue sections information

Sample (case) number	Gender	Tissue
1	Female	Pancreatic cancer tissue
2	Female	Pancreatic cancer tissue
3	Male	Pancreatic cancer tissue
4	Male	Pancreatic cancer tissue

Due to unavailability of normal human pancreases as control, healthy mouse pancreases were analysed. Mouse pancreases were provided by Professor Paul R Gard, School of Pharmacy and Biomolecular Sciences, University of Brighton, Brighton, UK.

Mouse pancreas tissue was fixed in 3.7% formalin (in PBS) for 4 hours at room temperature and then stored in PBS at 4°C. The samples were dehydrated by immersion into graded ethanol series as shown in Table 2-4. After dehydration, tissue samples were embedded into paraffin wax and paraffin blocks stored at room temperature.

Table 2-4 Tissue dehydration schedule

Serial number	Time (minutes)	Solution of ethanol (V/V)
1	45	70%
2	45	80%
3	45	90%
4	45	100%
5	60	100%

Paraffin embedded human pancreatic cancer and mouse pancreases blocks were sectioned; paraffin wax from the edges from samples blocks were removed to ensure even cutting and a firm position in the microtome cassette clamp. The blade holder of the rotary microtome (Leica RM 2235, Germany) was cleaned with histoclear (Fisher scientific, UK) before and after sectioning. A fresh blade was set into the microtome and the starting section cutting thickness was set at $10\mu\text{m}$. Paraffin from sample blocks was sectioned until the sample could be clearly seen, then the blade was replaced with a fresh blade and the cutting thickness was changed to $5\mu\text{m}$ and the sections were taken. At every four or five section intervals the sections were transferred to a water bath (40°C), these sections were then transferred to glass slides. The sections on slides were dried in a hot air oven at 60°C for two hour or overnight at room temperature to fix the sections on glass slides prior to staining.

2.2.7.1. *Haematoxylin and eosin staining*

In order to define morphology of tissue sections; haematoxylin and eosin staining was applied to tissue sections which are a combination of acid/base dye. Haematoxylin and eosin staining commonly named as H&E staining where H (haematoxylin) acts as basic dye and exists as cation (+ive charged) whereas E (eosin) acts as an acid dye existing as an anion (-ive charged) [293]. Basic haematoxylin binds to acidic nucleic acids in the nucleus and stains as blue, brown and black whereas acidic eosin binds to basic groups various proteins with in cytoplasm and stains pink to red.

Tissue sections ($5\mu\text{m}$) were mounted on glass slides were incubated for two hours in hot air oven at 60°C to fix sections on glass slides. The samples were deparaffinised by dipping sections into xylene for 10 minutes or twice for 5 minutes. Then sections were rehydrated by serial washing in ethanol (100% for 10 minutes, 90% for 5 minutes, 80% for 5 minutes, 50% for 5 minutes) and rinsed in distilled water for 5 minutes. Sections

were dipped into haematoxylin for 2 minutes followed by careful rinsing under tap water. Further to this sections were dipped (10 times) into 2% of acetic acid followed by 10 dips in tap water. For bluing sections were incubated into bluing solution (1.5% of ammonium hydroxide (30%) in 70% of ethanol) for 1 minute followed by 10 dips in tap water. To decolourise sections were dipped into 90% ethanol for 1 second. Sections were incubated in 1% eosin (% phloxin B, ethanol, acetic acid) for 5 minutes then excess eosin was removed by rinsing in 90% ethanol for 3 minutes. Then sections were dehydrated by incubating in ethanol (90% for 3 minutes, 100% for 3 minutes two times). Then sections were cleared in xylene and stained sections were mounted by adding DPX mounting solution on sections followed by placing coverslips very carefully by avoiding any air bubble. Examination was performed by light microscopy and images were captured at 5X, 10X and 40X magnification.

2.2.7.2. *Immunohistochemistry*

Immunohistochemistry techniques were employed to identify the specific antigen or protein of interest in the tissue samples using specific antibodies. In the present studies, a chromogenic detection method has been used, in which enzyme conjugated (horseradish peroxidase) to the antibody and on addition of substrate (3,3'-diaminobenzidine called as DAB) produce coloured (brown) precipitate at the location of specific protein and analysed by using light microscopy [293].

Tissue sections (5 μ m) were mounted on glass slides and incubated for two hours in the oven at 60°C to fix sections on glass slides. The samples were deparaffinised by dipping sections into xylene for 10 minutes or twice for 5 minutes. Then sections were rehydrated by serial washing in ethanol (100% for 10 minutes, 90% for 5 minutes, 80% for 5 minutes, 50% for 5 minutes) and rinsed in distilled water for 5 minutes. Antigen retrieval was carried out in sodium citrate buffer (10mM sodium citrate, 0.05% tween

20, pH 6.0) heated at 95°C in a water bath for 10 minutes. Following this, samples were cooled to room temperature and rinsed in PBS twice for 5 minutes. In order to detect intracellular antigens, tissue sections were permeabilized with 0.1% of triton X-100 in PBS for 10 minutes followed by 5 minute washes in PBS [294]. To stop non-specific binding of antibodies; samples were blocked with blocking buffer (10% goat serum, 5% BSA, 0.2% tween-20 and 0.7% glycerol in PBS) for 1 hour at room temperature in humidified chamber. Concentration of primary antibody varied depending upon the antibody being used. PDCD4 antibody was used at a concentration of 1:100. NF-κB and HIF-1α antibodies were used at a concentration of 1:200. Various primary antibodies were diluted in blocking buffer and applied on to the samples. Sample with primary antibody were incubated over night at 4°C in humidified chamber.

The following day samples were washed twice in wash buffer (2% BSA, 0.4% tween-20 and 0.7% glycerol in PBS) for 5 minutes each. In order to stop endogenous peroxidase activity samples were incubated in 3% of hydrogen peroxide in PBS for 10 minutes at room temperature followed by washing with PBS for 5 minutes. Samples were incubated for 1 hour in a humidified chamber with specific HRP conjugated secondary antibody (1:80) diluted in blocking buffer.

Detection of antigen/antibody interaction was achieved by in application of DAB substrate for 30 seconds to 1 minute followed by rinsing samples in tap water for 5 minutes.

Stained sections were counterstained with haematoxylin as stated above in section 2.2.7.1. Examination was performed by light microscopy and images were captured at 5X, 10X and 40X magnification.

2.2.8. Data and statistical analysis

All data was analysed using Graphpad Prism 5 software. MTT assay data and western blots densitometry values from three experiments were transformed into percentage control and mean \pm SEM was calculated for error bars. Statistical analyses were carried out using 2way ANOVA test. Significance was detected at p-value of <0.05 (*), <0.01 (**) and <0.001 (***).

Chapter 3. Cell Viability in Hypoxia

3.1. Introduction

Recent figures published by Cancer Research, UK suggest that 8773 people were diagnosed with pancreatic cancer in 2011 and of those, 8320 died of the disease making pancreatic cancer the 5th most common cause of cancer death [295]. Early onset of local invasion and distal metastasis with notoriously late presentation make any chance of a curative treatment virtually impossible, hence pancreatic cancer is one of the most lethal human malignancies [296]. The reasons and mechanisms behind the late presentation and malignancy are not known. However it has been proposed that the microenvironment of extreme hypoxia found inside the solid tumours of the pancreas may contribute [297]. Most mammalian tissues have a tissue oxygen concentration of 2 to 9%, ambient air is 21% oxygen. Hypoxia is usually defined as $\leq 2\%$ oxygen and $\leq 0.2\%$ oxygen is defined as anoxia [172]. Hypoxia is one of the clinical hallmarks of pancreatic cancer and a well-accepted reason for resistance against chemo- and radio-therapy [298, 299]. Therefore it is of great importance to make use of new technologies which allow cells to be studied under conditions of oxygen deprivation, to determine the behaviour of different pancreatic cell types under hypoxic condition. In low oxygenated microenvironment (hypoxia), cell and tissue viability depends upon the activation of several molecular processes that, ultimately decide the fate of cells [300].

The aim of this research was to utilise a hypoxic cell culture chamber to investigate the viability of rat pancreatic ductal (ARIP), human pancreatic adenocarcinoma (PSN-1) and mouse β -cells (MIN6) in normoxic (ambient 21% oxygen) and Hypoxic (1% oxygen) environment.

3.2. Viability assays

In order to determine the viability of PSN-1, ARIP and MIN6, cells were seeded in six well plates and incubated for 24 hours, followed by serum starvation (to reset cells to G0) overnight. The following day cells were stimulated with standard culture medium containing 10% FBS. Cells were cultured in hypoxic (1% oxygen) and normoxic (21% oxygen) oxygen concentrations for 12 or 24 hours. Viability was examined by MTT assay and HPI staining.

3.2.1. MTT assay

Following culture in normoxia and hypoxia (section 2.2.1), cells were incubated with MTT solution: this was reduced to purple insoluble formazan crystals by mitochondrial dehydrogenase enzymes present in the cells. The purple formazan crystals were dissolved in DMSO and absorbance was analysed at 540nm on plate reader (Multiscan plate reader, ThermoScientific®). Average of absorbance values and standard deviation from triplicate samples was calculated. GraphPad Prism 5 (version 5.03) software was used for graph plotting and two-way ANOVA (with Bonferroni posttest) statistical analysis was performed.

3.2.1.1. *Human pancreatic adenocarcinoma cells (PSN-1)*

PSN-1 cell viability was examined by MTT assay under hypoxic and normoxic conditions at 12 and 24 hour time points (doubling time for PSN-1 cell population was determined as 22.00 hours). Figure 3-1 shows that a low oxygen concentration did not have any effect on the viability of PSN-1 cells at either time point examined. No significant growth difference between hypoxic and normoxic conditions was observed at the 12 or 24 hour time points ($p > 0.05$).

3.2.1.2. *Pancreatic ductal cells (ARIP)*

ARIP cell viability was examined by MTT assay under hypoxic and normoxic conditions at 12 or 24 hour time points (doubling time for ARIP cell population was determined as 16.00 hours). Figure 3-2 shows that a low oxygen concentration did not have any effect on the viability of ARIP cells at any time point examined. No significant growth difference between hypoxic and normoxic conditions was observed at the 12 or 24 hour time points ($p>0.05$).

3.2.1.3. *β -cells (MIN6)*

MIN6 cells viability was negatively affected by hypoxia (time for MIN6 cell population was determined as 26.47 hours). Results indicated that a low oxygen concentration had a detrimental effect on the viability of MIN6 cells at both the 12 and 24 hour time point (Figure 3-3). Cell viability significantly decreased by approximately 50% at 12 hours and 70% at 24 hours compared to normoxic conditions. Cells under normoxic conditions continued to grow while the viability of cells in hypoxic condition was significantly reduced. Significant growth difference was observed between hypoxic and normoxic conditions at 12 hour ($p<0.001$) as well as 24 hour ($p<0.001$) time points.

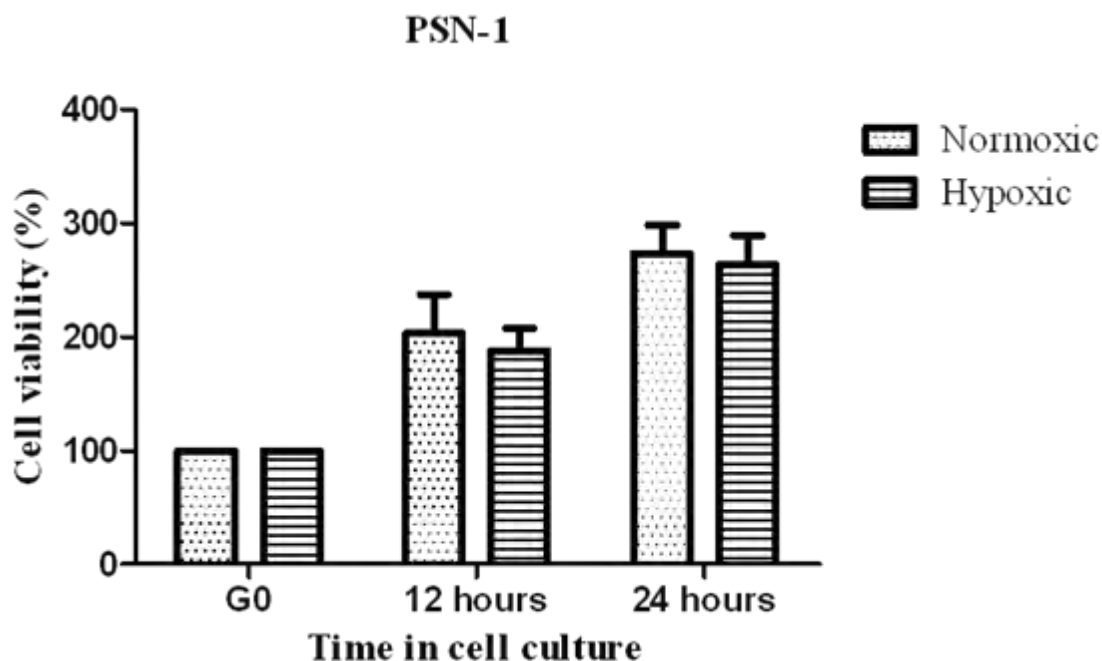


Figure 3-1: Viability of PSN-1 cells synchronised and grown in normoxic and hypoxic culture conditions by MTT assay

PSN-1 cells were seeded at 2×10^5 cells in each well of 6-well plate and serum starved overnight followed by addition of whole medium containing 10% FBS. MTT assay was performed ($n=3$, \pm SEM) after 12 or 24 hours. Results shown are representative of three separate experiments, error bar values represent mean \pm standard error. No significant growth difference between hypoxic and normoxic conditions at 12 or 24 hour time points ($p > 0.05$).

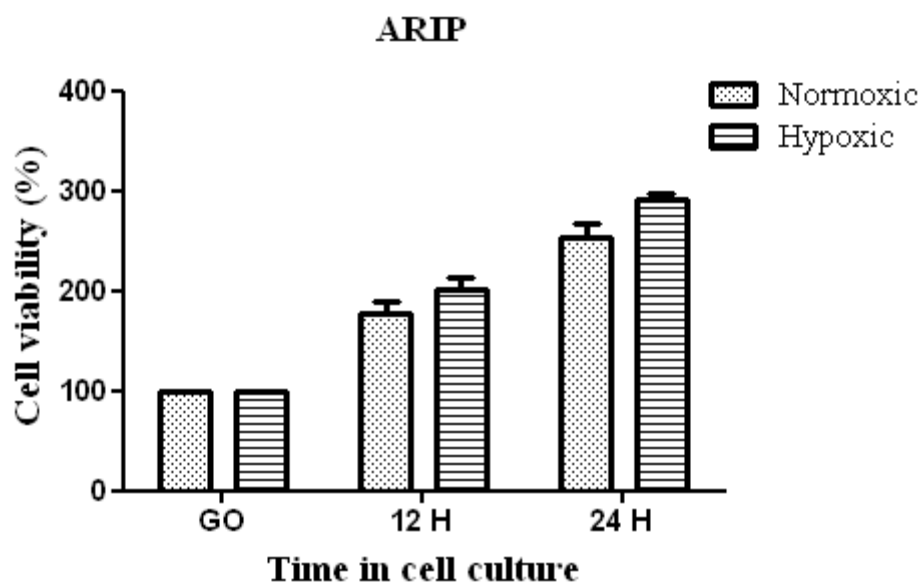


Figure 3-2: Viability of ARIP cells synchronised and grown in normoxic and hypoxic culture conditions by MTT assay

ARIP cell were seeded at 2×10^5 cells in each well of 6-well plate and serum starved overnight followed by addition of whole medium containing 10% FBS. MTT assay was performed (n=3, \pm SEM) after 12 or 24 hours. Results shown are representative of three separate experiments, error bar values represent mean \pm standard error. No significant growth difference between hypoxic and normoxic conditions at 12 or 24 hour time points ($p > 0.05$).

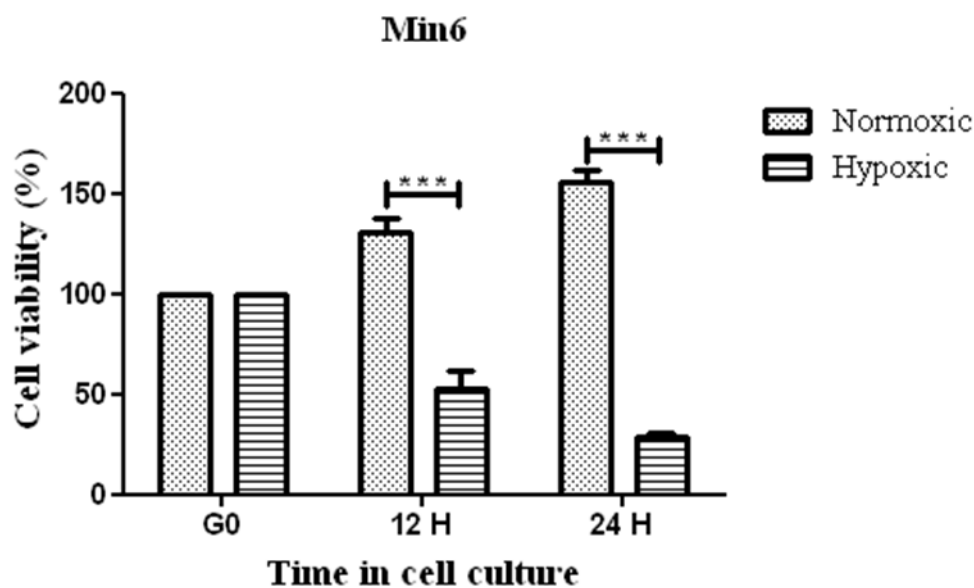


Figure 3-3: Viability of MIN6 cells synchronised and grown in normoxic and hypoxic culture conditions by MTT assay.

MIN6 cell were seeded at 2×10^5 cells in each well of 6-well plate and serum starved overnight followed by addition of whole medium containing 10% FBS. MTT assay was performed (n=3, \pm SEM) after 12 or 24 hours. Results shown are representative of three separate experiments, error bar values represent mean \pm standard error. Significant growth difference between hypoxic and normoxic conditions at 12 hour (***) p<0.001) as well as 24 hour (***) p<0.001) time points.

3.2.2. Hoechst Propidium Iodide (HPI) Staining

In order to assess cell viability by a different method and determine if any cells were dying by apoptosis or necrosis, HPI staining was performed. A solution of Hoechst/propidium iodide was prepared in cell culture medium and HPI staining was performed after the treatments explained in section 2.2.1.1. Cells were analysed by fluorescence microscopy (Zeiss Axiovert 25, Sweden) using DAPI filter: dead cells were stained red, bright blue stained nucleus indicated apoptotic cells and blue nucleus indicated cells normal cells.

3.2.2.1. *Human pancreatic adenocarcinoma cells (PSN-1)*

PSN-1 cell viability was examined by HPI staining under hypoxic and normoxic conditions at the 12 or 24 hour time points (Figure 3-4). These results indicate that, low oxygen concentration did not have any effect on the viability of PSN-1 cells at any of the time points examined. PSN-1 cells grew normally under normoxic or hypoxic condition at the 12 or 24 hour time points.

3.2.2.2. *Pancreatic ductal cells (ARIP)*

ARIP cell viability results (Figure 3-5) indicate that, hypoxia had some effect on the viability of ARIP cell at 24 hour time points; indicated by a substantial amount of apoptotic cells with bright blue nucleus. However, ARIP cell grew normally in normoxic condition (at the 12 or 24 hours) and at the hypoxic 12 hour time point.

3.2.2.3. *β -cells (MIN6)*

MIN6 cell viability was highly affected by hypoxia. Results indicate that hypoxia had a detrimental effect on the viability of MIN6 cells at 12 or 24 hour time points; indicated by substantial amount of apoptotic cells with bright blue nucleus and necrotic cells with

red nucleus. However, MIN6 cells grew normally in a normoxic condition at the 12 or 24 hour time points as shown in Figure 3-6.

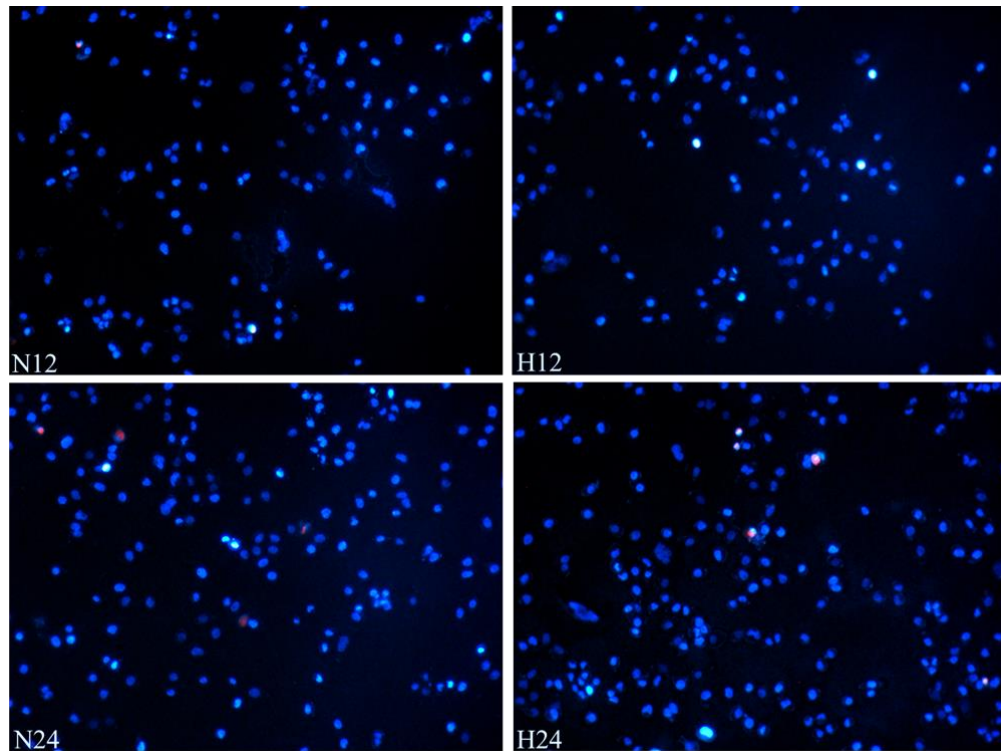


Figure 3-4: Viability of PSN-1 cells synchronised and grown in normoxic and hypoxic culture conditions by HPI staining

PSN-1 cell were seeded at 2×10^5 cells/ml in each well of 6-well plate and serum starved overnight followed by addition of whole medium containing 10% FBS. HPI staining was performed (n=3) at 12 or 24 hours. Cells were visualized by fluorescence microscopy. Images were captured at 10X magnification and results are representative of three separate experiments. Images were representative of six separate fields. All cells were viable at the 12 or 24 hour time points. Hypoxic conditions do not have any effect on viability of PSN-1 cells was observed.

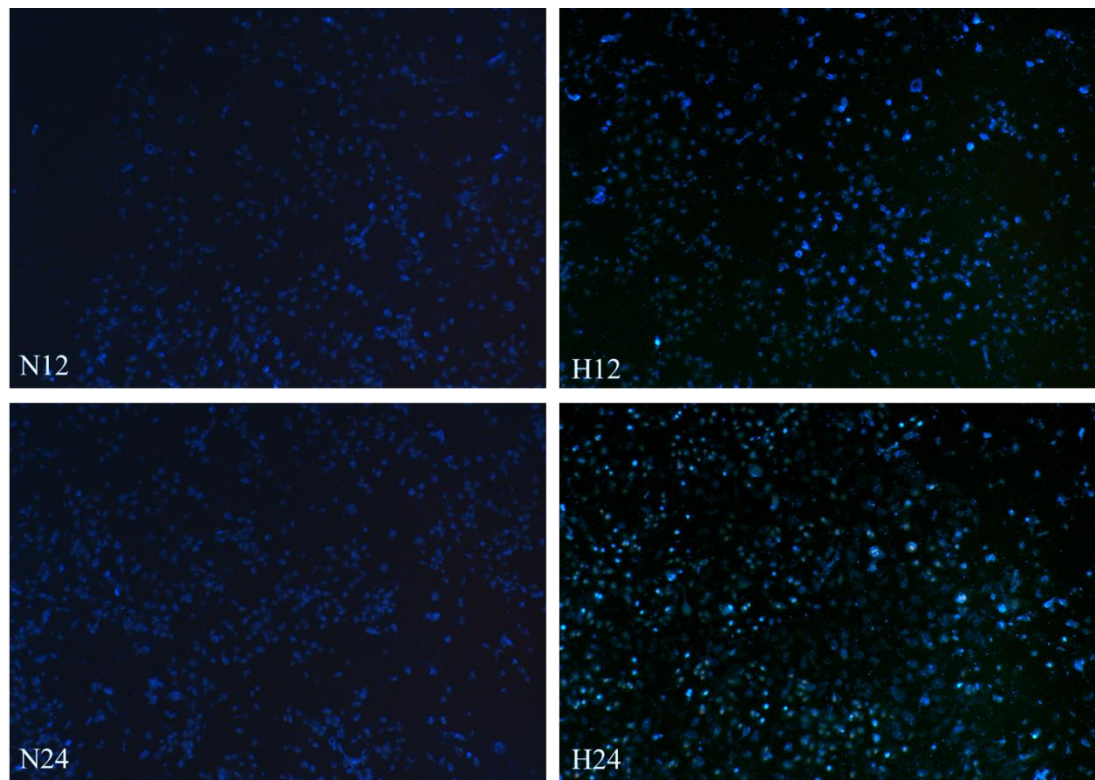


Figure 3-5: Viability of ARIP cells synchronised and grown in normoxic and hypoxic culture conditions by HPI staining

ARIP cell were seeded at 2×10^5 cells/ml in each well of 6-well plate and serum starved overnight followed by addition of whole medium containing 10% FBS. HPI staining was performed (n=3) at 12 or 24 hours. Cells were visualized by fluorescence microscopy. Images were captured at 10X magnification and results are representative of three separate experiments. Images were representative of six separate fields. Cells in normoxic conditions at 12 and 24 hour stained light blue, which means cells are viable. Cells in hypoxic conditions at 12 hour stained light blue however, at H24 cells with bright blue nucleus were observed indicating apoptosis triggered by hypoxia. No signs of necrosis were observed in any of the samples.

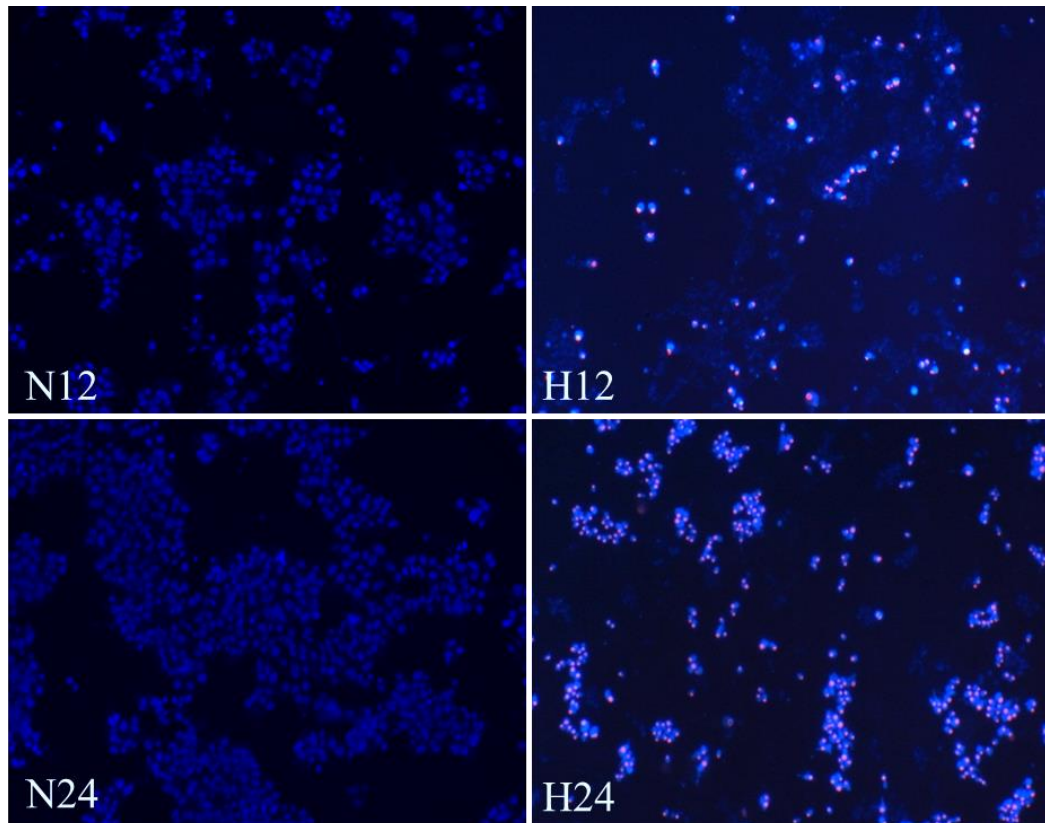


Figure 3-6: Viability of MIN6 cells synchronised and grown in normoxic and hypoxic culture conditions by HPI staining

MIN6 cell were seeded at 2×10^5 cells/ml in each well of 6-well plate and serum starved overnight followed by addition of whole medium containing 10% FBS. HPI staining was performed (n=3) at 12 or 24 hours. Cells were visualized by fluorescence microscopy. Images were captured at 10X magnification and results are representative of three separate experiments. Images were representative of six separate fields. Cells in normoxic conditions at 12 and 24 hour stained light blue, which means cells are viable. Cells in hypoxic conditions at 12 or 24 hours stained light blue indicating apoptosis and red coloured nucleus indicating necrosis. Hypoxic conditions trigger apoptosis and necrosis in MIN6 cell.

3.3. Discussion

Cell division and cell death are essential parts of the normal development and maturation cycle of mammalian cells [301]. Maintaining the balance between cell division and cell death is critical for the normal physiological process and an abnormal balance between these two can lead to diseases such as cancer and diabetes mellitus. Whereas uncontrolled cell proliferation and escape from cell death lead to cancer [302], low cell mass and high death of beta cells lead to diabetes mellitus [303].

The initial aim of this study was to investigate growth and viability of human pancreatic adenocarcinoma (PSN-1), rat pancreatic ductal (ARIP) and mouse β -cells (MIN6) in low oxygen as a clinically reflective model of the pancreatic tumour microenvironment. Firstly we investigated the growth of cells by the use of MTT assay to detect mitochondrial activity in normoxic and hypoxic conditions at 12 or 24 hours. Hypoxia did not have any effect on the growth of PSN-1 cells and there was no significant growth difference between cells grown in normoxic conditions compared to hypoxic conditions (Figure 3-1). The same pattern of growth was found on studying ARIP cells. There was no significant growth difference between cells grown in normoxic conditions compared to hypoxic conditions as shown in Figure 3-2. However, in the case of MIN6 cells, there was a significant reduction in cell growth under hypoxic conditions. Specifically there was a nearly 50% growth reduction within the first 12 hours of growth under hypoxic conditions and after 24 hours a 70% growth reduction was observed in MIN6 cells. Statistical analysis showed that there was a significant growth difference ($p < 0.001$) between the MIN6 cells grown in normoxic conditions compared to hypoxic conditions as shown in Figure 3-3. These results indicated that hypoxic conditions did not have any effect on growth of PSN-1 and ARIP cells. However, hypoxic conditions particularly at 24 hours had a catastrophic effect on the viability of MIN6 cells.

In order to confirm the findings from the MTT assay and to identify whether cells were undergoing apoptosis or necrosis under hypoxic conditions, a Hoescht propidium iodide (HPI) stain was performed. HPI staining of PSN-1 further confirmed the stable viability of PSN-1 cells under hypoxic conditions, as shown in Figure 3-4. PSN-1 cells were viable stained light blue under normoxic and hypoxic conditions at 12 or 24 hours. HPI staining of ARIP cells indicated that under normoxic conditions cells were viable, however, under hypoxic conditions at 24 hours cells with bright blue nuclei (apoptotic) were observed as shown in Figure 3-5. MTT results for ARIP cells indicated that there was no effect of hypoxia on growth of ARIP cells, whereas HPI indicated that hypoxia triggered apoptosis at H24. The MTT assay measures the reduction in metabolic activity; live cells can reduce MTT to purple formazan in the mitochondria however, dead cells cannot metabolize MTT. One potential explanation for the differing results by MTT and HPI might be that cells were in the early phase of apoptosis. The early phase of apoptosis does not affect membrane permeability, nor do they result in any alteration in the activity of mitochondria. Therefore the MTT assay might be more effective for detecting the later stages of apoptosis [304, 305]. The MTT assay may therefore underestimate the levels of apoptosis if this process is at an early stage. HPI staining of MIN6 cells indicated that the hypoxic conditions triggered both apoptosis and necrosis which leading to beta cell death (as shown in Figure 3-6).

It has been reported in many studies that cancer cells under hypoxia develop an efficient adaptive metabolic response to ensure their survival and proliferation [171, 306, 307]. Indeed hypoxic cancer cells activate glucose uptake and glycolysis to produce pyruvate which then converted into lactate instead of being oxidised via the tricarboxylic acid (TCA) cycle and oxidative phosphorylation as in normal cells under normoxic conditions. Cancer cell not only use glucose as energy source but also use glutamine as an energy source to survive under hypoxia [306, 308, 309]. This might be the reason

that PSN-1 cells adapt and proliferate under hypoxic conditions. It might be that PSN-1 cells have the option to switch between glucose and glutamine dependent anaerobic metabolic pathways, allowing PSN-1 cells to survive and proliferate under hypoxic conditions. It has been reported that pancreatic cancer cell lines even under normoxic conditions use glycolytic metabolic pathway and also able to metabolise glutamine [310]. However, hypoxia alter progression of normal cells division cycle especially G1/S phase [311]. However, Min6 and ARIP cells unable to cope with low oxygen condition, which may trigger the cycle arrest and ultimately cells under goes apoptosis and necrosis. Pancreatic beta cells secrete insulin in response to blood glucose for systemic metabolism. In order to secrete insulin beta cells require a large amount of oxygen to produce ATP [216]. This might be another reason that Min6 cells need more oxygen compared to normal pancreatic ductal (ARIP) cells, which triggered early (12 hour) apoptosis and necrosis in Min6 beta compared to ARIP cells.

The onset of both cancer and diabetes mellitus are complex, multistep processes however, microenvironment plays a critical role in both. A hypoxic microenvironment triggers the growth of cells in many cancers [312] and additionally has been shown to damage pancreatic beta cells in diabetes mellitus [313]. This study revealed that hypoxia has detrimental effects on MIN6 growth and viability. These results may have great relevance to the processes experienced by β -cells during the islet transplantation [314, 315]. Islet transplantation has the potential to cure type 1 diabetes and currently is the only treatment for type 1 diabetes which offers the patient the possibility of total insulin independence [316]. A normal pancreas consists of nearly 1 million islets [317] and with good isolation procedure 500,000 islets can be purified. However, many of these die even before transplantation [318] and nearly 30 to 70% transplanted islets die within few days [319]. Hypoxia is an inevitable result of the devascularisation which occurs during islet isolation and purification; the subsequent transplantation into an

environment without an oxygen supply ultimately results in a negative impact on beta-cell survival [320]. It is believed that after islet transplantation, revascularization of pancreatic islets may take several days [321] and beta cells experience hypoxia which may be detrimental effect to the beta cell function [320, 322, 323]. Revascularization and supply of sufficient oxygen to pancreatic islets can provide protection against hypoxia and ultimately can increase beta cell survival [323]. Our beta cell viability results support this need to maintain oxygen supply for beta cell survival which could have a positive impact on islet transplantation.

The MTT assay and HPI staining were performed to determine the viability of pancreatic cell lines however, in future work to study cell proliferation, cell cycle, detection of apoptosis, mitochondrial activity other methods and measurements could be employed such as DNA laddering (apoptosis DNA fragmentation), BrdU (cell proliferation and apoptotic cells), Ki67 (cell proliferation), Caspase 3 (apoptosis), cytochrome C oxidase (progress of apoptosis and apoptosis inducer).

From this study it can be concluded that, human pancreatic adenocarcinoma cells (PSN-1) are able to adapt to hypoxic conditions. Hypoxia did trigger apoptosis but not necrosis in ARIP cells, however, beta-cells (MIN6) do not survive under hypoxic conditions and hypoxia triggered both necrosis and apoptosis. Therefore it could be said that pancreatic ductal cells were able to adapt to hypoxic conditions more effectively than pancreatic beta-cells (MIN6).

Having determined the effect of hypoxia on pancreatic cell viability it was next important to investigate the change in morphology of all three cell types under hypoxic conditions and examine morphology of human pancreatic adenocarcinoma tissue samples.

Chapter 4. Cells morphology

4.1. Introduction

In order to maintain shape, cells undergo highly regulated biological processes controlled by interactions between the cytoskeleton, the membrane and various membrane-bound proteins which interact with the extracellular environment [324-326]. Morphology of cells can be used as an important measure for the cellular organization and the physiological state of the cells; be it differentiation, apoptosis, malignancy or lymphocyte activation. Indeed morphology of cells is a major factor used to determine the function of different cells and tissue types, thus it can be commonly used as a qualitative and quantitative measure using certain assay [327]. Microscopy techniques provide vital information on morphological characteristics of cancer cells. Cancerous cells differ from normal cells by morphologically characteristics such as: large size nucleus, high nucleus/cytoplasm ratio (low cytoplasmic amount), irregular size and shape of nucleus, prominent nucleolus, irregular shape and size of cells (Table 4-1) [328, 329].

Table 4-1: Morphological characteristics of normal and cancer cells.

Normal cell	Cancer cell
Large amount of cytoplasm compared to nuclear size	Large size of the nucleus compared to cell size
Smooth nuclear border	Irregular nuclear boarder and often multinucleated
Clear nuclear stain and fine chromatin granules in the nucleus	Dark staining of nucleus and larger size of chromatin clumps in the nucleus
Small nucleolus	Large nucleolus
Regular size and shape of cell	Variable pleomorphism in size and shape of cell

Scanning electron microscopy has become a vital tool to investigate surface features of cells, cell to cell interactions and cell organisation. SEM gives three dimensional (because of the secondary electron detection mode) information about on the cell surface and results are far easier to interpret compared with transmission electron microscopy (TEM)[330]. The cell creates several types of surface or plasma membrane protrusions such as microvilli, filopodia, lamellipodia and surface ruffles. These surface protrusive structures can be analysed under SEM [331]. Finger like protrusion structures on the plasma membrane can be filopodia (small size) and lamellipodia (large size). Filopodia and lamellipodia play important roles in cell to cell contact, adhesion, migration and angiogenesis [332]. Cell migration is one of the hallmark processes in cancer metastasis and angiogenesis. Increased filopodia formation has been associated with cancer cell migration [333] and invasion [334]. Spike extensions from plasma membrane are one of the major characteristics of cancer; however normal cells have a smooth membrane. These spike extension help cancer cells to invade surrounding tissue and undergoes metastasis in the process of EMT (Epithelial-mesenchymal transition). EMT is characterised by major changes in cell shape, formation of spindle like structures and irregular membrane borders [335].

Diagnostic imaging helps to distinguish between different types of neoplastic and non-neoplastic lesions. In order to give accurate treatment for any disease, it is vital that it should be accurately diagnosed, especially in the treatment of cancer. Pathology reports play a vital role in defining the type of tumour/cancer and staging/grade (nature of cancer, whether it is localised or metastasised and how abnormal cells looks under the microscope). The main reason for the low survival rate in pancreatic cancer is because of its notoriously late presentation, rarely shown symptoms in early stages until a late stage, highly aggressive metastatic potential and very poor outcome [22, 23]. By the

time symptoms appear it is often already too late, so early diagnosis is the key to fighting this deadly cancer.

The normal healthy pancreas is divided into lobules and these lobules are held together by connective tissue. The large lobules are divided into smaller lobules by intra-lobular connective tissue. Large blood vessels and nerve bundles runs through the septa of connective tissues [18]. Within each lobule numerous acini are arranged in a ring-like structure and connected with other acini through intercalated ducts. Small ducts collect digestive juices inside the lobules (intra-lobular) and outside the lobules (inter-lobular ducts). The islets of Langerhans (IL) are scattered throughout the pancreas [18, 19, 336].

Pancreatic cancer is classified according to the cell type or origin, structure and behaviour. It is divided into exocrine and endocrine cancer, but the majority of pancreatic cancers are adenocarcinomas and originate in ductal epithelial cells lining small gland like structures [70, 337, 338]. The purpose of this study was to identify histopathology of human pancreatic cancer tissue biopsies from four patients diagnosed with pancreatic cancer was studied.

In the present study we investigated morphological characteristics of three well-established cell lines (rat pancreatic ductal, human pancreatic adenocarcinoma and mouse β -cells line) cultured in hypoxic (1% oxygen) and normoxic (21% oxygen) conditions. In order to determine the morphology of normal pancreas, sections from mouse pancreas were analysed. In order to determine the histology stage of human tumour sections from human pancreatic cancer tissue (four case studies) sections were analysed. Various microscopy techniques were used such as light, confocal and scanning electron microscopy to define the morphological characteristics.

4.2. Morphology of cell lines

Most human cancer studies are largely dependent upon *ex vivo* cultured cell lines. In the present study we examined three pancreatic cell lines: rat pancreatic ductal (ARIP), human pancreatic adenocarcinoma (PSN-1) and mouse β -cells (MIN6) cultured in hypoxic (1% oxygen) and normoxic (21% oxygen) conditions. Morphological criteria of malignancy are defined by deviation from normal tissue architecture, poor demarcation, high nuclear cytoplasmic ratio, high rate of mitosis and pleomorphism [339].

In order to determine the morphology of PSN-1, ARIP and MIN6 cells, cells were seeded in six well plates on glass coverslips and incubated for 24 hours, followed by serum starvation (G0) overnight to synchronise cell populations. The following day cells were stimulated with standard culture medium containing 10% FBS. Cells were cultured in hypoxic (1% oxygen) and normoxic (21% oxygen) conditions for 12 or 24 hours. Cell morphology was analysed by an actin cytoskeleton study and scanning electron microscopy (SEM) observation.

4.2.1. Cytoskeleton analysis (Actin staining)

After various treatments cells were fixed with 3.7% formalin at 12 or 24 hour. Cells were incubated with phalloidin for 1 hour to stain actin filaments within the cells. Glass coverslips with stained cells were mounted on glass slides with DAPI which stained the nuclei of cells. Cells were analysed by confocal microscopy and images were captured at 20X and 65X magnifications.

4.2.1.1. *Human pancreatic adenocarcinoma cells (PSN-1)*

PSN-1 cell morphology was investigated by confocal microscopy using TRITC-labelled phalloidin toxin (Figure 4-1). The overall morphology at G0 was altered, as was an irregular shape of cells as well the nuclei, nuclear to cytoplasmic ratio was high (size of

nuclei were bigger compared to cytoplasm). Under normoxic conditions at 12 or 24 hours multinucleated (cell contains more than one) cells were observed with an irregular shape and size of nuclei. Under hypoxic conditions at 12 or 24 hours nuclei of the cells were not localized in the centre of the cells, also arc shaped nuclei were observed. The shape of the cells and growth pattern was irregular observed at H12 and H24 but the same as normoxic as shown in Figure 4-1.

4.2.1.2. *Pancreatic ductal cells (ARIP)*

ARIP cells morphology was investigated by confocal microscopy using TRIC-labelled phalloidin toxin (Figure 4-2). These results indicated that at G0, N12, N24 and H12 regular shape of cells with regular shaped nuclei was observed. Also the nuclei were localised in the centre of the cells and normal cytoplasm to nuclei ratio was observed. However, under hypoxic conditions at 24 hours a non-uniform cells pattern, irregular shape and size of cells was observed compared to cells under normoxic conditions as shown in Figure 4-2.

4.2.1.3. *β -cells (MIN6)*

Islet β cells grow in clusters, connected with each other via gap junctions. Cell to cell contact among β cells in islets is very important to coordinating the integrated secretory response of the whole islet [340]. MIN6 beta cell morphology was investigated by confocal microscopy using TRIC-labelled phalloidin toxin. These results are displayed in Figure 4-3. These results indicated that, under all conditions beta cells were growing in groups and cytoplasm to nuclei ratio was normal. Regular shape and size of cells as well as nuclei were observed at G0, N12 and N24. However, there was irregular shaped cell surface was observed at H12. Small sized beta cells were observed at H24 compared to the cells under normoxic conditions.

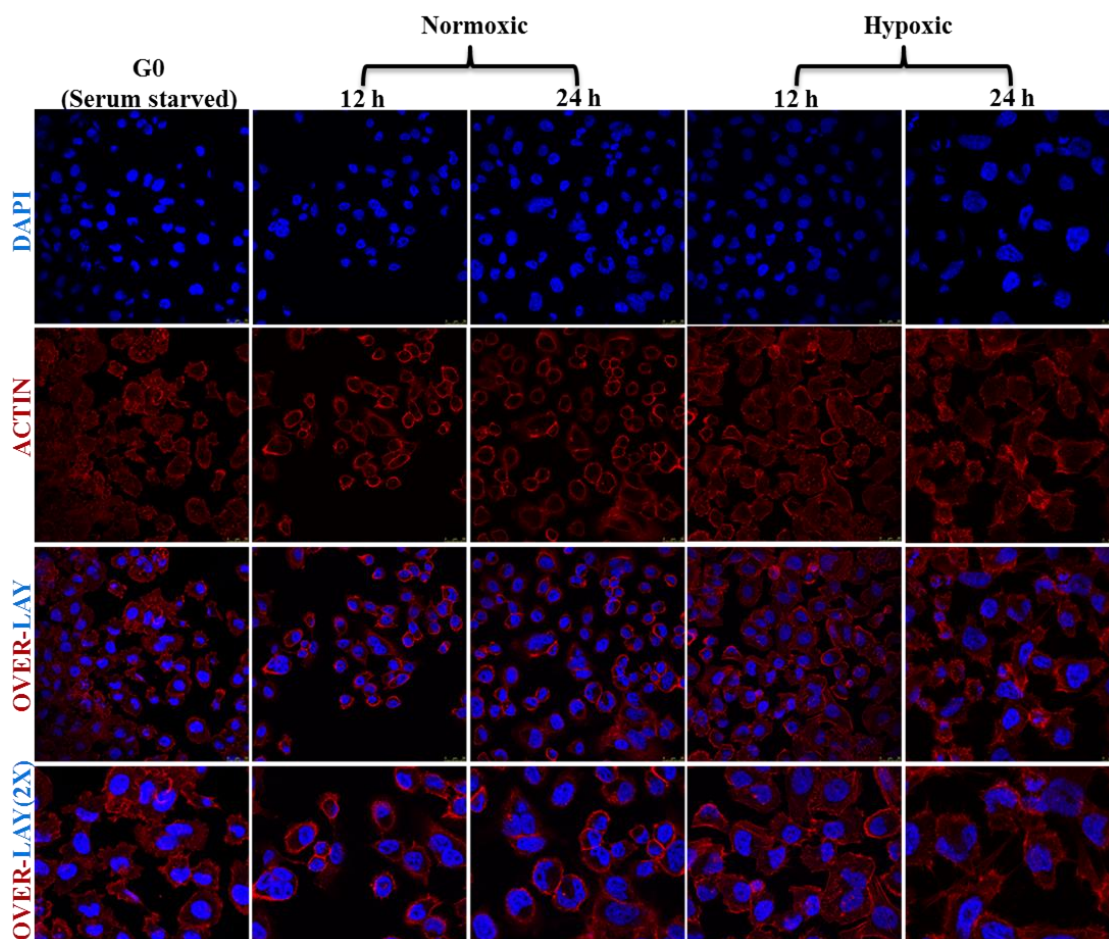


Figure 4-1: Morphology of PSN-1 cells under hypoxic and normoxic conditions.

PSN-1 cells were seeded at 2×10^5 cells in each well of 6-well plate on glass coverslips and serum starved overnight followed by addition of whole medium containing 10% FBS; cells were fixed with 3.7% of formalin at 12 or 24 hours and phalloidin staining was performed to stain actin filaments of cells. Cells were visualized by confocal microscopy and images were captured at 40X magnification. Results are representative of three separate experiments. Images were representative of six separate fields. These results indicate that at G0 there was irregular shape of cells as well nucleus and the nucleus to cytoplasmic ratio was high. Under normoxic conditions (N12 & N24) cells containing more than one nucleus with variable shape and size of nuclei was observed. Under hypoxic conditions (H12 & H24) irregular shape and size of the cells and nucleus was observed. Also the nucleus was not localized in the centre of the cells.

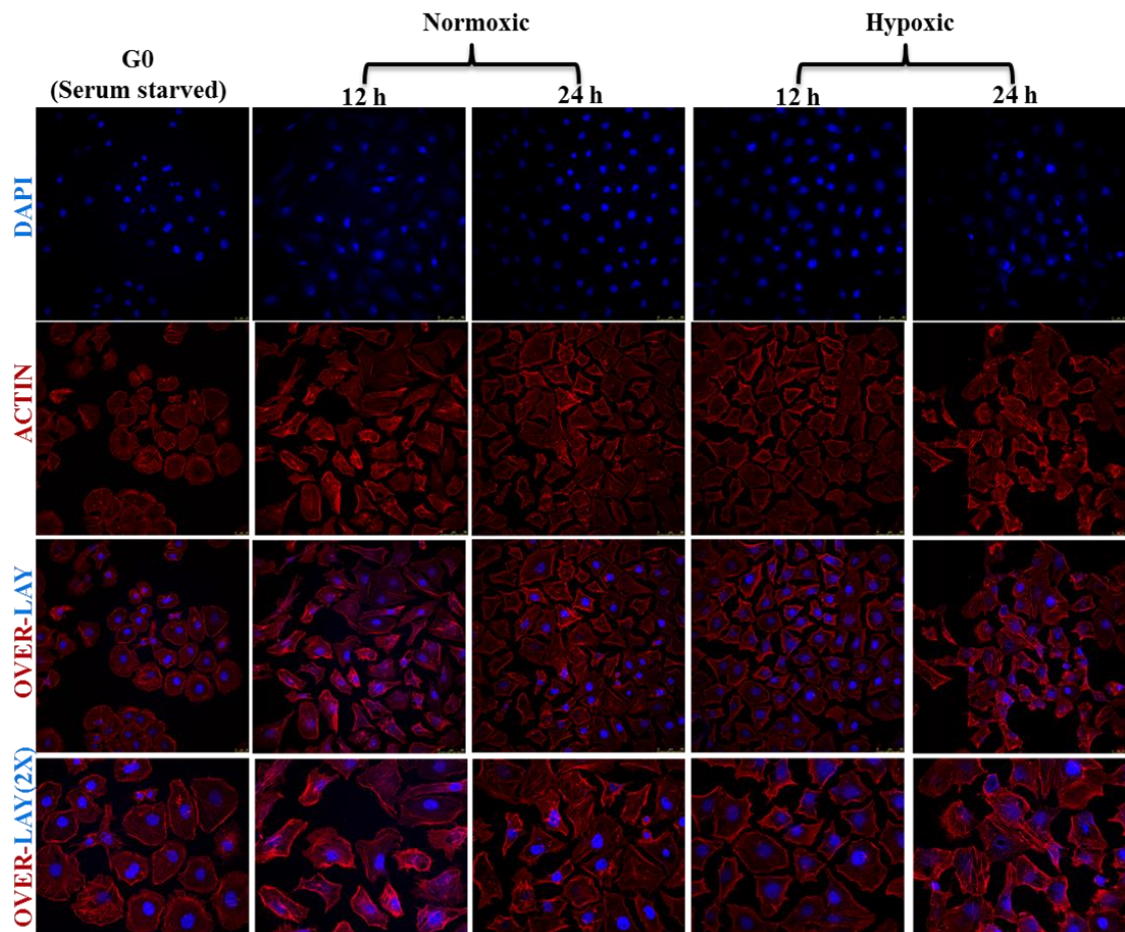


Figure 4-2: Morphology of ARIP cells under hypoxic and normoxic conditions. ARIP cell were seeded at 2×10^5 cells in each well of 6-well plate on glass coverslips and serum starved overnight followed by addition of whole medium containing 10% FBS; cells were fixed with 3.7% of formalin at 12 or 24 hours and phalloidin staining was performed to stain actin filaments of cells. Cells were visualized by confocal microscopy and images were captured at 40X magnification. Results are representative of three separate experiments. Images were representative of six separate fields. These results indicated that cells at G0, N12, N24 and H12 were with regular shape of cells as well as nucleus, also the nucleus of cells was localized in the centre of cells. Normal cytoplasm to nuclei ratio was observed. However, H24 shape and size of cells was irregular also growth pattern was irregular compared to cells under normoxic conditions.

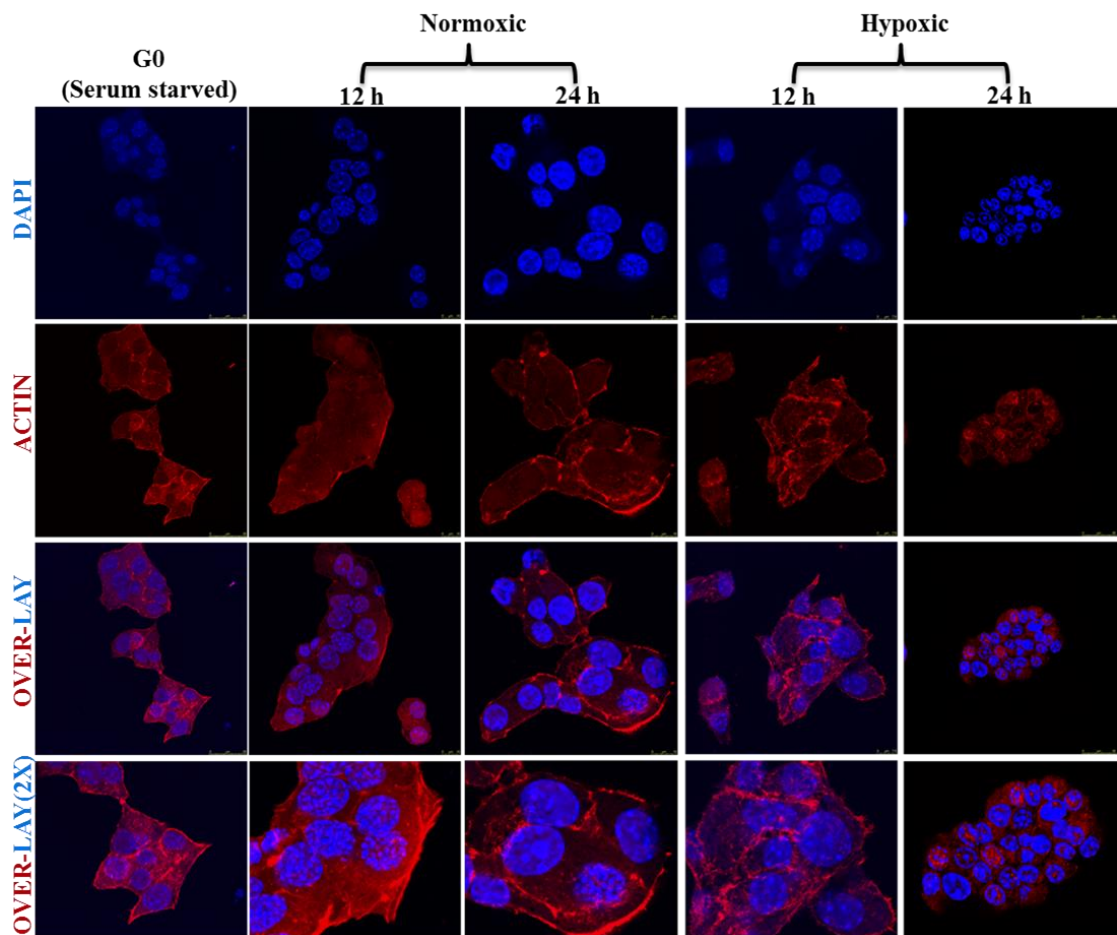


Figure 4-3: Morphology of MIN6 cells under hypoxic and normoxic conditions. MIN6 cell were seeded at 2×10^5 cells in each well of 6-well plate on glass coverslips and serum starved overnight followed by addition of whole medium containing 10% FBS; cells were fixed with 3.7% of formalin at 12 or 24 hours and phalloidin staining was performed to stain actin filaments of cells. Cells were visualized by confocal microscopy and images were captured at 40X magnification. Results are representative of three separate experiments. Images were representative of six separate fields. These results indicated that beta cells at all-time points under normoxic (N) or hypoxic (H) grow in groups (cell to cell contact). Regular shape and size of beta cells as well as nuclei was observed at G0 (serum starved), N12 and N24. Ruff surface of cells was observed at H12. At H24 small size of cells was observed.

4.2.2. Scanning Electron Microscopy (SEM)

In order to determine the cell surface morphology, SEM was performed. For SEM analysis, cells on coverslips were coated with platinum and examined using Zeiss Sigma field emission gun SEM (Zeiss NTS). Images were captured at 1K, 5K, 10K, 30K, 50K and 100K (1K=1000X) magnifications.

4.2.2.1. *Human pancreatic adenocarcinoma cells (PSN-1)*

PSN-1 cell surface morphology was investigated by SEM Zeiss Sigma field emission gun SEM (Zeiss NTS) and results are detailed in Figure 4-4. Results indicate that the PSN-1 cell population has two distinct morphology of cell: elongated fibroblast-like cells and rounded lymphocyte-like cells. However, it appears that the surface of all cells shares the same morphological features. At G0 and H12 PSN-1 cells were round shaped and in contact with each other with large lamellipodia. At G0 and H12 the surface of cells was covered with small microvilli structures as well as finger-like structures of filopodia. Cells under normoxic (N12 and N24) conditions were round shaped and contacted with each other with large lamellipodia, here too the cell surface was covered with finger-like filopodia. At H24 the surface of cells was fully covered with finger-like filopodia, these structures help pancreatic cancer cells to invade and metastasis to other body parts.

4.2.2.2. *Pancreatic ductal cells (ARIP)*

ARIP cell surface morphology was investigated by SEM Zeiss Sigma field emission gun SEM (Zeiss NTS) and results are shown in Figure 4-5. ARIP cells at G0 were connected with each other via large lamellipodia on the edges of the cell surface. Cells under normoxic (N12 and N24) and hypoxic (H12) conditions shared the same morphology; they were connected with each other via lamellipodia and plasma membrane and small bulges were observed. However at H24 cells were covered with

small filopodia, which is quite commonly found on the surface of cancer cells and been associated with cancer cell migration [333] and invasion [334].

4.2.2.3. *β -cells (MIN6)*

MIN6 cell surface morphology was investigated by SEM Zeiss Sigma field emission gun SEM (Zeiss NTS). Results indicated in Figure 4-6 showed that at G0 and normoxic (N12 and N24) conditions the surface of the cells shared the same morphological features, for example cells grew in groups and formed tight intercellular contact with each other via plasma membrane with bulges. This is characteristic of this cell type and is required for the beta-cell secretory response. At H12 the population of cells was quite low compared to controls and normoxic conditions. As identified in this study, under hypoxic conditions MIN6 beta cells die by undergoing apoptosis and necrosis. SEM analysis demonstrated that in hypoxia the MIN6 cell cytoskeleton appeared to break up and the membrane bulged outward in a process called blebbing. Population of the cells grown under hypoxic conditions for 24 hours was very low, also showing blebbing (apoptosis) as well as pores (necrosis) in plasma membrane was observed on comparing with cells under normoxic and serum starved conditions as shown in Figure 4-6.

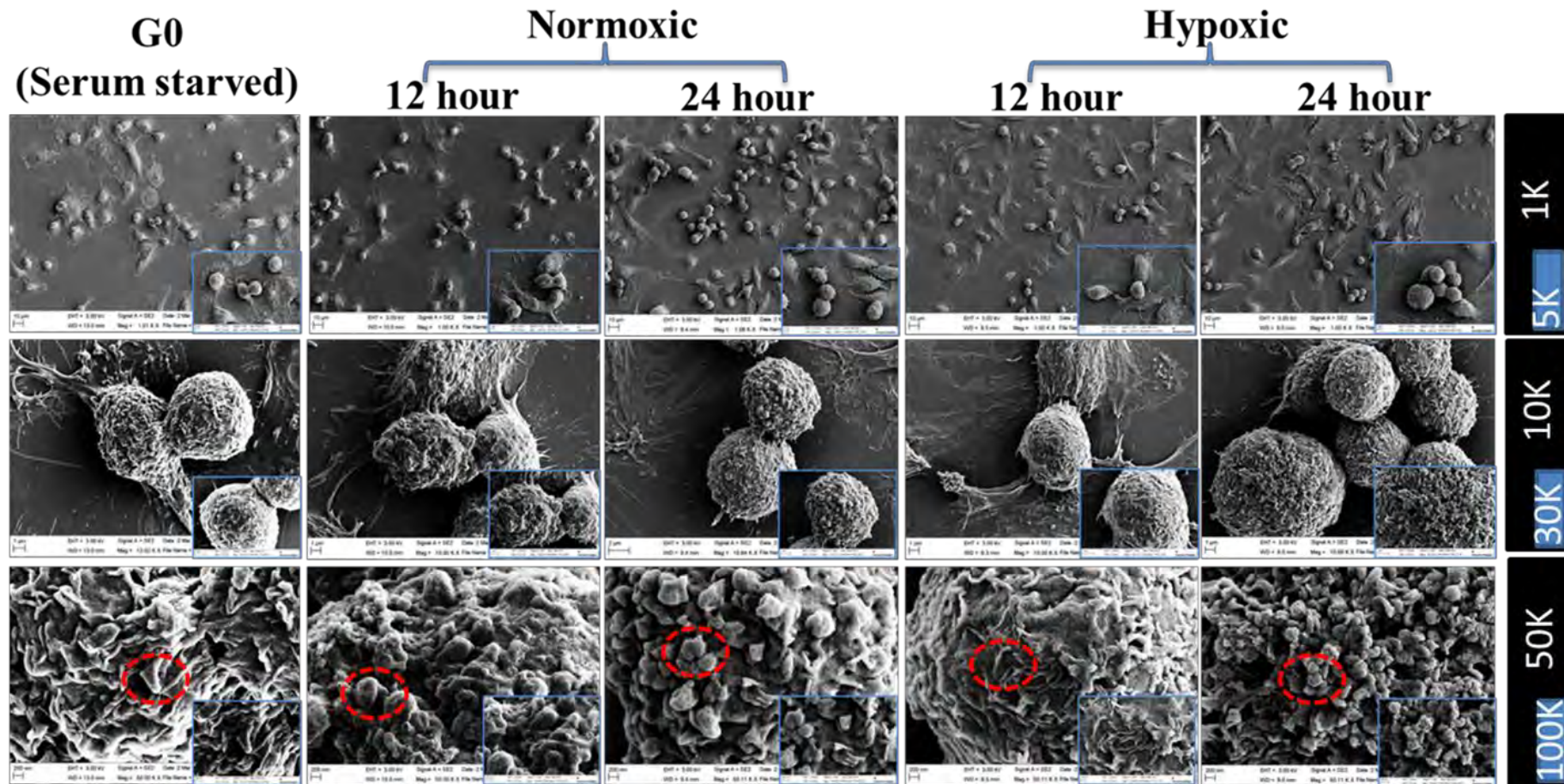


Figure 4-4: Scanning electron microscopy of the surface morphology of human pancreatic adenocarcinoma cells (PSN-1). PSN-1 cells were fixed with 2.5% of glutaraldehyde and coated with platinum coating (4nm). Cells were examined using Zeiss Sigma field emission gun SEM (Zeiss NTS). Images were captured at the magnifications shown (1K, 5K, 10K, 30K, 50K and 100K). Images were representative of six separate fields. At G0 & H12 surface of the cells was covered by small finger-like protrusion **filopodia and microvilli**. Under normoxic (12 or 24 hours) conditions the surface of the cells was covered by **filopodia** and cells were attached to each other with larger lamellipodia. Cells surface at H24 was fully covered with **filopodia**.

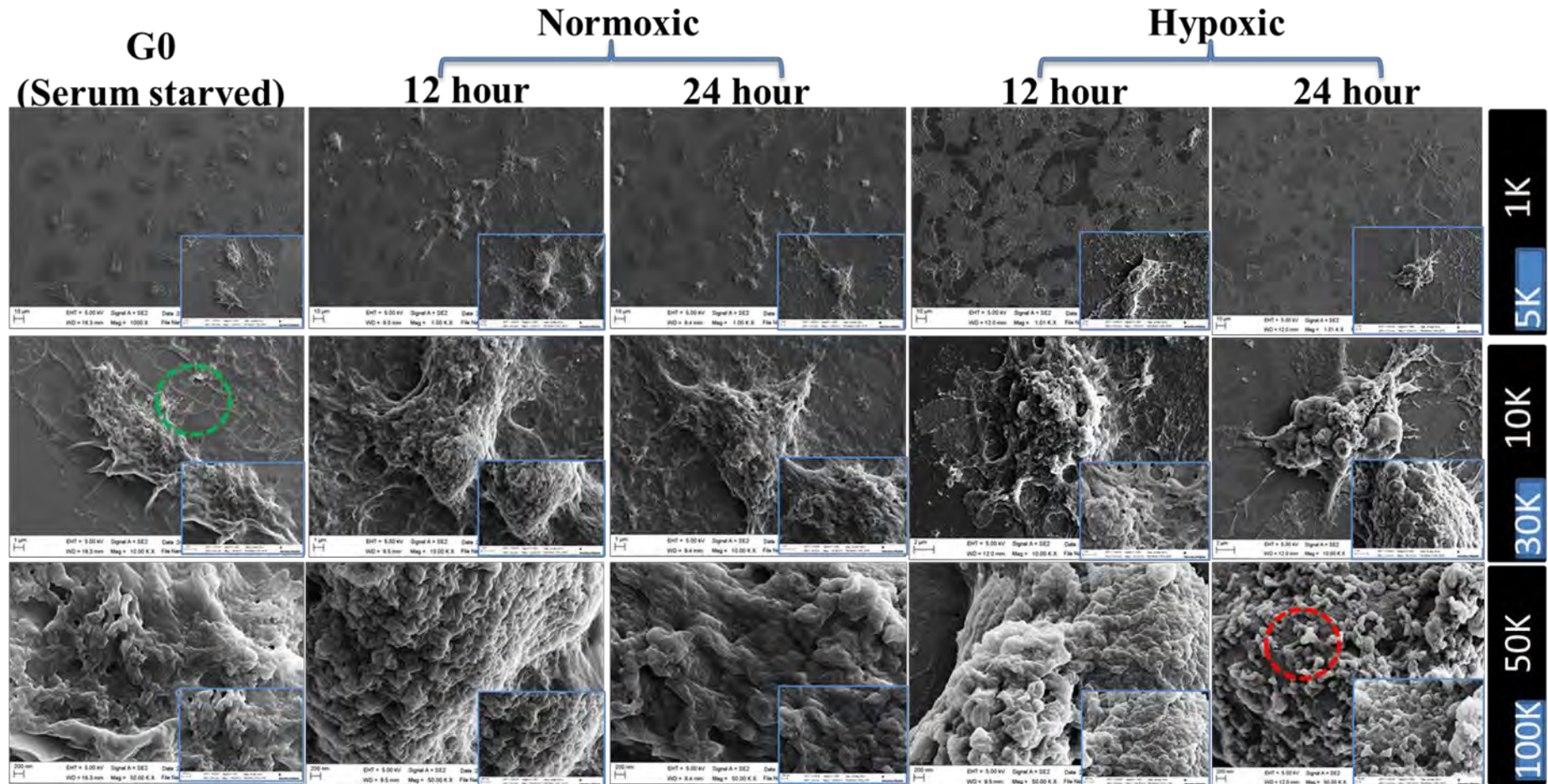


Figure 4-5: Scanning electron microscopy of the surface morphology of pancreases ductal cell (ARIP).

ARIP cells were fixed with 2.5% of glutaraldehyde and coated with platinum coating (4nm). Cells were examined using Zeiss Sigma field emission gun SEM (Zeiss NTS). Images were captured at the magnifications shown (1K, 5K, 10K, 30K, 50K and 100K). Images were representative of six separate fields. At G0 cells were connected with each other with long lamellipoida. Small bulges were observed on the surface of cells under normoxic (12 or 24 hours) and hypoxic conditions at 12 hours. Cells surface was fully covered with small filopodia under hypoxic conditions at 24 hours.

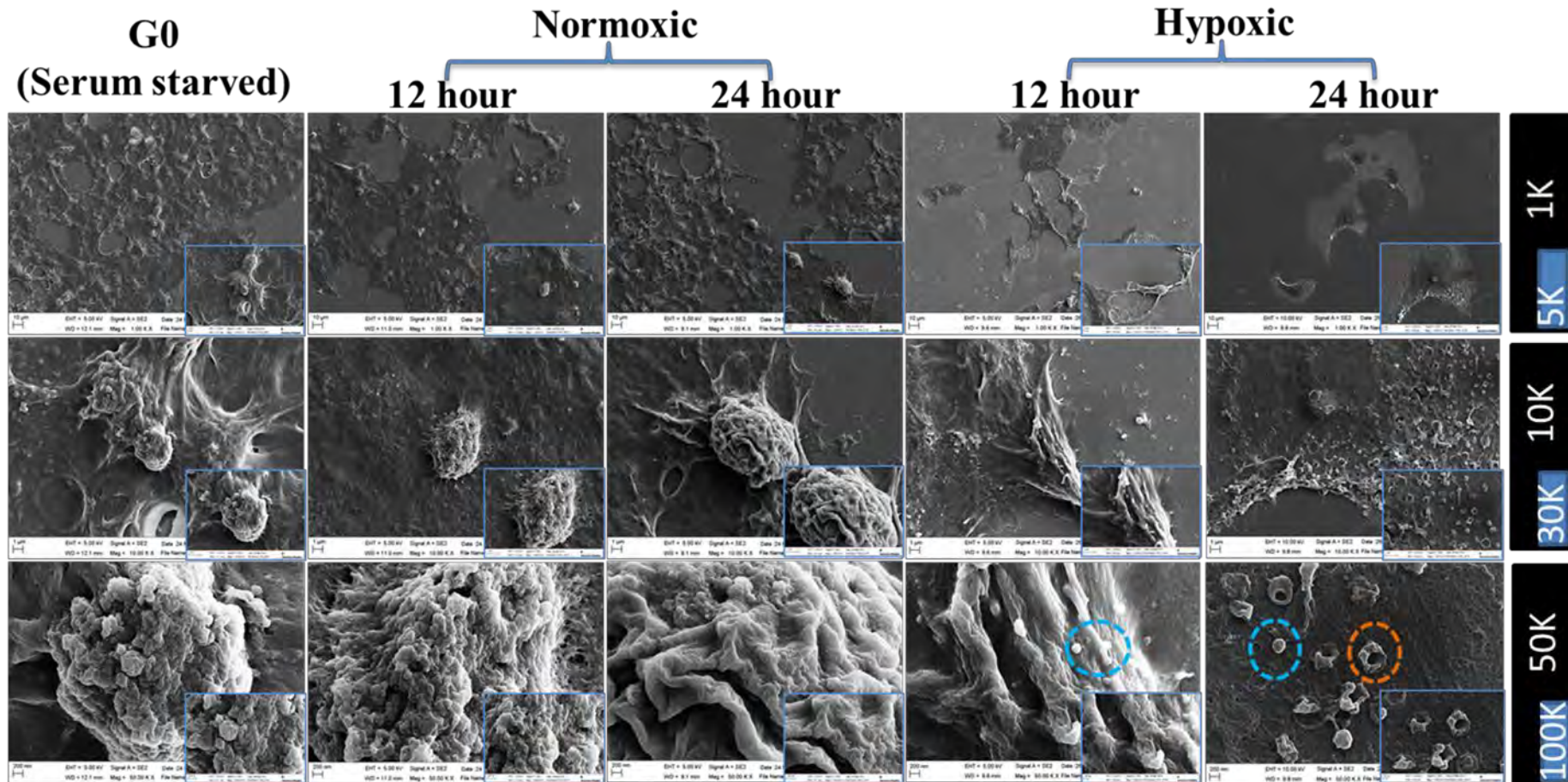


Figure 4-6: Scanning electron microscopy of the surface morphology of mouse pancreases beta cells (MIN6).

MIN6 cells were fixed with 2.5% of glutaraldehyde and coated with platinum coating (4nm). Cells were examined using Zeiss Sigma field emission gun SEM (Zeiss NTS). Images were captured at the magnifications indicated (1K, 5K, 10K, 30K, 50K and 100K). Images were representative of six separate fields. At G0, N12&N24 cells were grow in groups and formed tight intercellular (cell to cell) contacts. Under hypoxic conditions at 12 hours a low population of cells and **blebbing** (apoptosis) on the plasma membrane was observed. A very low population of cells and plasma membrane **pores** (necrosis), **blebbing** (apoptosis) was observed in cells under hypoxic conditions at 24 hours.

4.3. Morphology of normal and cancerous pancreases

In order to define the morphology of normal pancreas and the histopathology of pancreatic cancer tissue, sections were analysed by phalloidin and H&E staining. Due to unavailability of normal human pancreas, mouse pancreas was analysed and considered representative of normal pancreas because the mouse model is genetically closely related to humans [341]. H&E staining is the most common staining method to visualize tissue morphology and is used by pathologists in tissue based diagnosis. Using H&E staining analysis we can define normal and abnormal cell and tissue compartments. Pancreatic ductal adenocarcinomas are well to moderately differentiated, however, variation of differentiation within the same neoplasm is quite common. Poor differentiation is uncommon [80]. After staining our pancreas tissue sections it was possible to differentiate between normal and cancerous tissue. Cancerous tissue has large nuclei, with variation in the size and shape of the nuclei. Aside from the nuclei abnormalities, an increase in collagen fibres, equivalent to the intensity of stromal fibrosis is quite commonly observed in pancreatic cancer patients [342]. To define the histopathology of human pancreatic tissue sections (in all four cases) samples were stained with H&E staining and compared with healthy mouse pancreas as well as healthy human pancreas where data were available [18, 19, 336].

4.3.1. Mouse normal pancreas

In order to investigate the morphology of normal mouse pancreas; formalin fixed paraffin embedded pancreas tissue blocks were sectioned (5 μ m) and mounted on glass slides. Tissue sections were deparaffinised by dipping sections in xylene and rehydrated (gradient ethanol). Phalloidin and H&E staining were performed.

4.3.1.1. *Phalloidin cytoskeleton staining*

Phalloidin staining was performed and sections were mounted with fluorescent mounting medium containing DAPI. Stained sections were analysed by confocal microscopy and images were captured at 40X (Figure 4-7) and 100X (Figure 4-8) magnification. In Figure 4-7, it can be seen that acini (group of acinar cells) were present in a ring-like structure in an irregular profile and connected with intercalated ducts (panels A&C). Nuclei in acinar cells lie toward the basal region of the cell. Islets of Langerhans were observed within far more numerous acini and connected with intralobular ducts (B).

Under high magnification (100X) - Figure 4-8 panel A&C clearly show acini present in a circular and irregular profile inside the lobule. These acini were arranged around a narrow lumen and rounded nuclei lying toward the basal side of the acinar cell. Acini are clearly connected with very small intercalated ducts and these ducts were join together inside the lobule and ultimately open into intralobular duct. These results (panel B) also indicate that the intralobular islet of Langerhans (IL) was localised among far more numerous acini and connected to the intralobular duct.

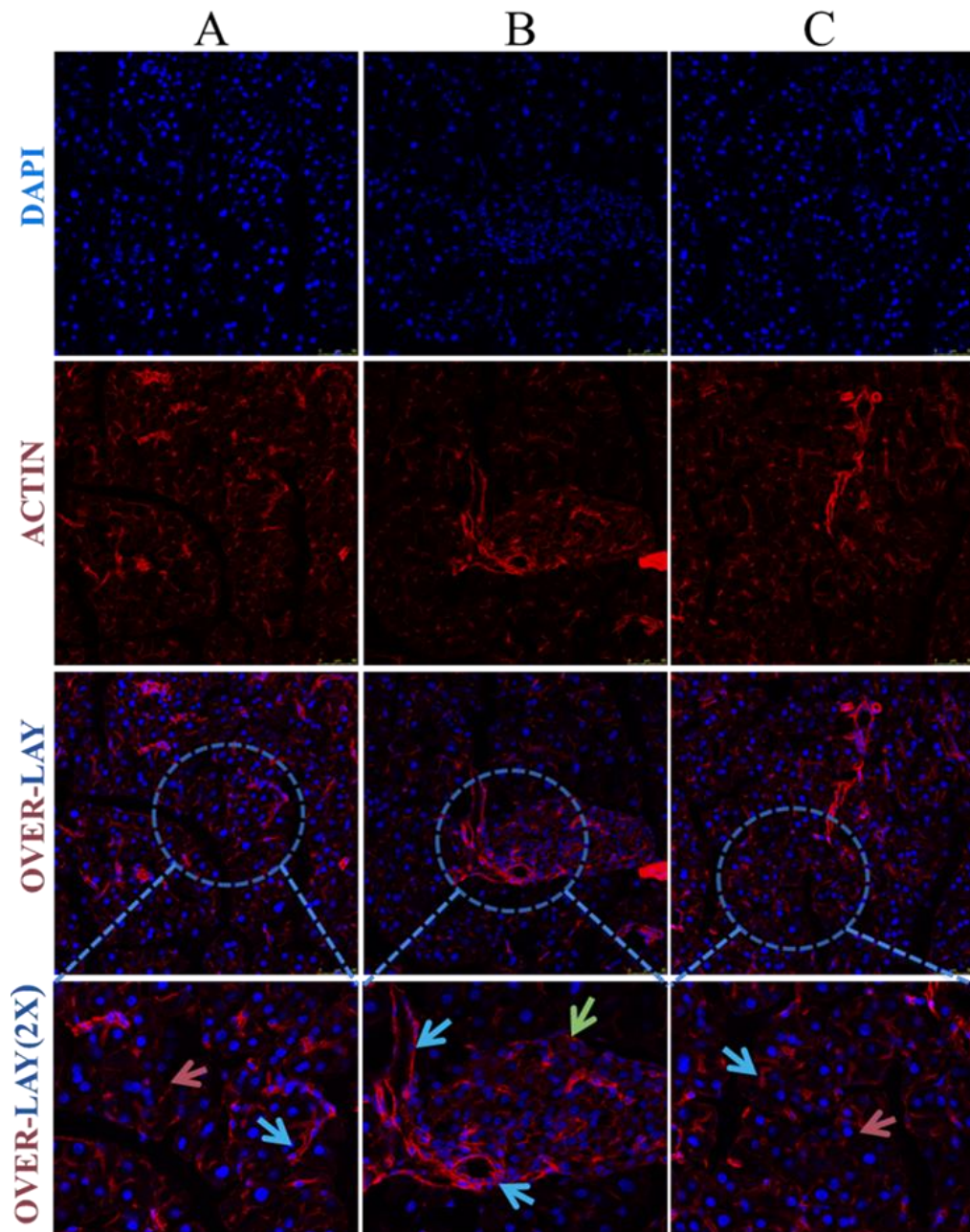


Figure 4-7: Morphology of normal mouse pancreas (40X magnification)

Formalin fixed, paraffin embedded tissue samples were sectioned (5 μ m) and mounted on glass slides. Phalloidin staining was performed in order to investigate detailed morphology of normal pancreas. Phalloidin stains the **cytoskeleton (actin filament)** and DAPI stains the **nucleus**. Stained sections were analysed by confocal microscopy and images were captured at 40X magnification. In panel A and C numerous **acini** are present in circular and irregular profile within the lobule. **Acini** with rounded nucleus and connected with very small **intercalated ducts**. Panel B large islet of Langerhans (IL) surrounded by numerous acini and **intralobular ducts** inside the lobule.

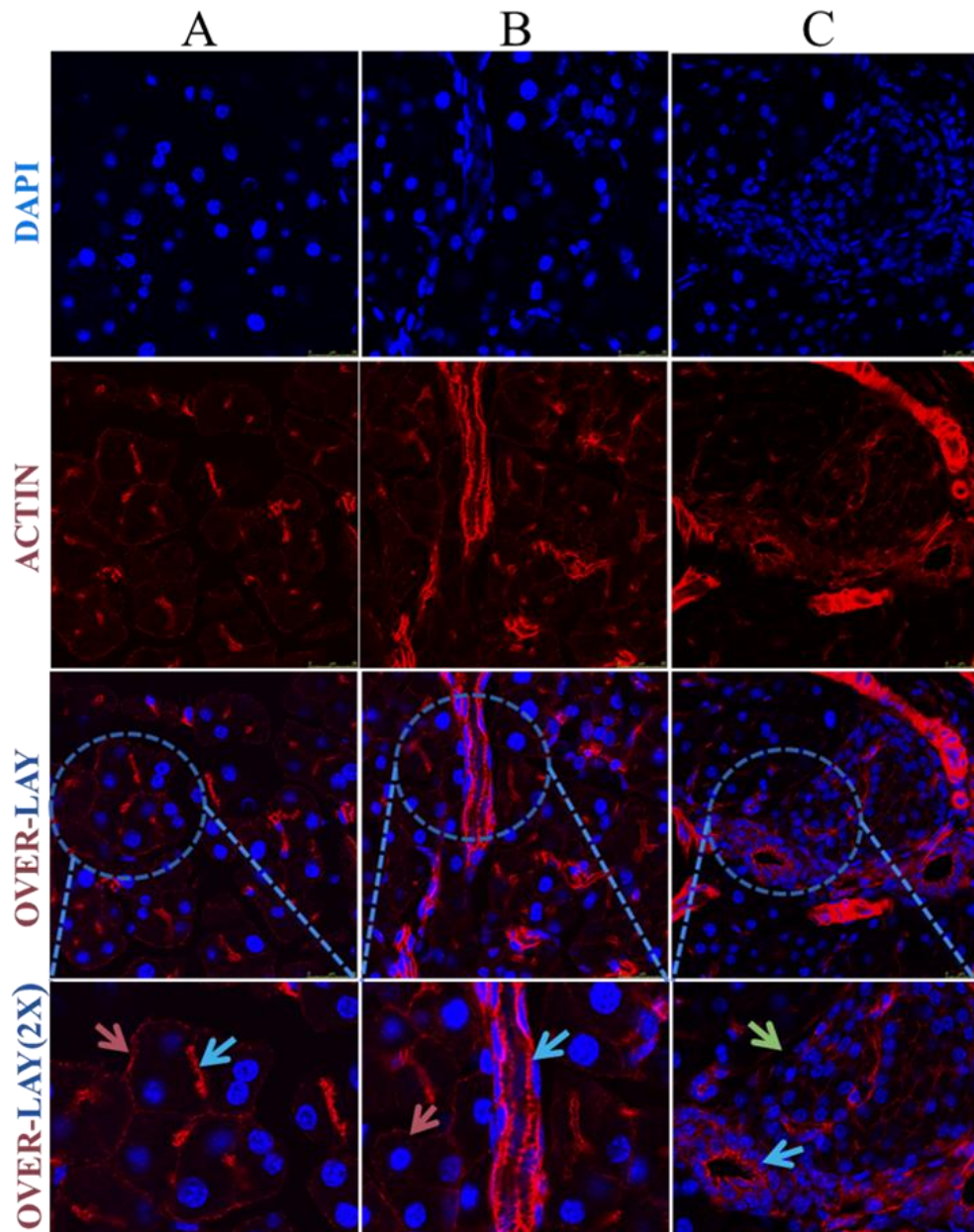


Figure 4-8: Morphology of normal mouse pancreas (100X magnification)

Formalin fixed, paraffin embedded tissue samples were sectioned (5 μ m) and mounted on glass slides. Phalloidin staining was performed in order to investigate detailed morphology of normal pancreas. Phalloidin stain **cytoskeleton (actin filament)** and DAPI stain the **nucleus**. Stained sections were analysed by confocal microscopy and images were captured at 100X magnification. Panel A and B acini are present in a circular and irregular profile. Pancreatic acini are arranged around a narrow lumen and with rounded nuclei located toward the basal side of the cell. Acini are connected with very small **intercalated ducts**. In panel C intralobular **islet of Langerhans (IL)** among far more numerous **acini** and **intralobular duct** next to **IL**.

4.3.1.2. *H&E staining*

In order to investigate the morphology of normal mouse pancreas H&E staining was performed. Stained sections were analysed by light microscopy and images were captured at 5X (Figure 4-9), 10X (Figure 4-10) and 40X (Figure 4-11). The pancreas is divided into small lobules and these lobules are connected with each other by connective tissue (CT). Each lobule contains numerous acini and these acini are present in a circular and irregular profile. Acini are arranged around a very narrow lumen and the cytoplasm of the cell has a dark red colour as it contains large granules which stain deeply red with eosin. Acini with rounded nuclei were located toward the basal side of the cell as observed and shown in Figure 4-11 (B). Inside the lobule, small intercalated ducts join together and make larger ducts and these join further to intralobular ducts (Figure 4-10 (A)). Large blood vessels run through and in between the lobules as well as in-side the lobule as shown in Figure 4-9 (A, B &D), Figure 4-10 (A) and Figure 4-11 (C). The islets of Langerhans (IL) were scattered throughout the lobules, some IL were among far more numerous acini and some were next to intralobular ducts as shown in Figure 4-9. Islets of Langerhans are easily recognised from the rest of the pancreas tissue because lighter stained clusters stand out in the more darkly stained acini. Cells in IL were arranged in a cluster with rounded nuclei as shown in Figure 4-11 (A).

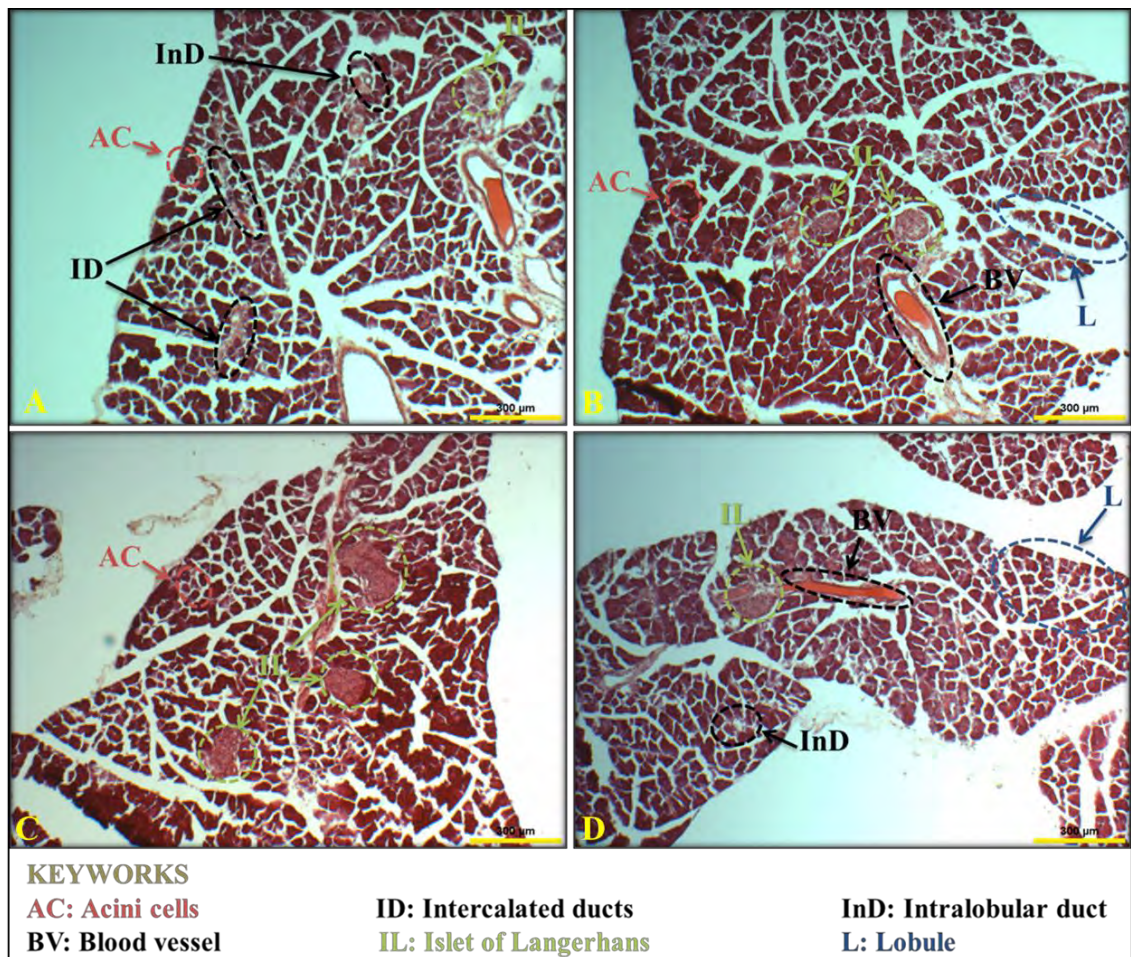


Figure 4-9: Morphology of normal mouse pancreas stained with H&E staining (5X magnification).

Formalin fixed, paraffin embedded pancreas tissue blocks were sectioned (5µm) and mounted on glass slides and H&E staining was performed. Images were captured by light microscopy at 5X magnification. Numerous **acini (AC)** (as highlight in **red circle**) were present in circular and irregular profile inside each lobule. Large blood vessels (**BV**) (as highlight in **black circle**) travel through connective tissue in between and inside the **lobules (L)** (as highlight in **blue circle**). Intercalated ducts run around **acini** and intralobular ducts lie inside the **lobules**. Intralobular and interlobular **islets of Langerhans (IL)** (as highlight in **green circle**) can be seen among far more numerous **acini** cells.

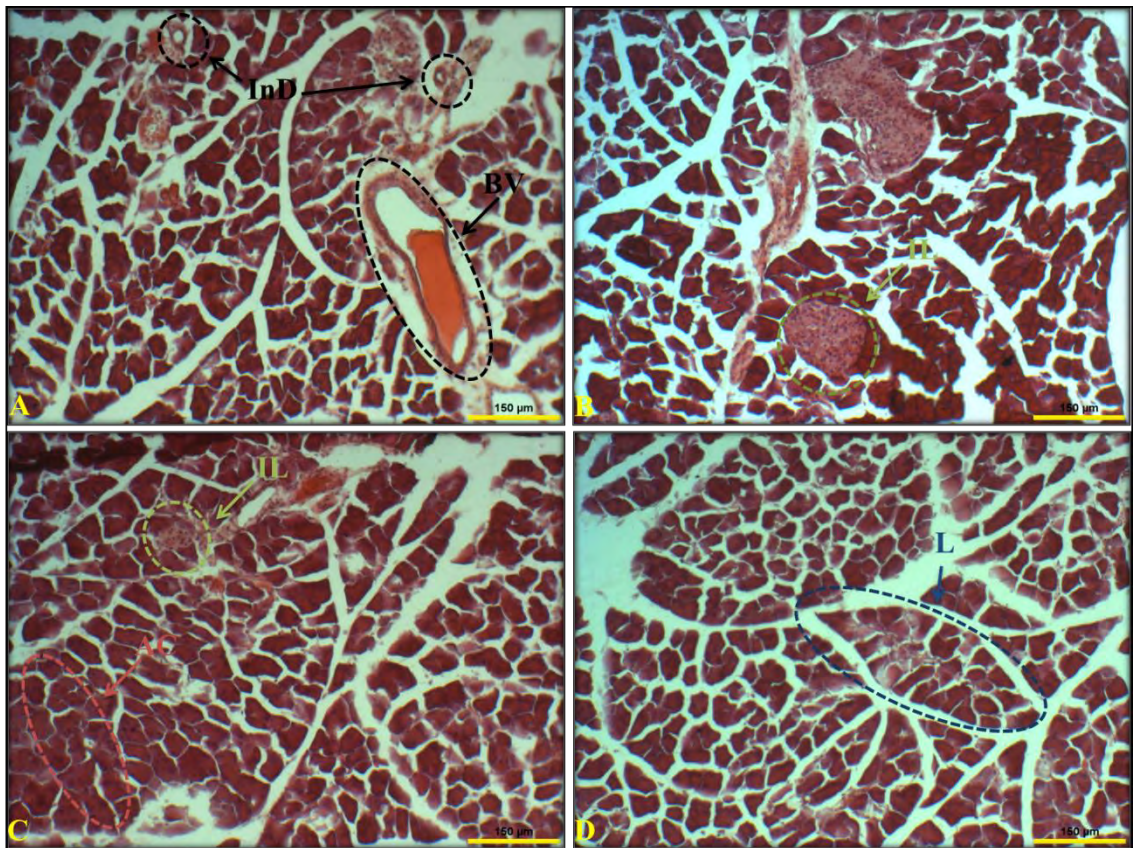


Figure 4-10: Morphology of normal mouse pancreas stained with H&E staining (10X magnification).

Formalin fixed, paraffin embedded pancreas tissue blocks were sectioned (5µm) and mounted on glass slides and H&E staining was performed. Images were captured by light microscopy at 10X magnification. Numerous **acini (AC)** are present in circular and irregular profile inside each lobule. Large blood vessels (BV) (as highlight in black circle) travel through connective tissue in between and inside the **lobules (L)** (as highlight in blue circle). Intercalated ducts run around **acini** and intralobular ducts lie inside the **lobules**. Variable sized intralobular **islets of Langerhans (IL)** (as highlight in green circle) are present among far more numerous **acini** cells.

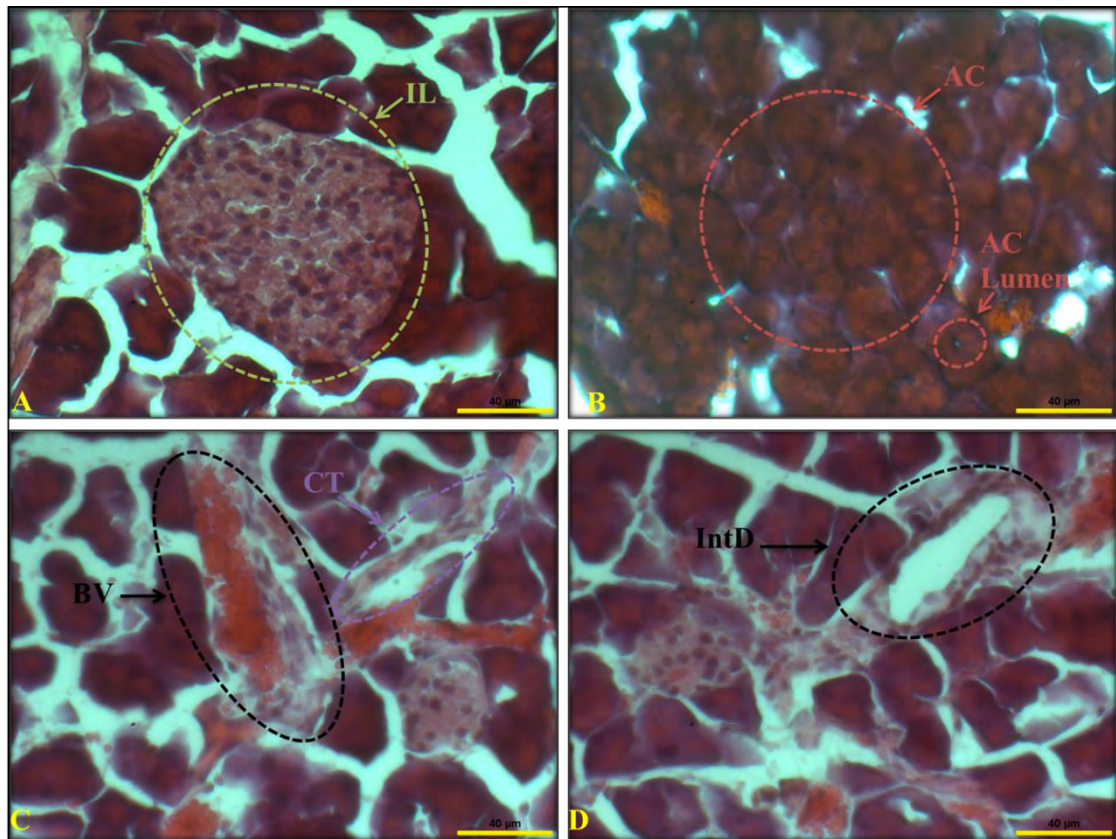


Figure 4-11: Morphology of normal mouse pancreas stained with H&E staining (40X magnification).

Formalin fixed, paraffin embedded pancreas tissue blocks were sectioned (5µm) and mounted on glass slides and H&E staining was performed. Images were captured by light microscopy at 40X magnification. A: Intralobular islet of Langerhans (IL) (as highlight in green circle) is surrounded by far more acini. In panel B numerous acini (AC) (as highlight in red circle) are present in circular and irregular profile. In panel C Connective tissue (CT) (as highlight in violet circle) has been identified around a blood vessel. An interlobular duct lies on the edge of the lobule as highlighted in black circle in panel D.

4.3.2. Morphology of human pancreatic cancer tissue

In order to investigate the morphology of human pancreatic cancer tissue samples; formalin fixed paraffin embedded pancreas tissue blocks were sectioned (5µm) and mounted on glass slides. Tissue sections were deparaffinised by dipping sections in xylene and rehydrated (gradient ethanol). H&E staining was performed and samples were analysed by light microscope and images captured at 5X, 10X and 40X magnifications.

4.3.2.1. Case study 1

The results from sample 1 are shown in Figure 4-12 (5X), Figure 4-13 (10X) and Figure 4-14 (40X). Results from Figure 4-12 (5X) indicated that sample 1 was moderate to poorly differentiated, as some part of the sections still retained the normal morphology i.e. acinar cells were still intact in lobular structure and surrounded by fibrous connective tissue as observed and as indicated in Figure 4-12 (A). However, in the rest of the tissue section total loss of normal morphology was observed. Invasion of fibrous connective tissue, rudimentary acini, pleomorphic malignant epithelial cells, and poorly differentiated gland like structures were observed as shown in Figure 4-12 (B, C &D). Figure 4-13(X10) demonstrates that acinar cells arranged in the lobular structure and interlobular duct surrounded by fibrous connective tissue was observed in Figure 4-13 (A) and Figure 4-14 (A). Rudimentary acinar cells and nerve cell bundle were surrounded by desmoplastic stromal cells as indicated in Figure 4-13 (B&C) and Figure 4-14(C). Pleomorphic malignant epithelial cells and ductal epithelial cells with pleomorphic nucleus were observed in Figure 4-13 (D) and Figure 4-14 (B&D). Results from H&E staining of case study 1 suggested that this tissue is well to moderately differentiated pancreatic adenocarcinoma; however, there some part of the tissue is poorly differentiated pancreatic adenocarcinoma.

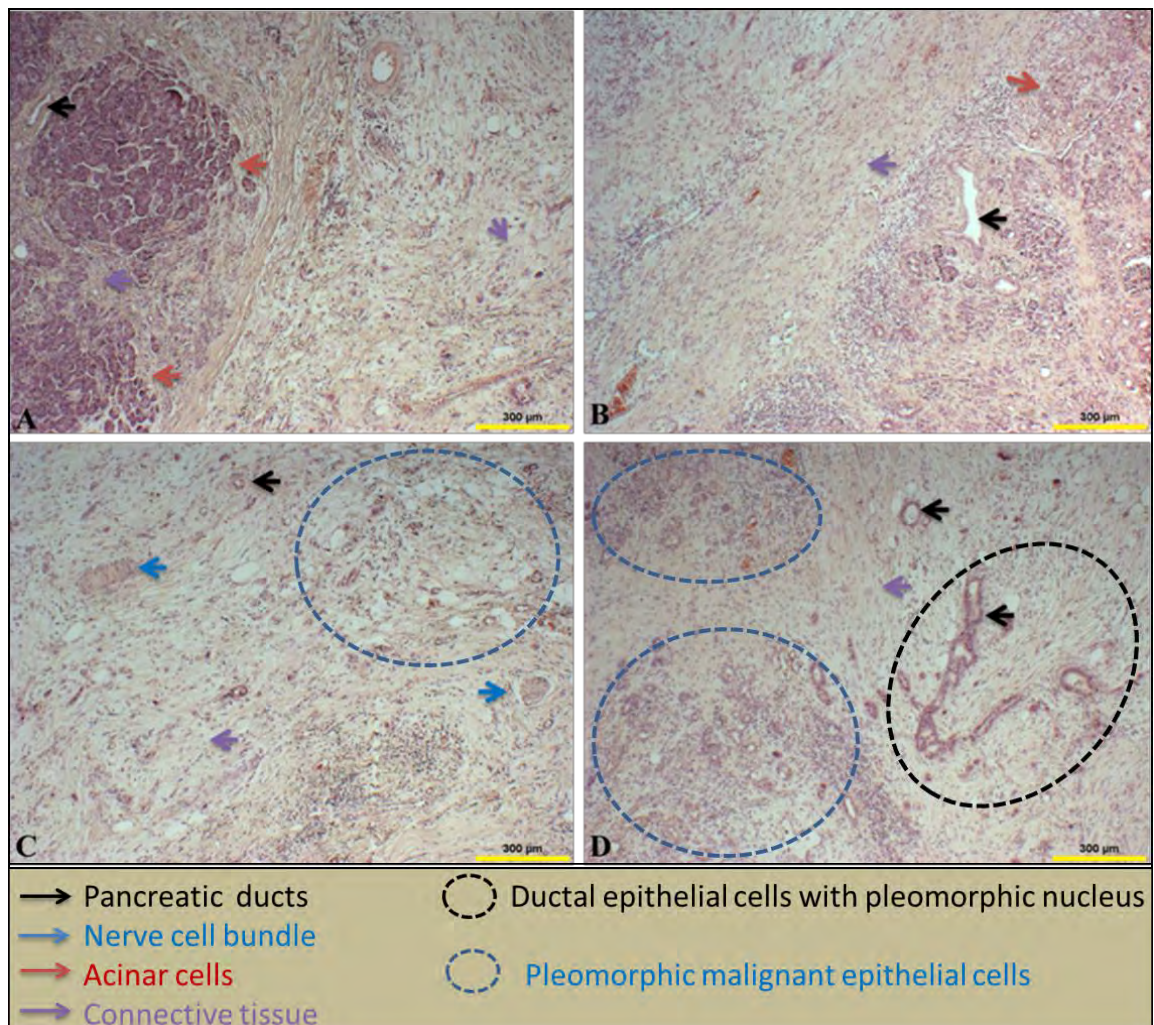


Figure 4-12: Haematoxylin and Eosin (H&E) staining of human adenocarcinoma pancreas tissue case study 1 (5X magnification).

Formalin fixed, paraffin embedded tissue samples were sectioned (5µm) and mounted on glass slides. H&E staining was performed and images were captured by light microscopy at 5X magnification. (A) **Acinar** (←) cells are still intact in the lobular structure and two lobules are divided by **fibrous connective tissue** (←), Inter-lobular (←) duct in between two lobules and surrounded by connective tissues. Half of the section has lost its integrity, invasion of fibrous connective tissue and lack of lobular structures can be seen as well as loss of acinar cells. (B) **Acini** like structure or rudimentary acini, no lobule structure, **desmoplastic stromal tissue**. (C) **Fibrous connective tissue** (←) invasion into **nerve** (←) cells, loss of exocrine and endocrine integrity of pancreas, pleomorphic malignant epithelial cells (inside the **circle**). (D) Desmoplastic stroma, duct (←) epithelial cells with pleomorphic nuclei (as highlight in black circle), pleomorphic malignant epithelial cells (inside the **circle**).

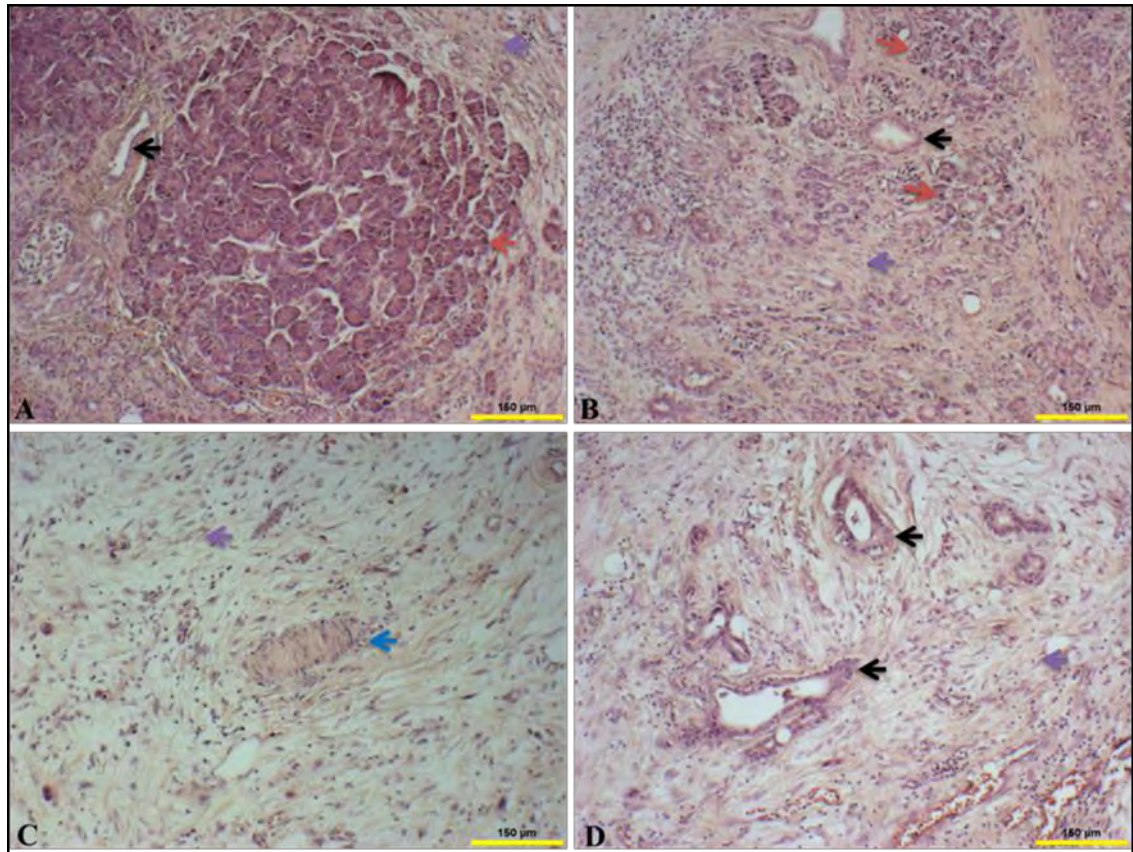


Figure 4-13: Haematoxylin and Eosin (H&E) staining of human adenocarcinoma pancreas tissue case study 1 (10X magnification).

Formalin fixed, paraffin embedded tissue samples were sectioned (5µm) and mounted on glass slides. H&E staining was performed and images were captured by light microscopy at 10X magnification. (A) **Acinar** (←) cells are still intact in lobular structure and two lobules are divided by **fibrous connective tissue** (←) and Inter-lobular (←) duct in between two lobules surrounded by connective tissues. (B) Invasion of **fibrous connective tissue** (←) can be seen in between the lobules and **acinar** (←) cells lost its integrity, also Intra-lobular (←) duct outside the lobules (C) Clear invasion of **fibrous connective tissue** (←) into the bundle of **nerve** (←) cells. (D) High invasion of **fibrous connective tissue** (←) surrounding ductal (←) epithelial cell with pleomorphic nucleus and no acinar cells found.

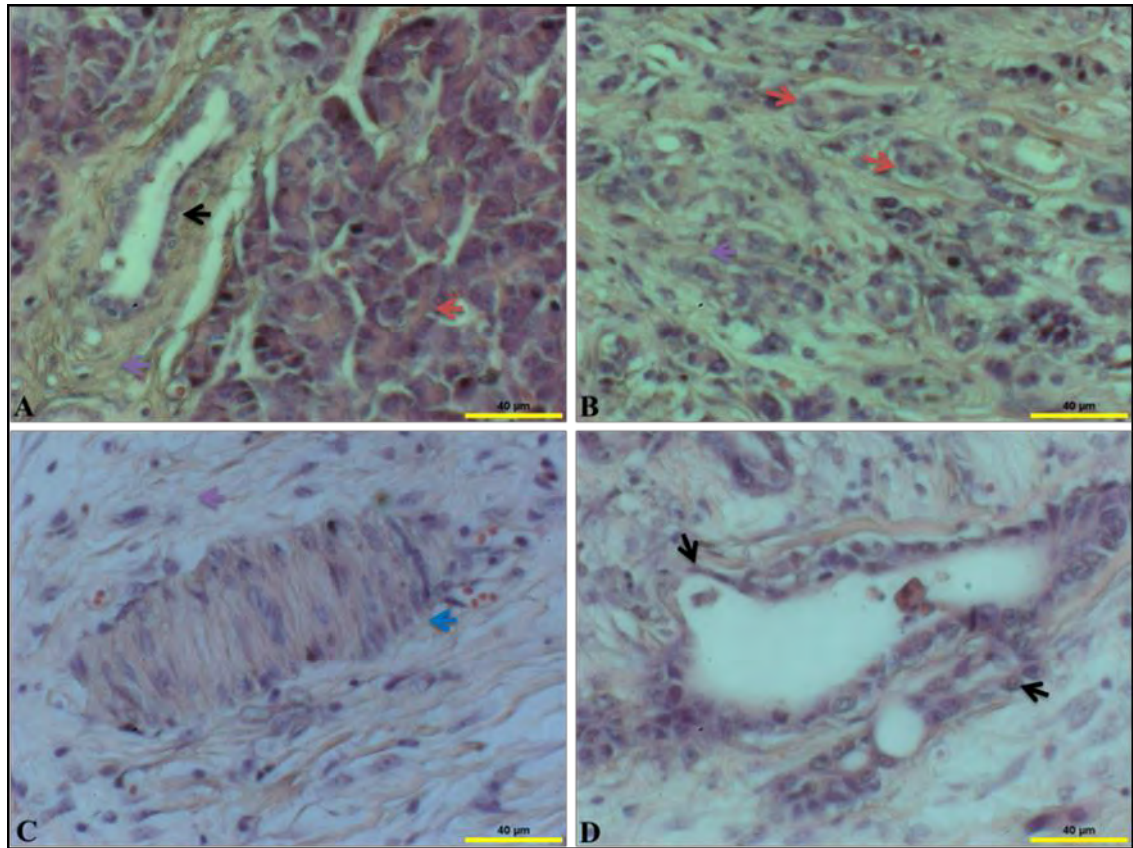


Figure 4-14: Haematoxylin and Eosin (H&E) staining of human adenocarcinoma pancreas tissue case study 1 (40X magnification).

Formalin fixed, paraffin embedded tissue samples were sectioned (5µm) and mounted on glass slides. H&E staining was performed and images were captured by light microscopy at 40X magnification. (A) **Acinar** (←) cells are organized in clusters and inter-lobular (←) duct in between two lobules are surrounded by connective tissues. (B) Pleomorphic malignant epithelial cells surrounded by **fibrous connective tissue** (C) **Fibrous connective tissue** (←) invasion into the **nerve** (←) cell bundle. (D) Duct (←) epithelial cell with pleomorphic nuclei as highlighted by black arrows.

4.3.2.2. *Case study 2*

The results from sample 2 are shown in Figure 4-15(5X), Figure 4-16(10X) Figure 4-17(40X). Results from Figure 4-15 indicated that half of tissue sections still have lobular morphology with acini and intralobular ducts. Invasion of fibrous connective tissue and invasion of pleomorphic malignant epithelial cells to the nerve cell bundle is also evident as shown in the red circle in Figure 4-15 (A). However, the rest of the section has lost its integrity and has rudimentary lobular morphology, with loss of acini observed in Figure 4-15 (A). There is also loss of lobular morphology: free standing islets of Langerhans and a large duct with irregular shaped and pleomorphic nucleus were surrounded by fibrous connective tissue as observed in Figure 4-15 (B). Figure 4-15 (C) highlights that rudimentary lobular morphology and ductal epithelial cells with pleomorphic nucleus were surrounded by desmoplastic connective tissue. Small gland like structure or pleomorphic malignant epithelial cells were surrounded by desmoplastic fibrous connective tissue as observed in Figure 4-15 (D). On analysing the stained tissue section under higher magnification (10X) it was clear that the presence of highly pleomorphic malignant epithelial cells and ductal epithelial cells with pleomorphic nucleus were observed. Also invasion of pleomorphic malignant epithelial cells and desmoplastic connective tissue to the nerve cell bundle was observed in Figure 4-16 (A, B &C). Instead of acinar cells, islet of Langerhans was surrounded by desmoplastic connective tissue as shown in Figure 4-16 (D). The results from this tissue section under higher magnification (40X) analysis show (Figure 4-16) the presence of small pleomorphic malignant cells (multinucleated, irregular shape and size of nucleus) and mitotic figures (chromosomes are visible as tangled and dark-staining threads) as observed in Figure 4-16 (A). Islets of Langerhans were surrounded by desmoplastic connective tissue and ductal epithelial cells with pleomorphic nucleus surrounded by fibrous connective tissue were observed as shown in Figure 4-16 (B, C &D).

These results from H&E staining of case study 2 indicated that this tissue is well to moderately differentiated human pancreatic adenocarcinoma.

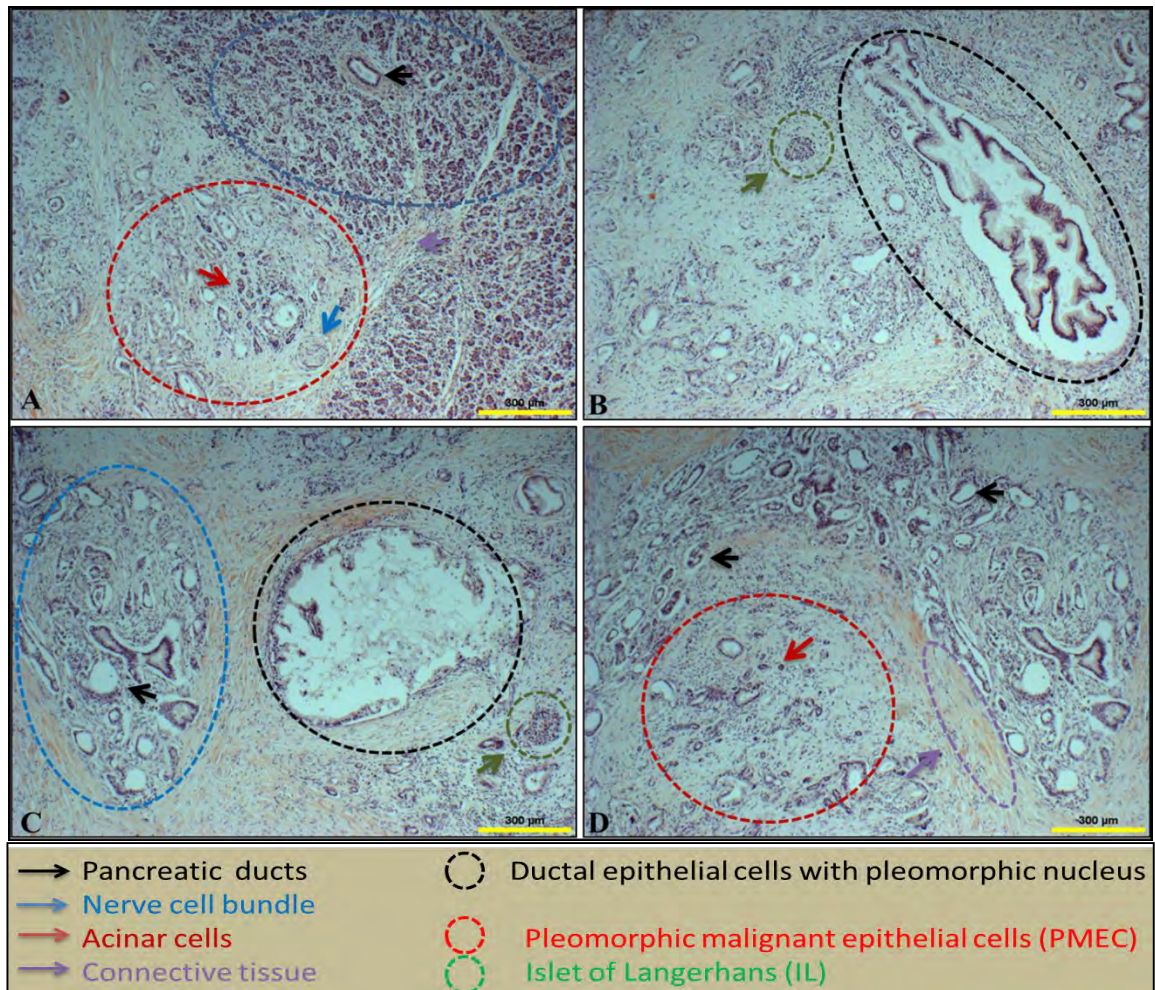


Figure 4-15: Haematoxylin and Eosin (H&E) staining of human adenocarcinoma pancreas tissue case study 2 (5X magnification).

Formalin fixed, paraffin embedded tissue samples were sectioned (5 μ m) and mounted on glass slides. H&E staining was performed and images were captured by light microscopy at 5X magnification. (A) Acinar cells were still intact in lobular structure and two lobules were divided by fibrous connective tissue (FTC) (\leftarrow). Inter-lobular (\leftarrow) duct in between two lobules was surrounded by connective tissues. Half of the section lost its integrity (no lobular structures and acinar cells) and invasion of FTC (\leftarrow) has been identified. Invasion of FTC (\leftarrow) into the bundle of nerve (\leftarrow) cells and PMEC (as highlight in red circle) can be seen. (B) Loss of lobular morphology, no acinar cells, duct (\leftarrow) epithelial cell with pleomorphic nucleus and free standing IL (not surrounded by acinar cell) has been identified. (C & D) Individual lobules lost their integrity (as highlight within the blue circle) and highly infiltrated with FTC (\leftarrow). PMEC and duct (\leftarrow) epithelial cell with pleomorphic nuclei were observed (as highlighted within the black circle in figure c).

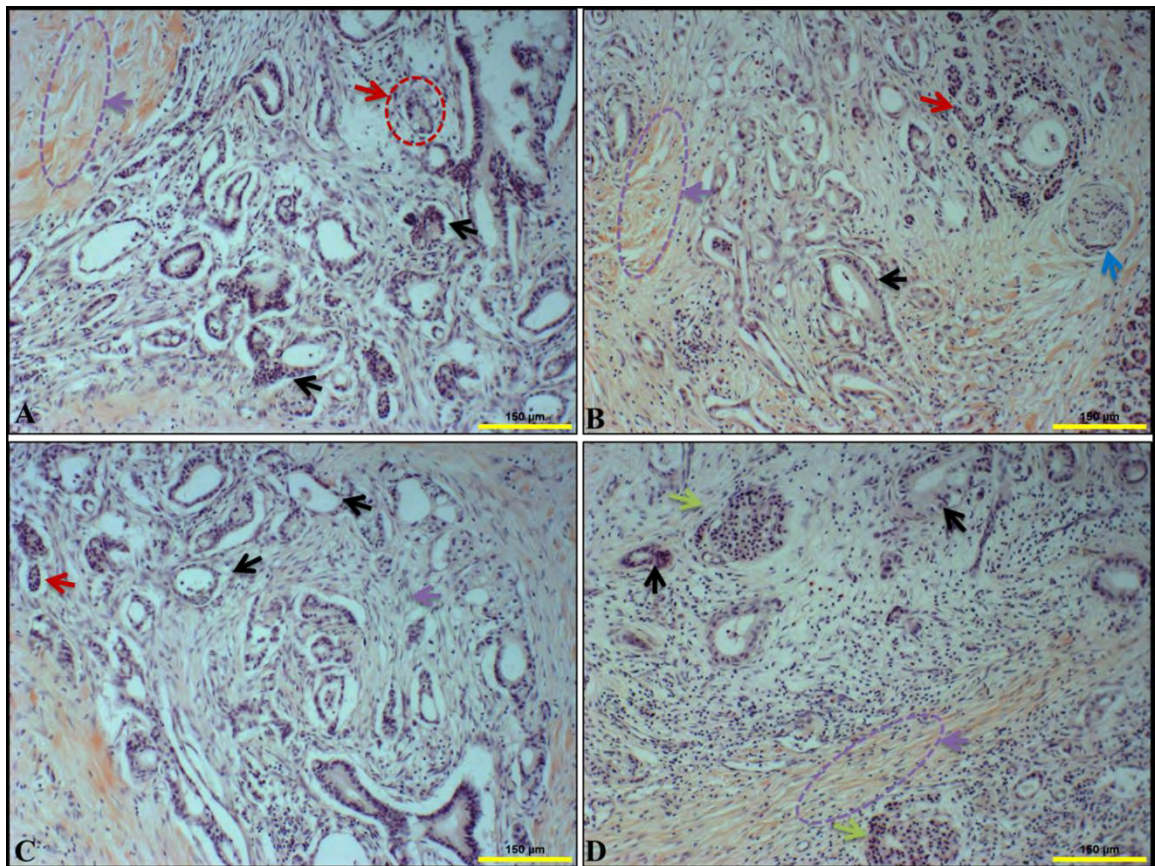


Figure 4-16: Haematoxylin and Eosin (H&E) staining of human adenocarcinoma pancreases tissue case study 2 (10X magnification).

Formalin fixed, paraffin embedded tissue samples were sectioned (5µm) and mounted on glass slides. H&E staining was performed and images were captured by light microscopy at 10X magnification. The key features are as follows: A and C rudimentary lobular morphology, no acini, **desmoplastic stromal tissue (in violet circle)**, **pleomorphic malignant epithelial cells (in red circle)** and duct (←) epithelial cell with pleomorphic nucleus. In panel B, loss of lobular morphology, **desmoplastic stromal tissue**, **pleomorphic malignant epithelial cells**, duct (←) epithelial cell with pleomorphic nuclei and glandular structure near to the **nerve (←) cells bundle (D) Duct (←) epithelial cell with pleomorphic nuclei**, infiltration of neutrophils and free standing **islets of Langerhans (←)** were surrounded by dense **fibrous connective tissue**.

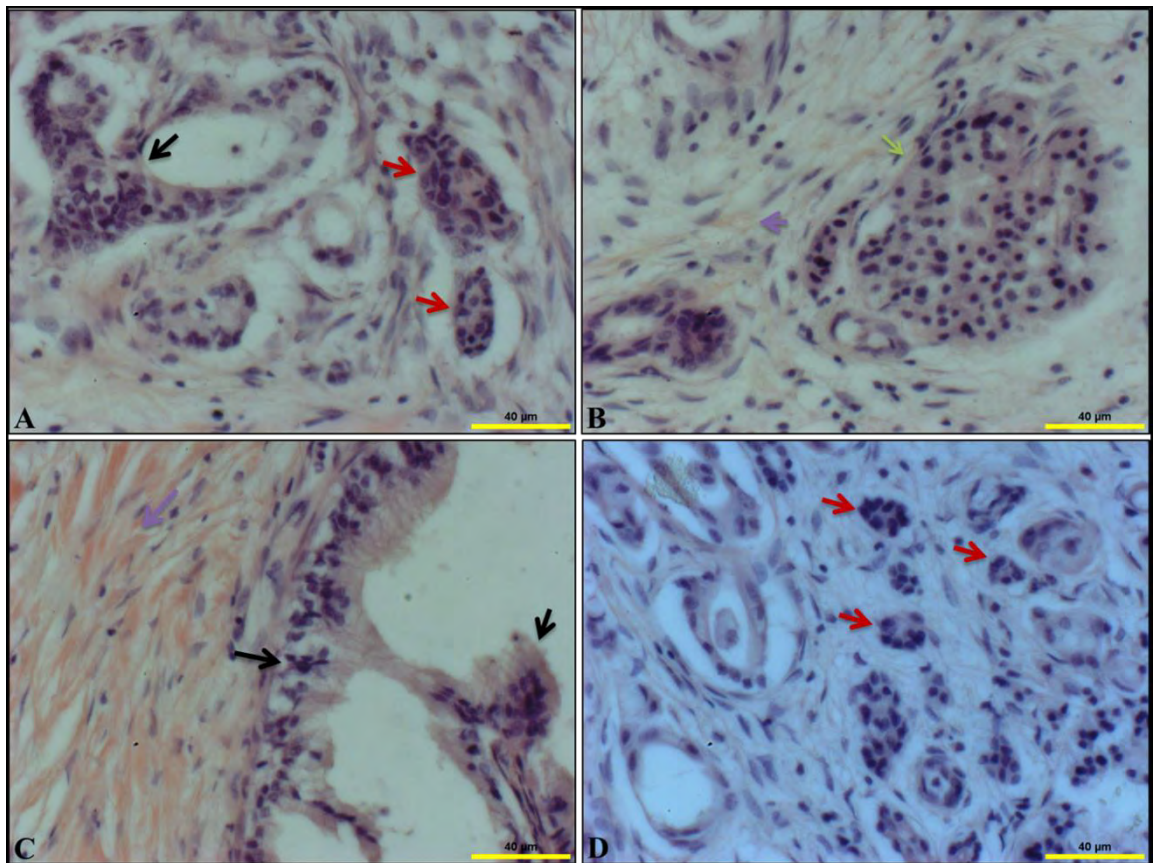


Figure 4-17: Haematoxylin and Eosin (H&E) staining of human adenocarcinoma pancreases tissue case study 2 (40X magnification).

Formalin fixed, paraffin embedded tissue samples were sectioned (5µm) and mounted on glass slides. H&E staining was performed and images were captured by light microscopy at 40X magnification. (A) **Pleomorphic malignant epithelial cells** and duct (←) epithelial cells with pleomorphic nuclei were observed. (B) **Fibrous connective tissue** (←) and free standing **islet of Langerhans**. (C) Duct (←) epithelial cells with pleomorphic nuclei and **desmoplastic connective tissue**. (D) **Pleomorphic malignant epithelial cells** were observed.

4.3.2.3. *Case study 3*

The results from sample 3 are shown in Figure 4-18 (5X), Figure 4-19 (10X) and Figure 4-20 (40X). As shown in Figure 4-18, there is a total loss of normal pancreas morphology: autolysis of tissue section was evident, and no lobular morphology, no acini and no islets of Langerhans were found. The tissue was highly infiltrated with fat cells all around and surrounded by connective tissue. Ductal epithelial cells with pleomorphic nuclei, irregular shaped cells and at some places loss of nuclei were observed in Figure 4-18 (A, B, C &D). On observing stained sections under higher magnification (10X) (Figure 4-19) it was clear that the tissue was highly infiltrated with desmoplastic connective tissue and ductal epithelial cells were with pleomorphic cytoplasm as well as nuclei were observed in Figure 4-19 (A,C&D). It has been observed that stromal cells were invaded into the nerve cell bundle as shown in Figure 4-19 (B). Lymphocytes (dark nucleus) were highly infiltrated throughout the tissue section. Pancreatic cancer tissue under higher magnification (40X) in Figure 4-20 shows irregular shapes ducts with irregular shape and size of the cytoplasm as well as nuclei surrounded by desmoplastic connective tissue was observed in Figure 4-20 (A, B, C &D).

Sample 3 analyses showed total loss of exocrine and endocrine glandular structure of pancreatic cancer tissue, indicating that this tissue is a poorly differentiated pancreatic adenocarcinoma.

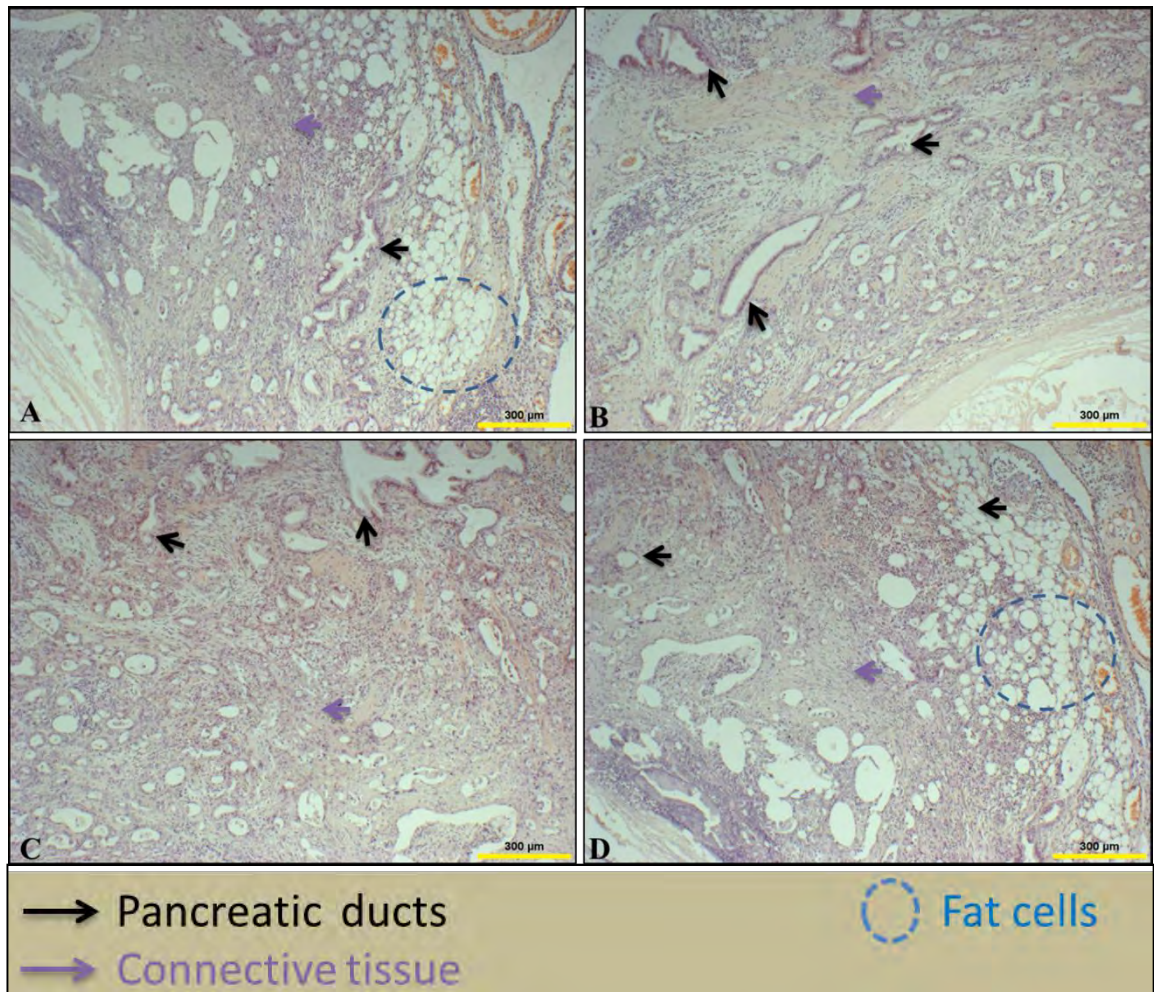


Figure 4-18: Haematoxylin and Eosin (H&E) staining of human adenocarcinoma pancreas tissue case study 3 (5X magnification).

Formalin fixed, paraffin embedded tissue samples were sectioned (5µm) and mounted on glass slides. H&E staining was performed in order to make cells visible and define general morphology of tissue sections. Images were taken under light microscope at 5X. (A, B, C&D) All ducts were surrounded by **desmoplastic connective tissue** (←) and total losses of pancreas morphology such as loss of lobular structure, no acinar as well as islet cells were observed. Ductal (←) epithelial cell with pleomorphic nuclei and fat cells around the tissue section (as **highlight in blue circle**) were observed.

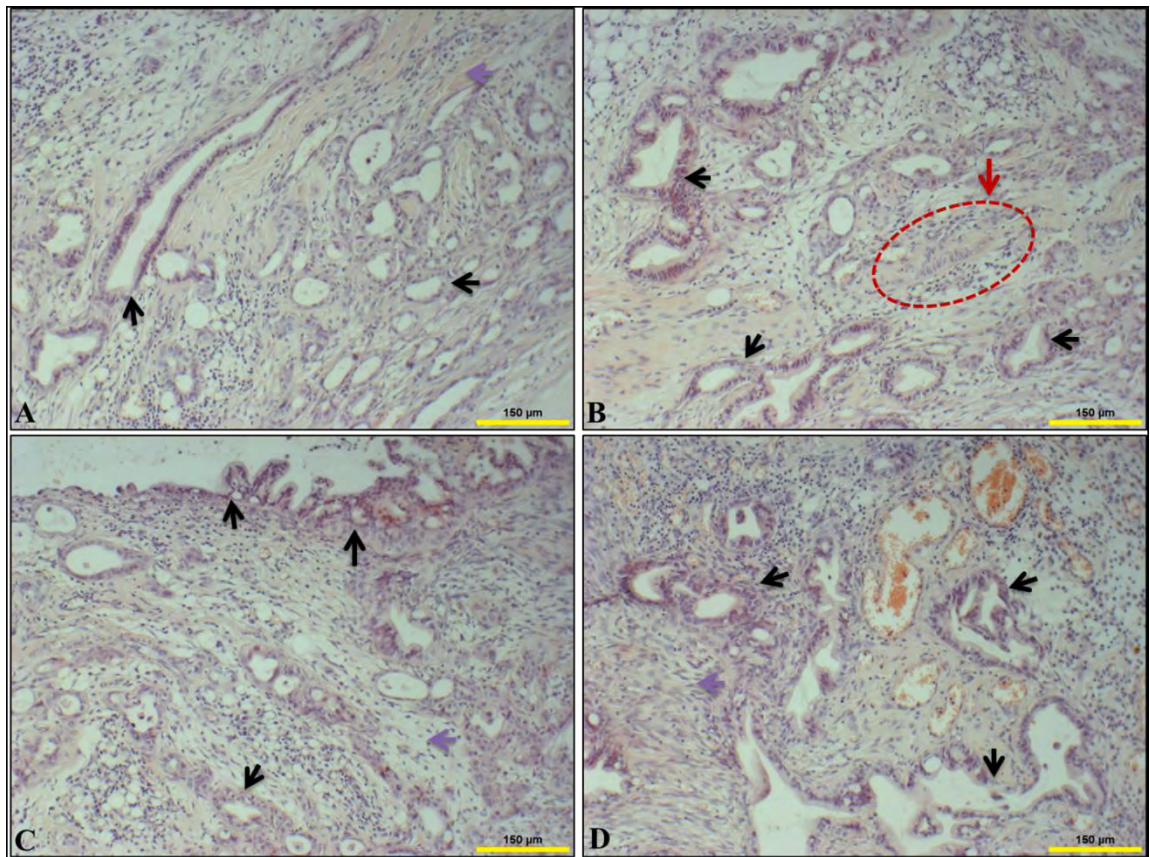


Figure 4-19: Haematoxylin and Eosin (H&E) staining of human adenocarcinoma pancreases tissue case study 3 (10X magnification).

Formalin fixed, paraffin embedded tissue samples were sectioned (5 μ m) and mounted on glass slides. H&E staining was performed in order to make cells visible and define morphology of tissue sections. Images were taken under light microscope at 10X. (A, B, C&D) All ducts were surrounded by **stromal cells or connective tissue** (\leftarrow) and total loss of the pancreatic structure such as loss of lobular structure, no acinar as well as islet cells was observed. Irregular shape and size of the nuclei of ductal (\leftarrow) cells and some of ductal cells with no nuclei was found. Invasion of connective tissue into the bundle of nerve cells (as highlighted in **red circle**) were observed.

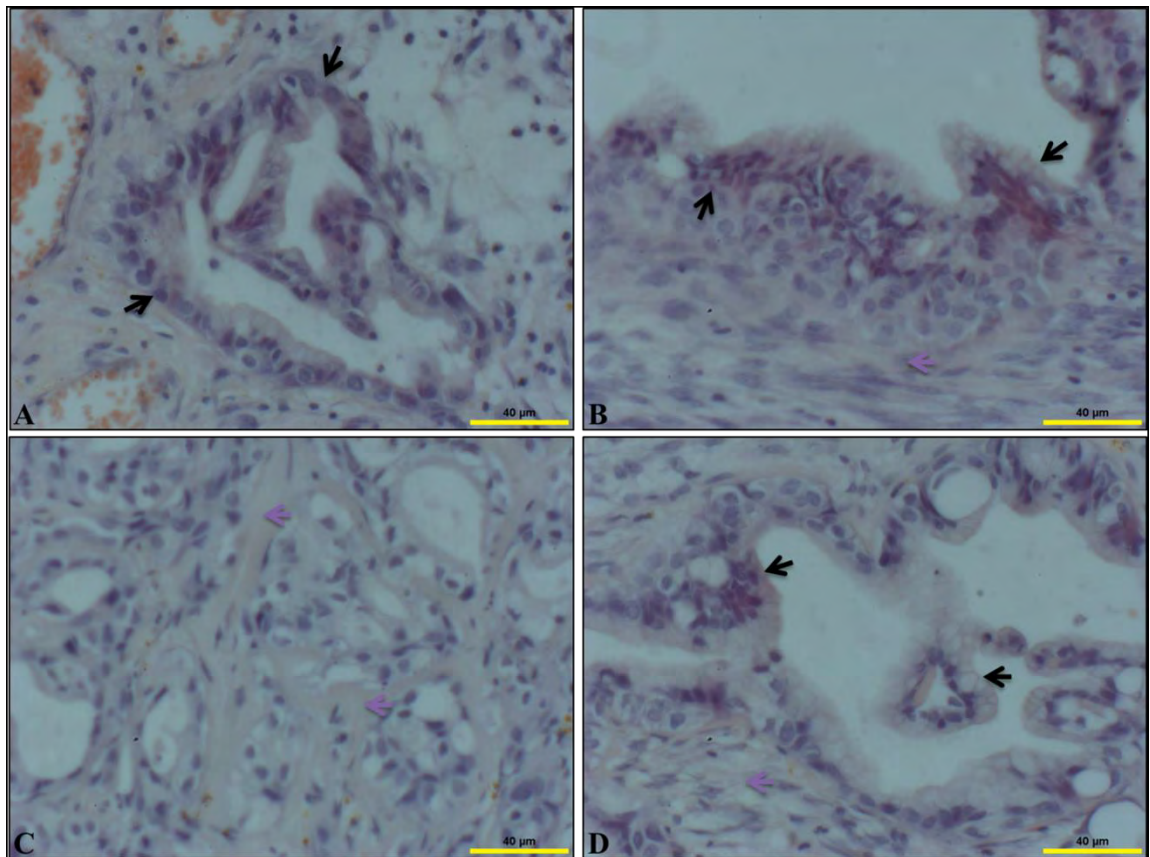


Figure 4-20: Haematoxylin and Eosin (H&E) staining of human adenocarcinoma pancreases tissue case study 3 (40X magnification).

Formalin fixed, paraffin embedded tissue samples were sectioned (5µm) and mounted on glass slides. H&E staining was performed in order to make cells visible and define morphology of tissue sections. Images were taken under light microscope at 40X. (A) Multinucleated, irregular shape and size of the nuclei of ductal (←) cells was found. (B &D) Multinucleated, irregular shape and size of nucleus of ductal (←) cells and **stromal or connective tissue** (←) invasion was observed. (C) All ducts and fat cells were surrounded by **fibrous connective tissue** (←).

4.3.2.4. *Case study 4*

The results from sample 4 are shown in Figure 4-21 (5X), Figure 4-22 (10X) and Figure 4-23 (40X). As shown in Figure 4-21 (A, B, C &D), there is loss of pancreas morphology: Pronounced autolysis of tissue section and loss of lobular morphology are evident. Variably sized and shaped islets of Langerhans are surrounded by desmoplastic connective tissue. Invasion of lymphocyte cells around the tissue section especially near the nerve cell bundle was found. A number of pleomorphic malignant epithelial cells near to the rudimentary exocrine structure were observed. On observing this stained tissue section at higher magnification (10X), Figure 4-22 (A) indicated that pleomorphic malignant epithelial cells were surrounded by desmoplastic connective tissue. Autolysis of islets of Langerhans and invasion of lymphocyte cells to the nerve cell bundle can be observed in Figure 4-22 (B). There were small duct like structures and variable sizes of islets of Langerhans were surrounded by desmoplastic connective tissue. Figure 4-22 (C &D) indicating that lymphocyte cells and pleomorphic malignant epithelial cells were invaded to the nerve cell bundle. On analysing this tissue section at higher magnification (40X) in Figure 4-23 (A) results indicated pleomorphic malignant epithelial cells and multinucleated ductal epithelial cells were surrounded by desmoplastic connective tissue. Also invasion of lymphocyte cell to the nerve cell bundle was observed in Figure 4-23 (B&C). Large size islets of Langerhans were surrounded by desmoplastic connective tissue as shown in Figure 4-23 (D).

H&E staining analyses of sample 4 shows a loss of lobular morphology, loss of acini and the presence of large number of islets of Langerhans, indicating that this tissue is moderately differentiated pancreatic adenocarcinoma.

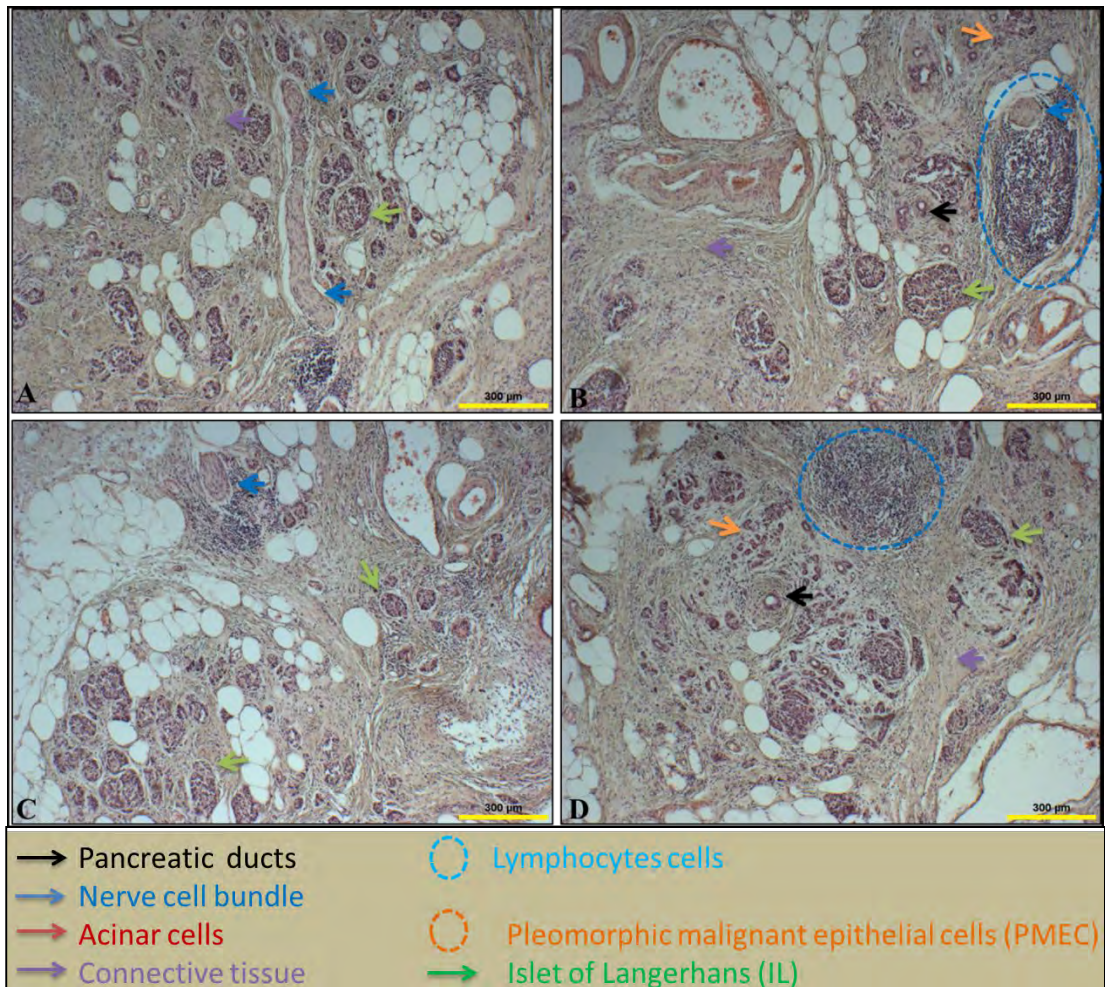


Figure 4-21: Haematoxylin and Eosin (H&E) staining of human pancreatic cancer tissue case study 4 (5X magnification).

Formalin fixed, paraffin embedded tissue samples were sectioned (5µm) and mounted on glass slides. H&E staining was performed and images were captured by light microscopy at 5X magnification. (A, B, C&D): Pronounced autolysis, loss of lobular morphology and acinar cells of pancreas tissue sections. Lymphocyte cells (dark nucleus in blue circle, as highlight in blue circle) invaded to nerve cell bundle. Variable sized and number of islet of Langerhans (←) surrounded by highly desmoplastic connective (←) tissue. (B&D): Pleomorphic malignant epithelial (←) cells at different places of tissue sections.

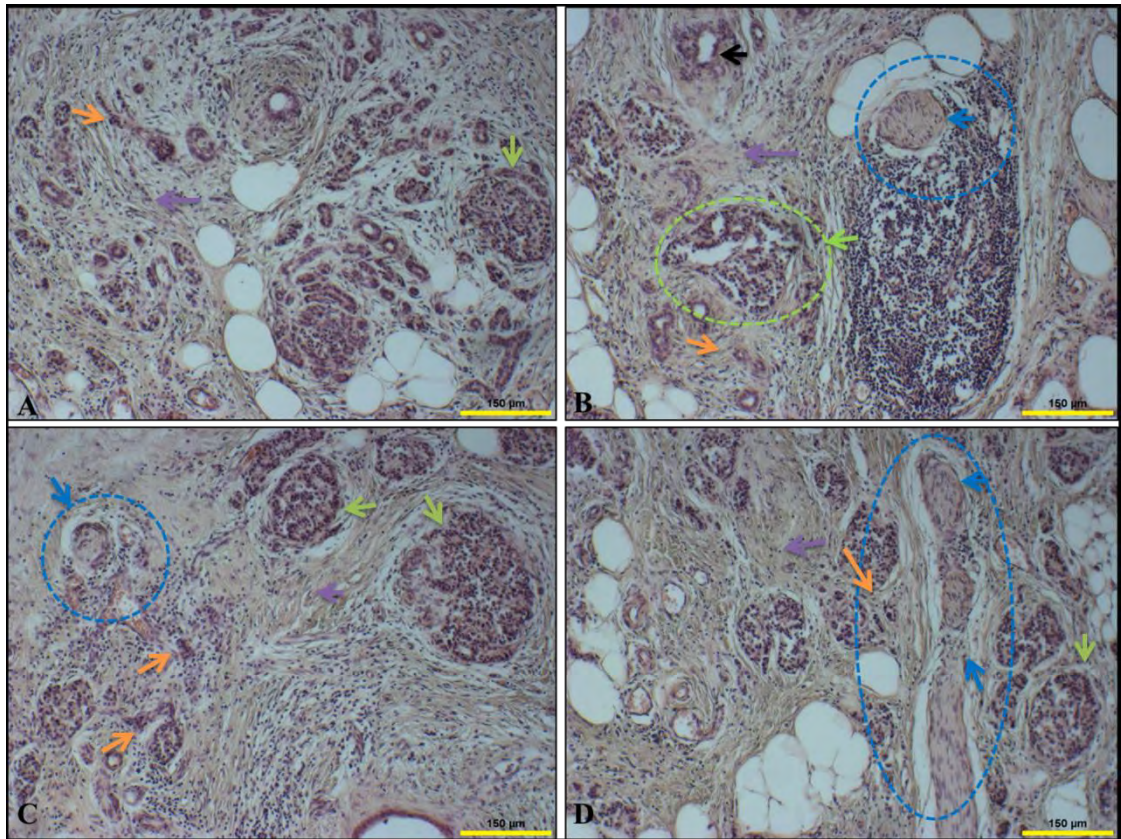


Figure 4-22: Haematoxylin and Eosin (H&E) staining of human pancreatic cancer tissue case study 4 (10X magnification).

Formalin fixed, paraffin embedded tissue samples were sectioned (5µm) and mounted on glass slides. H&E staining was performed and images were captured by light microscopy at 10X magnification. (A) Autolysis of lobular morphology and invasion of desmoplastic connective tissue. **Pleomorphic malignant epithelial (←)** cells around the small duct like structures. (B, C & D) Invasion of lymphocyte cells throughout the tissue section, autolysis of **islet of Langerhans (←)** (as highlighted in **green circle**), tissue section at different places and **pleomorphic malignant epithelial (←)** cells and invasion of fibrous connective tissue into or around the nerve cell bundle as highlighted in **blue circle**.

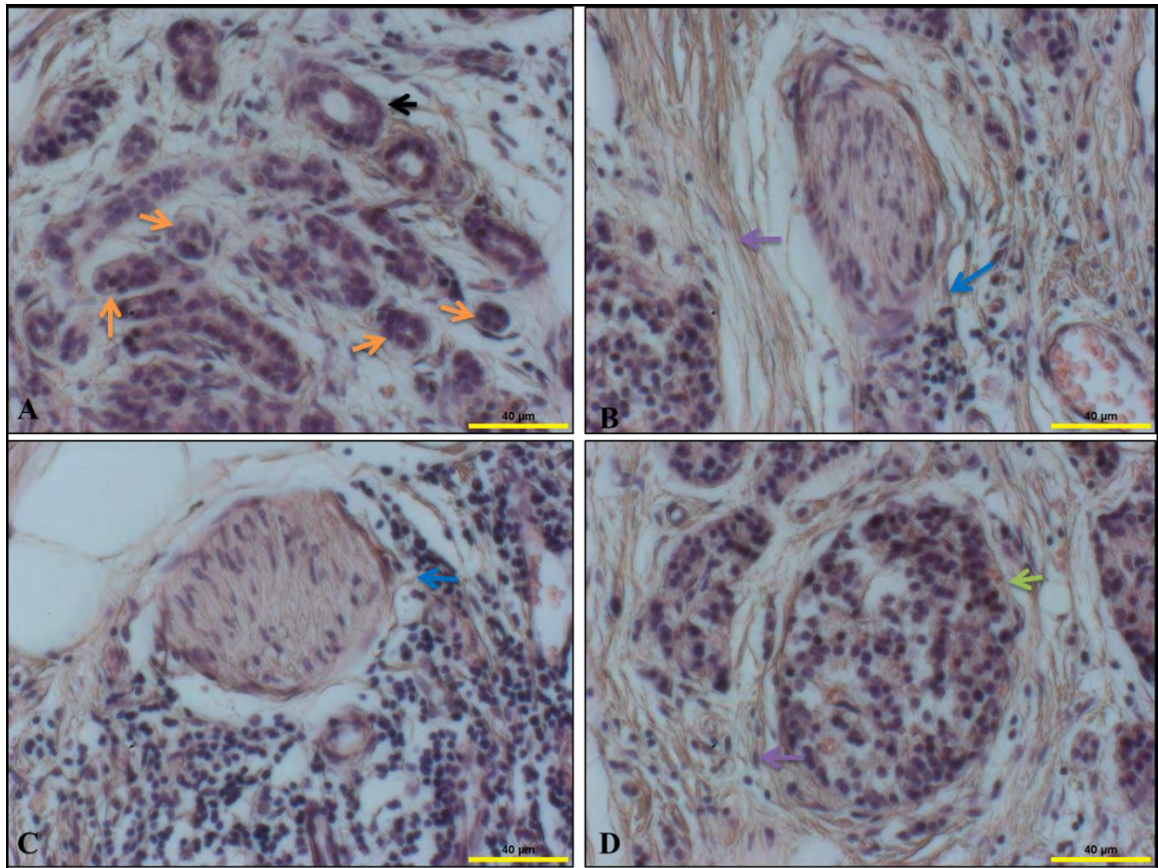


Figure 4-23: Haematoxylin and Eosin (H&E) staining of human pancreatic cancer tissue case study 4 (40X magnification).

Formalin fixed, paraffin embedded tissue samples were sectioned (5µm) and mounted on glass slides. H&E staining was performed and images were captured by light microscopy at 40X magnification. Key characteristics noted are: (A) Group of **pleomorphic malignant epithelial** (←) cells and multinucleated ductal cells (←) (B & C) Invasion of lymphocytes and **fibrous connective** (←) tissue into the **nerve** (←) cell bundle (D) Free standing islets surrounded by **fibrous connective** (←) tissue.

4.4. Discussion

This chapter focused specifically on the detailed morphology of normal and cancerous pancreas cells and tissues. Initial experiments were designed to investigate the morphology of pancreatic adenocarcinoma (PSN-1), rat pancreatic ductal (ARIP) and mouse β -cells (MIN6) under normoxic and hypoxic conditions by phalloidin staining and scanning electron microscopy. Firstly any change in morphology from a serum starved (G0) condition to normoxic and hypoxic condition at 12 or 24 hours of all three cell lines was investigated by staining with phalloidin which helps to visualise the cytoskeleton and DAPI to visualise the nucleus of the cells. Results from experiments demonstrated that PSN-1 cells (a human pancreatic adenocarcinoma cell line) have characteristics of cancer cells, such as cells with more than one nucleus, a high nucleus to cytoplasm ratio, irregular growth pattern, irregular shape of cytoskeleton and irregular shape and size of nucleus as shown in Figure 4-1. PSN-1 cells under normoxic and hypoxic conditions shared the same morphology and no effect of hypoxia on morphology was observed. Morphology of PSN-1 cells was further confirmed by SEM analysis as shown in Figure 4-4. SEM analysis showed that the PSN-1 cells surface was covered by small finger-like protrusions called filopodia and cells were connected with each other with long arm-like extensions called lamellipodia. These spiked extensions from the PSN-1 cell surface distinguish cancer cells from normal cells. These membrane extensions provide a mechanism for cancer cells to invade to adjacent tissue and further to migrate into blood stream and finally to attack other organs by metastasis [332]. Increased filopodia formation has been associated with cancer cell migration [333] and invasion [334] and plays important role in the process of EMT (Epithelial-mesenchymal transition [335]. Results from both studies (cytoskeleton and SEM) of PSN-1 cell, indicated that the cell population under hypoxic and normoxic conditions

remained approximately the same and that cells are characteristic of pancreatic cancer, as shown in Figure 4-1 and Figure 4-4.

On investigating the morphology of pancreatic ductal cells (ARIP cells), staining with phalloidin and DAPI showed that cells under hypoxic (12 hours) and normoxic conditions (12 or 24 hours) had large cytoplasm compared to the nuclei, regular shaped cytoskeleton as well as nucleus and rounded shaped nuclei which were localized in the centre of cells. However, following 24 hours in hypoxic conditions, ARIP cells were irregularly sized, shaped with rough cytoskeleton as shown in Figure 4-2. These results show that hypoxic condition does have some effect on the morphology of ARIP cell. Investigation of ARIP cell morphology was further studied by SEM analysis. SEM analysis shows that ARIP cells under normoxic (12 or 24 hours) and hypoxic (12 hours) conditions had a smooth cell surface (Figure 4-5) as compared to PSN-1 cells surface (Figure 4-4). However, following 24 hour in hypoxic conditions, ARIP cells surfaces were covered with filopodia (Figure 4-5), which is one the key characterises of cancer cells, as discussed earlier. It is quite interesting that ARIP cells are adapted to hypoxic conditions (no sign of necrosis was observed as shown in Figure 3-5) but change in the morphology occur from normal to cancerous, as shown by morphological analyses (Phalloidin and SEM analysis). There has been longstanding debate about the specific type and origin of cells that are transformed in pancreatic adenocarcinoma [343, 344]. Filopodia development (Figure 4-5) and no necrosis (Figure 3-5) under hypoxic conditions might be an adaptation or resistance response to the hypoxia; this was observed in ARIP cells. Hypoxia and easy adaptation (mutation) of ARIP (pancreatic ductal) cells may be the two reasons behind that most of pancreatic cancer cases arise from pancreatic ducts especially ductal adenocarcinoma [69, 70].

MIN6 cells morphology was also investigated by phalloidin staining and SEM. Phalloidin staining showed that MIN6 cells under hypoxic and normoxic conditions

have a regular shape and size. Cells grow in clusters with nuclei localised in the centre of cells and regular shape and size of nuclei was observed (Figure 4-3). SEM analysis further showed that MIN6 cells grow in groups connected with each other. Cell to cell contact is very important in β -cells in islets for integrated secretory responses [340]. Surface analysis showed that the MIN6 cell surface at G0 and N12 hour condition had rough surfaces, whereas at N24 cell surfaces were quite smooth, with small bulges. However, under hypoxic conditions MIN6 cells showed a change in the morphology, as the membrane showed blebbing (apoptosis) and pores (characteristic of necrosis). Also from SEM analysis it was clear that the population of MIN6 cells was increased from G0 to N12 and further by N24; however, from G0 to H12 and then H24 the cell population was decreasing, as shown in Figure 4-6. Both viability (Figure 3-6) and morphology (Figure 4-6) analysis indicated that MIN6 cells undergo apoptosis and necrosis under hypoxic conditions. β -cell death under hypoxic conditions particularly explains the huge loss of islet cell number and functions during the process of islet transplantation. Pancreatic islets are highly vascularized and the very first day after transplantation they face low oxygen concentration/availability (hypoxia), especially cells deep inside the islet (which may even face anoxia) resulting in detrimental effect on the cell number, survival and functions [345]. In addition to this reduced beta cell mass, which is a hallmark of type 1 diabetes and seen in advanced type 2 diabetes [346], it has previously been suggested that islet cells may be exposed to hypoxia in the disease process of diabetes [347]. From this study we can conclude that our data is consistent with the hypothesis that loss of beta cell mass in diabetes or loss of islet mass during the process islet transplantation, may be because of hypoxic conditions which ultimately induce apoptosis, resulting in direct loss of beta cells mass. Morphology studies also confirmed that, PSN-1, ARIP and MIN6 cells are true representatives of pancreatic cancer, pancreatic ductal and β -cells respectively.

In the present study we further studied human pancreatic adenocarcinoma tissue biopsies (paraffin embedded) from the patients diagnosed with pancreatic adenocarcinoma. In order to define the histopathology of pancreatic tissue biopsies (paraffin embedded) samples, H&E staining was performed. Due to unavailability of normal human pancreas tissue, mouse pancreas was utilised as a control and analysed by phalloidin staining and H&E staining. H&E and phalloidin staining demonstrated that the normal pancreas was divided into lobules and these lobules were composed of numerous ring-like structure called acini. Pancreatic acini are composed of acinar cells with rounded nuclei and are arranged around the very small lumen. These numerous acini are connected to intercalated ducts which further open into intralobular ducts. Islets of Langerhans (clusters of cells) are surrounded by numerous acini and scattered in a random pattern within or on the edge of lobules as shown in Figure 4-7 to Figure 4-11. This data confirms that the pancreas consists of different specialised cells allowing pancreas to perform as a multifunctional organ. The pancreas is divided into exocrine (acinar cells and ductal cells producing gastric juices) and endocrine (islet of Langerhans producing insulin & other hormones) pancreas [348]. The majority of pancreatic cancers arise in the exocrine part of the pancreas especially adenocarcinoma (ductal epithelial cell lining) and these account for ~90% of all pancreatic cancer [69, 70]. The second most common histological type of pancreatic cancer is mucin secreting tumour cancer also from exocrine part of pancreas and accounts for <10% of pancreatic cancer [71]. Whereas the tumours from endocrine cells are quite rare and these tumours arise from beta and alpha cells [349]. Histological evaluation remains a vital tool for diagnosis of any cancer. Most pancreatic cancers are well to moderately differentiated, however, variation of differentiation within the same neoplasm is quite common. Well to poor differentiation is uncommon [80, 338, 350]. Tumour microenvironment plays a vital role in the process of initiation, progression and invasion of pancreatic

adenocarcinoma [351, 352] including processes such as activation of pancreatic stellate cells leading to pancreatic fibrosis (desmoplasia) [353]. Desmoplastic pancreatic fibrosis (dense collagen-rich) is a major risk factor for malignant phenotype in pancreatic cancer [352, 354, 355].

In the present study, four human pancreas adenocarcinoma tissue samples were studied. Paraffin embedded human pancreas adenocarcinoma tissue were sectioned and stained with H&E staining and analysed by light microscopy. On gross examination by H&E staining of an four human pancreatic adenocarcinoma samples, we found that sample 1 and 2 were well to moderately differentiated but at some part poorly differentiated (total loss of pancreas integrity) (Figure 4-12 & Figure 4-15); sample 3 was moderately to poorly differentiated as show in Figure 4-18 and sample 4 was well differentiated pancreatic cancer (islet, rudimentary acinar and lobular structure) as showed in Figure 4-21. We found that case study 1, 2 and 4 highly were infiltrated with desmoplastic fibrous connective tissue as showed in Figure 4-13 (C), Figure 4-16 (C) and Figure 4-23 (B). It has been reported that desmoplastic reaction is known to contribute to invasion, malignancies and chemoresistance [74, 356]. Once desmoplastic connective tissue invades the nerve cell bundles at this stage, the tumour is highly metastatic and typically infiltrates into the biliary system of pancreas [357, 358]. On very careful examination of human pancreatic adenocarcinoma samples we found that in all case studies (1 to 4) fibrous connective tissue invaded to the nerve cell bundles as show in Figure 4-14 (C), Figure 4-16 (B), Figure 4-19 (B) and Figure 4-23 (B). Human pancreatic adenocarcinoma tissue samples (four case studies) were compared to heathy mouse pancreas as well as to healthy human pancreas data available [18, 19, 336], our results indicated that all cancer samples had loss of lobular structure, showed loss of acinar cells (some rudimentary in sample 1, 2 & 4) and invasion of small gland-like pleomorphic malignant epithelial cell structures. On histological examination small

gland-like pleomorphic malignant epithelial cells are quite commonly found in pancreatic cancer tissue [359, 360].

Clear conclusions can be drawn from our morphology analysis (phalloidin and SEM) that hypoxic conditions did not have any effect on the morphology and population (of human pancreatic adenocarcinoma cells (PSN-1). These results also demonstrated PSN-1 cells have characteristics of cancer cells which distinguish them from other normal cells. SEM and phalloidin analysis revealed that hypoxic conditions do trigger morphological changes in ARIP cells, from normal to cancer. Our results indicate that pancreatic ductal cells (ARIP) can be easily transformed or mutated into cancerous cells by hypoxia and this could be an explanation that most of pancreatic cancer cases arises from ductal epithelial cells especially adenocarcinoma. Beta cell morphological analysis demonstrated that hypoxic conditions have an effect on the morphology of MIN6 cells as well as the population number. Our findings are consistent with the hypothesis that the loss of beta cell mass in diabetes or loss of islet mass during the process islet transplantation, may be because of hypoxic conditions. This hypoxia may ultimately induce apoptosis or necrosis, resulting in direct loss of beta cells mass.

Variability of the severity of the disease (cancer) spread within the tissue sample of human pancreatic adenocarcinoma was found. Samples with well to moderately differentiated pancreatic adenocarcinoma (case study 1,2 &4), moderately to poorly differentiated pancreatic adenocarcinoma (case study 1) and poorly differentiated pancreatic adenocarcinoma (case study 3) were found. Histological examination data indicated the presence of desmoplastic fibrous connective tissue in all four tissue samples, which may ultimately cause tumour hypoxia and chemo-resistance to pancreatic cancer.

Having established that hypoxia does triggered change in the morphology and viability of pancreatic beta cells and ductal cells, whereas no effect was found on the

morphology as well as viability of pancreatic ductal adenocarcinoma cells. So it is essential to understand what molecular pathway pancreatic cancer cells adapt in order to survive under hypoxic conditions and also to investigate the genes play role to trigger apoptosis or necrosis in pancreatic beta and ductal cells? Tumour hypoxia environment has been linked to an aggressive progression and chemoresistance in pancreatic cancer, but the mechanisms by which hypoxic conditions affect progression still remain poorly understood [196]. New targets and more effective therapeutic intervention are required to improve diagnosis and prognosis for all patients with pancreatic cancer. Thus, molecular mechanism and genes involved in pancreatic cancer progression need to be better understood. Program cell death gene 4 (PDCD4), a tumour suppressor was originally identified during the investigation of genes up-regulated in the process of apoptosis. Loss of expression of PDCD4 has been reported in several cancers [111]. However, never been studied in pancreatic cancer and the reason for loss of its expression has never been studied. By answering this question, the role novel tumour suppressor PDCD4 was evaluated. The essential transcription factor up-regulated during hypoxia (HIF-1 α) and transcription factor (NF κ B) active in most of the cancers were evaluated. This research will now delve further in the role of PDCD4, HIF-1 α and NF κ B in human pancreatic adenocarcinoma.

Chapter 5. Programmed Cell Death 4 Gene (*PDCD4*)

5.1. Introduction

Programmed cell death 4 gene (*Pdcd4*) (also known as *MA-3*, *TIS*, *H731* and *DUG*) was first identified during an investigation into genes up-regulated in the process of apoptosis [104]. Now *PDCD4* is a novel tumour suppressor gene which has recently drawn attention because of its down-regulation or loss of expression in several types of cancer such as tongue tumour [136], invasive ductal breast carcinoma [137], skin cancer [123], human glioma [138], nasopharyngeal carcinoma [139], lung cancer [135], gastric cancer [140], colon cancer [141] and ovarian cancer [142]. While loss of *PDCD4* gene has been associated with certain cancers and up-regulation of the PDCD4 protein has been identified in both apoptotic and healthy cells [104]. How PDCD4 exert its effect is not known yet, however, it has been reported that in the cytoplasm PDCD4 protein interacts with eukaryotic translation initiation factor 4A and inhibits its helicase activity resulting in inhibition of protein translation [107, 113]. These findings suggest that the role of PDCD4 protein in protein translation may have a role in the nucleus also.

Interestingly it has been reported that treating cancer cells with various anti-cancerous drugs results in up-regulation of *PDCD4* [143, 361] and induced expression of miRNA-21 down-regulates expression of PDCD4 [145-148]. All these data suggest an important role of PDCD4 in tumour development, and suggest it is a potential target in novel cancer therapies.

PDCD4 comprises 469 amino acids and has multiple phosphorylation sites, but the importance of phosphorylation remained unclear for several years [120]. In 2005, Palamarchuk, *et al.*, reported that Akt phosphorylates PDCD4 and induces translocation of PDCD4 protein from the cytoplasm to nucleus of embryonic fibroblast cells, decreasing its ability to act as an inhibitor of activator protein (AP-1) mediated

transcription [116]. However, conflicting data exist about the subcellular localisation of PDCD4. Some studies have found that PDCD4 is localized in the nucleus in normal cells and in the cytoplasm in cancer cells [123, 124] whilst others have reported that PDCD4 localized in the nucleus in cancer tissues and in the cytoplasm in normal tissues [125]. This conflicting data might be because of the shuttling of PDCD4 between cytoplasm and nucleus [115] or cell type specific localisation of PDCD4 protein [126]. Subcellular localisation and expression of PDCD4 protein in pancreatic cancer, however, has not been extensively studied to date. Pancreatic cancer is one the most notorious malignancies in humans with very low survival rate. Pancreatic tumours often have extreme levels of hypoxia [196] and clinically it is well accepted that hypoxia is responsible for tumour metastasis [362], chemo-resistance and radio-resistance [363]. Hypoxia in tumours regulates and induces the expression of *HIF-1 α* , especially in pancreatic cancer [364]. The relationship between hypoxia (tumour microenvironment) and PDCD4 (novel tumour suppressor) has not been studied before in pancreas cancer. Hypoxia not only plays a crucial role in pancreatic cancer, but also in type 1 diabetes, type 2 diabetes and islets transplant outcome. Diabetes mellitus is a metabolic disorder occurring when beta cells no longer function normally or have been destroyed, resulting in dysfunction of the islets pancreatic and insulin dependency [365, 366]. Apoptosis of pancreatic beta-cells contributes significantly in both type 1 and type 2 diabetes [367, 368]; however, the molecular mechanism of beta-cell death and its regulation are poorly understood. Islets transplantation is a potential long term treatment for diabetes, but a high population of beta-cells die within a few days of transplantation [369]. Recently, PDCD4 has been linked to type 1 diabetes prevention [370], beta-cell neogenesis [280] and obesity linked disease [371]. So understanding the mechanism of beta-cell death and regulation could identify a novel site for therapeutic intervention in diabetes mellitus.

Apoptosis plays a very important role in both pancreatic cancer and diabetes mellitus; *PDCD4* is a novel gene which is up-regulated during apoptosis, thus making *PDCD4* a novel therapeutic target in both pancreatic cancer and diabetes mellitus. The aim of this research was to investigate the expression, regulation and subcellular localisation of *PDCD4* in three pancreatic cell lines (in hypoxic and normoxic environment), mouse pancreas and human pancreatic adenocarcinoma tissues.

5.2. Results

In order to determine the role of *PDCD4* in the pancreas; the expression, regulation and subcellular localisation of *PDCD4* was investigated in three different pancreatic cell lines by performing western blotting and immunocytochemistry. Also expression and subcellular localisation of *PDCD4* was investigated in mouse pancreas and human pancreatic adenocarcinoma tissues (four case studies) by performing immunohistochemistry.

5.2.1. *PDCD4* in pancreatic cells

This study was designed to investigate the influence of cell culture conditions which mimic the oxygen-deprived hypoxic conditions found in the core of a cancerous tumour i.e. hypoxic conditions (1% oxygen) and normal growth culturing conditions i.e. normoxic conditions (21% oxygen) on the expression, regulation and subcellular localisation of *PDCD4* protein in human pancreatic adenocarcinoma (PSN-1), mouse β -cells (MIN6) and rat ductal (ARIP) cell lines. This was investigated by performing western blotting and immunocytochemistry.

5.2.1.1. *Western blotting*

In order to identify the expression, regulation and subcellular localisation of *PDCD4* in PSN-1, MIN6 and ARIP cells; cells were cultured and pelleted at various time points i.e.

G0 (serum starvation), normoxic (N) and hypoxic (H) both at 12 and 24 hours. Cell protein extracts were quantified and separated on 10% SDS-PAGE. Western blotting was performed using a specific antibody to PDCD4 and densitometry analysis was performed using Image j software. Densitometry values from three separate experiments (n=3) were plotted and statistical analyses (2way ANOVA test) was performed on Graphpad prism 5 software. Error bar values represent +/- standard error mean (SEM).

5.2.1.1.1. Human pancreatic adenocarcinoma cells (PSN-1)

In order to determine expression of PDCD4 in human pancreatic adenocarcinoma cells (PSN-1) under different stimuli (serum starved, normoxic and hypoxic), whole cell protein extracts were extracted and western blotting was performed using a specific antibody to PDCD4. Densitometry analysis reveals the expression of PDCD4 is significantly lower at hypoxic 24 hours (H24) ($p < 0.001$) compared with serum starved (G0) and normoxic 24 hours (N24) conditions. PDCD4 expression was significantly higher at N24 ($p < 0.01$) compared to G0 as shown in Figure 5-1. Further subcellular (cytoplasmic and nuclear) localisation of PDCD4 in PSN-1 cells determined by western blot analysis. The results are detailed in Figure 5-2. The cytoplasm expression of PDCD4 is significantly lower at H24 ($p < 0.01$) and higher at N24 ($p < 0.05$) compared to G0 conditions. On comparing cytoplasmic to nuclear expression; PDCD4 was highly expressed in the cytoplasm compared to the nucleus of PSN-1 cells. Expression of PDCD4 in nucleus is not significantly different at any time point between hypoxic and normoxic conditions in PSN-1 cells as shown in Figure 5-2 (C).

5.2.1.1.2. Pancreatic ductal cells (ARIP)

Subcellular expression of PDCD4 in pancreatic ductal cells was investigated under different stimuli (serum starved, normoxic and hypoxic). Cytoplasmic and nuclear protein extracts were extracted from ARIP cells and western blotting was performed.

The results are displayed in Figure 5-3. Densitometry analysis indicated that in the cytoplasm PDCD4 was expressed significantly higher at H24 ($p < 0.01$) and significantly lower at N12 ($p < 0.01$) compared G0. On comparing cytoplasmic to nuclear expression; PDCD4 was highly expressed in the cytoplasm compared to the nucleus of ARIP cells. However, no significant expression difference of PDCD4 in the nucleus was found.

5.2.1.1.3. Pancreatic beta cells (MIN6)

The effect of hypoxia on the subcellular expression of PDCD4 in beta cells at different time points was investigated. Cytoplasmic and nuclear protein extracts were extracted from MIN6 cells and western blotting was performed. In Figure 5-4 it is clear from the densitometry analysis that in the cytoplasm, expression of PDCD4 was significantly higher at H24 ($p < 0.001$) compared to all time points and significantly lower at N24 ($p < 0.05$) compared to H12 and H24 conditions. In the nucleus PDCD4 expression was significantly lower at H12 ($p < 0.05$) compared to N12 as shown in Figure 5-4.

Pancreatic adenocarcinoma cells

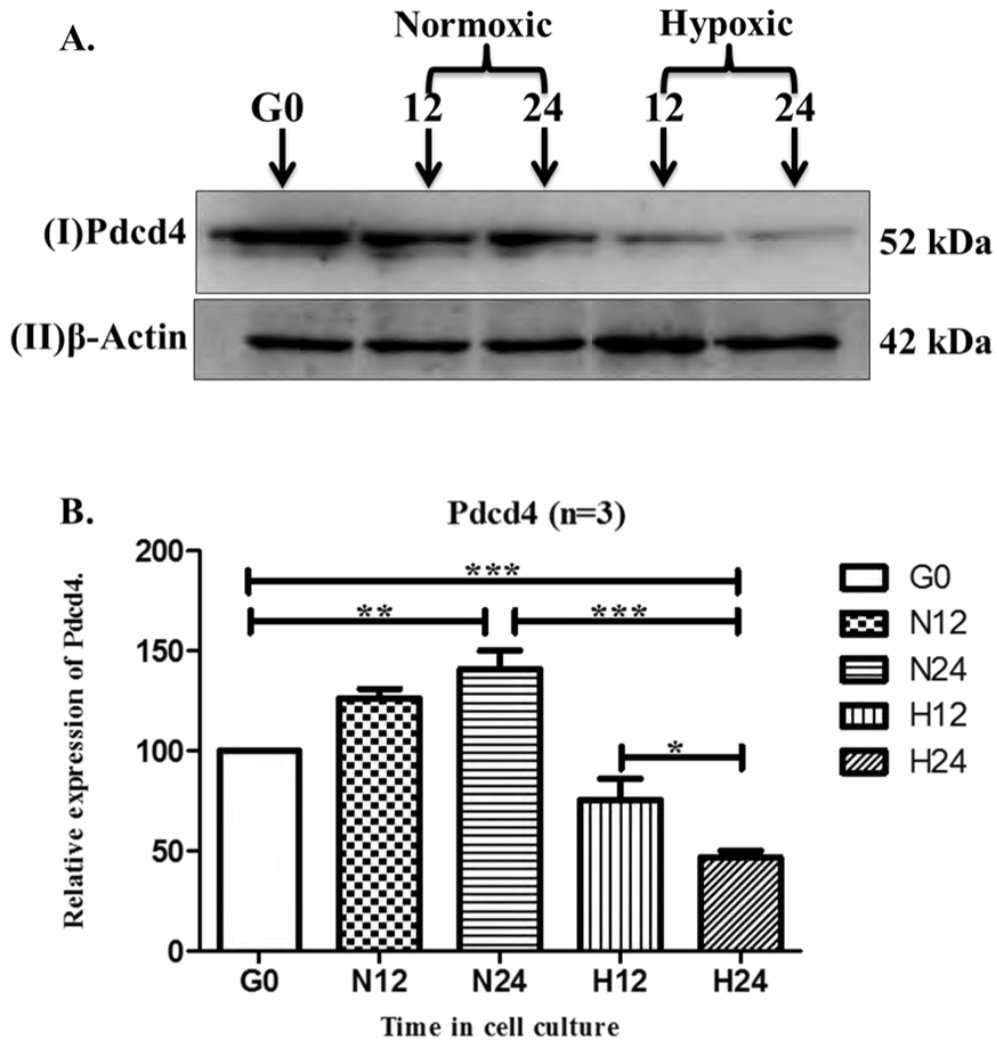


Figure 5-1: Expression of PDCD4 under hypoxic and normoxic conditions in human pancreatic adenocarcinoma cells.

PSN-1 cells were exposed to hypoxic or normoxic conditions over 24 hours. 10 μ g of whole cell extract was separated by 10% SDS-PAGE. Proteins were analysed by western blotting using an antibody specific to PDCD4. Panel A (I) represents PDCD4 (52kDa) protein expression and (II) represents protein loading control β -actin (42kDa). Panel B illustrates densitometry of PDCD4 relative to β -actin. These results were reproduced in at least three separate experiments. Error bar values represent mean \pm standard error. Expression of PDCD4 was significantly higher at N24 (**p<0.01) and significantly lower at H24 (**p<0.001) compared to G0. Expression of PDCD4 was significantly higher at N24 (**p<0.001) compared to H24 and expression at H12 (*p<0.05) was higher compared to H24.

Pancreatic adenocarcinoma cells

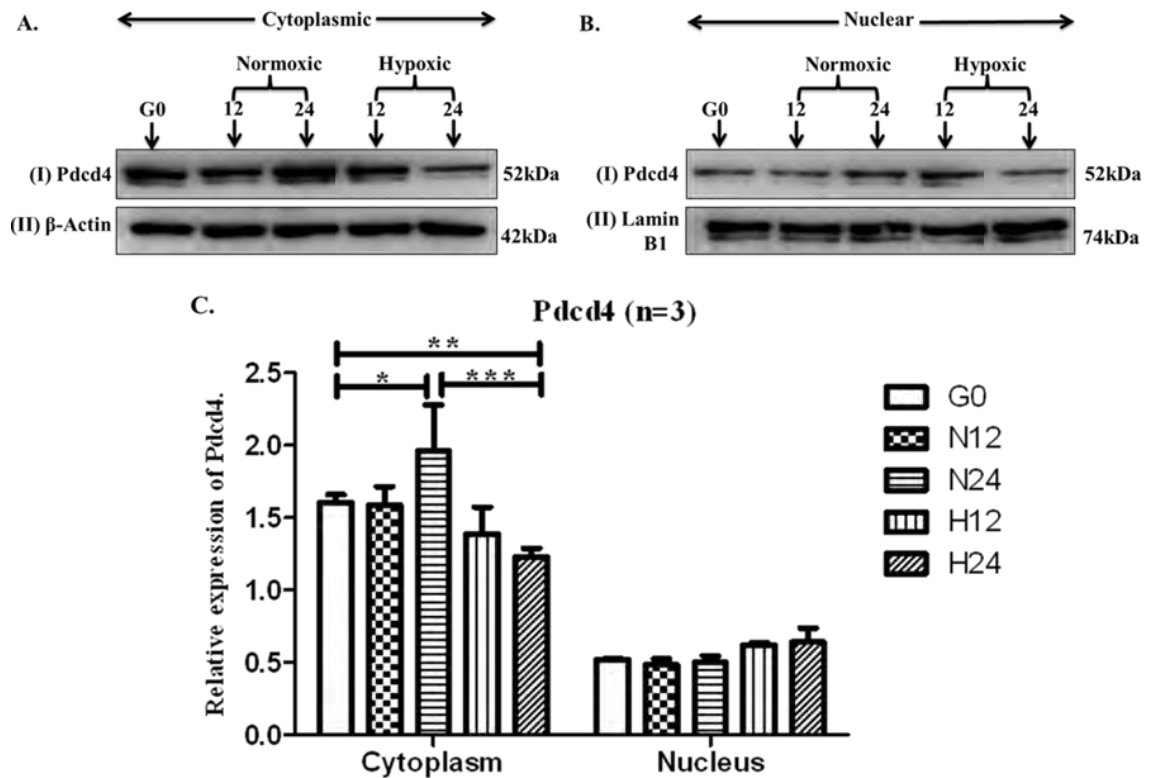


Figure 5-2: Subcellular expression (A) cytoplasm and (B) nucleus of PDCD4 in human pancreatic adenocarcinoma cells.

PSN-1 cells were cultured under G0 (serum starvation), normoxic or hypoxic conditions for 12 and 24 hours. Following incubation the cells were pelleted. Cytoplasmic and nuclear proteins were extracted and 10 μ g of cytoplasmic and nuclear cell extract were separated on a 10% SDS-PAGE. Proteins were analysed by western blotting using an antibody specific to PDCD4. Panel A (I) represents PDCD4 (52kDa) protein expression in the cytoplasm (II) represents protein loading control β -actin (42kDa). Panel B (I) represents PDCD4 (52kDa) protein expression in the nucleus (II) represents protein loading control lamin B1 (74kDa). Panel C illustrates densitometry analyses, showing cytoplasmic PDCD4 relative to control β -actin and nuclear PDCD4 relative to lamin B1. These results were reproduced in at least three separate experiments. Error bar values represent mean \pm standard error. PDCD4 was highly expressed in the cytoplasm as compared to the nucleus. Expression of PDCD4 was significantly higher at N24 (* p <0.05) and significantly lower at H24 (** p <0.01) compared to G0. However, no significant difference in expression between time points and conditions in the nucleus was found.

Pancreatic ductal cells

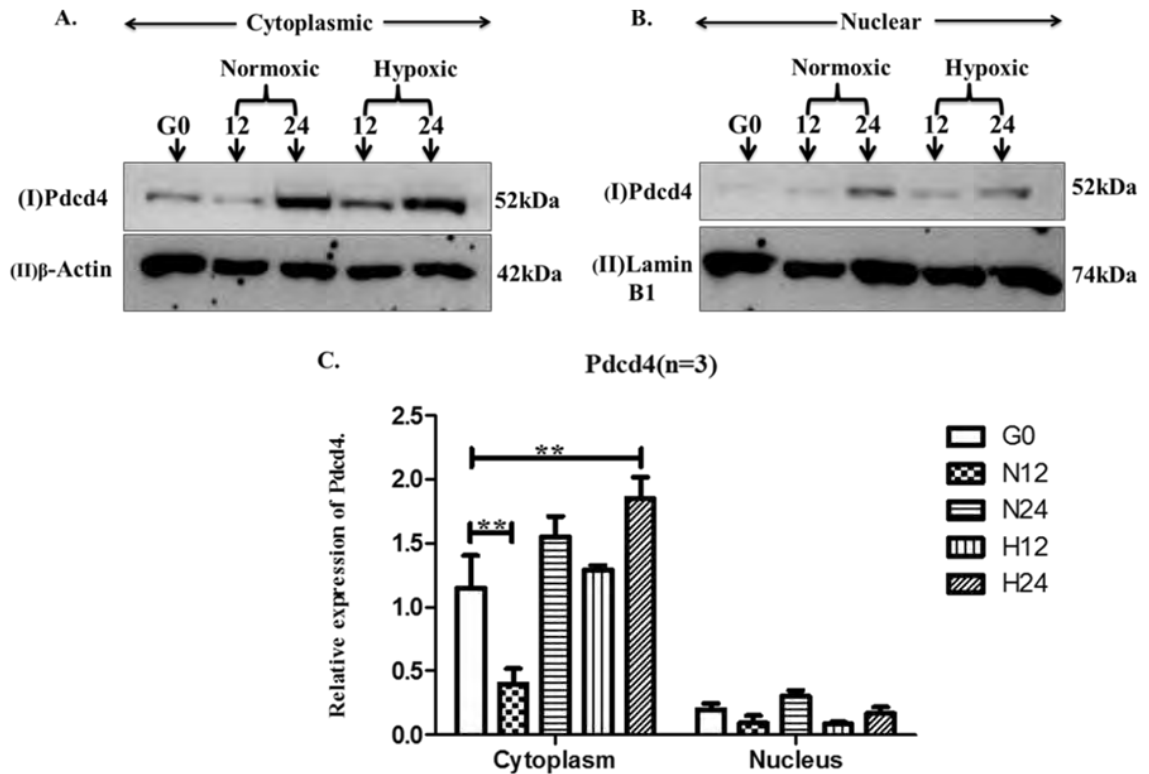


Figure 5-3: Subcellular expression (A) cytoplasm and (B) nucleus of PDCD4 in pancreatic ductal cells.

ARIP cells were cultured under G0 (serum starvation), normoxic or hypoxic conditions for 12 and 24 hours. Following incubation the cells were pelleted. Cytoplasmic and nuclear proteins were extracted and 10 μ g of cytoplasmic and nuclear cell extract were separated on a 10% SDS-PAGE. Proteins were analysed by western blotting using an antibody specific to PDCD4. Panel A (I) represents PDCD4 (52kDa) protein expression in the cytoplasm (II) represents protein loading control β -actin (42kDa). Panel B (I) represents PDCD4 (52kDa) protein expression in the nucleus (II) represents protein loading control lamin B1 (74kDa). Panel C illustrates densitometry analyses, showing cytoplasmic PDCD4 relative to β -actin and nuclear PDCD4 relative to lamin B1. These results were reproduced in at least three separate experiments. Error bar values represent mean \pm standard error. PDCD4 was highly expressed in the cytoplasm as compared to the nucleus. Expression of PDCD4 was significantly higher at H24 (**p<0.01) and significantly lower at N12 (**p<0.01) compared to G0. However, no significant difference in expression between time points and conditions in the nucleus was found.

Pancreatic beta cells

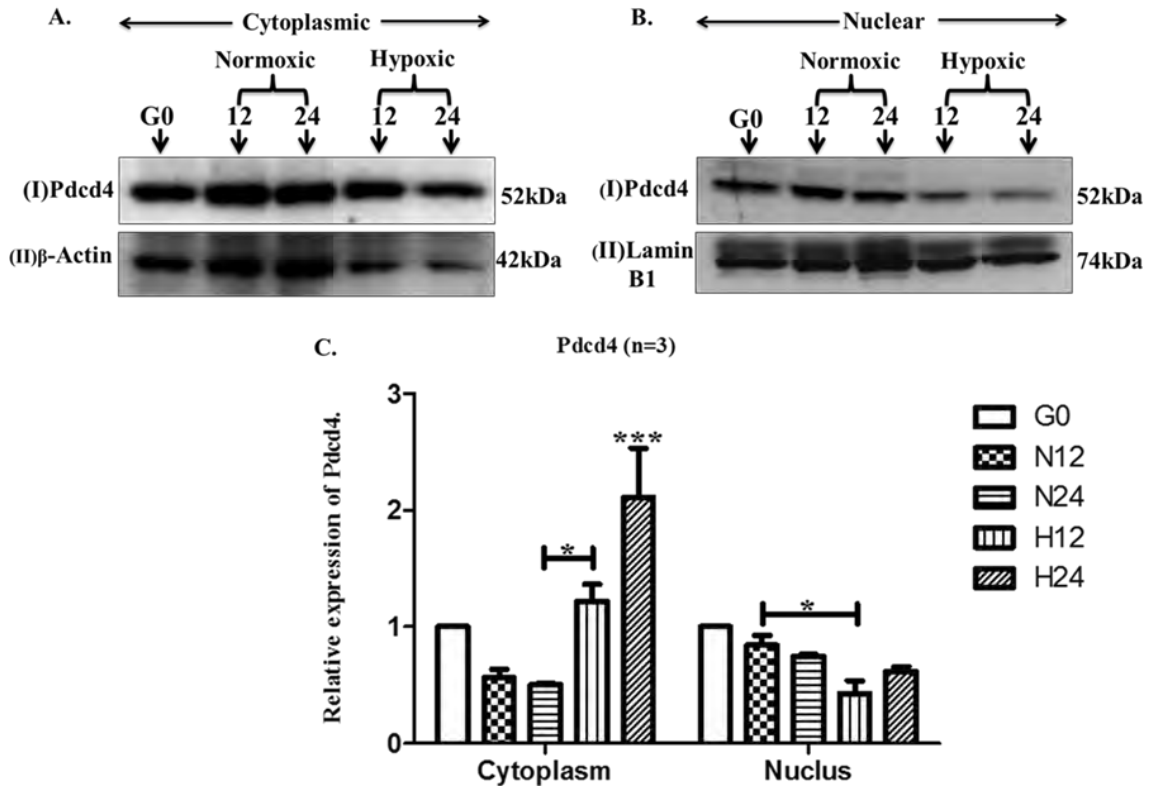


Figure 5-4: Subcellular expression (A) cytoplasm and (B) nucleus of PDCD4 in pancreatic beta cells.

MIN6 cells were cultured under G0 (serum starvation), normoxic and hypoxic conditions for 12 or 24 hours. Following incubation the cells were pelleted. Cytoplasmic and nuclear proteins were extracted and 10 μ g of cytoplasmic and nuclear cell extract were separated on a 10% SDS-PAGE. Proteins were analysed by western blotting using an antibody specific to PDCD4. Panel A (I) represents PDCD4 (52kDa) protein expression in the cytoplasm (II) represents protein loading control β -actin (42kDa). Panel B (I) Represents PDCD4 (52kDa) protein expression in the nucleus (II) represents protein loading control lamin B1 (74kDa). Panel C illustrates densitometry analysis, showing cytoplasmic PDCD4 relative to β -actin and nuclear PDCD4 relative to lamin B1. These results were reproduced in at least three separate experiments. Error bar values represent mean \pm standard error. PDCD4 was highly expressed in the cytoplasm as compared to the nucleus. Cytoplasmic expression of PDCD4 was significantly higher at H24 (** p <0.001) (low cells viability) compared to normoxic samples (high cells viability). However, PDCD4 nuclear expression at H12 (* p <0.05) was significantly lower compared to N12 and G0 samples.

These results indicated that hypoxia induced the expression of PDCD4 in pancreatic beta cells (MIN6) and ductal cells (ARIP); however, loss or reduced expression of PDCD4 was observed under hypoxic condition in human pancreatic adenocarcinoma cells (PSN-1).

5.2.1.2. *Immunocytochemistry*

In an attempt to further investigate subcellular localisation and expression of PDCD4 in PSN-1, ARIP and MIN6 cells: Cells were cultured and fixed with 3.7% formalin at various time points i.e. G0 (serum starvation), normoxic and hypoxic both for the 12 and 24 hours. Immunocytochemistry was performed using an antibody specific to PDCD4 and FITC and TRIC labelled secondary antibodies were used. Labelled cells on coverslips were mounted on glass slides with mounting medium containing DAPI to stain the nucleus. Samples were analysed by confocal microscopy (Leica TCS SP5 confocal microscope) and images were captured at 65X magnification. Experiments were repeated on at least three separate occasions with similar results seen.

5.2.1.2.1. **Human pancreatic adenocarcinoma cells (PSN-1)**

In order to determine subcellular localisation and expression of PDCD4 in human pancreatic adenocarcinoma cells (PSN-1) under different stimuli (serum starved, normoxic and hypoxic) at different time points by immunocytochemistry. These results are detailed in **Figure 5-5**. PDCD4 was exclusively expressed in the cytoplasm under all conditions at all-time points except normoxic 24 hours (N24) which shows low diffuse expression in the nucleus as well. PDCD4 was highly expressed at normoxic 12 and 24 hours compared to G0. However, very low expression of PDCD4 was observed under hypoxic (24 hours) conditions compared to G0 and normoxic 12 and 24 hours conditions, as shown in Figure 5-5.

5.2.1.2.2. Pancreatic ductal cells (ARIP)

Further subcellular localisation and expression of PDCD4 was investigated in pancreatic ductal cells (ARIP) under same stimuli (serum starved, normoxic and hypoxic) at different time points by immunocytochemistry. Immunocytochemistry results are detailed on Figure 5-6. From confocal image analysis of ARIP cells it is clear that PDCD4 was exclusively expressed inside the cytoplasm at G0, N12 and H12. However, PDCD4 was highly expressed in the cytoplasm with diffused expression in nucleus at N24 and H24. It was also clear that PDCD4 is highly expressed at N24 and H24 compared to G0, N12 and H12 as shown in Figure 5-6.

5.2.1.2.3. Pancreatic beta cell (MIN6)

The effect of hypoxia on the subcellular localisation and expression of PDCD4 in beta cells under same stimuli (serum starved, normoxic and hypoxic) at different time points was investigated by immunocytochemistry. Results are displayed on Figure 5-7. Confocal image analysis of MIN6 cells showed that PDCD4 at all-time points was highly expressed in the cytoplasm and diffusely expressed inside the nucleus, excluding H24 where PDCD4 was exclusively and highly expressed in the cytoplasm only as shown in Figure 5-7.

These results suggest that PDCD4 was mostly localised in the cytoplasm of PSN-1, ARIP and MIN6 cells under hypoxic and normoxic conditions. These results further confirmed loss or reduced expression of PDCD4 under hypoxic conditions in PSN-1 cells, however, higher expression of PDCD4 under hypoxic conditions was observed in MIN6 and ARIP cells.

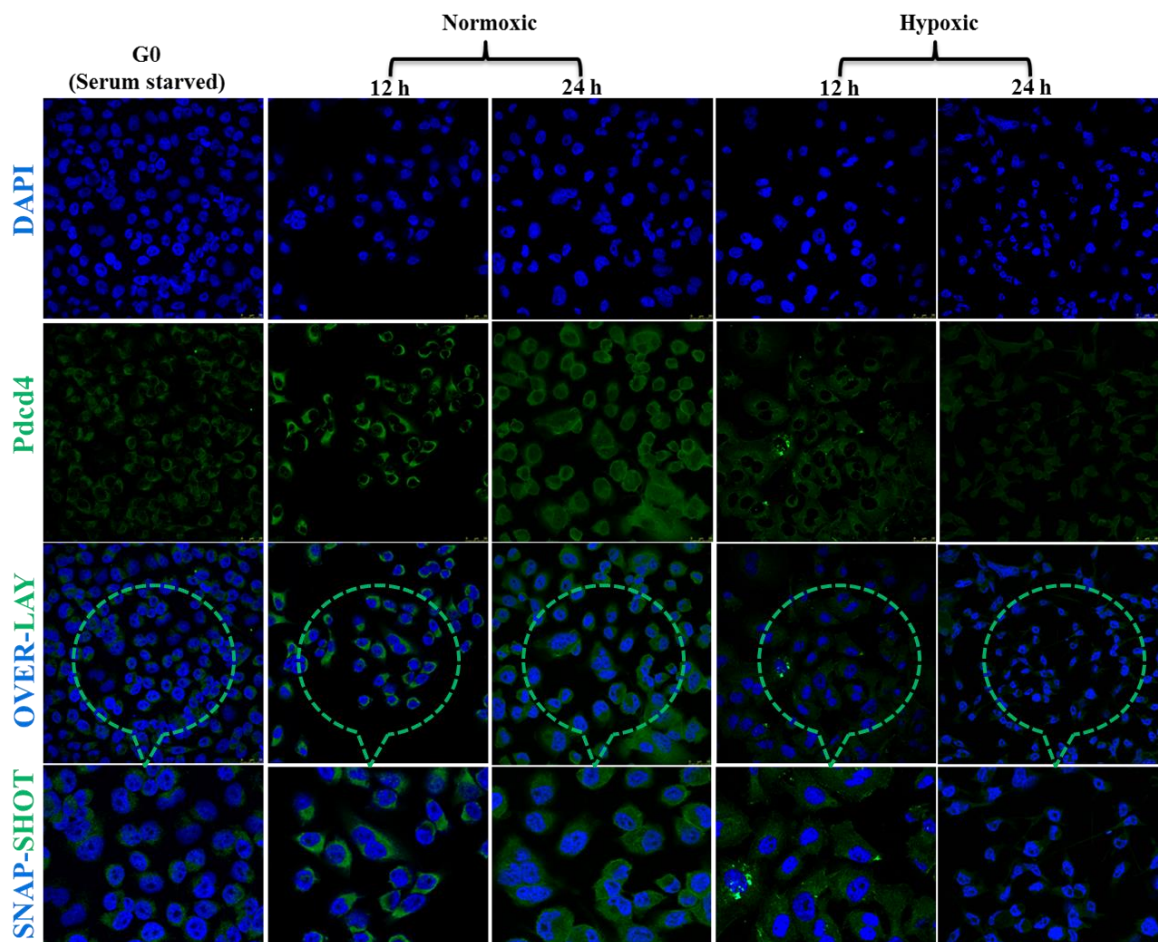


Figure 5-5: Sub-cellular localisation and expression of PDCD4 in human pancreatic adenocarcinoma cells.

PSN-1 cells were grown on glass cover slips in six well plates and fixed at various time points i.e. at G0 (Serum starvation), N12 & N24 (Normoxic) and H12 & H24 (Hypoxic). Immunocytochemistry was performed using a specific antibody to **PDCD4** and FITC labelled secondary antibody was used. Coverslips with cells were mounted on glass slides with mounting medium containing **DAPI (Blue)**, which stains the nucleus of the cells. Cells were analysed by confocal microscopy and images were captured at 65X magnification. Results are representative of three separate experiments and images were representative of six separate fields. **PDCD4** localized and expressed At G0: Cytoplasmic and low expression; At N12: Cytoplasmic; At N24: Cytoplasmic and very low nuclear; At H12: Cytoplasmic and low expression and At H24 very low and cytoplasmic expression. Over-all **PDCD4** was highly expressed in the cytoplasm, with very low expression under hypoxic conditions.

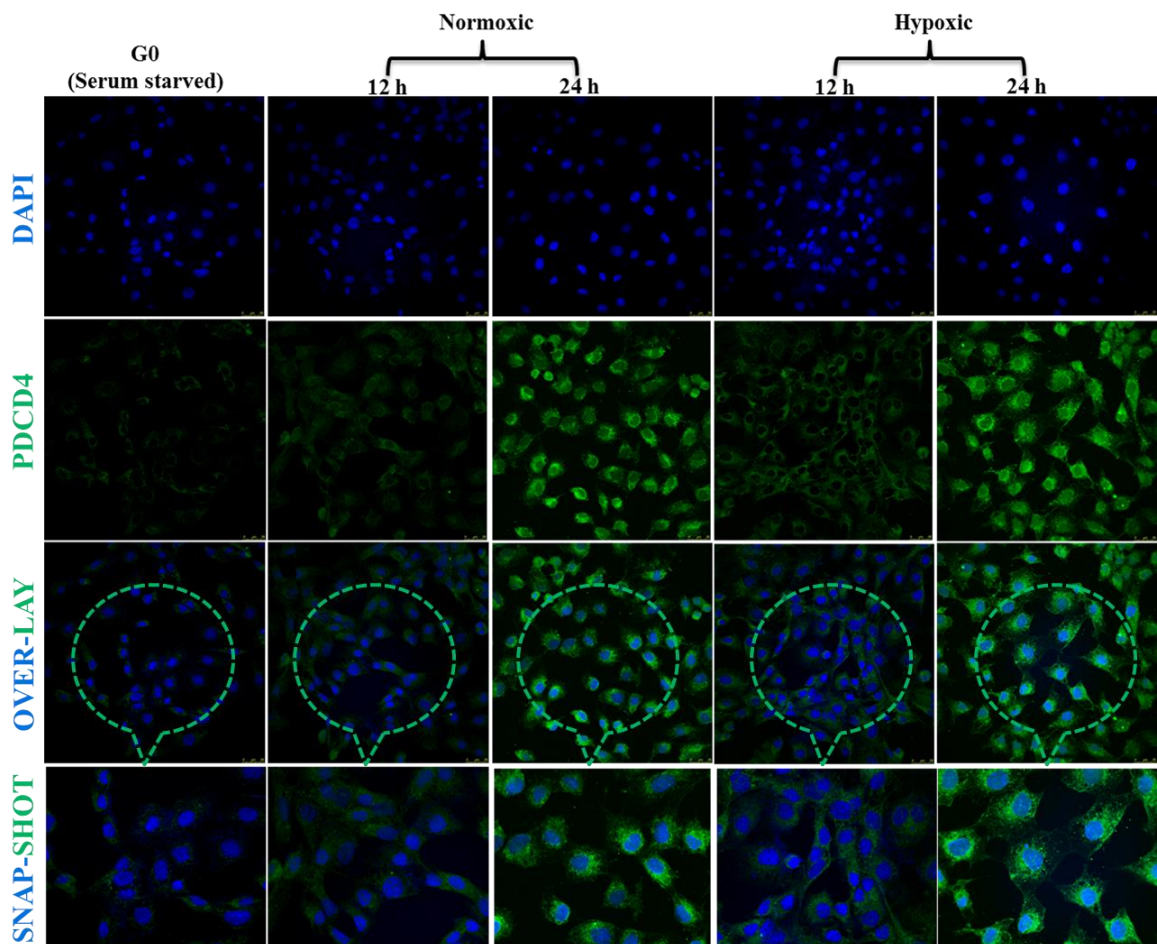


Figure 5-6: Sub-cellular localisation and expression of PDCD4 in pancreatic ductal cells.

ARIP cells were grown on glass cover slips in six well plates and fixed at various time points i.e. at G0 (Serum starvation), N12 & N24 (Normoxic) and H12 & H24 (Hypoxic). Immunocytochemistry was performed using a specific antibody to **PDCD4** and FITC labelled secondary antibody was used. Coverslips with cells were mounted on glass slides with mounting medium containing **DAPI (Blue)** which stains the nucleus of the cells. Cells were analysed by confocal microscopy and images were captured at 65X magnification. Results are representative of three separate experiments and images were representative of six separate fields. **PDCD4** localized and expressing At Go: Cytoplasmic and very low expression; At N12: Cytoplasmic and low expression; At N24: very high cytoplasmic and low nuclear expression; At H12: Cytoplasmic expression and At H24 very high cytoplasmic and low nuclear expression. Over-all **PDCD4** was highly expressed in the cytoplasm, with very low expression under serum starved conditions.

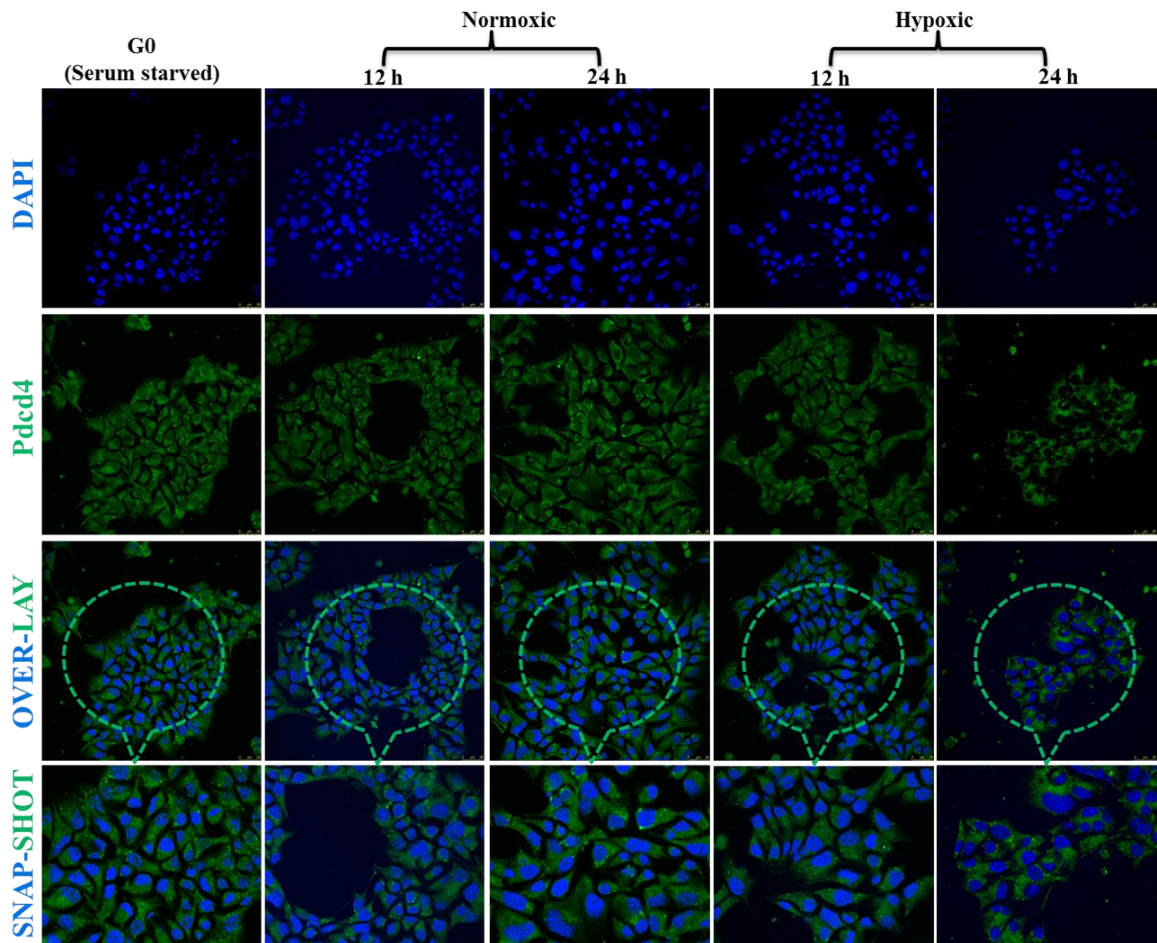


Figure 5-7: Sub-cellular localisation and expression of PDCD4 in mouse pancreatic beta cells.

MIN6 cells were grown on glass cover slips in six well plates and fixed at various time points i.e. at G0 (serum starvation), N12 & N24 (normoxic) and H12 & H24 (hypoxic). Immunocytochemistry was performed using a specific antibody to **PDCD4** and FITC labelled secondary antibody was used. Coverslips with cells were mounted on glass slides with mounting medium containing **DAPI (Blue)** which stains the nucleus of the cells. Cells were analysed by confocal microscopy and images were captured at 65X magnification. Results are representative of three separate experiments and images were representative of six separate fields. **PDCD4** localized and expressing At Go, N12, N24 and H12: Cytoplasmic and very low nuclear expression; At H24: High cytoplasmic expression. Over-all **PDCD4** was highly expressed in the cytoplasm, with very low nuclear expression.

5.2.2. PDCD4 expression and subcellular localisation in normal and adenocarcinoma pancreas tissue

In order to investigate expression and subcellular localisation of PDCD4 in normal pancreas and human pancreatic adenocarcinoma tissue sections, immunohistochemistry was performed. Due to unavailability of normal human pancreas, mouse pancreas was analysed and considered because the mouse model is genetically closely related to humans [341]. Formalin fixed paraffin embedded pancreas tissue blocks were sectioned (5µm) and mounted on glass slides. Tissue sections were deparaffinised by dipping sections in xylene and rehydrated using an ethanol gradient. Immunohistochemistry was performed using a specific antibody to PDCD4 with HRP conjugated secondary antibody. PDCD4 immuno-stained sections were counterstained with haematoxylin. Sections were mounted using DPX mounting medium and analysed by light microscopy; images were captured at 10X and 40X magnifications.

5.2.2.1. *PDCD4 in Mouse pancreas*

Immunohistochemistry was performed to reveal expression and subcellular localisation of PDCD4 in mouse pancreas. Immunohistochemistry results are shown in Figure 5-8 (10X) and Figure 5-9 (40X). PDCD4 was expressed in the cytoplasm of intercalated ducts and acinar cells as shown in Figure 5-8 (A) and Figure 5-9 (D). PDCD4 was strongly expressed in Islets of Langerhans (IL) and blood vessels as shown in Figure 5-8 (C &D). On observing at higher magnification it is also cleared that PDCD4 was expressed in the cytoplasm as well as in the nucleus of Islets of Langerhans (IL) and intralobular ducts as shown in Figure 5-9. These results suggest that PDCD4 was differentially expressed in different types of pancreas cells.

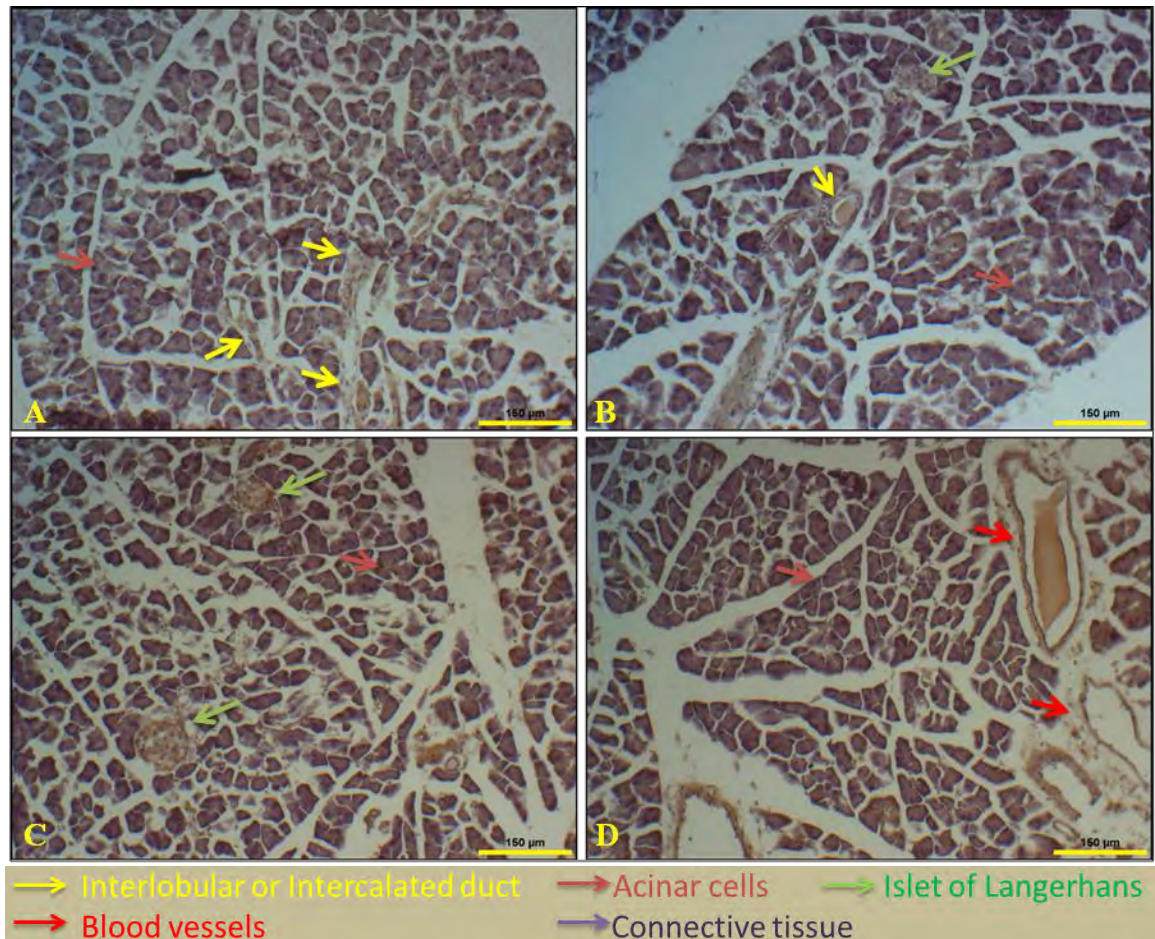


Figure 5-8: Immunohistochemical analysis of the expression of PDCD4 in mouse pancreas (10X magnification).

Formalin fixed, paraffin embedded mouse pancreas tissue blocks were sectioned (5µm) and mounted on glass slides. Immunohistochemistry was performed using a specific antibody to PDCD4. PDCD4 immunostained sections were counter stained with haematoxylin and sections were mounted using mounting medium. Stained sections were analysed by light microscopy and images were captured at 10X magnification. Results are representative of three separate experiments and images were representative of six separate fields. (A & B) Weak cytoplasmic expression of PDCD4 was observed in **acinar cells**, **intralobular** and **intercalated ducts**. (C) Cytoplasmic expression of PDCD4 observed in **islets of Langerhans**. (D) With strong cytoplasmic expression of PDCD4 seen in **blood vessels**.

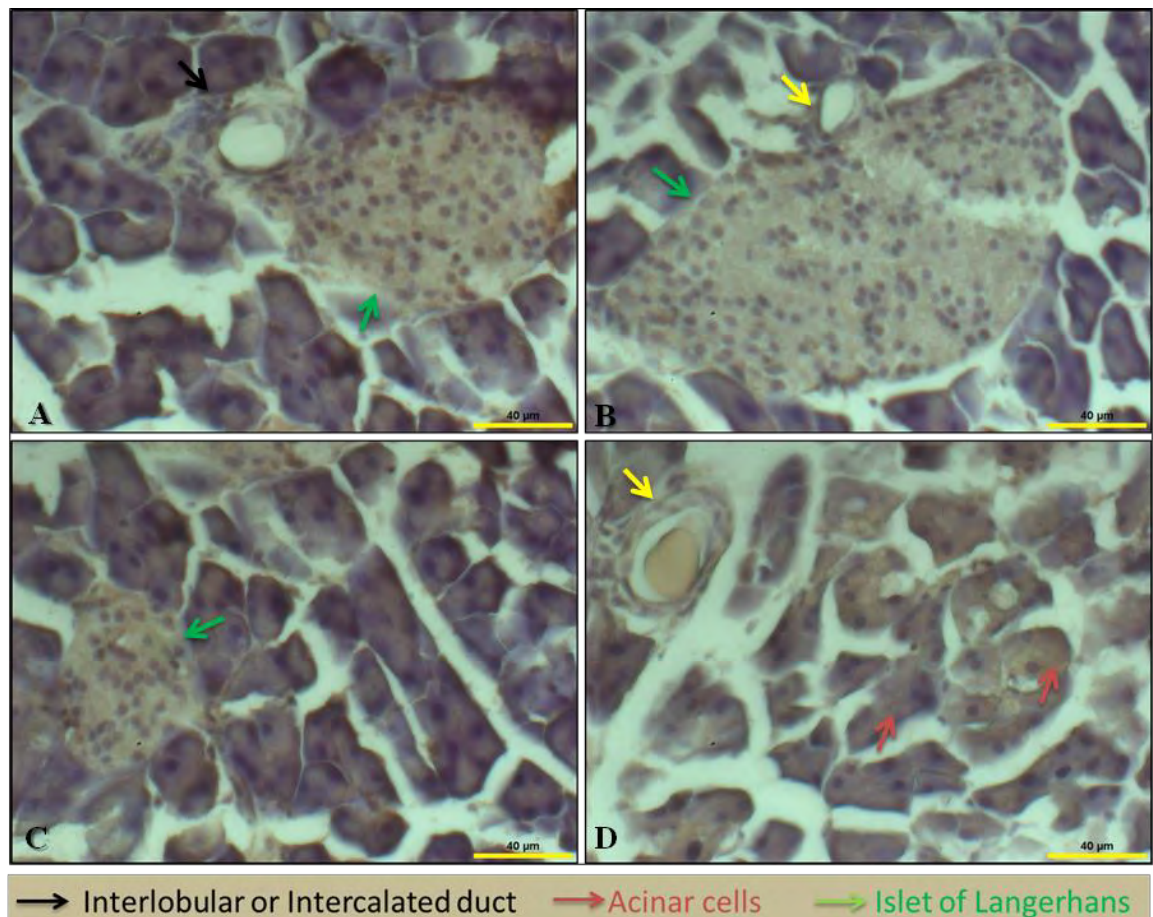


Figure 5-9: Immunohistochemical expression of PDCD4 in mouse pancreas (40X magnification).

Formalin fixed, paraffin embedded mouse pancreas tissue blocks were sectioned (5µm) and mounted on glass slides. Immunohistochemistry was performed using a specific antibody to PDCD4. PDCD4 immunostained sections were counter stained with haematoxylin and sections were mounted using mounting medium. Stained sections were analysed by light microscopy and images were captured at 40X magnification. Results are representative of three separate experiments and images were representative of six separate fields. (A, B, C & D) PDCD4 was expressed in the cytoplasm and nucleus of **Islets of Langerhans**. However, PDCD4 was exclusively expressed in the cytoplasm in **acinar** and **ductal cells**.

5.2.2.2. *PDCD4 in human pancreatic adenocarcinoma tissues*

In order to investigate expression of PDCD4 in human pancreatic adenocarcinoma tissue sections (provided by Zemskov Centre for Hepato-Pancreato-Biliary Surgery, Kiev, Ukraine) immunohistochemistry was performed. In the present study, human pancreatic adenocarcinoma tissue sections from four patients were studied for the expression of PDCD4 by immunohistochemistry.

5.2.2.2.1. **Case study 1**

Immunohistochemistry was performed to reveal expression and subcellular localisation of PDCD4 in human pancreatic adenocarcinoma tissue (sample 1). Immunohistochemistry results are shown in Figure 5-10 (5X), Figure 5-11 (10X) and Figure 5-12 (40X). The findings from our previous morphology (Figure 4-12, Figure 4-13 and Figure 4-14) study on sample 1 showed that, it is moderately to poorly differentiated pancreatic adenocarcinoma. This means that some parts of the tissue still resemble normal pancreatic morphology (moderate) but most of the tissue section lacks normal tissue morphology (poor). Tissue sections still have normal pancreatic morphology such as acinar cell, nerve cell bundle and lobular structure showing positive cytoplasmic expression of PDCD4 as shown in Figure 5-10 (B). Fibrous connective tissue or stromal cells around rudimentary acinar and lobular structure show expression of PDCD4 as shown in Figure 5-10 (D). However, fibrous connective tissue around the pleomorphic malignant epithelial tissue shows negative expression of PDCD4 as shown in Figure 5-10 (A, B &C). Analysing tissue sections on higher magnification, PDCD4 is not expressed in ductal cells (Figure 5-11(B &C) and Figure 5-12 (A, B & D)). Rudimentary acinar cells in lobular structure show positive cytoplasmic and nuclear expression of PDCD4 as shown in Figure 5-11(A), however, acinar cells which have lost full integrity show no expression of PDCD4 (Figure 5-12 (C)).

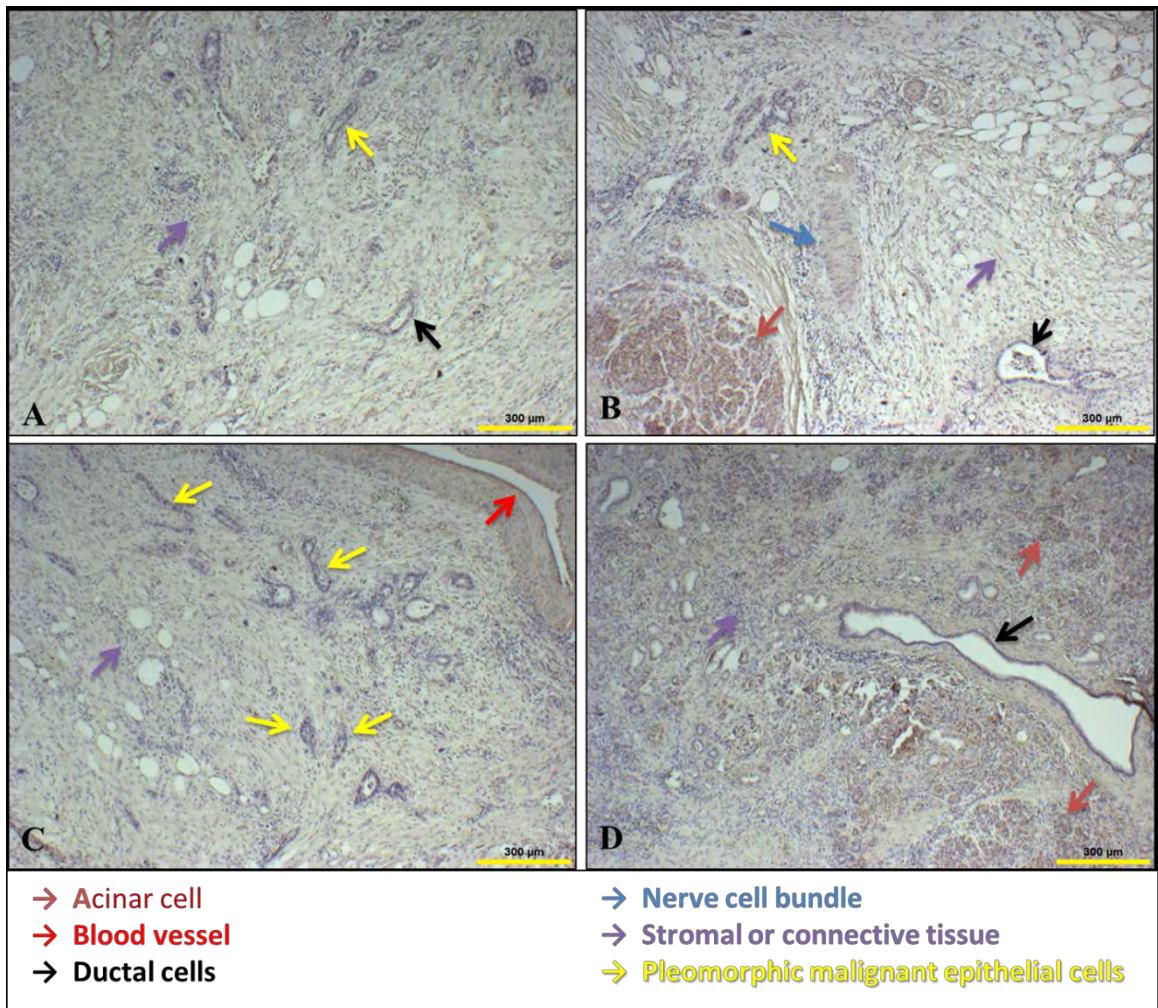


Figure 5-10: Immunohistochemical expression analysis of the PDCD4 in human pancreatic adenocarcinoma tissue case study 1 (5X magnification).

Formalin fixed, paraffin embedded pancreatic adenocarcinoma tissue blocks were sectioned (5µm) and mounted on glass slides. Immunohistochemistry was performed using a specific antibody to PDCD4. PDCD4 immunostained sections were counter stained with haematoxylin and sections were mounted using mounting medium. Stained sections were analysed by light microscopy and images were captured at 5X magnification. (A&C) There was no expression of PDCD4 in ductal cells (←), and **pleomorphic malignant epithelial cells (←)** (B &D) Weak cytoplasmic expression was observed in **fibrous connective or stromal (←)** cells and **acinar (←)** cells were positive for PDCD4 expression.

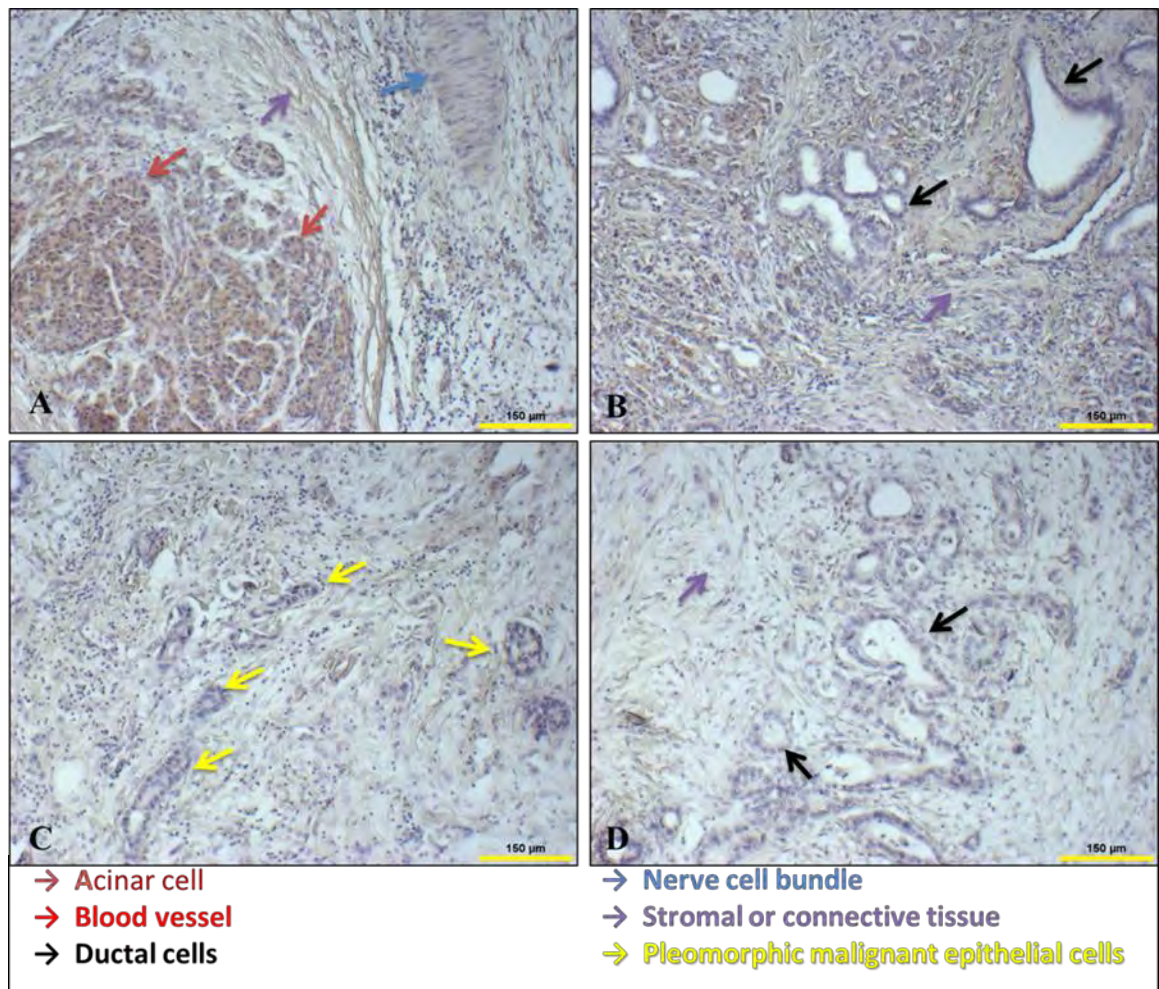


Figure 5-11: Immunohistochemical expression analysis of the PDCD4 in human pancreatic adenocarcinoma tissue case study 1 (10X magnification).

Formalin fixed, paraffin embedded pancreatic adenocarcinoma tissue blocks were sectioned (5µm) and mounted on glass slides. Immunohistochemistry was performed using a specific antibody to PDCD4. PDCD4 immunostained sections were counter stained with hematoxylin and sections were mounted using mounting medium. Stained sections were analysed by light microscopy and images were captured at 10X magnification. (A) Positive expression of PDCD4 was observed in **acinar cells** and low cytoplasmic expression of PDCD4 was identified in **nerve cell bundle**. (B) There was no expression of PDCD4 in ductal cells and cytoplasmic expression in **stromal cells** was observed. (C & D) Negative expression of PDCD4 was identified in **pleomorphic malignant epithelial** and ductal cell; however, **stromal cells** show weak cytoplasmic expression of PDCD4.

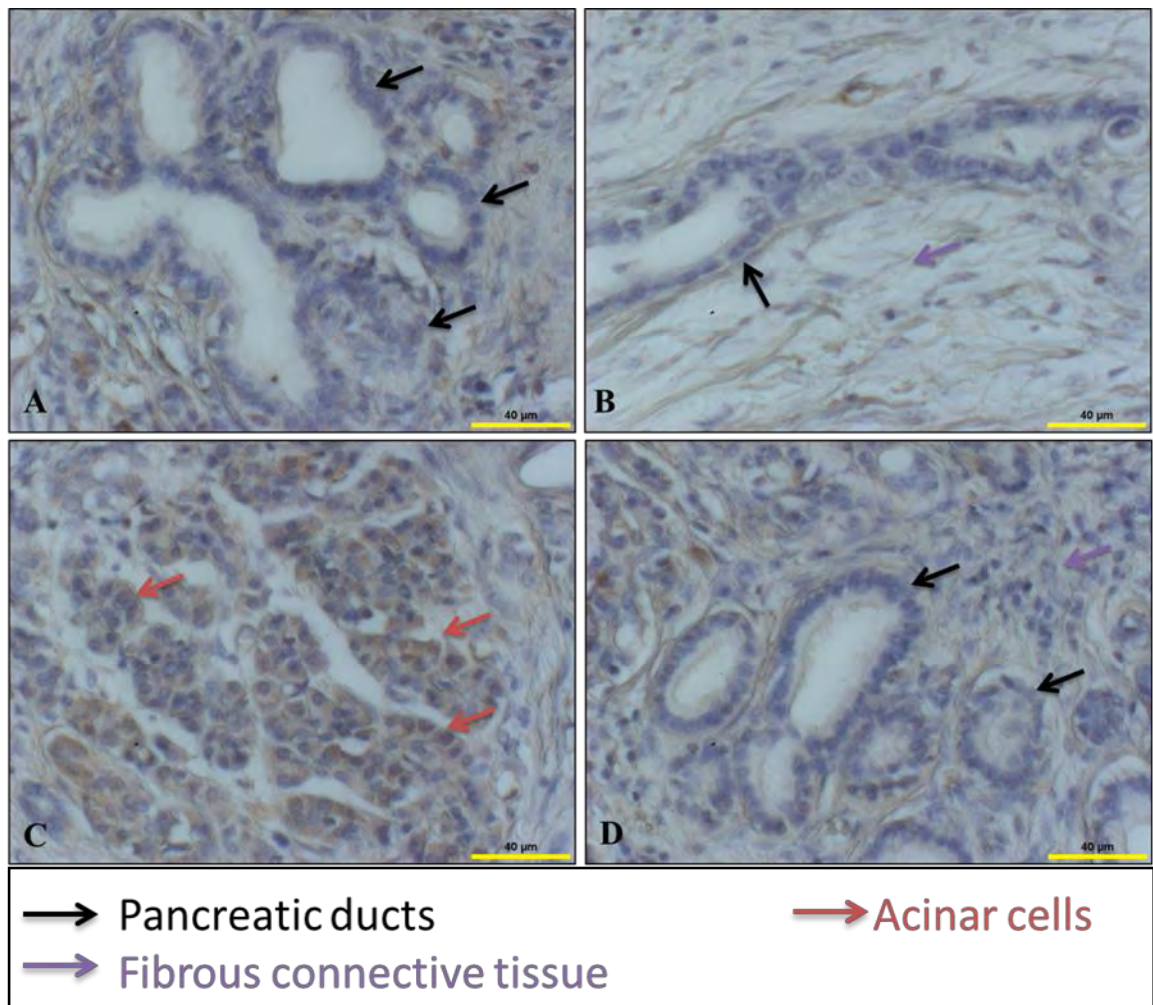


Figure 5-12: Immunohistochemical expression analysis of the PDCD4 in human pancreatic adenocarcinoma tissue case study 1 (40X magnification).

Formalin fixed, paraffin embedded pancreatic adenocarcinoma tissue blocks were sectioned (5µm) and mounted on glass slides. Immunohistochemistry was performed using a specific antibody to PDCD4. PDCD4 immunostained sections were counter stained with haematoxylin and sections were mounted using mounting medium. Stained sections were analysed by light microscopy and images were captured at 40X magnification. (A, B &D) There was no expression of PDCD4 observed in ductal cells; however, **fibrous connective tissue** shows weak cytoplasmic expression of PDCD4. (C) High expression of PDCD4 was identified in rudimentary **acinar cells**.

These results suggest that loss of PDCD4 expression occurs in poorly differentiated pancreatic adenocarcinoma tissue and weak cytoplasmic expression of PDCD4 is observed in moderately differentiated pancreatic adenocarcinoma tissue.

5.2.2.2.2. Case study 2

Immunohistochemistry was performed to reveal expression and subcellular localisation of PDCD4 in human pancreatic adenocarcinoma tissue (sample 2). Immunohistochemistry results are shown in Figure 5-13 (5X), Figure 5-14 (10X) and Figure 5-15 (40X). The findings from our previous morphology (Figure 4-15, Figure 4-16 and Figure 4-17) study on sample 2 showed that it is well to moderately differentiated but at some parts of tissue is poorly differentiated pancreatic adenocarcinoma. The well differentiated tissue section shows strong expression of PDCD4 as shown in Figure 5-13 (A & B); however, the tissue sections which have lost integrity show weak expression of PDCD4 as shown in Figure 5-13 (C & D). On analysing well differentiated sections under higher magnification; PDCD4 expression was observed in the nucleus and the cytoplasm of ductal cells and acinar cells (Figure 5-14 (A)). On analysing moderately differentiated section, weak cytoplasmic expression of PDCD4 was observed in fibrous connective tissue and ductal cell, however, islets of Langerhans showed positive expression of PDCD4 as shown in Figure 5-14 (B, C & D). It is clear from Figure 5-15 (A & B) that acinar cells show positive (nuclear and cytoplasmic) expression of PDCD4, however, rudimentary acinar (highlighted in red circle) cells show weak cytoplasmic expression of PDCD4. Ducts in poorly differentiated pancreatic adenocarcinoma tissue section indicated that PDCD4 was not expressing and weak cytoplasmic expression of PDCD4 was observed in fibrous connective tissue as shown in Figure 5-15 (C). PDCD4 was expressing in the cytoplasm and the nucleus of Islets of Langerhans cells as observed in Figure 5-15 (D). Results from this case study suggest that PDCD4 was expressing in the pancreatic cancer tissue

with normal morphology or well differentiated human pancreatic adenocarcinoma tissue. However, poorly differentiated human pancreatic adenocarcinoma tissue showed no or weak cytoplasmic expression of PDCD4.

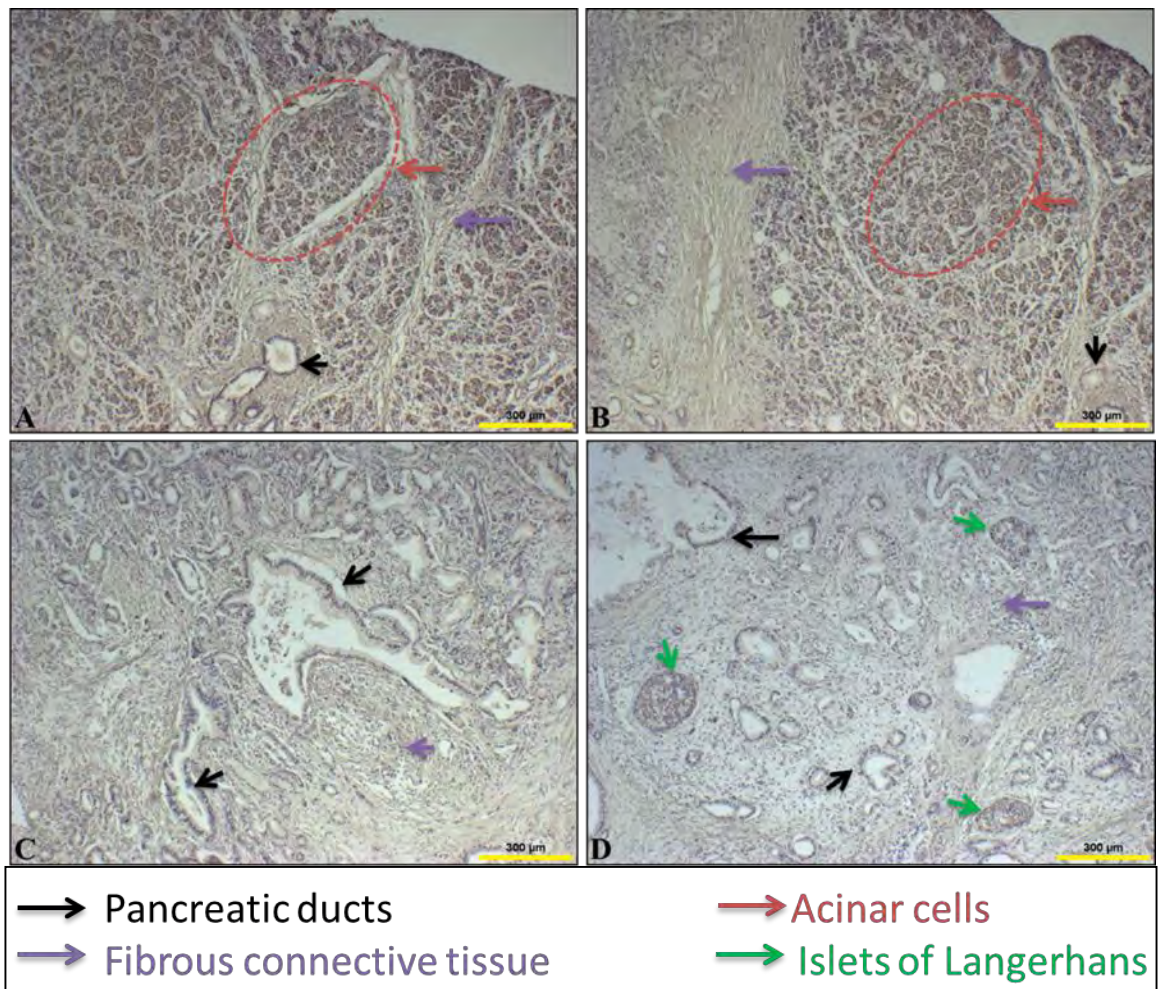


Figure 5-13: Immunohistochemical expression analysis of the PDCD4 in human pancreatic adenocarcinoma tissue case study 2 (5X magnification).

Formalin fixed, paraffin embedded pancreatic adenocarcinoma tissue blocks were sectioned (5µm) and mounted on glass slides. Immunohistochemistry was performed using a specific antibody to PDCD4. PDCD4 immunostained sections were counter stained with haematoxylin and sections were mounted using mounting medium. Stained sections were analysed by light microscopy and images were captured at 5X magnification. (A & B) PDCD4 was expressing in **acinar** cells (as highlighted in **red circle**), ductal cells and **fibrous connective tissue**. (C) Weak expression of PDCD4 was observed in ductal cells and **fibrous connective tissue**. (D) PDCD4 was observed in the **Islets of Langerhans**.

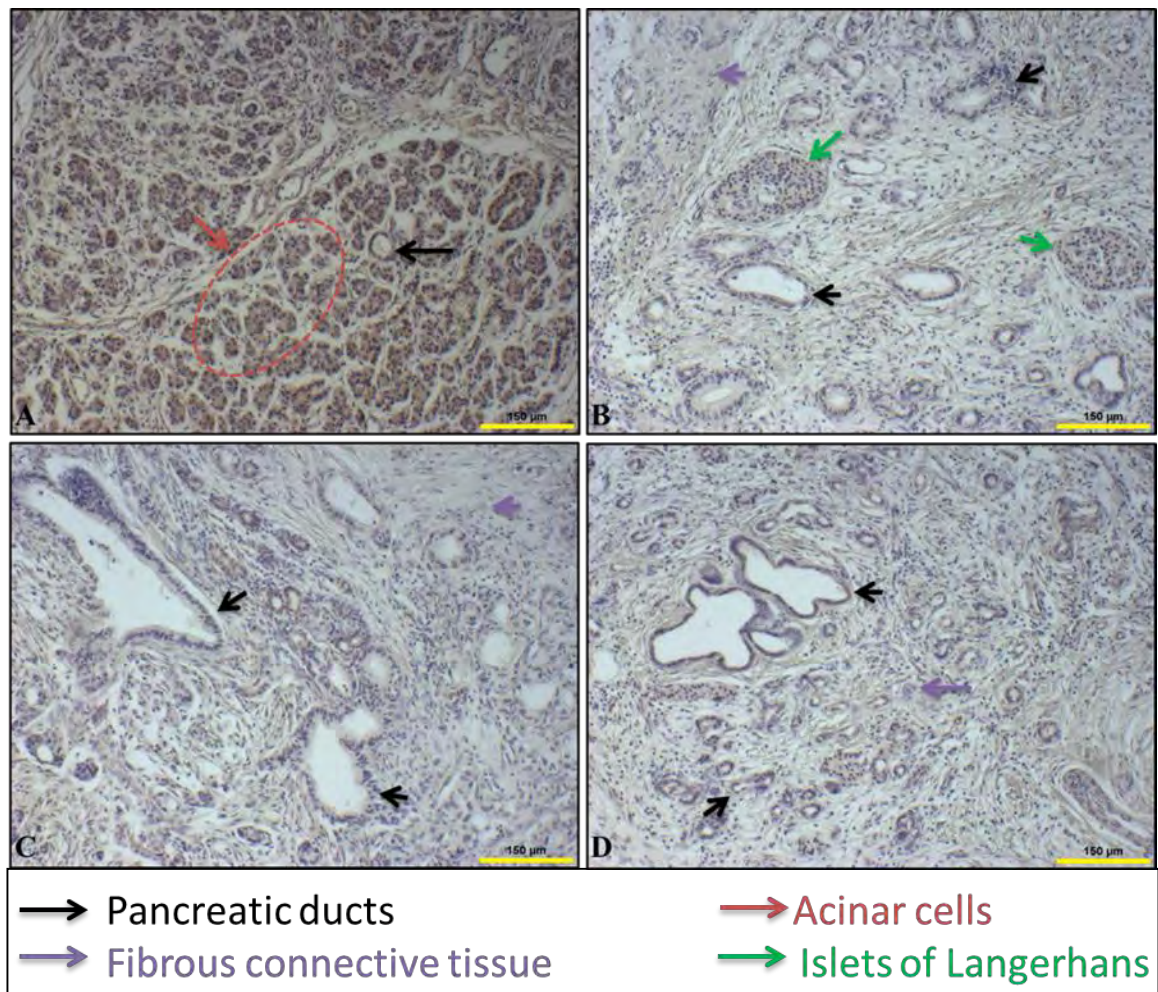


Figure 5-14: Immunohistochemical expression analysis of the PDCD4 in human pancreatic adenocarcinoma tissue case study 2 (10X magnification).

Formalin fixed, paraffin embedded pancreatic adenocarcinoma tissue blocks were sectioned (5µm) and mounted on glass slides. Immunohistochemistry was performed using a specific antibody to PDCD4. PDCD4 immunostained sections were counter stained with haematoxylin and sections were mounted using mounting medium. Stained sections were analysed by light microscopy and images were captured at 10X magnification. (A) Nuclear and cytoplasmic expression of PDCD4 was observed in ductal and **acinar** cells (as highlighted in **red circle**) and cytoplasmic expression of PDCD4 was found in **fibrous connective tissue**. (B) PDCD4 was expressing in **Islets of Langerhans**, ductal and **fibrous connective tissue**. (C & D) Cytoplasmic expression of PDCD4 was observed in ductal cells and **fibrous connective tissue**.

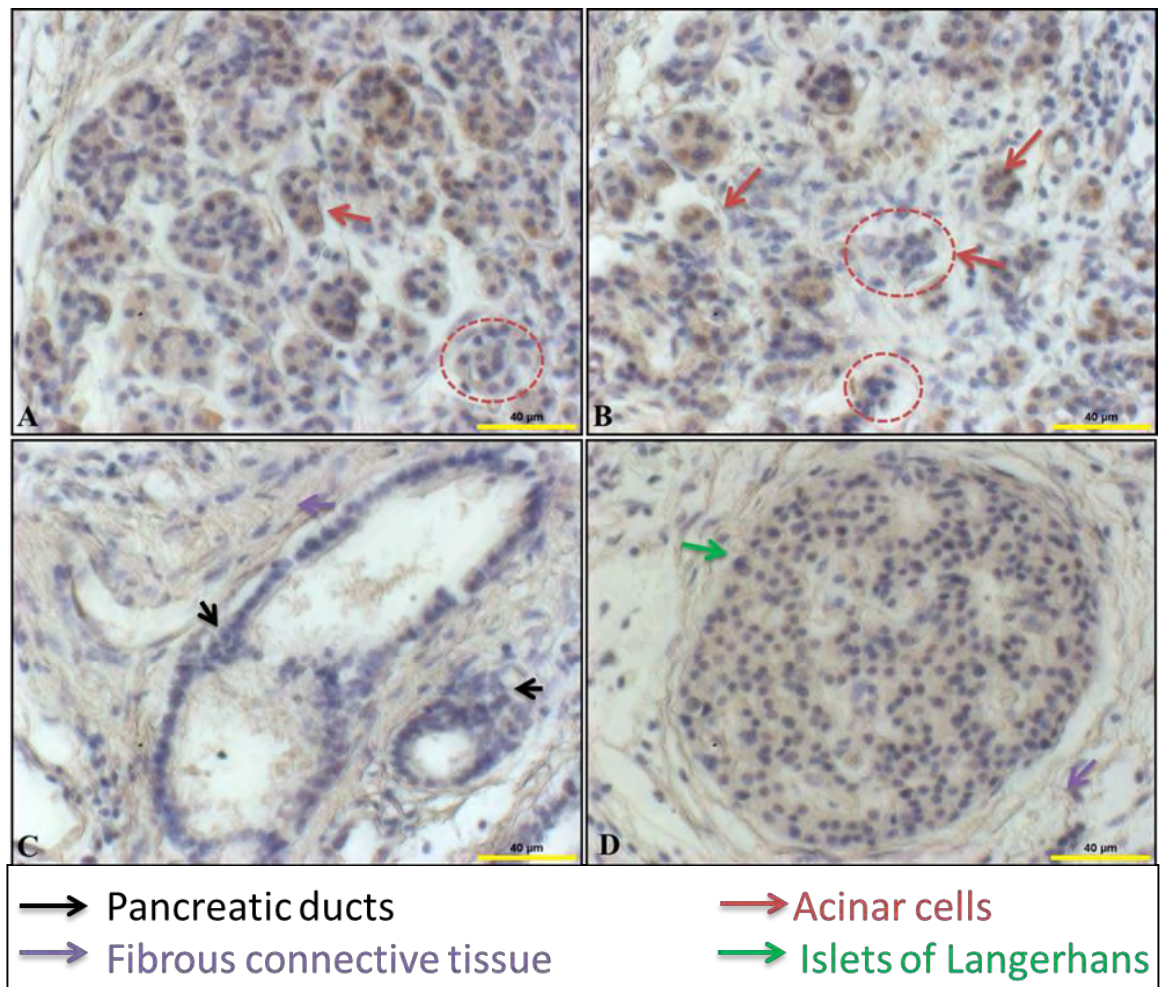


Figure 5-15: Immunohistochemical expression analysis of the PDCD4 in human pancreatic adenocarcinoma tissue case study 2 (40X magnification).

Formalin fixed, paraffin embedded pancreatic adenocarcinoma tissue blocks were sectioned (5µm) and mounted on glass slides. Immunohistochemistry was performed using a specific antibody to PDCD4. PDCD4 immunostained sections were counter stained with haematoxylin and sections were mounted using mounting medium. Stained sections were analysed by light microscopy and images were captured at 40X magnification. (A & B) Nuclear and cytoplasmic expression of PDCD4 was identified in acinar cells (ring like structure) however, **acinar** which has lost normal structure shows weak cytoplasmic expression of PDCD4 as highlighted in red circle. (C) Weak cytoplasmic expression of PDCD4 was observed **fibrous connective** tissue and PDCD4 was not expressing in ductal cells (D) PDCD4 was expressing in the nucleus and the cytoplasm of **Islets of Langerhans** cells.

5.2.2.2.3. Case study 3

Expression and subcellular localisation of PDCD4 in human pancreatic adenocarcinoma tissue (sample 3) was investigated by immunohistochemistry. Results are displayed in Figure 5-16 (5X), Figure 5-17 (10X) and Figure 5-18 (40X). The findings from our previous morphology (Figure 4-18, Figure 4-19 and Figure 4-20) study on sample 3 showed that sample 3 is a poorly differentiated pancreatic adenocarcinoma. Immunohistochemistry revealed weak cytoplasmic expression of PDCD4 in fibrous connective tissue and ductal cells as shown in Figure 5-16, Figure 5-17 and Figure 5-18. This tissue section was highly infiltrated with lymphocytes showing high expression of PDCD4 as shown in Figure 5-17 (B &C). On analysis under higher magnification, weak cytoplasmic expression of PDCD4 in ductal epithelial cells and fibrous connective tissue was observed as shown in Figure 5-18.

Results from sample 3 suggest weak cytoplasmic expression of PDCD4 expression in poorly differentiated pancreatic adenocarcinoma tissue however, infiltrating lymphocytes show high expression of PDCD4.

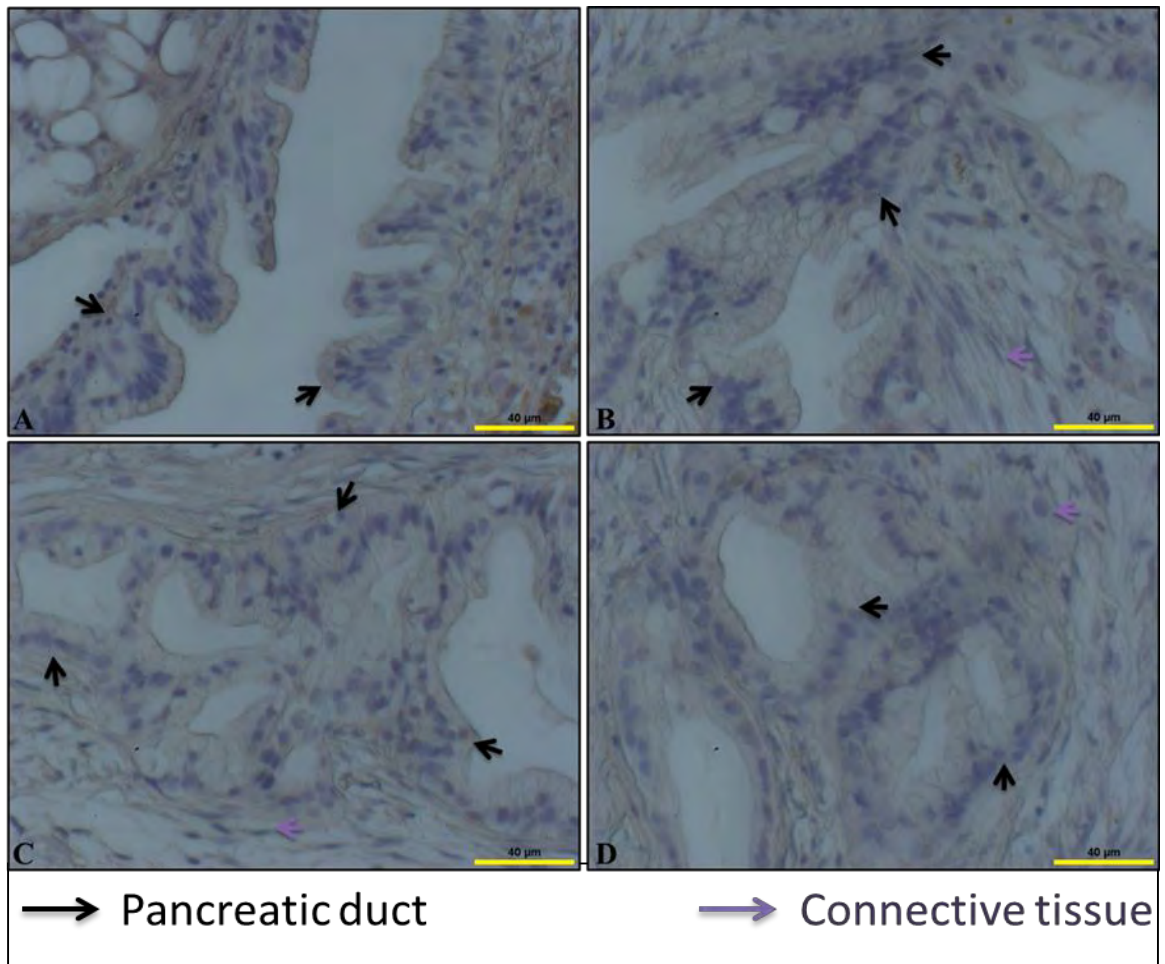


Figure 5-18: Immunohistochemical expression analysis of the PDCD4 in human pancreatic adenocarcinoma tissue case study 3 (40X magnification).

Formalin fixed, paraffin embedded pancreatic adenocarcinoma tissue blocks were sectioned (5µm) and mounted on glass slides. Immunohistochemistry was performed using a specific antibody to PDCD4. PDCD4 immunostained sections were counter stained with haematoxylin and sections were mounted using mounting medium. Stained sections were analysed by light microscopy and images were captured at 40X magnification. (A, B, C &D) Weak cytoplasmic expression of PDCD4 was observed in ductal cells and **fibrous connective or stromal** cells.

5.2.2.2.4. Case study 4

Immunohistochemistry was performed to reveal the expression and subcellular localisation of PDCD4 in human pancreatic adenocarcinoma tissue (sample 4). Immunohistochemistry results are detailed in Figure 5-19 (5X), Figure 5-20 (10X) and Figure 5-21(40X). H&E staining of sample 4 showed moderately differentiated pancreatic cancer and pronounced autolysis of tissue sections (Figure 4-21, Figure 4-22 and Figure 4-23). Immunohistochemistry results showed positive expression of PDCD4 in sample 4 as shown in Figure 5-19. PDCD4 was highly expressed in pleomorphic malignant epithelial cells, as well as in islets of Langerhans (Figure 5-20). Fibrous connective tissue and nerve cell bundles showed positive expression of PDCD4 as shown in Figure 5-20 (B&D). Ductal cells showed differential expression of PDCD4; multinucleated ductal cells showed cytoplasmic expression, however, epithelial (single nucleated) type ductal cells show nuclear expression of PDCD4 was observed in Figure 5-20 (C). Nuclear expression of PDCD4 was observed in islets of Langerhans and fibrous connective tissue as shown in Figure 5-21(A&B). Differential expression of PDCD4 was observed in ductal cells. In multinucleated ductal cells, PDCD4 expression was observed in the cytoplasm (Figure 5-21 (C)) however; nuclear expression of PDCD4 was observed in single nucleated ductal cells (Figure 5-21 (D)).

Results from this case study suggest that PDCD4 was highly expressed in this sample (case study 4). Nuclear expression of PDCD4 was found in islets of Langerhans, normal ductal cell (single nucleated) and fibrous connective tissue. However, multinucleated ductal cells only weakly expressed PDCD4 in the cytoplasm.

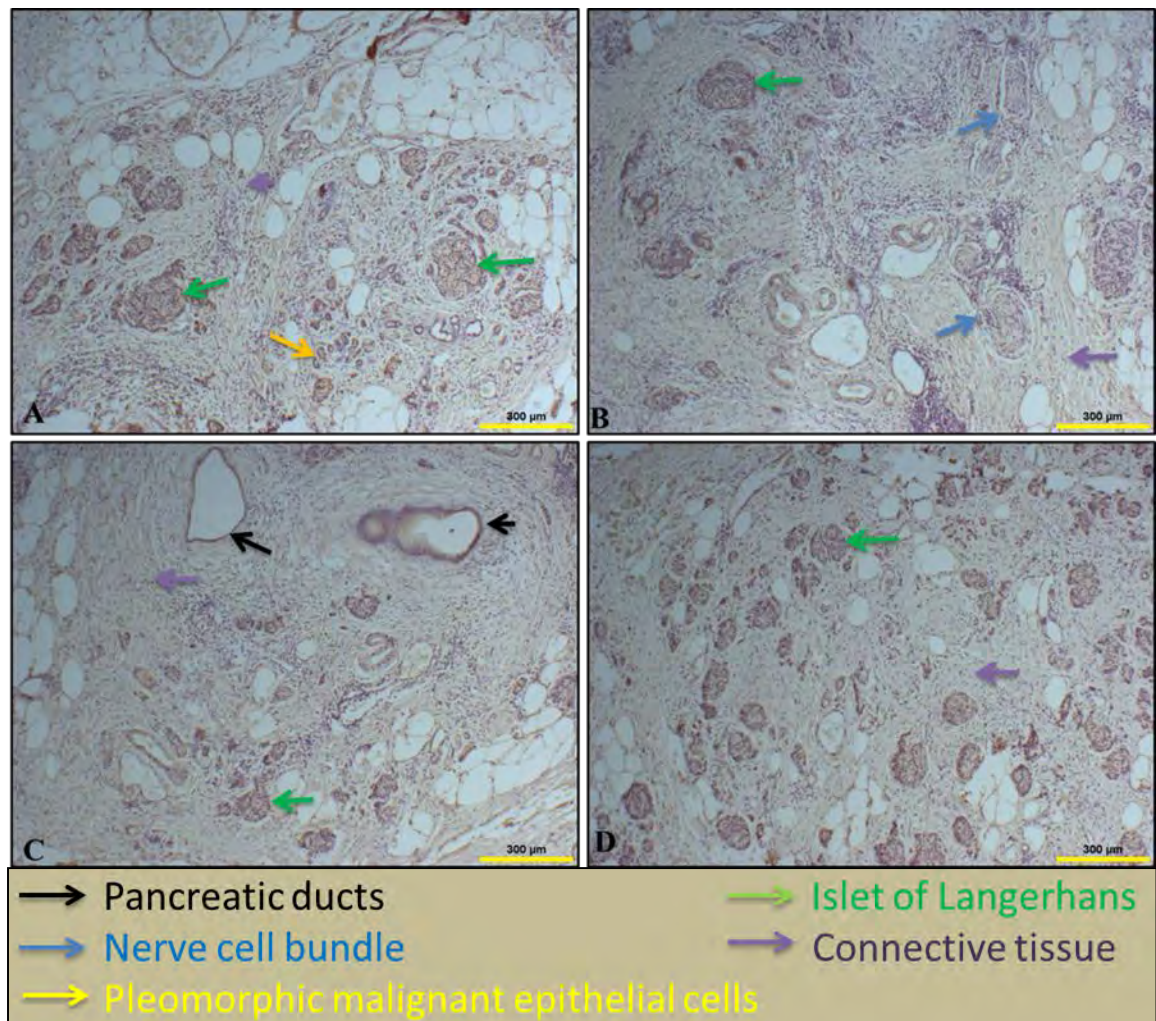


Figure 5-19: Immunohistochemical expression analysis of the PDCD4 in human pancreatic adenocarcinoma tissue case study 4 (5X magnification).

Formalin fixed, paraffin embedded pancreatic adenocarcinoma tissue blocks were sectioned (5µm) and mounted on glass slides. Immunohistochemistry was performed using a specific antibody to PDCD4. PDCD4 immunostained sections were counter stained with haematoxylin and sections were mounted using mounting medium. Stained sections were analysed by light microscopy and images were captured at 5X magnification. (A) High expression of PDCD4 observed in **islets** cells and **pleomorphic malignant epithelial**. (B) Cytoplasmic expression of PDCD4 was observed in bundle of **nerve** cells and **fibrous connective or stromal** cells. (C) Nuclear and cytoplasmic expression of PDCD4 was observed in the ductal cells. (D) PDCD4 was highly expressed in the **Islets of Langerhans**.

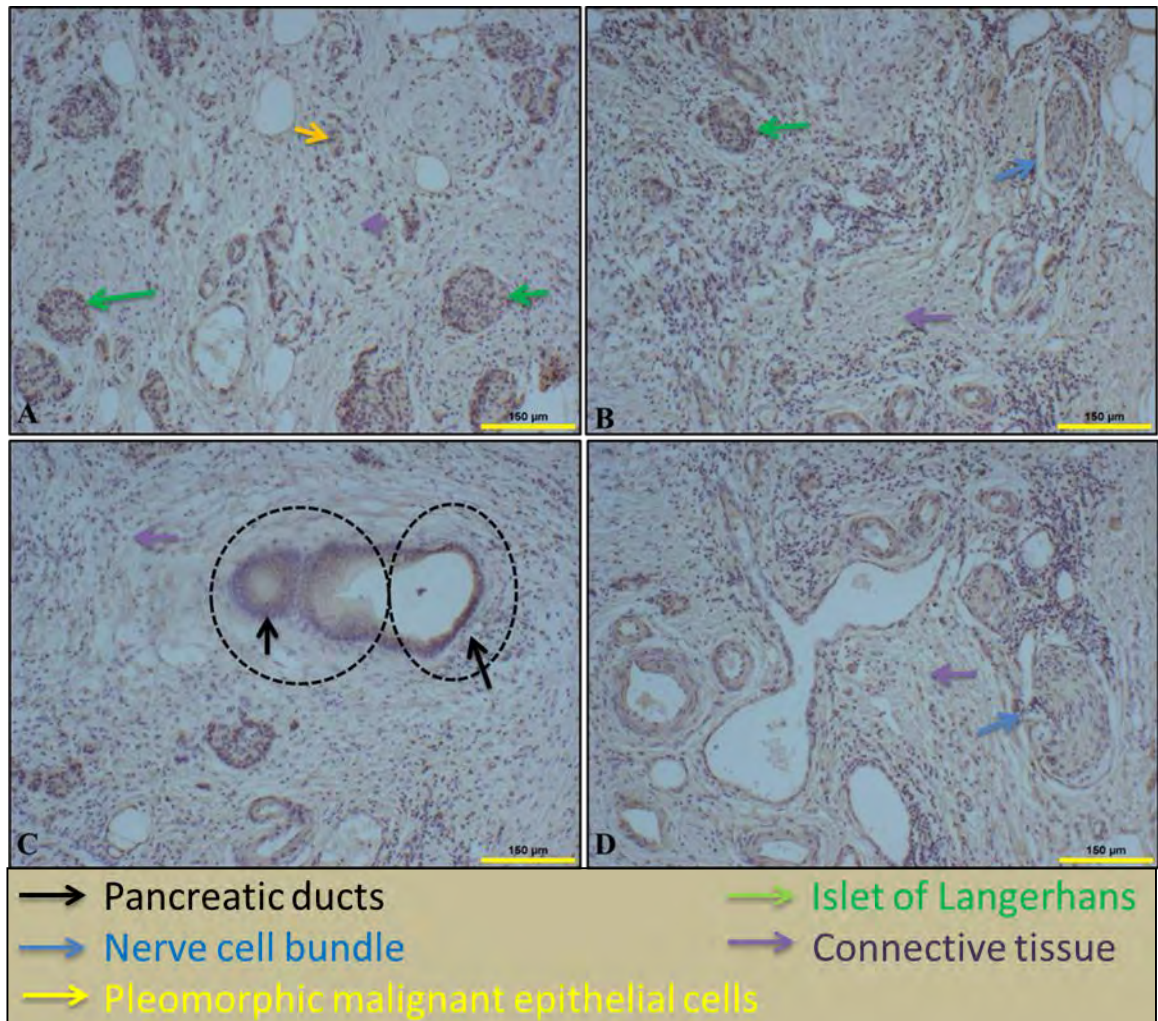


Figure 5-20: Immunohistochemical expression analysis of the PDCD4 in human pancreatic adenocarcinoma tissue case study 4 (10X magnification).

Formalin fixed, paraffin embedded pancreatic adenocarcinoma tissue blocks were sectioned (5µm) and mounted on glass slides. Immunohistochemistry was performed using a specific antibody to PDCD4. PDCD4 immunostained sections were counter stained with haematoxylin and sections were mounted using mounting medium. Stained sections were analysed by light microscopy and images were captured at 10X magnification. (A) Positive expression of PDCD4 expression in **islets** cells and low expression in **pleomorphic malignant epithelial**. (B &D) Cytoplasmic expression of PDCD4 was observed in bundle of **nerve** cells and **fibrous connective or stromal** cells. (C) Cytoplasmic expression of PDCD4 was observed in multinucleated ductal cells however, nuclear expression of PDCD4 was observed in single nucleated ductal cells as highlighted in black circle.

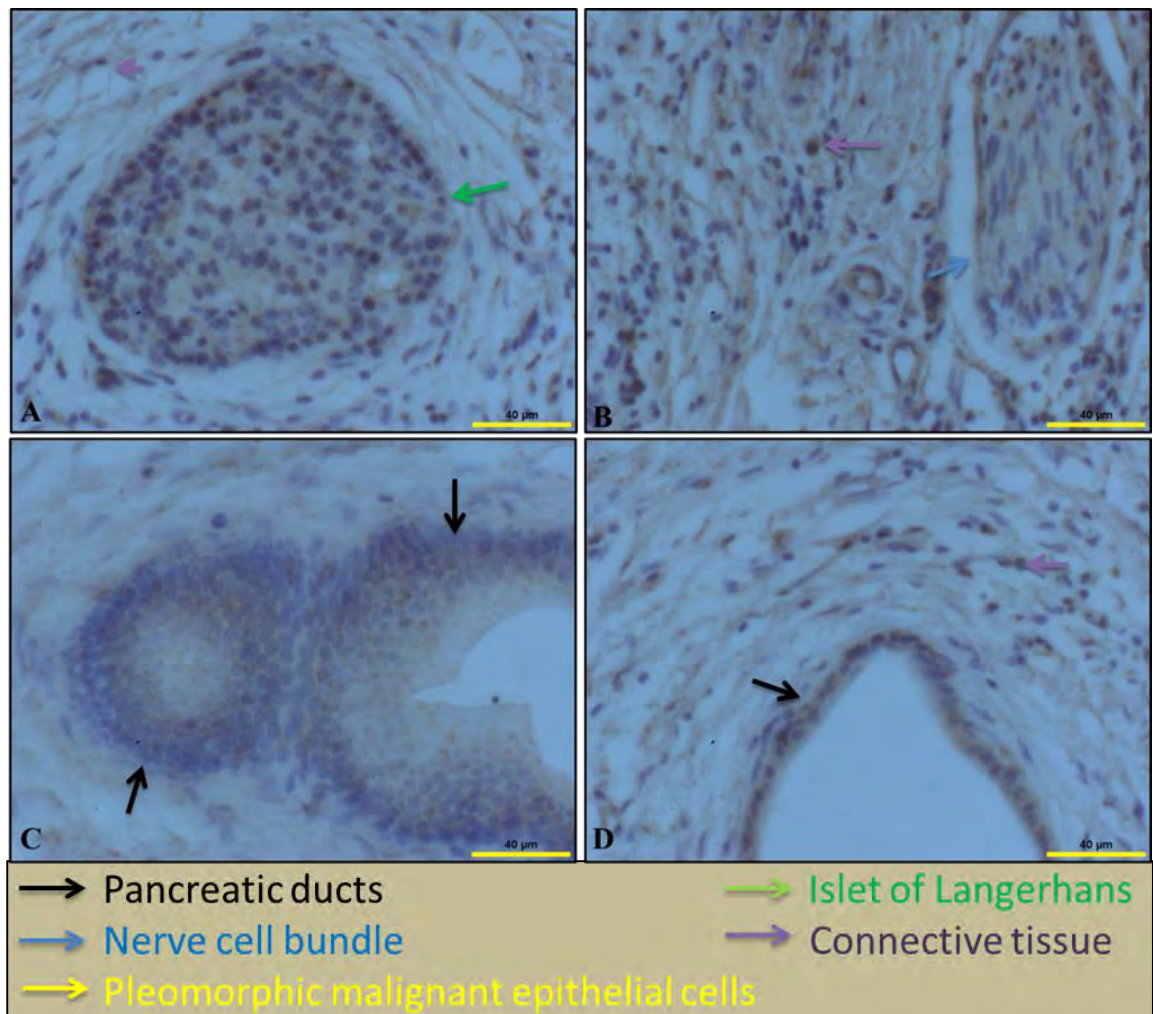


Figure 5-21: Immunohistochemical expression analysis of the PDCD4 in human pancreatic adenocarcinoma tissue case study 4 (40X magnification).

Formalin fixed, paraffin embedded pancreatic adenocarcinoma tissue blocks were sectioned (5µm) and mounted on glass slides. Immunohistochemistry was performed using a specific antibody to PDCD4. PDCD4 immunostained sections were counter stained with haematoxylin and sections were mounted using mounting medium. Stained sections were analysed by light microscopy and images were captured at 40X magnification. (A) Nuclear expression of PDCD4 expression in **islets** and **fibrous connective or stromal** cells. (B) Positive expression of PDCD4 in **nerve** cells bundle and **fibrous connective or stromal** cells. (B &D) Cytoplasmic expression of PDCD4 in **nerve** cells bundle and **fibrous connective or stromal** cells. (C &D) Cytoplasmic expression of PDCD4 was observed in multinucleated ductal cells however, nuclear expression of PDCD4 was observed in single nucleated ductal cells.

5.3. Discussion

Our studies designed and began to define the expression pattern of novel tumour suppressor, PDCD4 in human pancreatic adenocarcinoma cells. Many studies have reported loss or down-regulation of PDCD4 expression in several types of cancer such as tongue tumour [136], invasive ductal breast carcinoma [137], skin cancer [123], human glioma [138], nasopharyngeal carcinoma [139], lung cancer [135], gastric cancer [140], colon cancer [141] and ovarian cancer [142]. PDCD4 has recently been linked with type 1 diabetes [370] and pancreatic cancer [372] but the role has not been definitively defined especially under the influence of hypoxic microenvironment in human pancreatic adenocarcinoma. Tumour microenvironment interestingly plays a very important role in tumour progression and patient prognosis. Decreased oxygen availability (hypoxia) in the core of a tumour is an important characteristic of tumour microenvironment often associated with pancreatic tumours [196].

In order to determine expression of PDCD4 under hypoxic conditions in PSN-cells, cells were cultured under hypoxic (1% oxygen) conditions which mimic the tumour microenvironment and compared that to the normal growth culturing conditions i.e. normoxic conditions (21% oxygen). Interestingly it has observed that expression of PDCD4 decreased significantly ($p < 0.001$) compared to normoxic condition in PSN-1 cells (Figure 5-1). This is a novel response of PDCD4 expression under the influence of hypoxia and has never been reported before in any study. Continuing this investigation the subcellular expression of PDCD4 in PSN-1 cells was determined under the influence of hypoxia and it was found that PDCD4 was highly expressed in the cytoplasm compared to the nuclear expression. Densitometry analysis showed significantly ($p < 0.001$) lower expression of PDCD4 under hypoxia (24 hours) compared to normoxic and serum starved (G0) as shown in Figure 5-2. Our cell viability studies (Figure 3-1 and Figure 3-4) have shown that hypoxia does not have any effect on

viability of PSN-1, but it does down-regulate the expression of PDCD4. As mentioned earlier many studies have reported loss of PDCD4 expression in several type of cancer, but the reason behind this loss of expression has not yet been elucidated, our results suggest that hypoxia may be the factor or reason behind the loss or reduced expression of PDCD4, which ultimately contributes to cancer invasion and migration. Recently, it has been reported that depleting PDCD4 function by siRNA mediated knockdown in breast cancer cells resulted in an increase in cancer cell migration and invasion [373]. In another study, knockdown of PDCD4 in colon cancer cells promoted migration as well as metastasis [374] however, overexpression of PDCD4 inhibited tumour cell invasion [375-377]. The present study has revealed that loss or reduced expression of PDCD4 may play an important role in pancreatic cancer cells survival under hypoxia.

The subcellular expression and localisation of PDCD4 has been investigated in normal pancreatic ductal (ARIP) cells under hypoxic and normoxic conditions. Western blotting analysis was performed in order to determine the subcellular expression of PDCD4. Interestingly the expression of PDCD4 under hypoxic conditions was significantly higher ($p < 0.01$) compared to normoxic and serum starved (G0) conditions as shown in Figure 5-3. These results also indicated that PDCD4 was highly expressed in the cytoplasm compared to the nucleus of ARIP cells, as shown in Figure 5-3. Cell viability analysis of ARIP cells showed that hypoxia triggers apoptosis (Figure 3-5) and this study has revealed that hypoxia triggers the high expression of PDCD4 in ARIP cells. These results suggest that higher expression of PDCD4 may induces apoptosis in ARIP cells or as reported before, that expression of PDCD4 is higher during the process of apoptosis [104].

Further subcellular expression and localisation of PDCD4 has been investigated in beta cells (MIN6) under hypoxic and normoxic conditions. Western blotting results showed that PDCD4 was highly expressed in the cytoplasm compared to the nucleus of the beta-

cells as shown in Figure 5-4. Densitometry analysis showed that expression of PDCD4 was significantly higher ($p < 0.001$) under hypoxic conditions compared to the normoxic conditions as well as serum starved conditions as shown in Figure 5-4. Our previous study has shown that up-regulation of PDCD4 during the process of islets neogenesis [280] and recently PDCD4 has been linked to type 1 diabetes [370]. MIN6 cells viability as well as morphology analyses have shown that hypoxia triggered apoptosis and necrosis in beta cells as (Figure 3-3 and Figure 3-6). The high expression of PDCD4 and apoptosis or necrosis induction in beta cells under hypoxic conditions, suggest that PDCD4 may play a role in inducing apoptosis or necrosis in beta cells (MIN6).

The exact role of PDCD4 during the process of apoptosis remains to be defined, as some studies have identified it as up-regulated [104] and others as down-regulated during the process of apoptosis [378]. Our results of ARIP and MIN6 cells viability and PDCD4 western blotting analysis suggest that PDCD4 up-regulated during the process of apoptosis in healthy pancreatic cells. However, high expression of PDCD4 was observed in the full population of cells (ARIP and MIN6) under hypoxic conditions (24 hours) but not in individual populations of only apoptotic or necrotic cells. So present data suggest that may be there is a link between high expression of PDCD4 observed and apoptosis or necrosis induced under hypoxic conditions in ARIP and MIN6 cells. Significantly lower expression of PDCD4 and no change in the viability of PSN-1 cells under hypoxic conditions further links low expression of PDCD4 and survival (no apoptosis) of cells under hypoxic conditions. A schematic representation of the proposed effect of PDCD4 expression on cell survival in the pancreas has been drawn out from the findings from cell viability and western blotting analysis as shown in Figure 5-22.

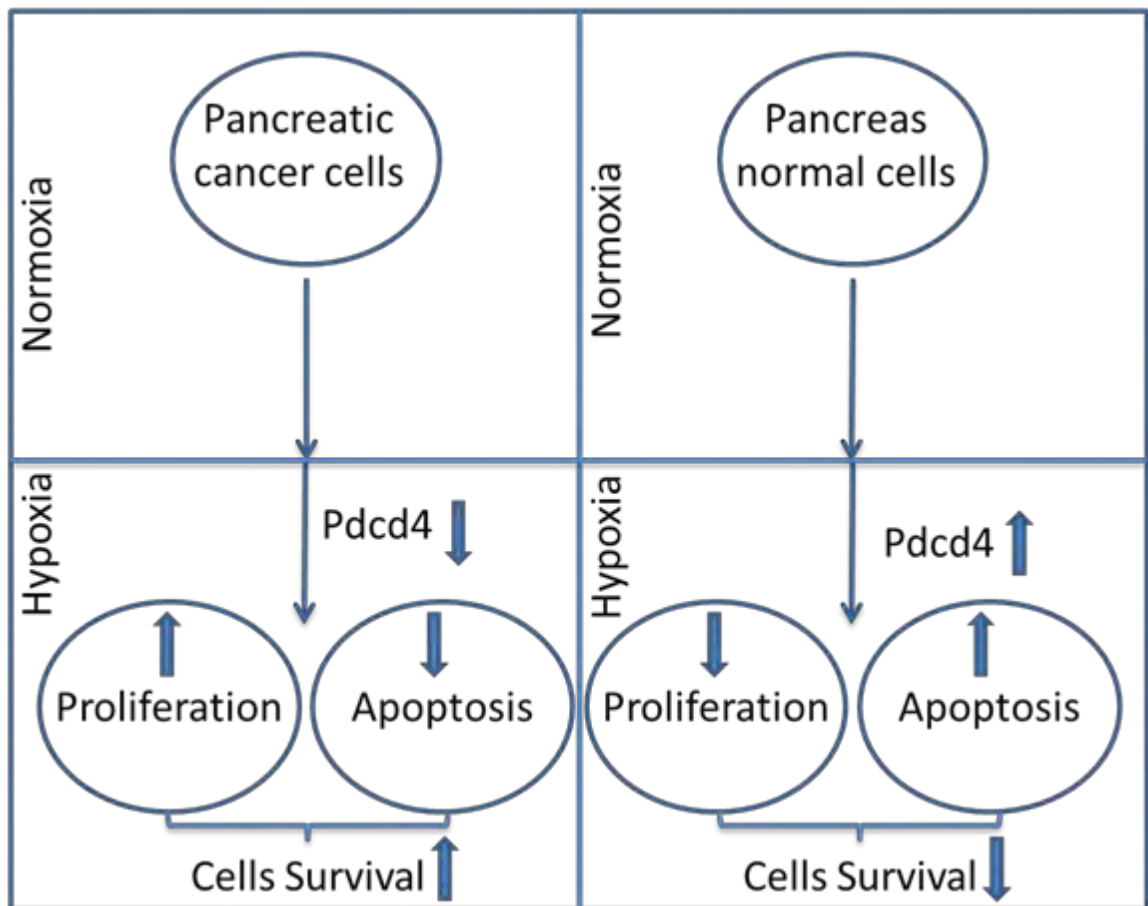


Figure 5-22: Schematic representation of the proposed effect of PDCD4 expression on cell survival in the pancreas

Hypoxia induces expression of PDCD4 in normal pancreatic cells such as MIN6 and ARIP cells, resulting in low proliferation and the triggering of apoptosis. However, in pancreatic cancer cells (PSN-1) under hypoxia, expression of PDCD4 decreases, resulting in no apoptosis and continued cells proliferation.

In order to further elucidate the potential role of PDCD4 in the pancreas the subcellular localisation and expression of PDCD4 was determined by immunocytochemistry. PDCD4 was mostly localized in the cytoplasm under hypoxic and normoxic conditions, however, after 24 hour growth in normoxic conditions it start diffusing inside the nucleus of PSN-1 cells as indicated in Figure 5-5. These results also complement the results from western blotting that expression of PDCD4 under the influence of hypoxia was very weak compared to the normoxic conditions (Figure 5-5). However, western blotting analysis also showed nuclear expression of PDCD4 as shown in Figure 5-2. Immunocytochemistry analysis demonstrates that PDCD4 was highly expressed or localized near to the nuclear membrane. An explanation for this apparent discrepancy could be that during the process of nuclear/cytoplasmic protein extraction it might be that some cytoplasmic protein bound to the nuclear membrane has cross contaminated the nuclear protein extracts, which appeared in western blotting of nuclear PDCD4 expression blot as seen in Figure 5-2 (B). Subcellular localisation and expression of PDCD4 in ARIP cells was determined and it was found that PDCD4 was mostly localised and expressed in the cytoplasm of ARIP cell however, at 24 hours, where expression of PDCD4 is quite high; diffuse expression in the nucleus was observed (Figure 5-6). These results also complement the western blotting results as shown in Figure 5-3. Further investigation of PDCD4 localisation in MIN6 cells revealed that PDCD4 was highly expressed in the cytoplasm, with very weak diffused expression in the nucleus of MIN6 cells as observed in Figure 5-7. These results also complemented western blotting analysis as shown in Figure 5-4.

From these analyses it is clear that in different pancreatic cells, although PDCD4 was mostly localized inside the cytoplasm, different cells show different patterns of expression under different conditions. Subcellular localisation of PDCD4 is still a topic of some controversy, as some studies have reported PDCD4 localized in the nucleus in

normal cells and in the cytoplasm in case of cancer [123, 124] whilst others reported that PDCD4 localized in the nucleus in cancer tissues and in the cytoplasm in normal tissues [125]. However, some reported that conflicting these data on PDCD4 localisation might be because PDCD4 shuttles between the nucleus and the cytoplasm, or on serum starvation PDCD4 is localized to the cytoplasm of cells [115, 379]. Our results have shown that PDCD4 is expressed in the cytoplasm of pancreatic cells and serum starvation did not have any effect on the localisation of PDCD4. It is also clear from our studies that PDCD4 does not translocate from the cytoplasm to the nucleus, however, weak diffuse expression of PDCD4 was observed in the nucleus under normoxic conditions at 24 hours in PSN-1 cells as well as ARIP cells.

How PDCD4 exerts its effects still it is not clear, but it has been reported that inside the cytoplasm PDCD4 inhibits helicase activity of eIF4a as well as interfering in the interaction of eIF4a with eIF4G, ultimately resulting in an inhibitory effect on protein translation [107, 113]. Studies into the role of PDCD4 in apoptosis have also given inconsistent findings; PDCD4 has a role in apoptosis in the case of lung [380] and breast cancer [361] however, no apoptotic effect has been found in other tissues [381, 382]. In some studies even overexpression of PDCD4 in ovarian cancer did not induce apoptosis [379]. Induced expression of PDCD4 in normal pancreatic (ARIP and MIN6) cells and loss or reduced expression of PDCD4 in pancreatic ductal adenocarcinoma cells under hypoxic conditions suggest the great importance of PDCD4 expression in deciding pancreatic cell fate. Our data suggest PDCD4 as a promising target for pancreatic cancer. Further work needs to be done to investigate if restoration of normal PDCD4 expression levels in pancreatic cancer cells under hypoxia induces cell death or senescence.

Most of the studies of PDCD4 in different types of cancers were studied in cell culture experiments and only a few studies have been done in animal models, as well as human

cancer tissues. It is very important to study the role of any *gene* in primary tissue sections which give very important information. So in the present investigation expression of PDCD4 was also observed in human pancreatic adenocarcinoma tissue (four case studies) and in healthy mouse pancreatic tissue. In 2010, PDCD4 expression was studied in 108 cases of intraductal papillary mucinous neoplasm of pancreas by immunohistochemistry and it was reported that PDCD4 was expressed in both the nucleus and cytoplasm [271]. This study also reported that, PDCD4 expression shifted from the nucleus to the cytoplasm as well as expression from high to low with the increase in the severity of disease [271]. Recently, it has been reported that PDCD4 was exclusively expressed in the nucleus of normal pancreatic cells whereas adenocarcinoma showed cytoplasmic expression [383], the same pattern of PDCD4 expression reported in colorectal and breast cancer [384, 385]. Different patterns of PDCD4 expression in intraductal papillary mucinous neoplasm (IPMN's) and in adenocarcinoma may vary according to the type of tumour cells. This warrants further investigation. Also PDCD4 expression may vary with different stages and severity of disease, such as from well differentiated to moderately differentiated and to poorly differentiated carcinoma; but in pancreatic adenocarcinoma PDCD4 expression had not yet been investigated. So in order to investigate PDCD4 expression in pancreatic tissues with different severity of disease spread, PDCD4 expression and localisation were determined by immunocytochemistry.

The role of PDCD4 in normal pancreas, as well as in human pancreatic adenocarcinoma tissues was investigated in the present study. Due to unavailability of healthy human pancreas to study as control (also it is hard to obtain), healthy mouse pancreas was analysed as an indicator of a non-cancerous control. In the present investigation four different human pancreatic adenocarcinoma tissue samples and healthy mouse pancreas were studied by immunohistochemistry analysis. Pancreatic adenocarcinoma tissue

sample morphology was defined by H&E staining and showed different morphological characteristics and severity of disease from well to moderate and poorly differentiated. On investigating PDCD4 expression in healthy mouse pancreatic tissue and weak cytoplasmic expression of PDCD4 in acinar cells and nuclear/cytoplasmic expression in ductal as well as islets cells was observed as shown in Figure 5-8 and Figure 5-9. These results suggested that PDCD4 was expressed in normal pancreatic cells, however, differential expression in different cells was observed as PDCD4 expression was found in ARIP cells (Figure 5-6) as well as MIN6 cells(Figure 5-7). Also all of these investigations suggest that PDCD4 was mostly localized in the cytoplasm, however, its expression increased or decreased depended upon the type of cells or environment.

Further PDCD4 expression and localisation was investigated in four human pancreatic adenocarcinoma tissue samples. In sample 1 which is moderately to poorly differentiated pancreatic adenocarcinoma tissue (sample 1), differential expression of PDCD4 was found. Part of the tissue section which still had normal pancreas tissue morphology such as lobular structure with acinar cells, showed positive nuclear and cytoplasmic expression of PDCD4. However, poorly differentiated parts of tissue section showed weak cytoplasmic expression and negative expression in ductal as well as pleomorphic malignant epithelial cells. These results suggest that part of the tissue with greater severity of malignancy showed loss or weak expression of PDCD4 and weak to strong cytoplasmic expression in moderately differentiated cancerous part of tissue sections as shown in Figure 5-10, Figure 5-11 and Figure 5-12.

Further expression of PDCD4 was investigated in pancreatic adenocarcinoma tissue section with severity of disease from well to moderate and poorly differentiated (sample 2). The well differentiated tissue section with lower severity of disease showed high nuclear and cytoplasmic expression of PDCD4 as shown in Figure 5-13 (A &B) also found that within well differentiated tissue section, cells with normal morphology

showed nuclear and cytoplasmic expression of PDCD4 such as acinar, intralobular ductal cells and islets of Langerhans as shown in Figure 5-15 (A& C). Even on the same section, acinar cells with loss of morphology of ring like structure showed lost or weak cytoplasmic expression of PDCD4 as shown in Figure 5-15 (A& B). Ductal cell lying with-in well differentiated tissue sections showed positive nuclear and cytoplasmic expression (Figure 5-14(A)), ductal cells lied in moderately differentiated tissue section showed weak cytoplasmic expression (Figure 5-14 (B)) and ductal cells lied in poorly differentiated tissue sections showed very weak or loss of PDCD4 expression as shown Figure 5-15 (C). These results suggest that with an increase in severity of malignancy expression of PDCD4 was decreased or lost.

Further expression of PDCD4 was determined in poorly differentiated pancreatic adenocarcinoma tissue and weak cytoplasmic expression of PDCD4 in ductal as well as fibrous connective tissue as shown in Figure 5-18.

PDCD4 expression was further evaluated in moderately differentiated pancreatic adenocarcinoma tissue sections with pronounced autolysis of tissue. High expression of PDCD4 was found as shown in Figure 5-19. Positive nuclear expression of PDCD4 was observed in islets and fibrous connective tissues as shown in Figure 5-21(A&B). Multinucleated ductal cells showed cytoplasmic expression and single nucleated ductal cells showed positive expression in the nucleus as shown Figure 5-21(C&D).

Clear conclusions can be drawn from our immunohistochemistry analysis of PDCD4 expression in human pancreatic adenocarcinoma tissue samples (1 to 4); that, expression of PDCD4 was reduced with progression of malignancy and has an inverse correlation with the advance stage of malignancy. PDCD4 might inhibit tumour progression as it was observed that low malignancy or normal morphology of tissue sections showed higher expression of PDCD4. Another important conclusion can be drawn out of these results that PDCD4 shows differential expression and localisation in

normal tissue but highly malignant pancreatic tissue showed weak cytoplasmic expression or localisation. The present study demonstrated that PDCD4 expression as well as localisation can be used as additional diagnostic tool to discriminate between normal tissues, benign and malignant pancreatic cancer tissues.

Overall our results from pancreatic cell lines (cancerous and normal) and tissue (normal and adenocarcinoma) have identified that PDCD4 as a new and novel target with great potential to fight two notorious diseases of pancreas i.e. pancreatic cancer and diabetes. More work needs to be done in the future in order to have full control of PDCD4 expression, but if we can carefully and deliberately increase or decrease the expression of PDCD4 we have the potential to give or take life to pancreatic cells.

Chapter 6. Hypoxia Inducible Factor -1 alpha (HIF-1 α)

6.1. Introduction

Pancreatic cancer is a lethal malignancy; 90% of cases are ductal adenocarcinoma and these are the dominant cause of cancer death. Currently there is no effective therapy for pancreatic cancer; chemotherapy and radiotherapy have very limited effect. One of the main reasons for this is the extreme hypoxic conditions found in pancreatic cancer, which provide the cancer cells with resistance against chemotherapy and radiotherapy [209, 386]. Hypoxia is one of the key pathological characteristics of solid tumours, especially in pancreatic cancer [209] and it plays a key role in cancer development and progression as illustrated in Figure 6-1[387].

However, the precise role of hypoxia in pancreatic cancer progression still remains poorly understood. It has been reported that, hypoxia triggers the expression or elevation of hypoxia inducible factor 1 alpha (HIF-1 α) in pancreatic cancer; however, in normal pancreatic tissue, very low levels of HIF-1 α have been observed [210, 388-390].

HIF-1 is a heterodimeric transcription factor consisting of an oxygen sensitive inducible subunit HIF-1 α and constitutively expressed HIF-1 β subunit. HIF-1 α under normoxic conditions is hydroxylated by prolyl hydroxylase, bound to the von Hippel-Lindau (VHL) tumour suppressor protein and rapidly degraded. Under hypoxic conditions hydroxylases are inactive resulting in HIF-1 α stabilization and translocation to the nucleus where it binds to HIF-1 β and ultimately results in transactivation of gene expression [279]. It has been reported that increases in expression of HIF-1 α increases tumour growth, vascularization and glucose metabolism, however, loss of HIF-1 α expression suppresses all of these responses [260, 391].

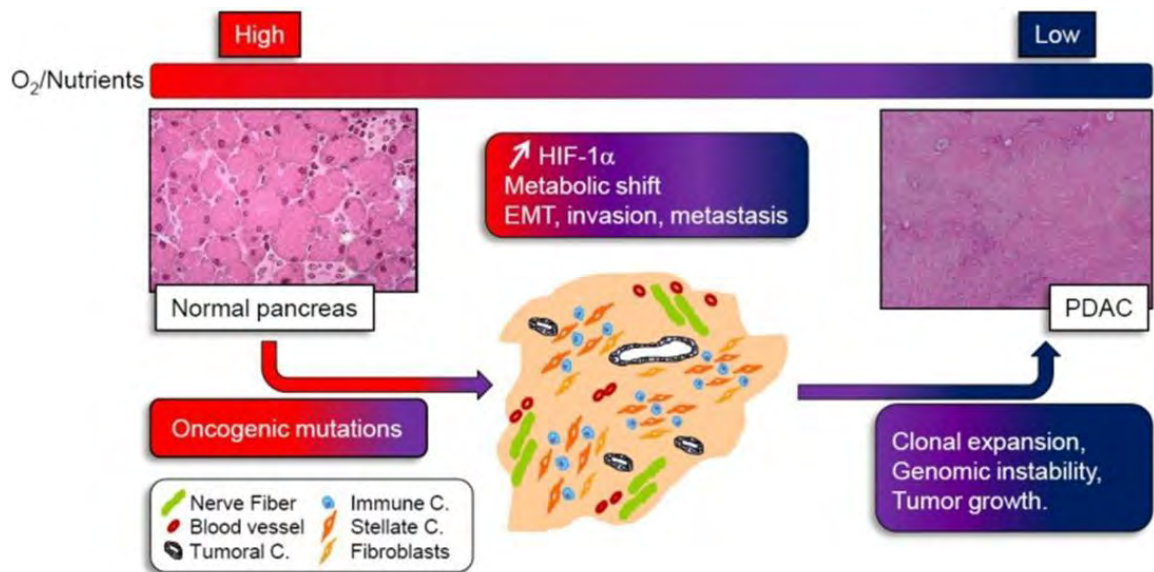


Figure 6-1: Role of hypoxia in pancreatic tumour development:

Loss of tumour suppressors and activation of various oncogenes results into tumour progression. In this tumour, cells are quickly surrounded by dense stroma which gradually reduces oxygen and nutrient supply to cancer cells. In response to these stress conditions cancer cells activate hypoxia-inducible factor 1 α (HIF-1 α), resulting in cell adaptation and survival. Pancreatic tumour cells under very hypoxic and nutrient deprived conditions promotes epithelial to mesenchymal transition (EMT) in pancreatic tumour. However, cells under extreme stress undergo apoptosis and those that survive are subject to genomic mutations, resulting in aggressive, invasive and metastatic pancreatic ductal adenocarcinoma (PDCA) formation.

Adapted from Vasseur, S., et al., Hypoxia induced tumor metabolic switch contributes to pancreatic cancer aggressiveness. Cancers (Basel), 2010. 2(4): p. 2138-52 [387].

Constitutive expression of HIF-1 α provides resistance to apoptosis induced by hypoxia and nutrient deprivation in pancreatic cancer cells. This study also revealed that HIF-1 α was constitutively expressed in most pancreatic cells even under normoxic conditions [215]. In 2010, Schwartz *et al.* reported that 88% of pancreatic adenocarcinomas showed nuclear expression of HIF-1 α . However, only 16% of normal pancreases showed HIF-1 α expression [197] and eradication of HIF-1 α expressing hypoxic cells resulted in suppression of tumour progression and dissemination [392]. HIF-1 α can induce apoptosis under hypoxic and hypoglycaemic conditions [393] however, it can prevent apoptosis as well [215]. The exact mechanism by which HIF-1 α induces apoptosis is not yet clear; it might be some other factor or involvement of other genes which may decide what role HIF-1 α should play, either apoptosis inducer or preventer. As our previous results suggest that, hypoxia induced apoptosis in normal pancreatic cells and does not have any effect on cell viability in pancreatic cancer cells. We also found that PDCD4 (tumour suppressor) expression under hypoxic conditions decreased in pancreatic cancer cells but was up regulated in normal pancreatic cells (Figure 5-1, Figure 5-2, Figure 5-3 and Figure 5-4).

The aim of this chapter is to examine the expression of HIF-1 α in normal and cancerous cells of the pancreas. We hypothesise that PDCD4 may be an extra factor influencing whether HIF-1 α induces or prevents apoptosis, or HIF-1 α might be an extra factor which decides the role for PDCD4 to play. A connection between HIF-1 α and PDCD4 has never been studied before in pancreatic cancer. In the present study we investigated the role of HIF-1 α in PSN-1 and ARIP cells only. In present investigation we did not include MIN6 cells, as the role of HIF-1 α in MIN6 cells already been extensively studied by Dr Michelle Barry (Oct 2013) in our research group.

6.2. Results

In order to determine the role HIF-1 α in pancreatic cells we investigated expression, regulation and subcellular localisation of HIF-1 α in two pancreatic cell lines by performing western blotting and immunocytochemistry. We also investigated expression and subcellular localisation of HIF-1 α in mouse pancreas and human pancreatic adenocarcinoma tissues (four case studies) by performing immunohistochemistry.

6.2.1. HIF-1 α in pancreatic cells

This study was designed to investigate the influence of culture which mimics the oxygen-deprived core of cancerous tumour i.e. hypoxic conditions (1% oxygen) and normal growth culturing conditions i.e. normoxic conditions (21% oxygen) on the expression, regulation and subcellular localisation of HIF-1 α in human pancreatic adenocarcinoma (PSN-1) and rat ductal (ARIP) cell lines as investigated by western blotting and immunocytochemistry.

6.2.1.1. *Western blotting*

In order to identify the expression, regulation and subcellular localisation of HIF-1 α in PSN-1 and ARIP cells; cells were cultured and pelleted at various time points i.e. G0 (serum starvation), normoxic and hypoxic conditions both at 12 and 24 hours. Cell protein extracts were quantified and separated on 10% SDS-PAGE. Western blotting was performed using a specific antibody to HIF-1 α and densitometry analysis was performed using Image j software. Densitometry values from three separate experiments (n=3) were plotted and statistical analyses (2way ANOVA test) were performed on Graphpad prism 5 software. Error bar values represent +/- standard error mean (SEM).

6.2.1.1.1. Human pancreatic adenocarcinoma cells (PSN-1)

In order to determine expression of HIF-1 α in human pancreatic adenocarcinoma cells under different stimuli (serum starved, normoxic and hypoxic), we began our investigation in PSN-1 cells; whole cell proteins were extracted and western blotting was performed. The results are detailed in Figure 6-2. From the densitometry analysis it is clear that expression of HIF-1 α was significantly higher at N24 and H24 ($p < 0.001$) compared to G0. There was no significant expression difference in HIF-1 α between normoxic and hypoxic conditions either time point. We further investigated subcellular (cytoplasmic and nuclear) expression of HIF-1 α in PSN-1 by western blotting analysis. The results are detailed in Figure 6-3. From the densitometry data it is clear that expression of HIF-1 α was significantly higher at N24 and H24 ($p < 0.001$) compared to G0. HIF-1 α was exclusively expressed in the nucleus of PSN-1 cells under hypoxic and normoxic conditions, as shown in Figure 6-3. There was no significant expression difference of HIF-1 α between normoxic and hypoxic at either time point.

6.2.1.1.2. Pancreatic ductal cells (ARIP)

We further investigated subcellular expression of HIF-1 α in pancreatic ductal cells under different stimuli (serum starved, normoxic and hypoxic). Cytoplasmic and nuclear protein extracts were extracted from ARIP cells and western blotting was performed. The results are detailed in Figure 6-4. From the densitometry data it is clear that expression of HIF-1 α was significantly higher at H24 ($p < 0.001$) compared to G0. Also expression of HIF-1 α at H24 ($p < 0.01$) was significantly higher compared N24. HIF-1 α was exclusively expressed in the nucleus of ARIP cells under hypoxic and normoxic conditions as shown in Figure 6-4.

Western blotting results suggest that in human pancreatic adenocarcinoma cells hypoxia does not have any effect on expression of HIF-1 α as there was no significant difference

of expression between hypoxic and normoxic conditions. However, in normal ductal cells hypoxia triggered the expression of HIF-1 α . It is also clear from these results that HIF-1 α was exclusively expressed inside the nucleus of pancreatic cells, either normal or cancerous, under both hypoxic and normoxic conditions.

Pancreatic adenocarcinoma cells

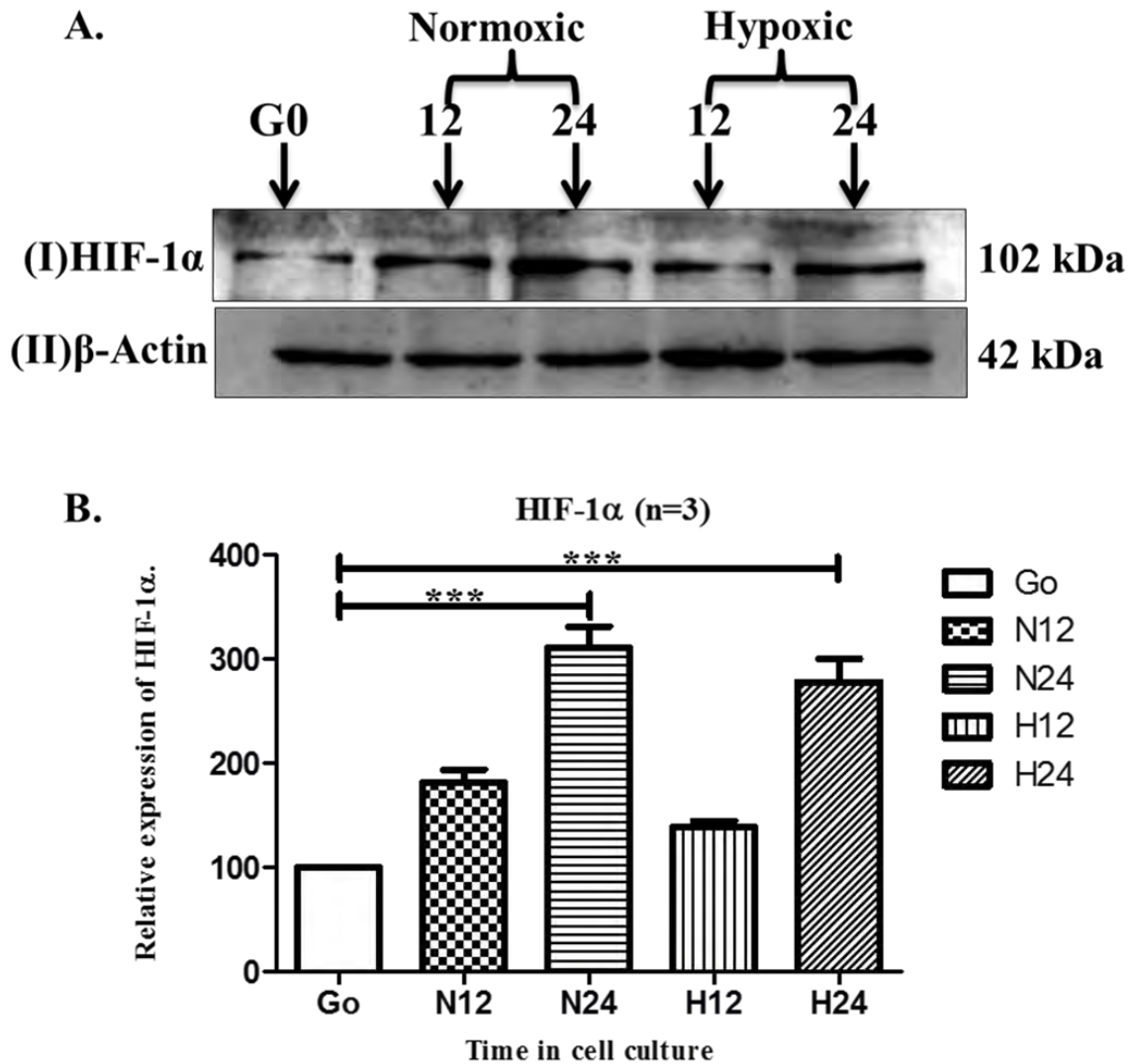


Figure 6-2: Expression of HIF-1 α under hypoxic and normoxic conditions in human pancreatic adenocarcinoma cells.

PSN-1 cells were exposed to hypoxic or normoxic conditions for 24 hours. 10 μ g of whole cell extract was separated by 10% SDS-PAGE. Proteins were western blotted using an antibody specific to HIF-1 α . Panel A (I) represents HIF-1 α (102kDa) protein expression and (II) represents protein loading control β -Actin (42kDa). Panel B illustrates densitometry of HIF-1 α relative to β -Actin. These results were reproduced in at least three separate experiments. Error bar values represent mean \pm standard error. Expression of HIF-1 α was significantly higher at N24 (***) and H24 (***) compared to G0.

Pancreatic adenocarcinoma cells

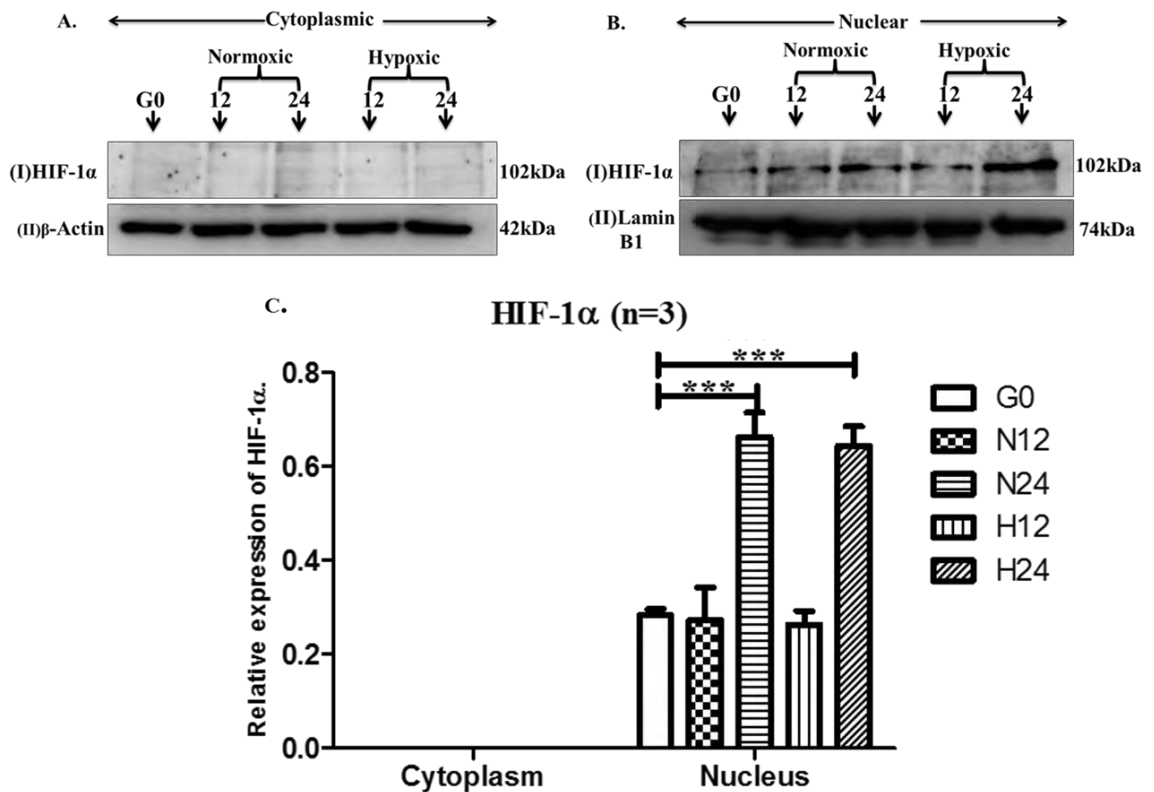


Figure 6-3: Subcellular expression (A) cytoplasm and (B) nucleus of HIF-1α in human pancreatic adenocarcinoma cells.

PSN-1 cells were cultured under G0 (serum starvation), normoxic or hypoxic conditions for 12 or 24 hours. After each indicated incubation period, the cells were pelleted. Cytoplasmic and nuclear proteins were extracted and 10μg of cytoplasmic or nuclear cell extract were separated on a 10% SDS-PAGE. Proteins were western blotted using an antibody specific to HIF-1α. Panel A (I) represents HIF-1α (102kDa) protein expression in the cytoplasm (II) represents protein loading control β-Actin (42kDa). Panel B (I) represents HIF-1α (102kDa) protein expression in the nucleus (II) represents protein loading control lamin B1 (74kDa). Panel C illustrates densitometry analysis showing cytoplasmic HIF-1α relative to control β-Actin and nuclear HIF-1α relative to lamin B1. These results were reproduced in at least three separate experiments. Error bar values represent mean +/- standard error. HIF-1α was exclusively expressed in the nucleus under normoxic and hypoxic conditions. Expression of HIF-1α was significantly higher at N24 and H24 (**p<0.001) compared to G0.

Pancreatic ductal cells

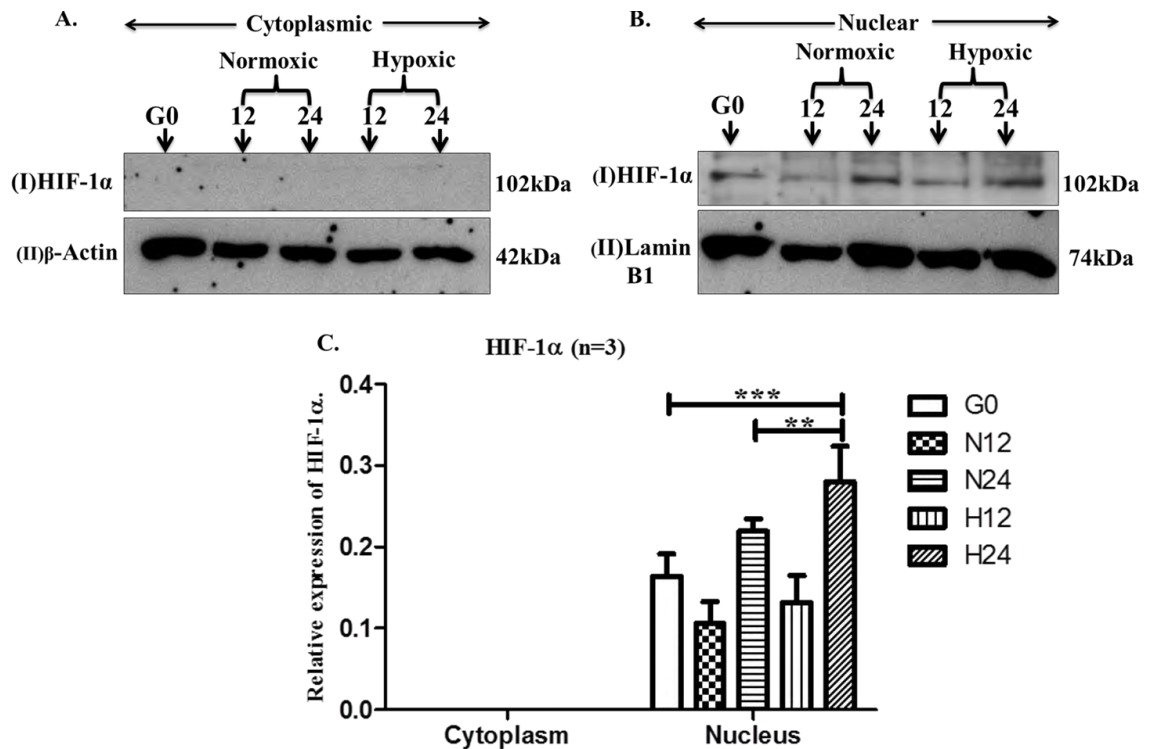


Figure 6-4: Subcellular expression (A) cytoplasm and (B) nucleus of HIF-1α in pancreatic ductal cells.

ARIP cells were cultured under G0 (serum starvation), normoxic or hypoxic conditions for 12 or 24 hours. After each indicated incubation period, the cells were pelleted. Cytoplasmic and nuclear proteins were extracted and 10μg of cytoplasmic and nuclear cell extract were separated on a 10% SDS-PAGE. Proteins were western blotted using an antibody specific to HIF-1α. Panel A (I) represents HIF-1α (102kDa) protein expression in the cytoplasm (II) represents protein loading control β-Actin (42kDa). Panel B (I) represents HIF-1α (102kDa) protein expression in the nucleus (II) represents protein loading control lamin B1 (74kDa). Panel C illustrates densitometry analysis showing cytoplasmic HIF-1α relative to control β-Actin and nuclear HIF-1α relative to lamin B1. These results were reproduced in at least three separate experiments. Error bar values represent mean +/- standard error. HIF-1α was exclusively expressed in the nucleus under normoxic and hypoxic conditions. Expression of HIF-1α was significantly higher at H24 (**p<0.01) compared to G0. Also HIF-1α was significantly higher at H24 (**p<0.01) compared to N24.

6.2.1.2. *Immunocytochemistry*

In order to further investigate subcellular localisation and expression of HIF-1 α in PSN-1 and ARIP cells: cells were cultured and fixed with 3.7% formalin at various experimental time points i.e. G0 (serum starvation), normoxic and hypoxic conditions for 12 or 24 hours. Immunocytochemistry was performed using a specific antibody to HIF-1 α and FITC labelled secondary antibody. Labelled cells on coverslips were mounted on glass slides with mounting medium containing DAPI to stain the nucleus. Samples were analysed by confocal microscope (Leica TCS SP5 confocal microscope) and images were captured at 65X magnification. All immunocytochemistry results are representative of at least three separate experiments (n=3).

6.2.1.2.1. **Human pancreatic adenocarcinoma cells (PSN-1)**

In order to determine subcellular localisation and expression of HIF-1 α in human pancreatic adenocarcinoma cells under different stimuli (serum starved, normoxic and hypoxic) at different time points by immunocytochemistry, we began our investigation with PSN-1 cells; immunocytochemistry results are detailed in Figure 6-5. From confocal image analysis of PSN-1 cells it is clear that HIF-1 α was exclusively expressed in the nucleus under normoxic as well as hypoxic conditions at all-time points. Expression of HIF-1 α increased at N24 and H24 compared to G0 as shown in Figure 6-5.

6.2.1.2.2. **Pancreatic ductal cells (ARIP)**

Further we investigated subcellular localisation and expression of HIF-1 α in pancreatic ductal cells (ARIP) under different stimuli (serum starved, normoxic and hypoxic) at different time points by immunocytochemistry. Immunocytochemistry results are detailed in Figure 6-6. From confocal image analysis of ARIP cells it is clear that HIF-1 α was exclusively expressed in the nucleus under normoxic as well as hypoxic

conditions at all-time points except N12. Expression of HIF-1 α increased at H24 compared to G0 as shown in Figure 6-6.

Immunocytochemistry results suggest that HIF-1 α was exclusively expressed in the nucleus of pancreatic cancer cells as well as normal cells. Expression of HIF-1 α was positive in human pancreatic adenocarcinoma as well ductal cells under hypoxic as well as normoxic conditions. Expression of HIF-1 α was elevated in human pancreatic adenocarcinoma cells under hypoxic and normoxic conditions compared to serum starved cells. However, in ARIP cells expression of HIF-1 α was quite low in normoxic compared to hypoxic conditions.

We next investigated expression and localisation of HIF-1 α in normal pancreatic tissue (mouse) and human pancreatic adenocarcinoma tissue samples (four case studies) by immunohistochemistry.

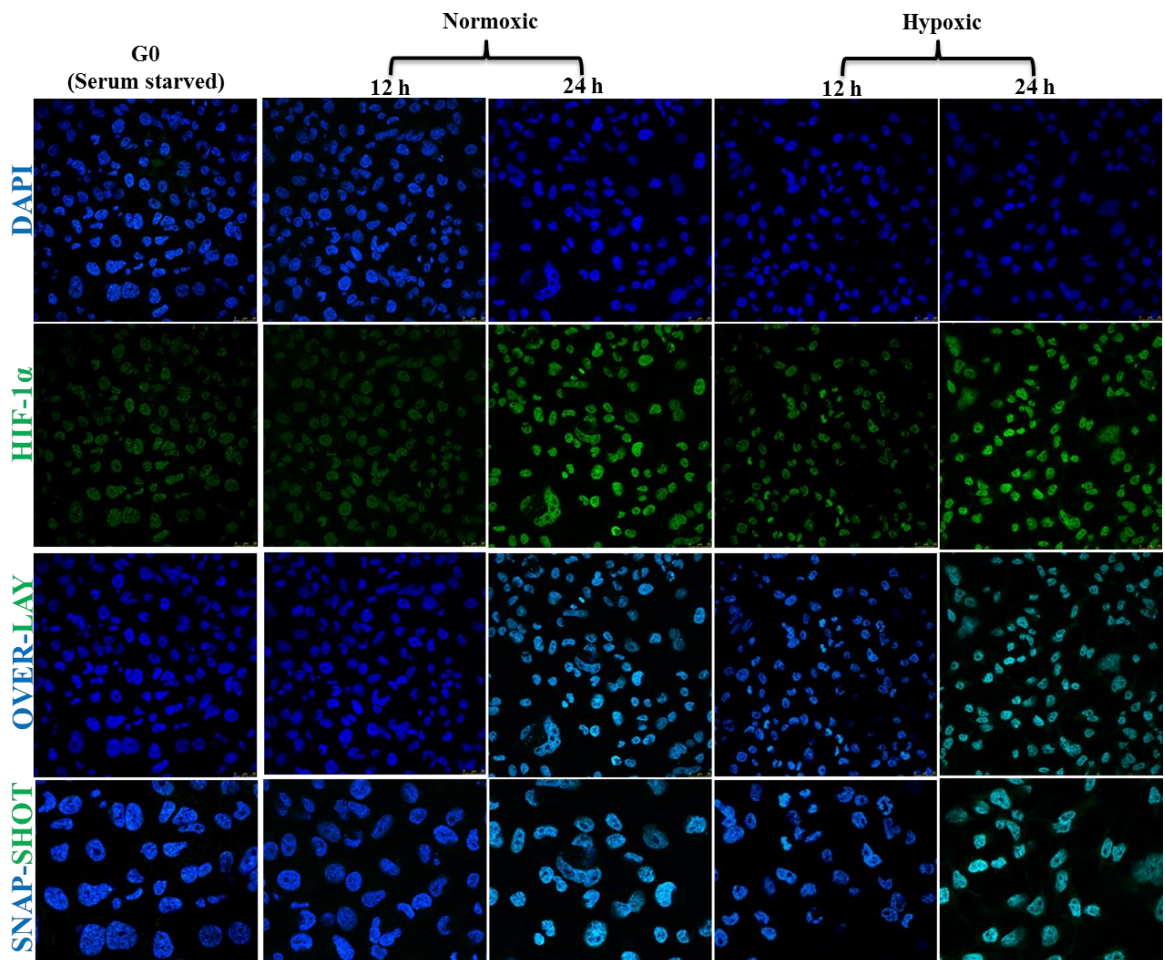


Figure 6-5: Sub-cellular localisation and expression of HIF-1 α in human pancreatic adenocarcinoma cells.

PSN-1 cells were grown on glass cover slips in six well plates and fixed at various time points i.e. at G0 (Serum starvation), N12 & N24 (Normoxic) and H12 & H24 (Hypoxic). Immunocytochemistry was performed using a specific antibody to HIF-1 α and FITC labelled secondary antibody. Coverslips with cells were mounted on glass slides with mounting medium containing DAPI which stains the nucleus of cells. Cells were analysed by confocal microscopy and images were captured at 65X magnification. Results are representative of three separate experiments and images were representative of six separate fields. HIF-1 α was exclusively localized and expressed in the nucleus of PSN-1 cells. However, expression of HIF-1 α was increased at N24 and H24 compared to G0.

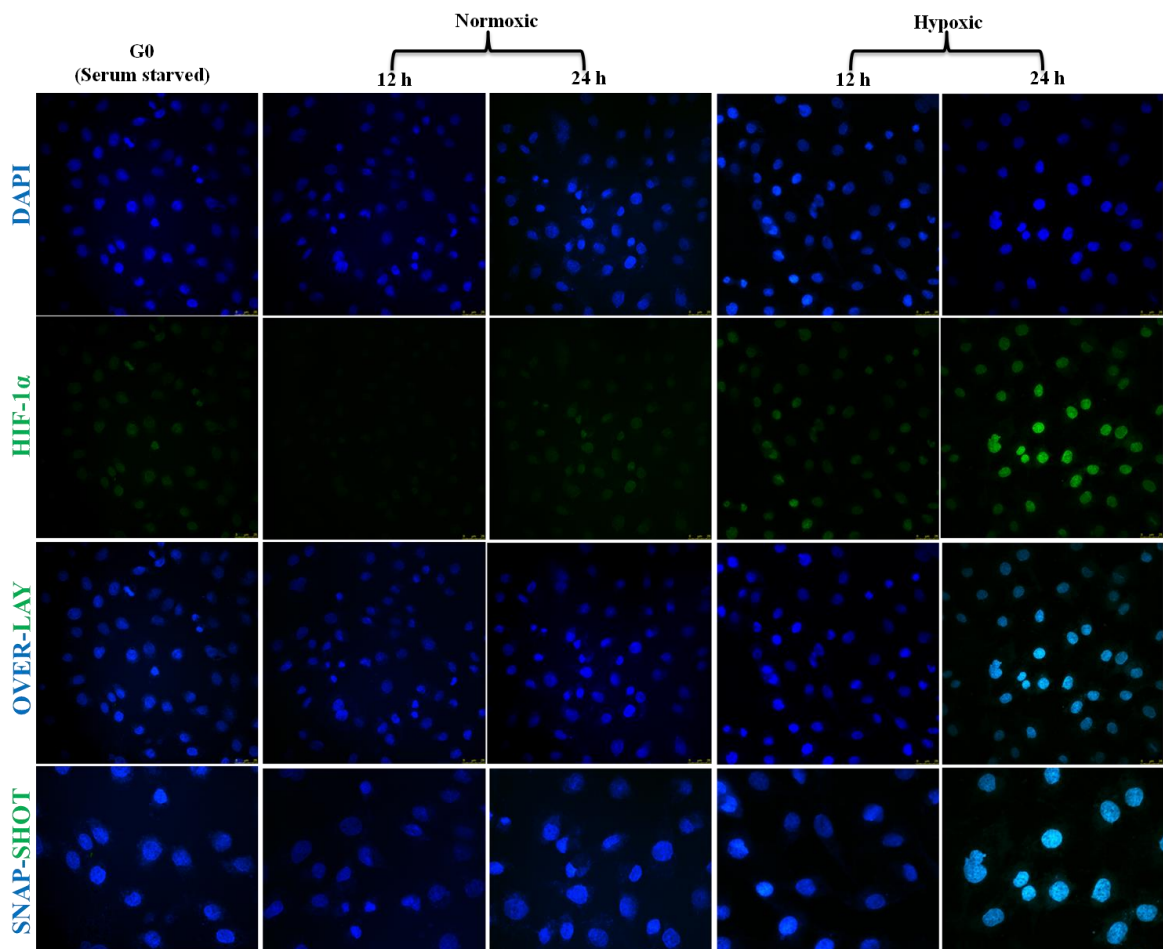


Figure 6-6: Sub-cellular localisation and expression of $\text{HIF-1}\alpha$ in pancreatic ductal cells.

ARIP cells were grown on glass cover slips in six well plates and fixed at various time points i.e. at G0 (Serum starvation), N12 & N24 (Normoxic) and H12 & H24 (Hypoxic). Immunocytochemistry was performed using a specific antibody to $\text{HIF-1}\alpha$ and a FITC labelled secondary antibody. Coverslips with cells were mounted on glass slides with mounting medium containing DAPI which stains the nucleus of cells. Cells were analysed by confocal microscopy and images were captured at 65X magnification. Results are representative of three separate experiments and images were represented in six separate fields. $\text{HIF-1}\alpha$ was exclusively localized and expressed in the nucleus of PSN-1 cells. However, expression of $\text{HIF-1}\alpha$ was increased at H24 compared to G0.

6.2.2. HIF-1 α expression and subcellular localisation in normal and adenocarcinoma pancreas tissue

In order to investigate expression and subcellular localisation of HIF-1 α in normal pancreas (mouse) and human pancreatic adenocarcinoma tissue sections, immunohistochemistry was performed. Formalin fixed paraffin embedded pancreas tissue blocks were sectioned (5 μ m) and mounted on glass slides. Tissue sections were deparaffinised by dipping sections in xylene and rehydrated (gradient ethanol). Immunohistochemistry was performed using a specific antibody to HIF-1 α and an HRP conjugated secondary antibody. HIF-1 α immuno-stained sections were counterstained with haematoxylin. Sections were mounted using DPX mounting medium and analysed by light microscopy and images were captured at 10X and 40X magnification.

6.2.2.1. *HIF-1 α in Mouse pancreas*

Immunohistochemistry was performed to reveal expression and subcellular localisation of HIF-1 α in mouse pancreas. Immunohistochemistry results are shown in Figure 6-7 (10X) and Figure 6-8 (40X). It is clear from these results that HIF-1 α was expressed in normal pancreas; however, HIF-1 α shows differential expression within the tissue sections as shown in Figure 6-7. From higher magnification analysis it is clear that, connective tissue surrounding ductal cells show positive expression of HIF-1 α ; however, ductal cells show very weak expression of HIF-1 α as shown in Figure 6-8 (A). It is clear from Figure 6-8 (B&C) that, acinar cells show weak cytoplasmic expression of HIF-1 α . Islets of Langerhans as well as intercalated ducts in-between acinar cells show positive expression of HIF-1 α , as shown in Figure 6-8 (D).

These results suggest that: HIF-1 α was expressed in normal pancreas, however, very weak expression was observed in ductal and acinar cells. Stroma tissue, Islets and intercalated ducts show positive expression.

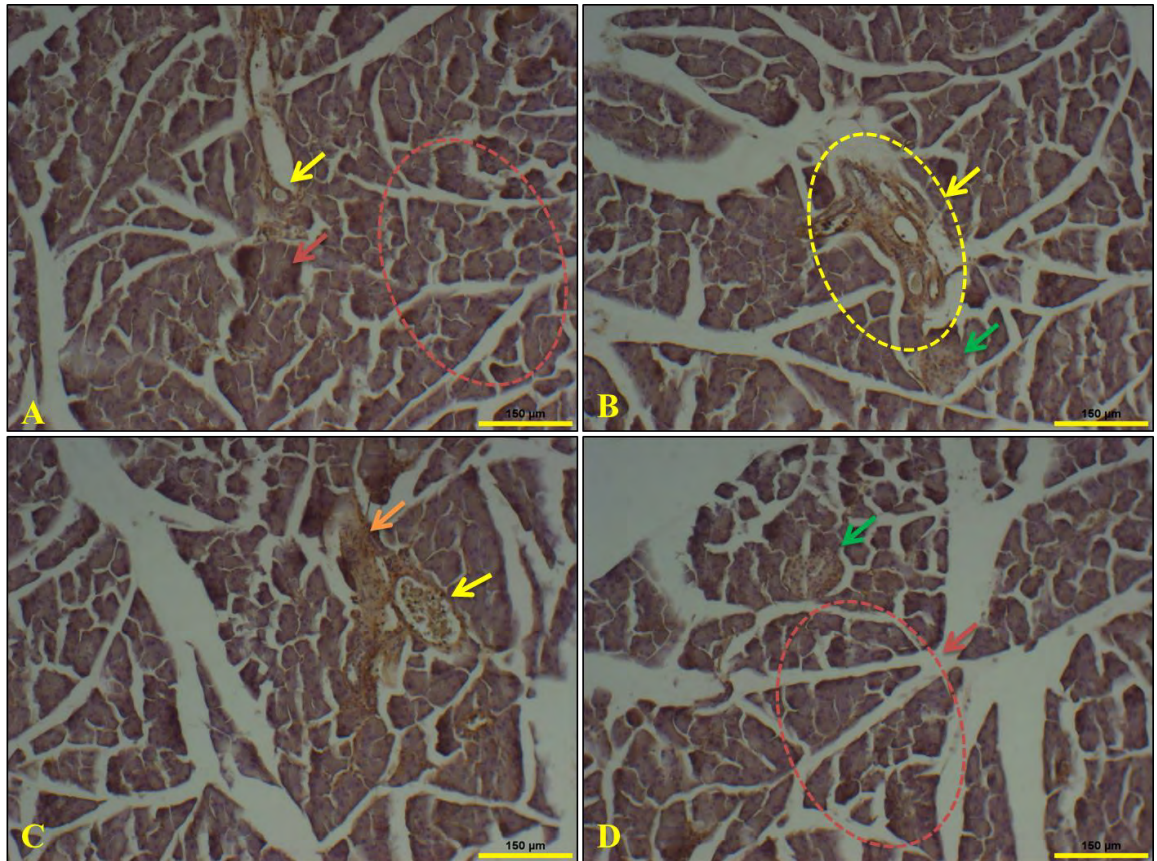


Figure 6-7: Immunohistochemical analysis of the expression of HIF-1 α in mouse pancreas (10X magnification).

Formalin fixed, paraffin embedded mouse pancreas tissue blocks were sectioned (5 μ m) and mounted on glass slides. Immunohistochemistry was performed using a specific antibody to HIF-1 α . HIF-1 α immunostained sections were counter stained with haematoxylin and sections were mounted using mounting medium. Stained sections were analysed by light microscopy and images were captured at 10X magnification. Results are representative of three separate experiments and images were representative of six separate fields.

Acinar (←) cells: Very weak cytoplasmic expression of HIF-1 α .

Blood vessels (←) cells: Positive cytoplasmic expression of HIF-1 α .

Connective or stromal (←) tissue: Cytoplasmic expression of HIF-1 α .

Islets (←) cells: Cytoplasmic expression of HIF-1 α .

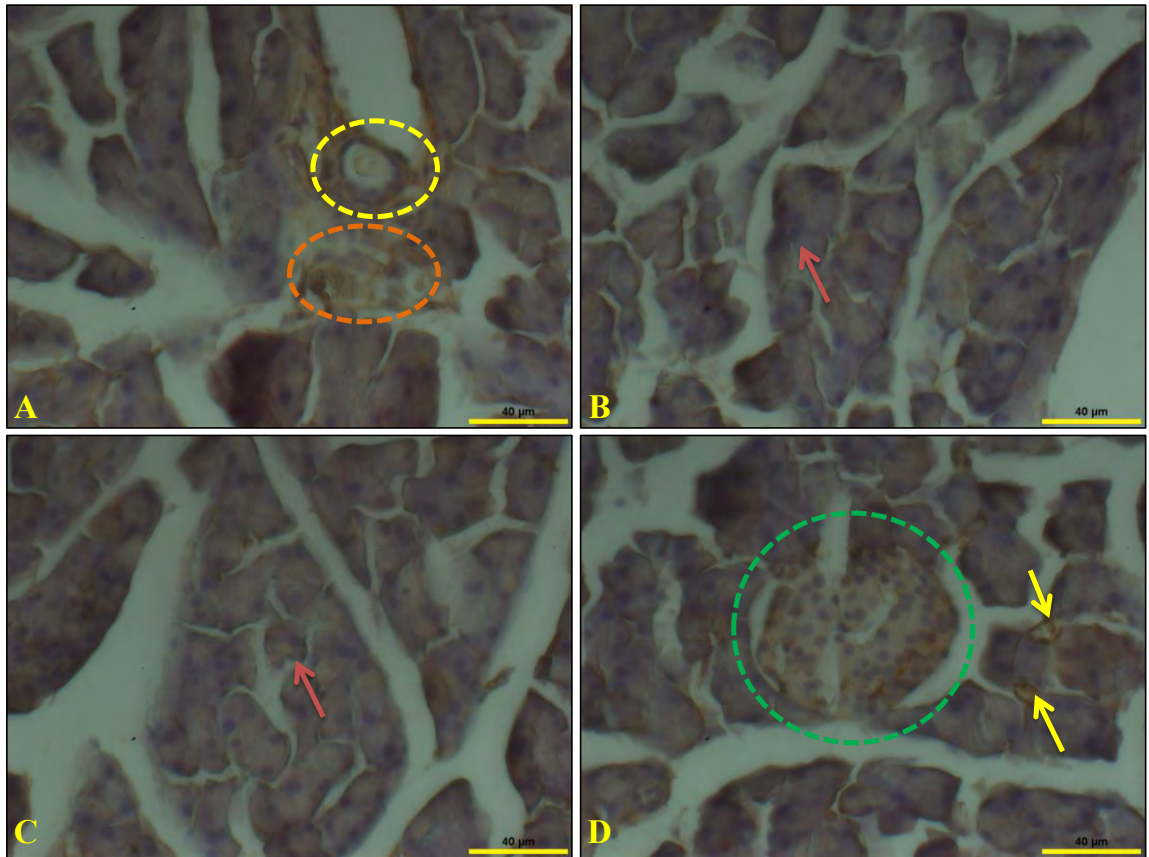


Figure 6-8: Immunohistochemical analysis of the expression of HIF-1 α in mouse pancreas (40X magnification).

Formalin fixed, paraffin embedded mouse pancreas tissue blocks were sectioned (5 μ m) and mounted on glass slides. Immunohistochemistry was performed using a specific antibody to HIF-1 α . HIF-1 α immunostained sections were counter stained with haematoxylin and sections were mounted using mounting medium. Stained sections were analysed by light microscopy and images were captured at 40X magnification. Results are representative of three separate experiments and images were representative of six separate fields. (A) Cytoplasmic expression of HIF-1 α in **stroma cells** and weak expression in **ductal cells**. (B&C) Weak cytoplasmic expression of HIF-1 α was observed in **acinar cells**. (D) Positive cytoplasmic expression of HIF-1 α was observed in **Islets of Langerhans** (as highlighted in **green circle**) and **intercalated ducts**.

6.2.2.2. *HIF-1 α in human pancreatic adenocarcinoma tissues*

In order to investigate expression of HIF-1 α in human pancreatic adenocarcinoma tissue sections immunohistochemistry was performed. In the present study human pancreatic adenocarcinoma tissue sections from four patients were studied for the expression of HIF-1 α by immunohistochemistry.

6.2.2.2.1. **Case study 1**

Immunohistochemistry was performed to reveal expression and subcellular localisation of HIF-1 α in human pancreatic adenocarcinoma tissue (sample 1). Immunohistochemistry results are shown in Figure 6-9 (5X), Figure 6-10 (10X) and Figure 6-11 (40X). It is clear from immunohistochemistry analysis for HIF-1 α expression in human adenocarcinoma sample 1 that: HIF-1 α was highly expressed throughout the tissue section on gross examination as shown in Figure 6-9 (5X). Analysis of samples under higher magnification indicated that HIF-1 α was highly expressed in rudimentary acinar, ductal, pleomorphic malignant epithelial and stroma cells as shown in Figure 6-10 (10X). In order to determine subcellular expression of HIF-1 α , samples were analysed at higher magnification (40X) and it was observed that HIF-1 α was expressed in the nucleus of malignant epithelial ductal cells and acinar cells as shown in Figure 6-11(A, B&C). It was also observed that stroma or fibrous connective tissue showed nuclear as well as cytoplasmic expression and pleomorphic malignant epithelial cells showed high expression of HIF-1 α in the cytoplasm and nucleus as shown in Figure 6-11(D).

The results of immunohistochemistry analysis for HIF-1 α in sample 1 suggest that HIF-1 α was highly expressed in this tissue section and most of the cells showed expression in the nucleus.

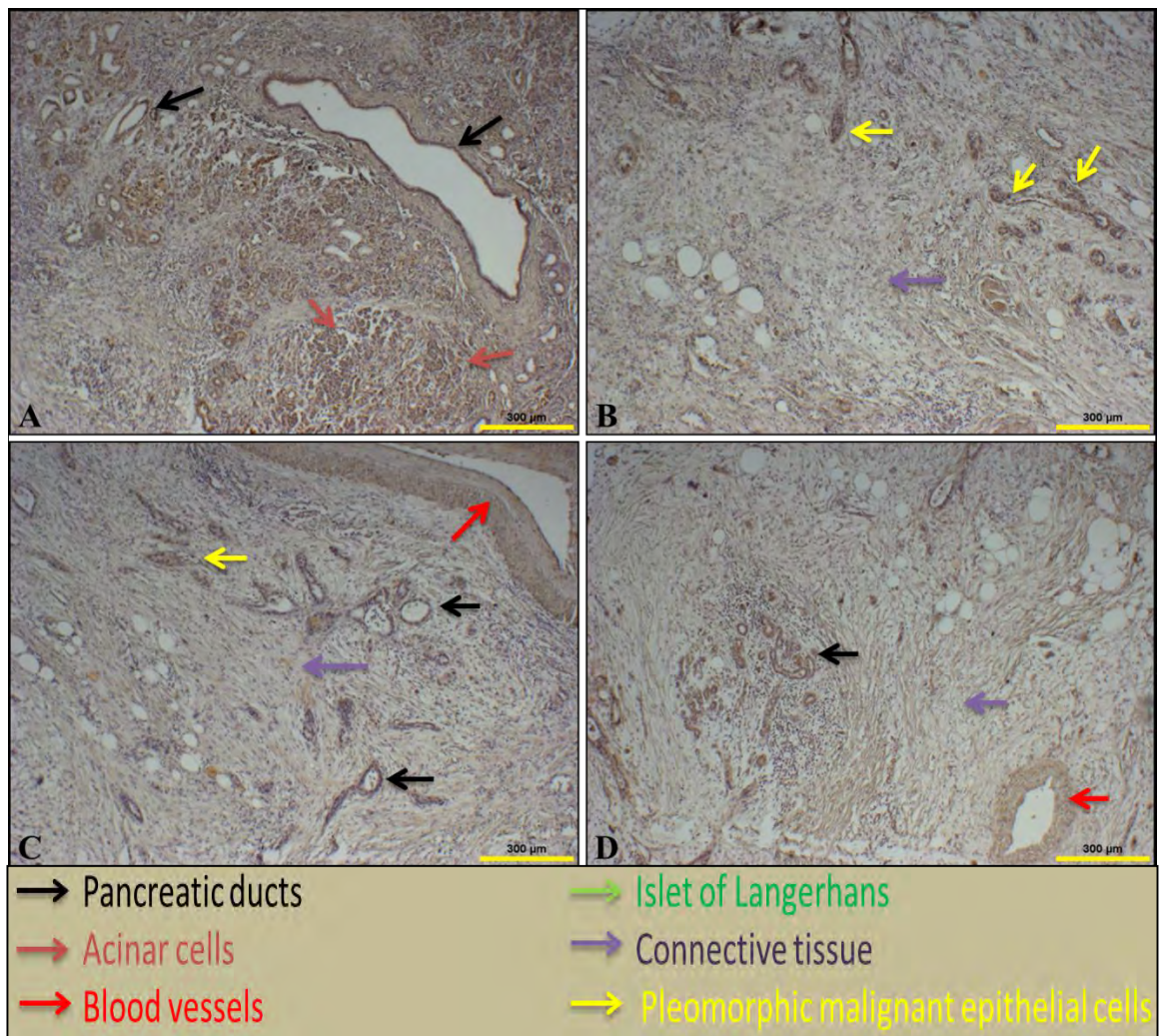


Figure 6-9: Immunohistochemical analysis of the expression of HIF-1 α in human pancreatic adenocarcinoma tissue case study 1 (5X magnification).

Formalin fixed, paraffin embedded pancreatic adenocarcinoma tissue blocks were sectioned (5 μ m) and mounted on glass slides. Immunohistochemistry was performed using a specific antibody to HIF-1 α . HIF-1 α immunostained sections were counter stained with haematoxylin and sections were mounted using mounting medium. Stained sections were analysed by light microscopy and images were captured at 5X magnification. HIF-1 α was highly expressed in ductal, fibrous connective tissue, acinar cells, pleomorphic malignant epithelial and blood vessels.

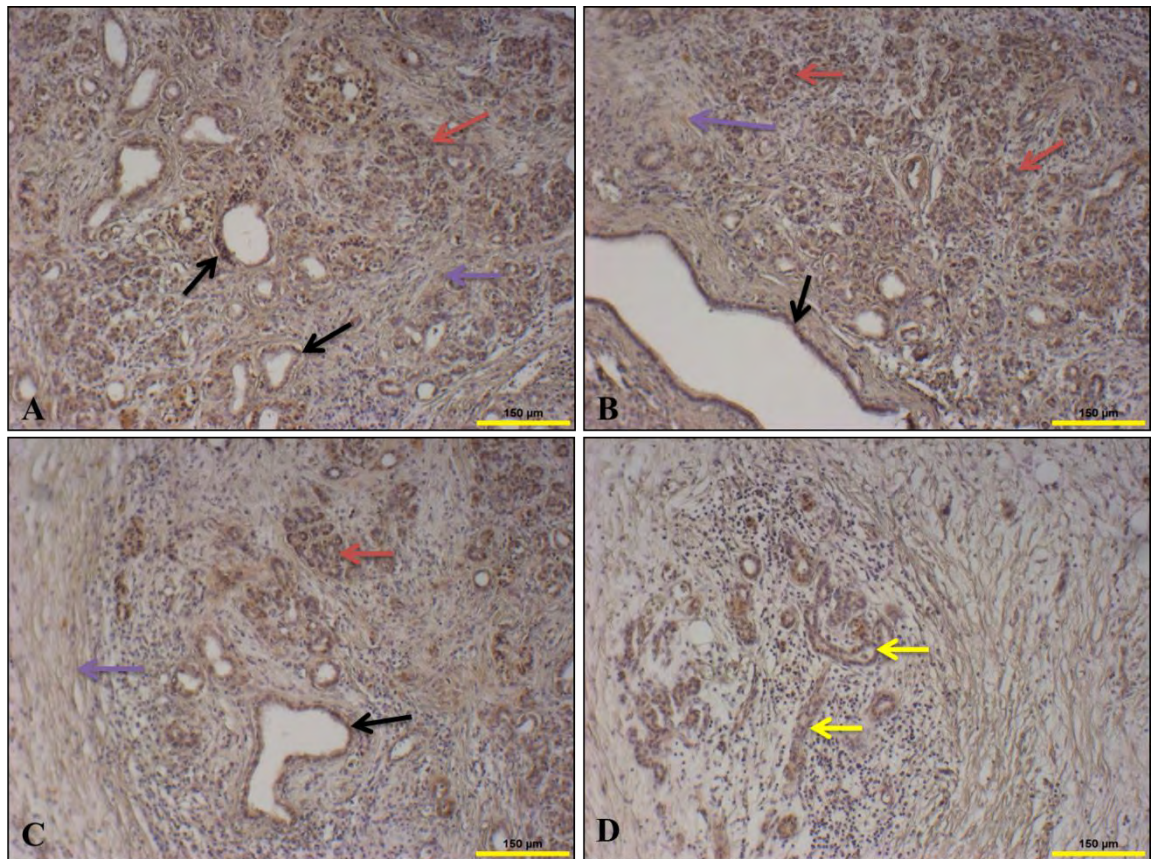


Figure 6-10: Immunohistochemical analysis of the expression of HIF-1 α in human pancreatic adenocarcinoma tissue case study 1 (10X magnification).

Formalin fixed, paraffin embedded pancreatic adenocarcinoma tissue blocks were sectioned (5 μ m) and mounted on glass slides. Immunohistochemistry was performed using a specific antibody to HIF-1 α . HIF-1 α immunostained sections were counter stained with haematoxylin and sections were mounted using mounting medium. Stained sections were analysed by light microscopy and images were captured at 10X magnification. HIF-1 α was highly expressed in ductal, fibrous connective tissue, and acinar cells, pleomorphic malignant epithelial and blood vessels.

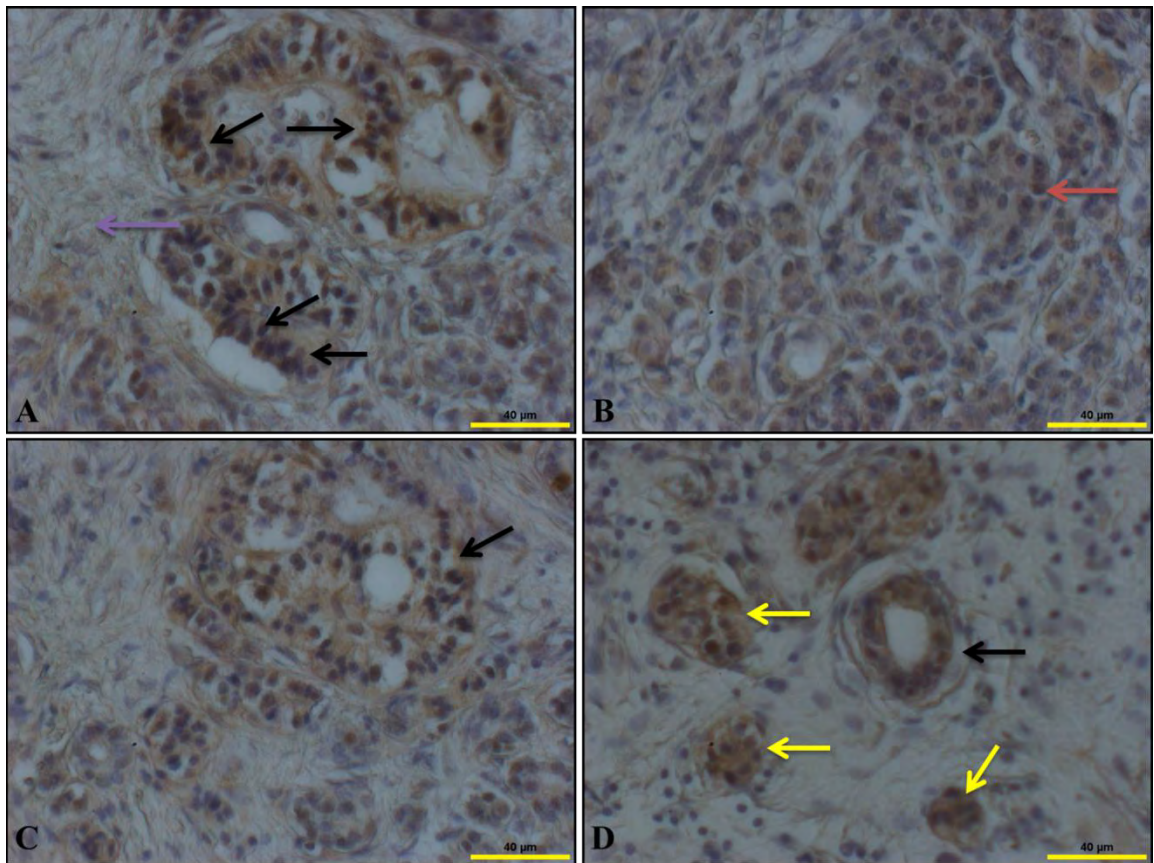


Figure 6-11: Immunohistochemical analysis of the expression of HIF-1 α in human pancreatic adenocarcinoma tissue case study 1 (40X magnification).

Formalin fixed, paraffin embedded pancreatic adenocarcinoma tissue blocks were sectioned (5 μ m) and mounted on glass slides. Immunohistochemistry was performed using a specific antibody to HIF-1 α . HIF-1 α immunostained sections were counter stained with haematoxylin and sections were mounted using mounting medium. Stained sections were analysed by light microscopy and images were captured at 40X magnification. (A & C) HIF-1 α was highly expressed in the nucleus of ductal epithelial cells and positive expression in fibrous connective tissue. (B) Positive nuclear expression of HIF-1 α in acinar cells. (D) HIF-1 α was highly expressed in the nucleus of pleomorphic malignant epithelial and ductal cells.

6.2.2.2.2. Case study 2

In order to determine the expression and subcellular localisation of HIF-1 α in human pancreatic adenocarcinoma tissue (sample 2), immunohistochemistry was performed and results are shown in Figure 6-12(5X), Figure 6-13(10X) and Figure 6-14(40X). It was clear from gross examination of immunohistochemistry of HIF-1 α results of sample 2 that; HIF-1 α was highly expressed throughout the tissue section, either sections showing normal or adenocarcinoma morphology as shown in Figure 6-12. On analysing at higher magnification at 10X it is clear that; HIF-1 α was highly expressed in ductal, islets, acinar and pleomorphic malignant epithelial and fibrous connective tissue as shown in Figure 6-13. In order to determine the subcellular expression of HIF-1 α further we analysed sample 2 under higher magnification at 40X. It was clear from these analyses that; acinar cells with normal and abnormal morphology showed positive nuclear and cytoplasmic expression of HIF-1 α as shown in Figure 6-14 (A). Islets of Langerhans showed positive nuclear and cytoplasmic expression of HIF-1 α as shown in Figure 6-14 (B). Fibrous connective tissue and malignant epithelial ductal cells showed positive nuclear and cytoplasmic expression of HIF-1 α as shown in Figure 6-14 (C). Ductal cells showed positive nuclear expression of HIF-1 α as shown in Figure 6-14 (D). The results from immunohistochemistry analysis for HIF-1 α in sample 2 suggested that HIF-1 α was highly expressed in this tissue section and most of the cells showed nuclear and cytoplasmic expression.

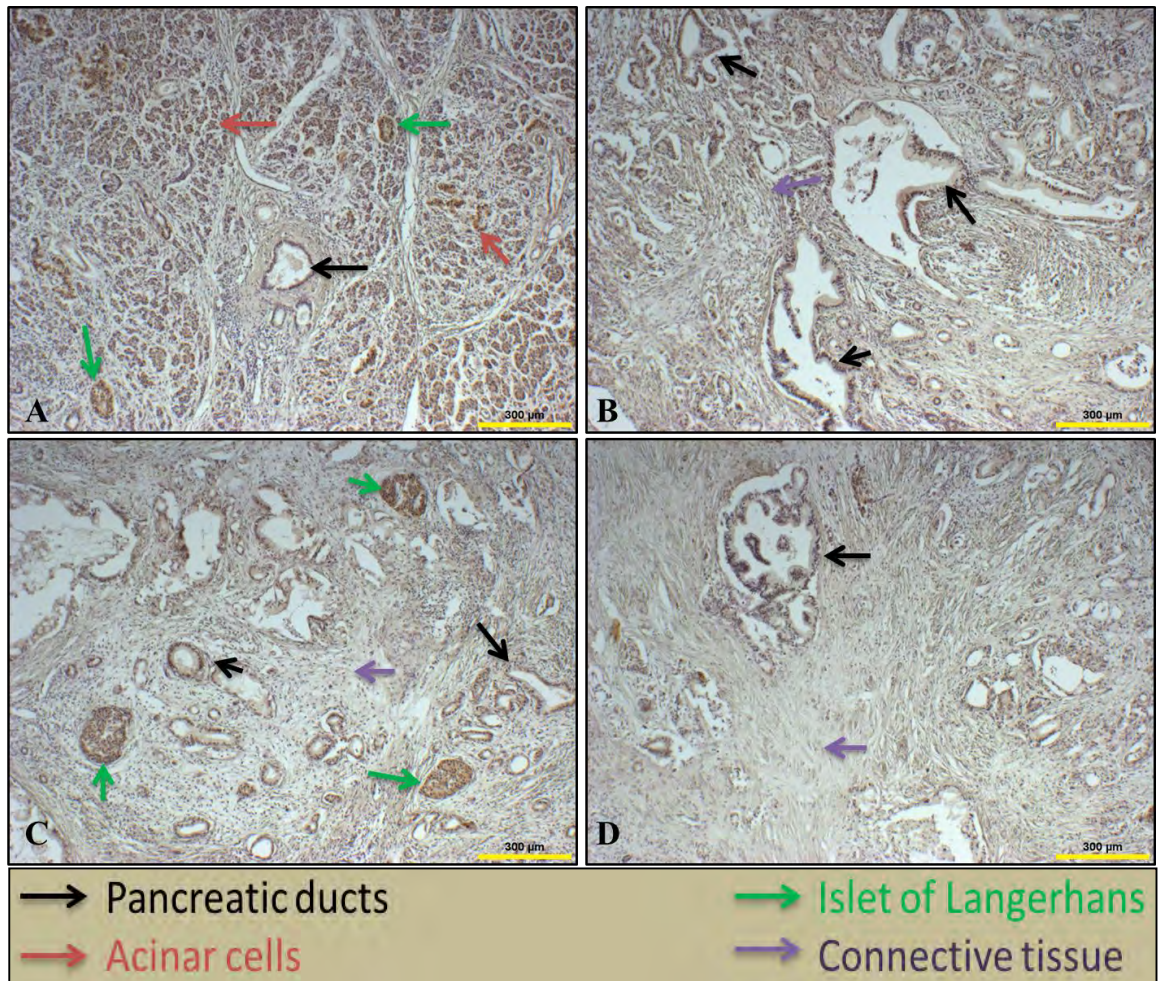


Figure 6-12: Immunohistochemical analysis of the expression of HIF-1 α in human pancreatic adenocarcinoma tissue case study 2 (5X magnification).

Formalin fixed, paraffin embedded pancreatic adenocarcinoma tissue blocks were sectioned (5 μ m) and mounted on glass slides. Immunohistochemistry was performed using a specific antibody to HIF-1 α . HIF-1 α immunostained sections were counter stained with haematoxylin and sections were mounted using mounting medium. Stained sections were analysed by light microscopy and images were captured at 5X magnification. HIF-1 α was highly expressed in ductal, fibrous connective tissue, acinar cells and Islets of Langerhans.

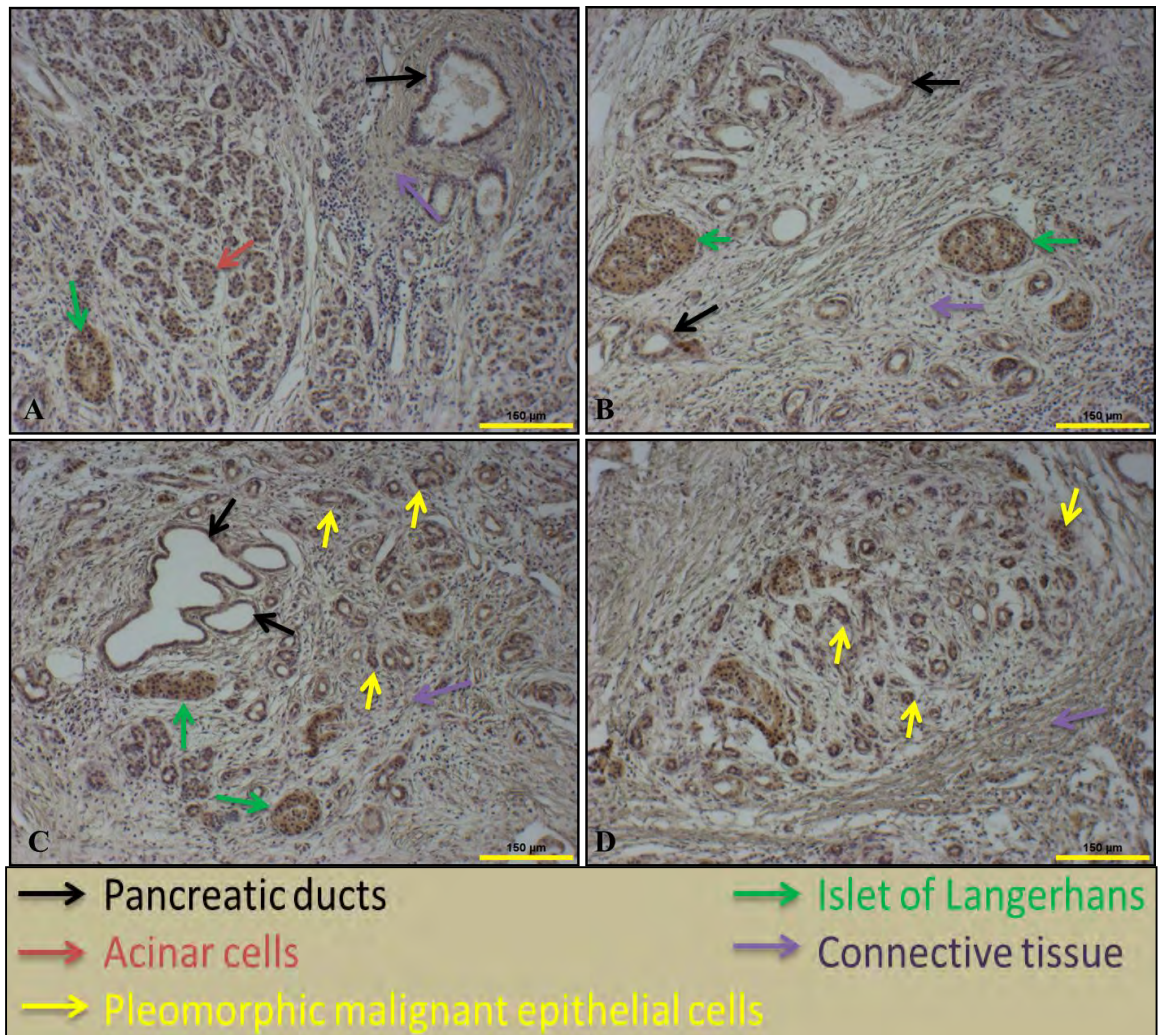


Figure 6-13: Immunohistochemical analysis of the expression of HIF-1 α in human pancreatic adenocarcinoma tissue case study 2 (10X magnification).

Formalin fixed, paraffin embedded pancreatic adenocarcinoma tissue blocks were sectioned (5 μ m) and mounted on glass slides. Immunohistochemistry was performed using a specific antibody to HIF-1 α . HIF-1 α immunostained sections were counter stained with haematoxylin and sections were mounted using mounting medium. Stained sections were analysed by light microscopy and images were captured at 10X magnification. HIF-1 α was highly expressed in ductal, fibrous connective tissue, acinar cells, pleomorphic malignant epithelial and Islets of Langerhans.

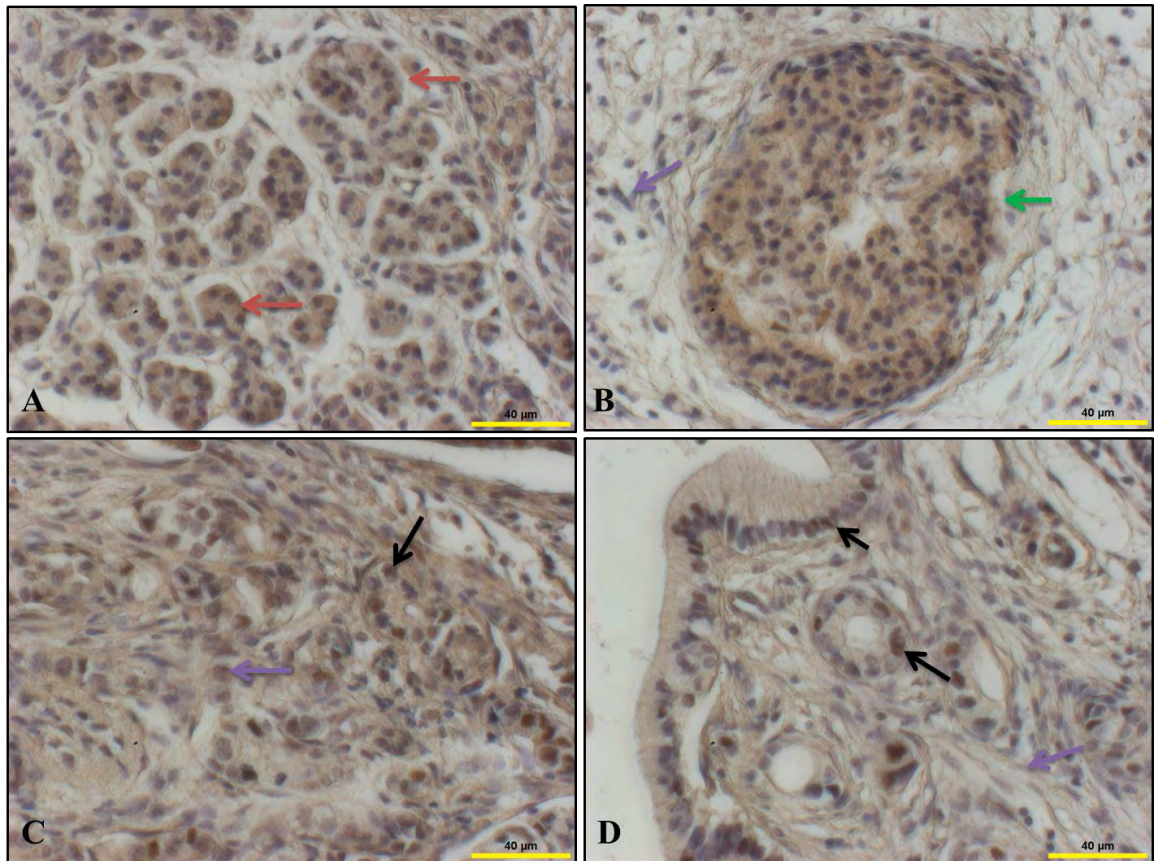


Figure 6-14: Immunohistochemical analysis of the expression of HIF-1 α in human pancreatic adenocarcinoma tissue case study 2 (40X magnification).

Formalin fixed, paraffin embedded pancreatic adenocarcinoma tissue blocks were sectioned (5 μ m) and mounted on glass slides. Immunohistochemistry was performed using a specific antibody to HIF-1 α . HIF-1 α immunostained sections were counter stained with haematoxylin and sections were mounted using mounting medium. Stained sections were analysed by light microscopy and images were captured at 40X magnification. (A) HIF-1 α was highly expressed in the nucleus of **acinar cells** and (B) **islets of Langerhans**. (C) Very high nuclear and cytoplasmic expression of HIF-1 α was observed in malignant epithelial ductal cells and **fibrous connective tissue**. (D) Positive nuclear expression of HIF-1 α in ductal cells.

6.2.2.2.3. Case study 3

Immunohistochemistry was performed in order to determine the expression and subcellular localisation of HIF-1 α in human pancreatic adenocarcinoma tissue (sample 3). Immunohistochemistry results are shown in Figure 6-15 (5X), Figure 6-16 (10X) and Figure 6-17 (40X). It was clear from gross examination of immunohistochemistry of HIF-1 α results of sample 3 that; HIF-1 α was positively expressed throughout the tissue section as shown in Figure 6-15. On analysing at higher magnification at 10X it was clear that; HIF-1 α was highly expressed in ductal and fibrous connective tissue as shown in Figure 6-16. In order to determine the subcellular expression of HIF-1 α further we analysed sample 3 at higher magnification at 40X. It was clear from these analyses that; nuclear and cytoplasmic expression of HIF-1 α was observed in ductal and fibrous connective tissue as shown in Figure 6-17.

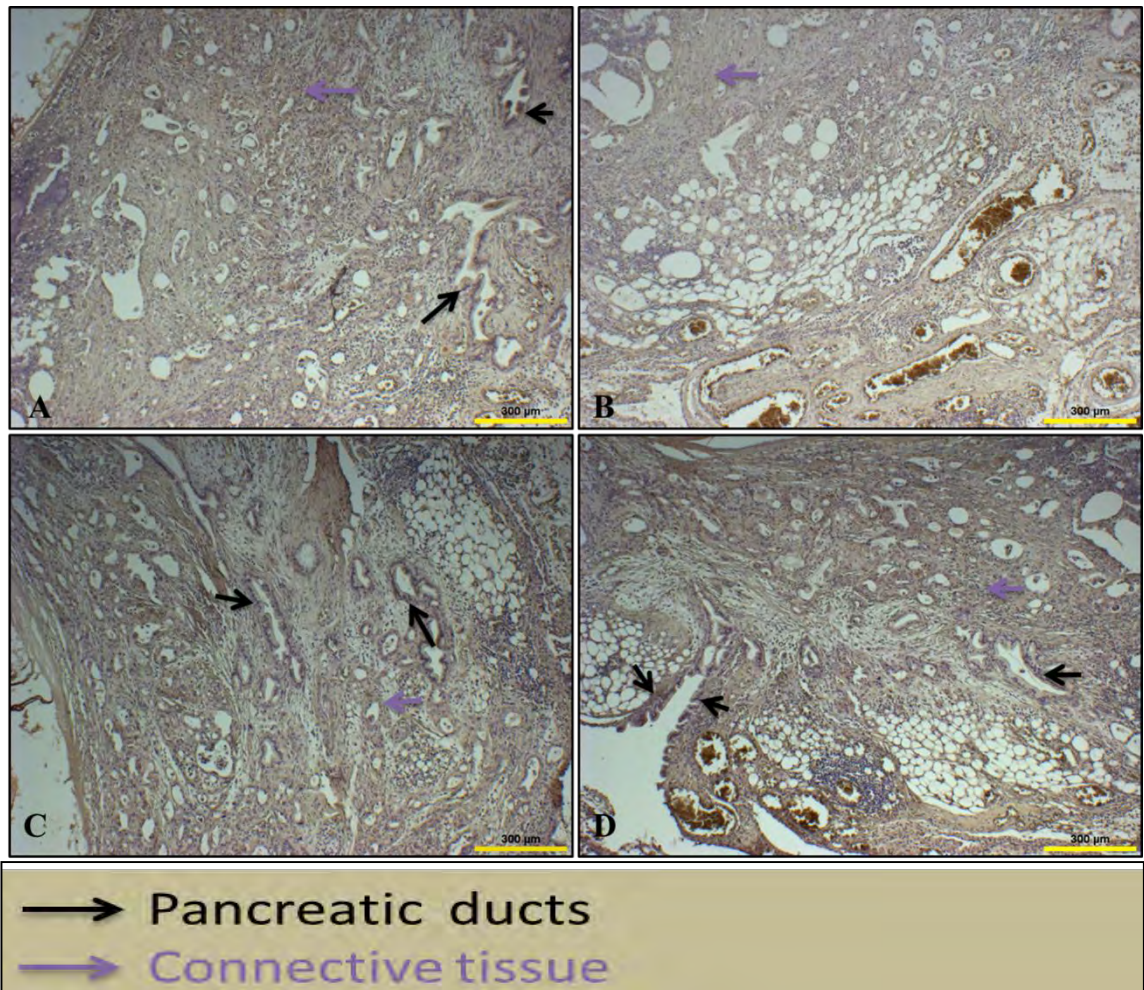


Figure 6-15: Immunohistochemical analysis of the expression of HIF-1 α in human pancreatic adenocarcinoma tissue case study 3 (5X magnification).

Formalin fixed, paraffin embedded pancreatic adenocarcinoma tissue blocks were sectioned (5 μ m) and mounted on glass slides. Immunohistochemistry was performed using a specific antibody to HIF-1 α . HIF-1 α immunostained sections were counter stained with haematoxylin and sections were mounted using mounting medium. Stained sections were analysed by light microscopy and images were captured at 5X magnification. HIF-1 α was positively expressed in ductal and fibrous connective tissue.

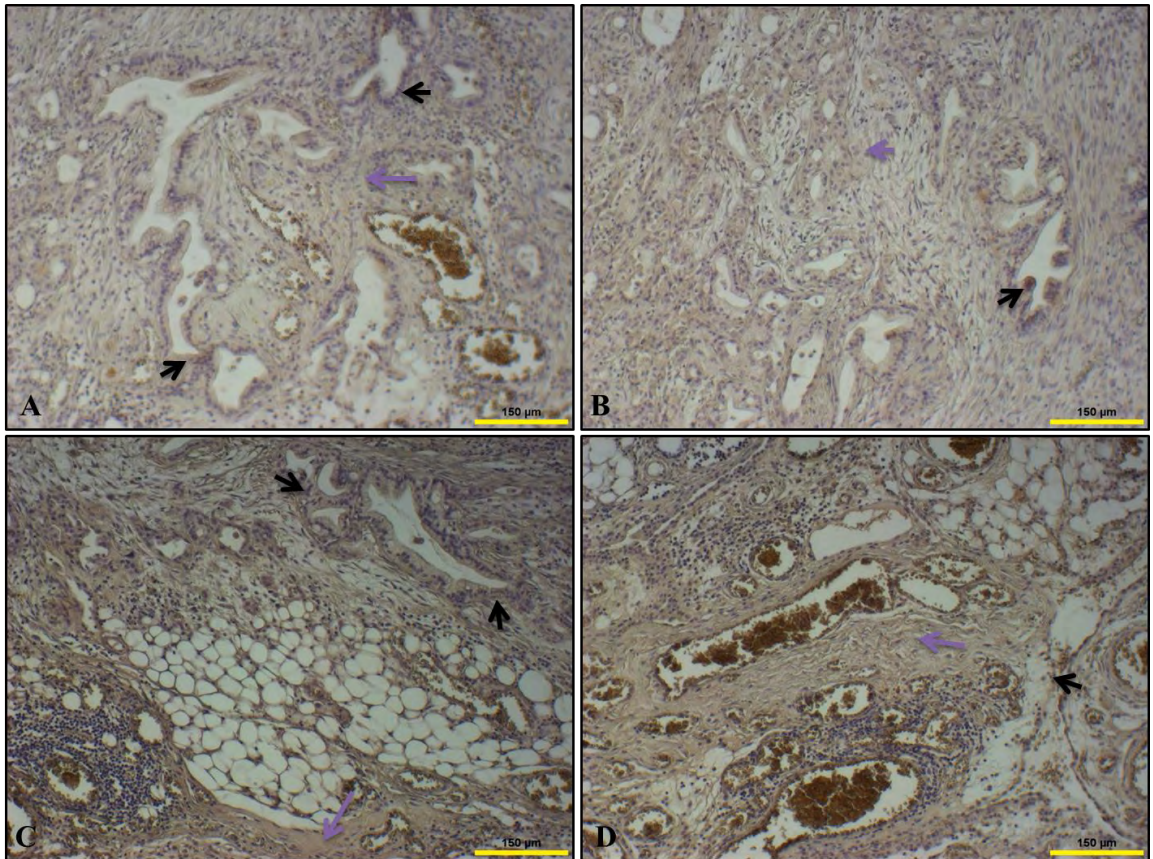


Figure 6-16: Immunohistochemical analysis of the expression of HIF-1 α in human pancreatic adenocarcinoma tissue case study 3 (10X magnification).

Formalin fixed, paraffin embedded pancreatic adenocarcinoma tissue blocks were sectioned (5 μ m) and mounted on glass slides. Immunohistochemistry was performed using a specific antibody to HIF-1 α . HIF-1 α immunostained sections were counter stained with haematoxylin and sections were mounted using mounting medium. Stained sections were analysed by light microscopy and images were captured at 10X magnification. HIF-1 α was positively expressed in ductal and fibrous connective tissue.

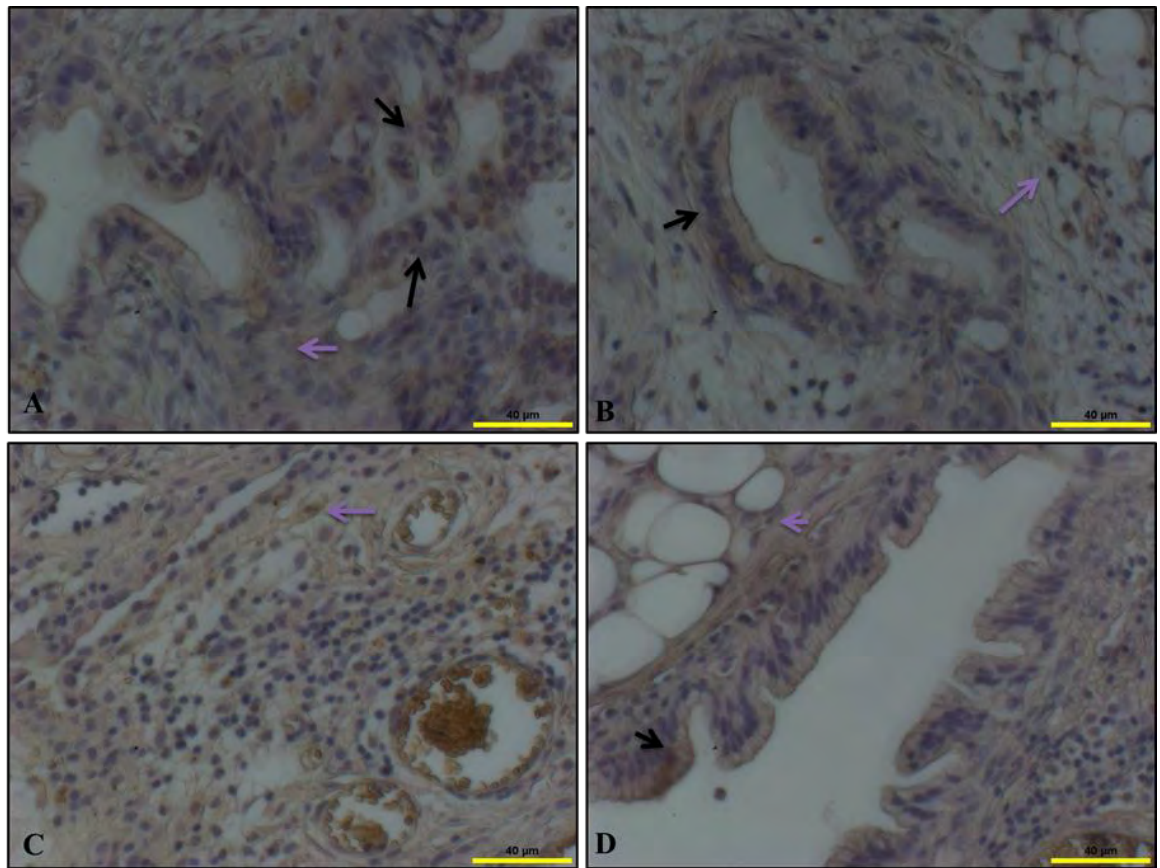


Figure 6-17: Immunohistochemical analysis of the expression of HIF-1 α in human pancreatic adenocarcinoma tissue case study 3 (40X magnification).

Formalin fixed, paraffin embedded pancreatic adenocarcinoma tissue blocks were sectioned (5 μ m) and mounted on glass slides. Immunohistochemistry was performed using a specific antibody to HIF-1 α . HIF-1 α immunostained sections were counter stained with haematoxylin and sections were mounted using mounting medium. Stained sections were analysed by light microscopy and images were captured at 40X magnification. HIF-1 α was positively expressed in the nucleus as well the cytoplasm of ductal and fibrous connective tissue.

6.2.2.2.4. Case study 4

In order to determine the expression and subcellular localisation of HIF-1 α in human pancreatic adenocarcinoma tissue (sample 4), immunohistochemistry was performed and results are shown in Figure 6-18 (5X), Figure 6-19 (10X) and Figure 6-20 (40X). It was clear from gross examination of immunohistochemistry of HIF-1 α results of sample 4 that; HIF-1 α was highly expressed throughout the tissue section, in sections showing either normal or adenocarcinoma morphology as shown in Figure 6-18. On analysing at higher magnification (10X) it was clear that; HIF-1 α was highly expressed in ductal, islet, pleomorphic malignant epithelial and fibrous connective tissue as shown in Figure 6-19. In order to determine the subcellular expression of HIF-1 α further we analysed sample 4 at higher magnification (40X). It was clear from these analyses that; malignant epithelial ductal cells showed strong nuclear expression of HIF-1 α as shown in Figure 6-20 (A), it was also clear from Figure 6-19 (D) that ductal cells showed strong nuclear expression of HIF-1 α . Cells in the islets of Langerhans showed strong nuclear expression of HIF-1 α as shown in Figure 6-20 (B&C). Connective tissue and blood vessel epithelial cells showed positive nuclear expression of HIF-1 α as shown in Figure 6-20 (D).

The results from immunohistochemistry analysis for HIF-1 α in samples 4 suggested that HIF-1 α was highly expressed throughout the tissue section and HIF-1 α was strongly expressed and localized inside the nucleus of ductal cells and cells of the islets of Langerhans.

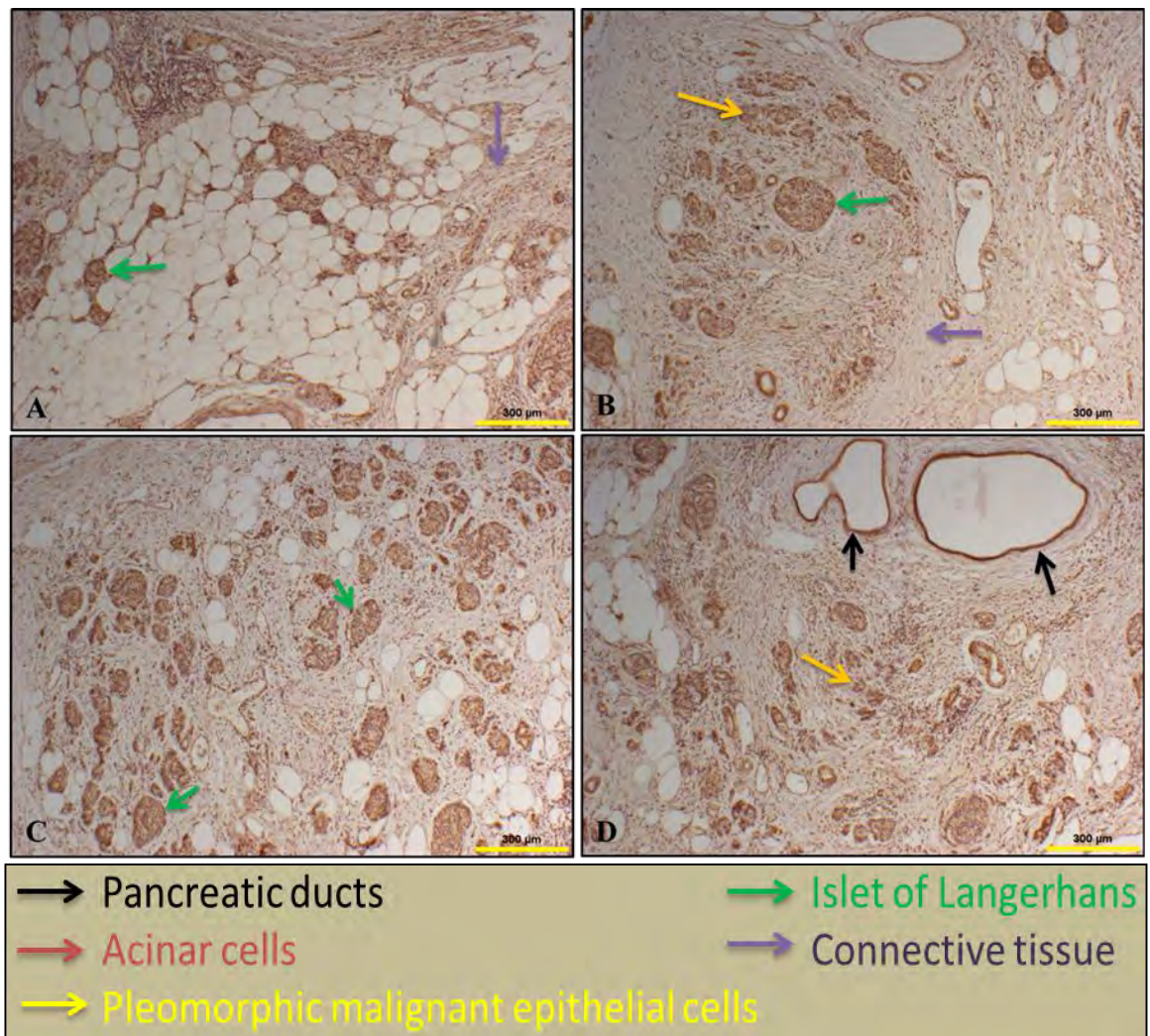


Figure 6-18: Immunohistochemical analysis of the expression of HIF-1 α in human pancreatic adenocarcinoma tissue case study 4 (5X magnification).

Formalin fixed, paraffin embedded pancreatic adenocarcinoma tissue blocks were sectioned (5 μ m) and mounted on glass slides. Immunohistochemistry was performed using a specific antibody to HIF-1 α . HIF-1 α immunostained sections were counter stained with haematoxylin and sections were mounted using mounting medium. Stained sections were analysed by light microscopy and images were captured at 5X magnification. HIF-1 α was highly expressed in ductal, fibrous connective tissue, acinar cells, pleomorphic malignant epithelial and Islets of Langerhans.

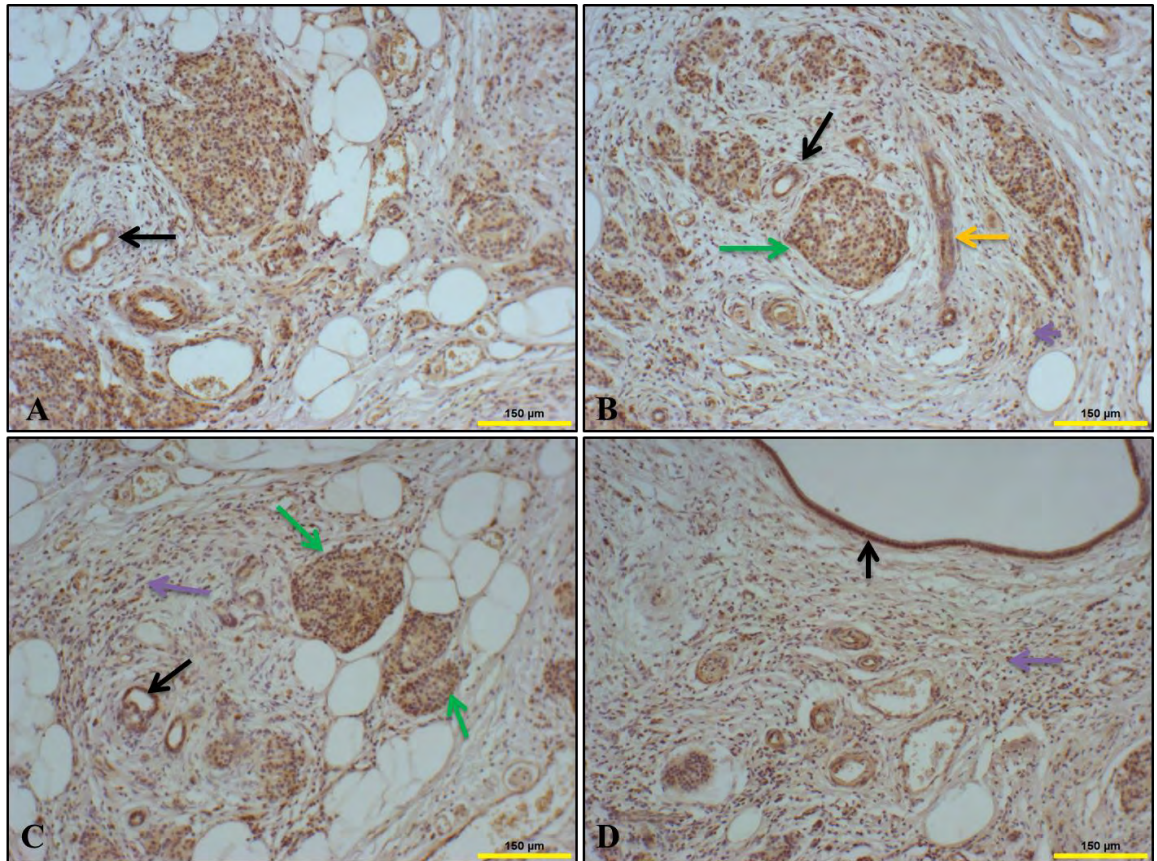


Figure 6-19: Immunohistochemical analysis of the expression of HIF-1 α in human pancreatic adenocarcinoma tissue case study 4 (10X magnification).

Formalin fixed, paraffin embedded pancreatic adenocarcinoma tissue blocks were sectioned (5 μ m) and mounted on glass slides. Immunohistochemistry was performed using a specific antibody to HIF-1 α . HIF-1 α immunostained sections were counter stained with haematoxylin and sections were mounted using mounting medium. Stained sections were analysed by light microscopy and images were captured at 10X magnification HIF-1 α was highly expressed in ductal, fibrous connective tissue, acinar cells, pleomorphic malignant epithelial and Islets of Langerhans.

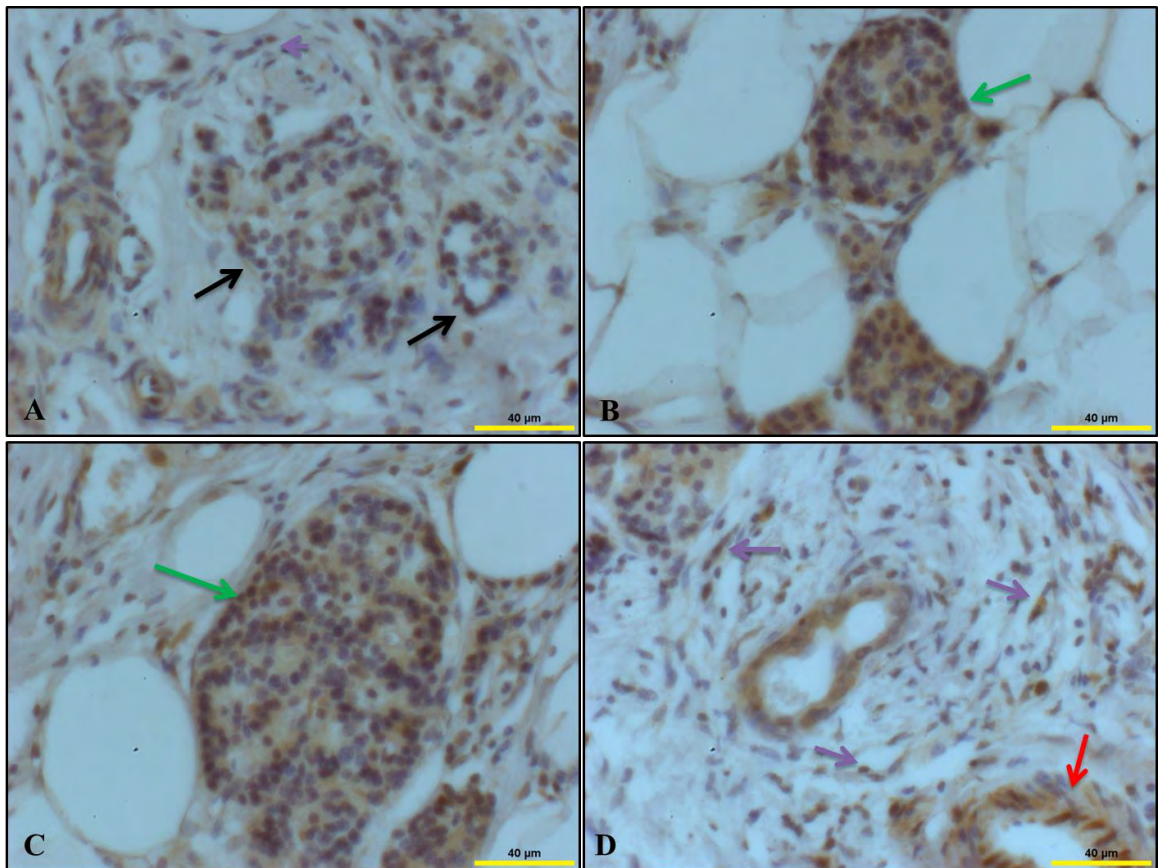


Figure 6-20: Immunohistochemical analysis of the expression of HIF-1 α in human pancreatic adenocarcinoma tissue case study 4 (40X magnification).

Formalin fixed, paraffin embedded pancreatic adenocarcinoma tissue blocks were sectioned (5 μ m) and mounted on glass slides. Immunohistochemistry was performed using a specific antibody to HIF-1 α . HIF-1 α immunostained sections were counter stained with haematoxylin and sections were mounted using mounting medium. Stained sections were analysed by light microscopy and images were captured at 40X magnification. (A) HIF-1 α was highly expressed in the nucleus of malignant epithelial ductal cells. (B & C) HIF-1 α was highly expressed in the nucleus of **Islets of Langerhans**. (D) Blood vessel and connective tissue showed positive nuclear expression of HIF-1 α .

6.3. Discussion

It has been reported that a hypoxic microenvironment plays an important role in the progression of pancreatic cancer and several studies have revealed that hypoxia might be the reason for selection of the most aggressive cell clones in solid tumours [394]. HIF-1 α is one of the most important and vital transcription factors, with expression increasing dramatically with any decrease in the concentration of oxygen and localisation to the nucleus, where it regulates the expression of many genes. However, it has been reported that under normoxic conditions HIF-1 α undergoes proteasomal degradation [184, 395, 396]. HIF-1 α plays a dual role: its higher expression can induce [397] or inhibit apoptosis [394]. The potential role of HIF-1 α in solid tumours, regarding apoptosis induction or inhibition is still a matter of controversy, as some studies reported that overexpression of HIF-1 α correlated with a low apoptosis index in oral squamous cancer cells [398] however, in the case of breast cancer cells, the opposite correlation has been reported [399]. The results of this study show that PDCD4 may play role as apoptosis inducer (increase expression of PDCD4) or inhibitor (decrease or loss expression of PDCD4) in pancreatic cells (normal and cancerous cells) under hypoxic conditions. The role of PDCD4 under hypoxic conditions might be decided by the master regulator of oxygen homeostasis i.e. HIF-1 α . Further investigations are needed in order to fully determine the role of HIF-1 α in the regulation of apoptosis under hypoxic conditions and understanding of these mechanisms might lead us to more specific treatment of pancreatic cancer

We began our investigation of the role of HIF-1 α in pancreatic adenocarcinoma cells (PSN-1) by western blotting whole cell extracts and nuclear and cytoplasmic extracts. We found that HIF-1 α expression was significantly higher at 24 hours under hypoxic and normoxic conditions compared to controls (G0). However, we found that there was

no significant difference in expression between normoxic and hypoxic conditions as shown in Figure 6-2.

We further investigated subcellular expression and localisation of HIF-1 α in PSN-1 cells by western blotting and immunocytochemistry. Densitometry analysis showed that HIF-1 α expression was significantly higher at 24 hours under hypoxic and normoxic conditions compared to controls (G0). Also this analysis revealed that, HIF-1 α was exclusively expressed in the nucleus of PSN-1 cells under hypoxic as well as normoxic conditions as shown in Figure 6-3. These results were further confirmed by immunocytochemistry analysis as shown in Figure 6-5.

Further subcellular expression and localisation of HIF-1 α in normal ductal (ARIP) cells was investigated by western blotting and immunocytochemistry. Densitometry analysis showed that HIF-1 α expression was significantly higher at 24 hours under hypoxic conditions compared to controls (G0) well as normoxic (N24) conditions as shown in Figure 6-4. HIF-1 α was exclusively expressed in the nucleus of ARIP cells as it was observed in PSN-1 cells. These results were further confirmed by immunocytochemistry and similar results were observed (Figure 6-6) a similar trend HIF-1 α expression was observed in 2002 by Moritz *et al*, suggesting that hypoxia does trigger the expression of HIF-1 α and localities to the nucleus in beta cells of pancreas [373].

The present study revealed that, hypoxia does not affect the expression of HIF-1 α in pancreatic adenocarcinoma cells however; hypoxia does induce the expression of HIF-1 α in normal ductal cells (ARIP). Subcellular localisation analysis showed that HIF-1 α was exclusively localised to the nucleus of PSN-1 cells as well as ARIP cells under hypoxic and normoxic conditions. Normal as well as adenocarcinoma cells of the pancreas shown expression of HIF-1 α under normoxic conditions a finding in keeping with results of Akakura *et al*, (2001) which suggested that several human pancreatic cancer cell lines express HIF-1 α under normoxic conditions [215]. It can be concluded

from the present study that pancreatic adenocarcinoma cells show positive expression of HIF-1 α which may be because of some other factors but not because of hypoxia. Also we can hypothesise that hypoxia is not the factor which stabilized HIF-1 α and translocated to the nucleus in pancreatic cells, as we found that HIF-1 α was exclusively localised in the nucleus of pancreatic cells under normoxic conditions. Further investigation needs to be done in order to determine the reason behind the up-regulation and nuclear localisation of HIF-1 α under normoxic and hypoxic conditions in pancreatic cells.

Expression and localisation of HIF-1 α in normal (mouse) pancreas as well as human pancreatic adenocarcinoma tissue samples (four case studies) was investigated by immunohistochemistry analysis. Immunohistochemistry analysis of normal pancreatic tissue sections showed differential expression of HIF-1 α . Ductal cells and islets of Langerhans showed positive expression of HIF-1 α . However, acinar cells showed very weak cytoplasmic expression of HIF-1 α . Our results confirmed that normal pancreatic tissue expresses HIF-1 α ; however expression was very low and it shown nuclear and cytoplasmic expression as shown in Figure 6-7 and Figure 6-8.

Expression and localisation of HIF-1 α in four pancreatic adenocarcinoma tissue samples was investigated. We began our investigation on moderately to poorly differentiated pancreatic adenocarcinoma tissue (sample 1) and very high expression of HIF-1 α was observed as shown in Figure 6-9. It was also clear from these analyses that HIF-1 α was expressed in the nucleus of different types of cells in this tissue sample, especially ductal cells, however, some of the cells showed nuclear and cytoplasmic expression of HIF-1 α as shown in Figure 6-10 and Figure 6-11.

Further expression of HIF-1 α was investigated in pancreatic adenocarcinoma tissue section with severity of disease from well to moderate and poorly differentiated (sample 2). We found very high expression of HIF-1 α in sample 2 as shown in Figure 6-12.

Higher magnification analysis showed that HIF-1 α was highly expressed inside the nucleus of cells such as ductal, acinar, malignant epithelial ductal cells, islets of Langerhans and fibrous connective tissue as shown in Figure 6-13. However, many different cells showed high nuclear and cytoplasmic expression as shown in Figure 6-14. Further expression of HIF-1 α was determined in poorly differentiated pancreatic adenocarcinoma tissue and we found nuclear and cytoplasmic expression of HIF-1 α in ductal cells as well fibrous connective tissue as shown in Figure 6-15, Figure 6-16 and Figure 6-17.

Further expression of HIF-1 α was evaluated in moderately differentiated pancreatic adenocarcinoma tissue section with pronounced autolysis of tissue. We found very high expression of HIF-1 α as shown in Figure 6-18. This analysis also indicated that HIF-1 α was highly expressed inside the nucleus of ductal cells, islets of Langerhans and connective tissues as shown in Figure 6-19 and Figure 6-20.

On comparing expression of HIF-1 α in sample 1, 2 and 4 with normal pancreatic tissue it was quite clear that HIF-1 α was highly expressed in pancreatic adenocarcinoma tissue and mostly localised inside the nucleus of cells.

Immunohistochemistry analysis showed similar results for HIF-1 α expression as observed in both PSN-1 and ARIP cells (western blotting and immunocytochemistry). So normal ductal cell line (ARIP), pancreatic adenocarcinoma cell line, normal pancreatic tissue or different regions of human adenocarcinoma pancreatic tissue (well differentiated, moderately differentiated or poorly differentiated) all showed positive expression of HIF-1 α . Mostly HIF-1 α was localised in the nucleus of the cells.

From the present investigation we can conclude that HIF-1 α was expressed in normal pancreatic cells as well as normal tissue however, it was highly expressed in human adenocarcinoma cell lines or tissue. We hypothesised that high expression of HIF-1 α

might help pancreatic adenocarcinoma cells to survive under hypoxic and nutrient deprived conditions and may act as an apoptosis inhibitor. On the other hand, once normal pancreatic cells are under stress, such as hypoxia, HIF-1 α may act as apoptosis inducer.

Chapter 7. Nuclear Factor kappa B (NFκB)

7.1. Introduction

NFκB is a family of transcription factors that modulate expression of genes with diverse functions. NFκB is constitutively expressed in the cytoplasm in an inactive state and activity of NFκB is regulated by an inhibitory protein called inhibitor of kappa B (IκB), that binds and sequesters NFκB. Various pathological stimuli activate IκB kinase (IKK) which results in phosphorylation and proteasomal mediated degradation of IκB, ultimately resulting in activation of NFκB. NFκB activation plays an important role in chemotherapy resistance in pancreatic cancer, which makes it a potential target in pancreatic cancer [271, 384, 385]. It has been reported that NFκB is constitutively activated in pancreatic cancer tumour tissue [383, 388, 389] but is inactive in normal pancreatic tissues and normal pancreatic cell lines [234, 260, 400]. In 2003, Liptay *et al*, reported that NFκB promoted proliferation and inhibited apoptosis in pancreatic cell lines and xenografts [260]. Many studies have reported that hypoxia regulates the activation of NFκB [391, 400] and recently, it has been reported that overexpression of HIF-1α induces epithelial to mesenchymal transition (EMT) in pancreatic cancer in an NFκB dependent manner [279]. NFκB was also recently linked to unique regulation of *PDCD4* in pancreatic beta cells through the miRNA-21 axis. In this study it was reported that activation of NFκB induces miRNA-21 activation which in turn inhibits *PDCD4*, consequently promoting apoptosis resistance in beta cells [370]. It is believed that up-regulation of miRNA-21 results in loss of *PDCD4* expression in many cancers [401-404]. Overexpression of miRNA-21 has been observed in early pancreatic lesions, pancreatic cancer cell lines and pancreatic tumours [386, 405]. NFκB may play crucial role in regulation of *PDCD4* in pancreatic adenocarcinoma. In order to investigate the role of NFκB in pancreatic adenocarcinoma, we examined the subcellular localisation,

expression and regulation of NFκB (p65) under hypoxic and normoxic conditions in normal as well as pancreatic adenocarcinoma cells and tissue sections. In the present study we investigated the role of NFκB in PSN-1 and ARIP cells only. In present investigation we did not include MIN6 cells, as the role of NFκB in MIN6 cells already been extensively studied by Dr Michelle Barry (Oct 2013) in our research group.

7.2. Results

In order to determine the role of NFκB in the pancreas we investigated subcellular localisation, expression and regulation of NFκB under hypoxic and normoxic conditions in two pancreatic cell lines by western blotting and immunocytochemistry. We also investigated expression and subcellular localisation of NFκB in whole mouse pancreas and human pancreatic adenocarcinoma tissues (four case studies) by immunohistochemistry.

7.2.1. NFκB in pancreatic cells

This study was designed to investigate the influence of cell culture conditions which mimic the oxygen-deprived hypoxic environment found in the core of a cancerous tumour i.e. hypoxic conditions (1% oxygen) and normal growth culturing conditions i.e. normoxic conditions (21% oxygen) on the expression, regulation and subcellular localisation of NFκB in human pancreatic adenocarcinoma (PSN-1) and rat ductal (ARIP) cell lines. This was investigated by western blotting and immunocytochemistry.

7.2.1.1. *Western blotting*

In order to identify the expression, regulation and subcellular localisation of NFκB in PSN-1 and ARIP cells, cells were cultured under normoxic or hypoxic conditions for 12 and 24 hours. Protein extracts were quantified and separated on 10% SDS-PAGE. Western blotting was performed using a specific antibody to NFκB and densitometry

analysis was performed using Image j software. Densitometry values from three separate experiments (n=3) were plotted and statistical analyse (2way ANOVA test) was performed using Graphpad prism 5software. Error bar values represent +/- standard error mean (SEM).

7.2.1.1.1. Human pancreatic adenocarcinoma cells (PSN-1)

In order to determine expression of NFκB in human pancreatic adenocarcinoma cells in response to different stimuli (serum starved, normoxic and hypoxic), we began our investigation in PSN-1 cells; whole cell protein extracts were prepared and western blotting was performed. The results are detailed on Figure 7-1. From the densitometry data it was clear that expression of NFκB was significantly higher at N24 ($p<0.005$) compared with control (G0).

We further investigated subcellular (cytoplasmic and nuclear) expression of NFκB in PSN-1 cells by western blotting analysis. The results are detailed in Figure 7-2. From the densitometry data it was clear that in the cytoplasm expression of NFκB was significantly higher at N24 ($p<0.01$) compared to control (G0) and at H24 ($p<0.001$) expression of NFκB was significantly higher compared to N12. It was also clear that hypoxia stimulated the accumulation of NFκB in the nucleus at H24 ($p<0.001$) where expression was significantly higher compared than control (G0).

These results suggest that a hypoxic environment may trigger activation and nuclear accumulation of NFκB in human pancreatic adenocarcinoma cells (PSN-1).

7.2.1.1.2. Pancreatic ductal cells (ARIP)

We further investigated subcellular expression of NFκB in pancreatic ductal cells in response to different stimuli (serum starved, normoxic and hypoxic). Cytoplasmic and nuclear protein extracts were prepared from ARIP cells and western blotting was performed. The results are detailed in Figure 7-3. It is clear from densitometry analysis

that NFκB was highly expressed in the cytoplasm in comparison with nuclear expression, however, no significant expression difference of NFκB in ARIP cells was observed under any conditions.

These results suggest that a hypoxic environment does not have any effect on NFκB expression in normal pancreatic ductal cells (ARIP).

Pancreatic adenocarcinoma cells

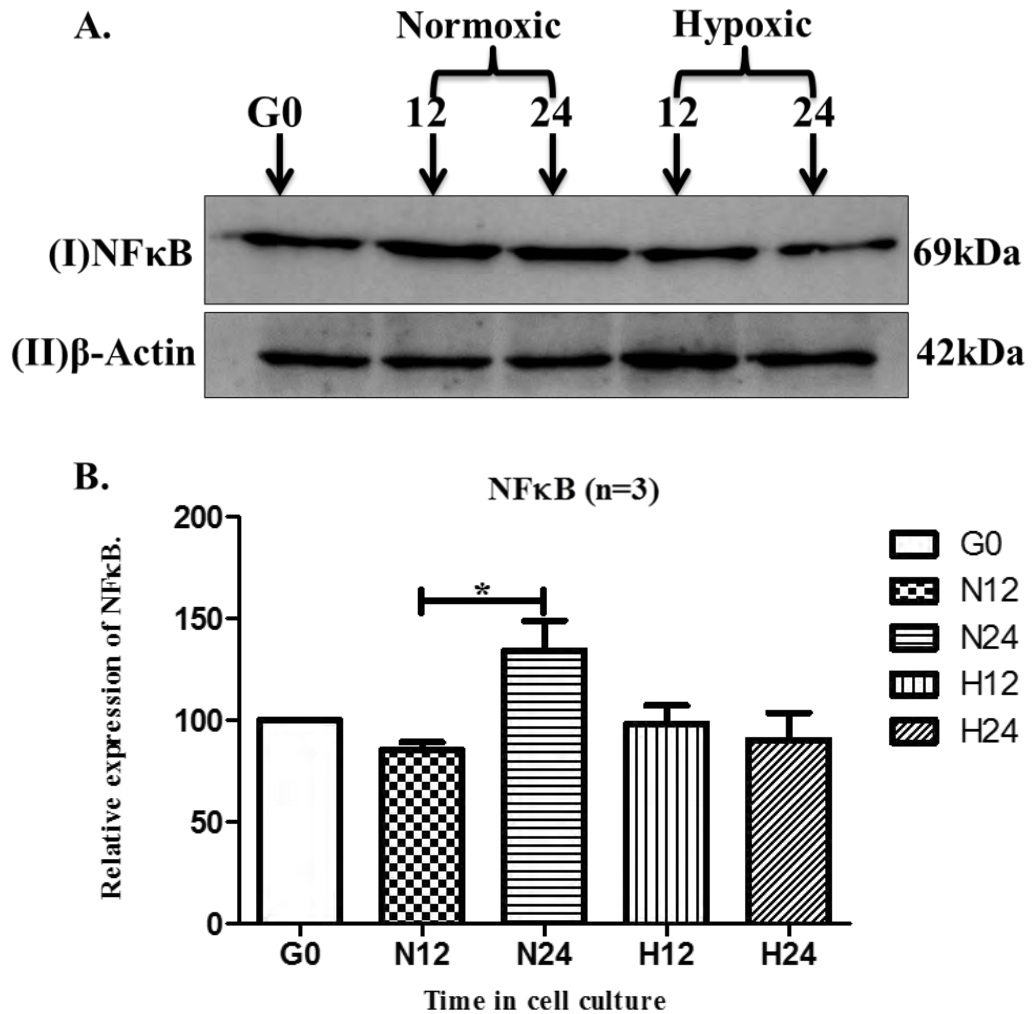


Figure 7-1: Expression of NFκB under hypoxic and normoxic conditions in human pancreatic adenocarcinoma cells.

PSN-1 cells were exposed to hypoxic or normoxic conditions over 24 hours. 10μg of whole cell extract was separated by 10% SDS-PAGE. Proteins were western blotted using an antibody specific to NFκB. Panel A (I) represents NFκB (69kDa) protein expression and (II) represents protein loading control β-Actin (42kDa). Panel B illustrates densitometry analysis, of NFκB relative to β-Actin. These results were reproduced in at least three separate experiments. Error bar values represent mean +/- standard error. Expression of NFκB was significantly higher at N24 (*p<0.05) compared to G0 samples.

Pancreatic adenocarcinoma cells

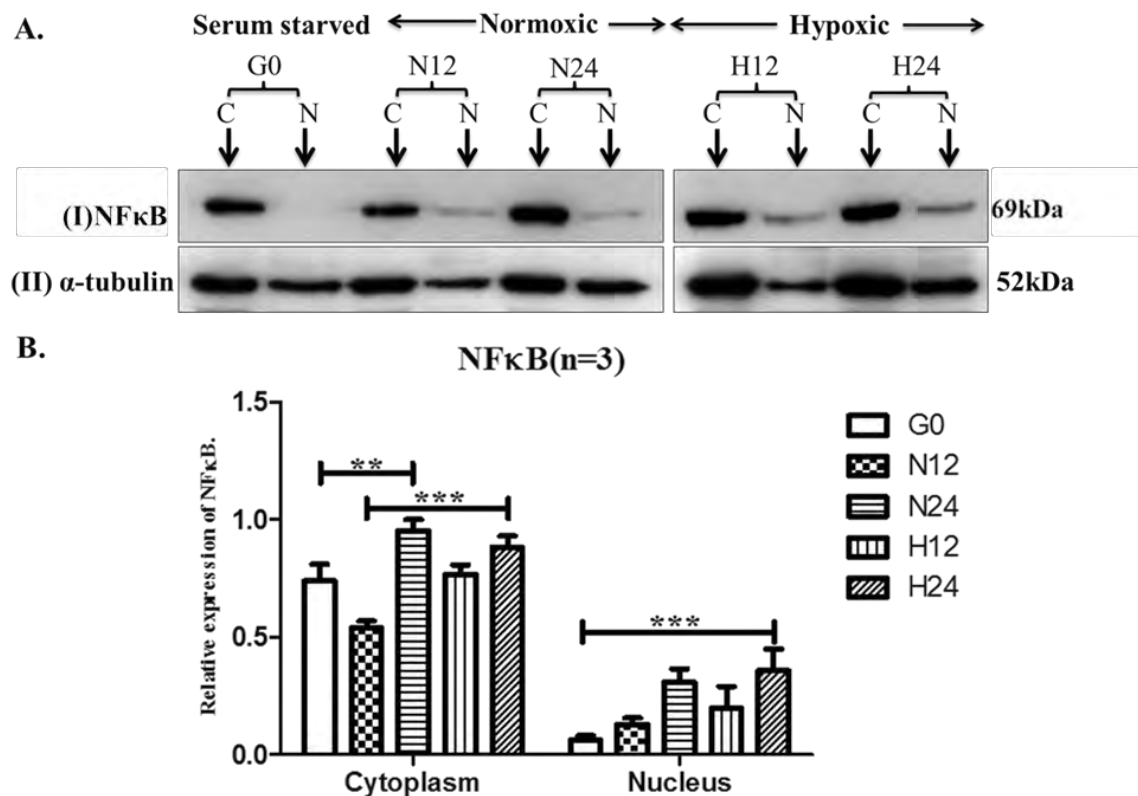


Figure 7-2: Subcellular expression of NFκB in human pancreatic adenocarcinoma cells.

PSN-1 cells were cultured under G0 (serum starvation), normoxic or hypoxic conditions for 12 and 24 hours. After each indicated incubation period, the cells were pelleted. Cytoplasmic and nuclear proteins were extracted and 10μg of cytoplasmic and nuclear cell extract were separated on a 10% SDS-PAGE. Proteins were western blotted using an antibody specific to NFκB. Panel A (I) represents NFκB (69kDa) protein expression in the cytoplasm (C) and nucleus (N). Panel A (II) represents protein loading control α-tubulin (52kDa). Panel B illustrates densitometry analysis, showing NFκB relative to control α-tubulin. These results were reproduced in at least three separate experiments. Error bar values represent mean +/- standard error. NFκB was highly expressed in the cytoplasm as compared to the nucleus. Expression of NFκB in the cytoplasm was significantly higher at N24 (**p<0.01) compared to G0 and H24 (***p<0.001) compared to N12 samples. Expression of NFκB in the nucleus was significantly higher at H24 (***p<0.001) compared to G0 samples.

Pancreatic ductal cells

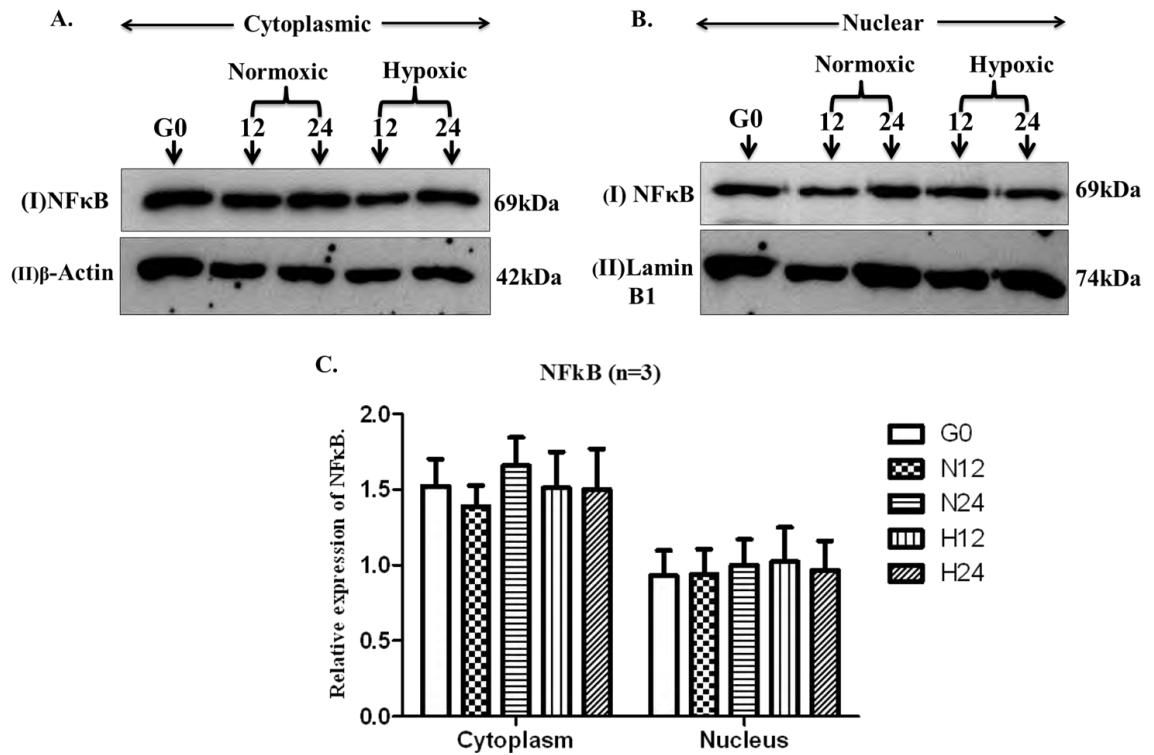


Figure 7-3: Subcellular expression (A) cytoplasm and (B) nucleus of NFκB in pancreatic ductal cells.

ARIP cells were cultured under G0 (serum starvation), normoxic or hypoxic conditions for 12 and 24 hours. After each indicated incubation period, the cells were pelleted. Cytoplasmic and nuclear proteins were extracted and 10μg of cytoplasmic and nuclear cell extract were separated on a 10% SDS-PAGE. Proteins were western blotted using an antibody specific to PDCD4. Panel A (I) represents NFκB (69kDa) protein expression in the cytoplasm (II) represents protein loading control β-actin (42kDa). Panel B (I) represents NFκB (69kDa) protein expression in the nucleus (II) represents protein loading control lamin B1 (74kDa). Panel C illustrates densitometry analysis, showing cytoplasmic NFκB relative to β-actin and nuclear NFκB relative to lamin B1. These results were reproduced in at least three separate experiments. Error bar values represent mean +/- standard error. NFκB was highly expressed in the cytoplasm as compared to the nucleus. No significant expression difference of NFκB was found in the cytoplasm as well as the nucleus.

7.2.1.2. *Immunocytochemistry*

In an attempt to further investigate the subcellular localisation and expression of NFκB in PSN-1 and ARIP cells, cells were cultured and fixed with 3.7% formalin at various time points i.e. G0 (serum starvation), normoxic and hypoxic both at 12 and 24 hours. Immunocytochemistry was performed by using a specific antibody to NFκB and FITC and TRIC labelled secondary antibodies were used. Labelled cells on coverslips were mounted on glass slides with mounting medium containing DAPI to stain the nucleus. Samples were analysed by confocal microscopy (Leica TCS SP5 confocal microscope) and images captured at 65X magnification. All immunocytochemistry results represent from at least three separate experiments (n=3).

7.2.1.2.1. **Human pancreatic adenocarcinoma cells (PSN-1)**

In order to determine subcellular localisation and expression of NFκB in human pancreatic adenocarcinoma cells under different stimuli (serum starved, normoxic and hypoxic) at different time points by immunocytochemistry, we began our investigation with PSN-1 cells. Immunocytochemistry results are detailed in Figure 7-4. From confocal image analysis of PSN-1 cells it is clear that under normoxic conditions NFκB was exclusively expressed in the cytoplasm however, under hypoxic conditions NFκB was highly expressed in the cytoplasm as well as the nucleus of PSN-1 cells.

These results suggest that NFκB is mostly localized in the cytoplasm of PSN-1 cells under normoxic conditions. However, hypoxia may trigger the nuclear accumulation of NFκB in PSN-1 cells.

7.2.1.2.2. **Pancreatic ductal cells (ARIP)**

Further we investigated the subcellular localisation and expression of NFκB in pancreatic ductal cells (ARIP) under different stimuli (serum starved, normoxic and hypoxic) at different time points by immunocytochemistry. Immunocytochemistry

results are detailed in Figure 7-5. From confocal image analysis of ARIP cells it is clear that NFκB was highly expressed in the nucleus as well as the cytoplasm of cells at G0 as well as under normoxic conditions. However, under hypoxic conditions NFκB was highly expressed in the nucleus of ARIP cells. It was also clear from H12 and H24 that NFκB was highly expressed near the nuclear membrane.

These results suggest that hypoxia may trigger nuclear expression of NFκB in ARIP cells however; these results also suggest that NFκB was highly expressed on or near the nuclear membrane, which may explain the difference between these results and the western blotting results for NFκB in ARIP cells.

In summary, western blotting as well as immunocytochemistry results suggests that NFκB was mostly localized in the cytoplasm of normal pancreatic ductal (ARIP) and adenocarcinoma (PSN-1) cells at G0 and under normoxic conditions. Hypoxia appears to trigger expression of NFκB in the nucleus of normal pancreatic ductal cells (ARIP) as well as human pancreatic adenocarcinoma (PSN-1) cells.

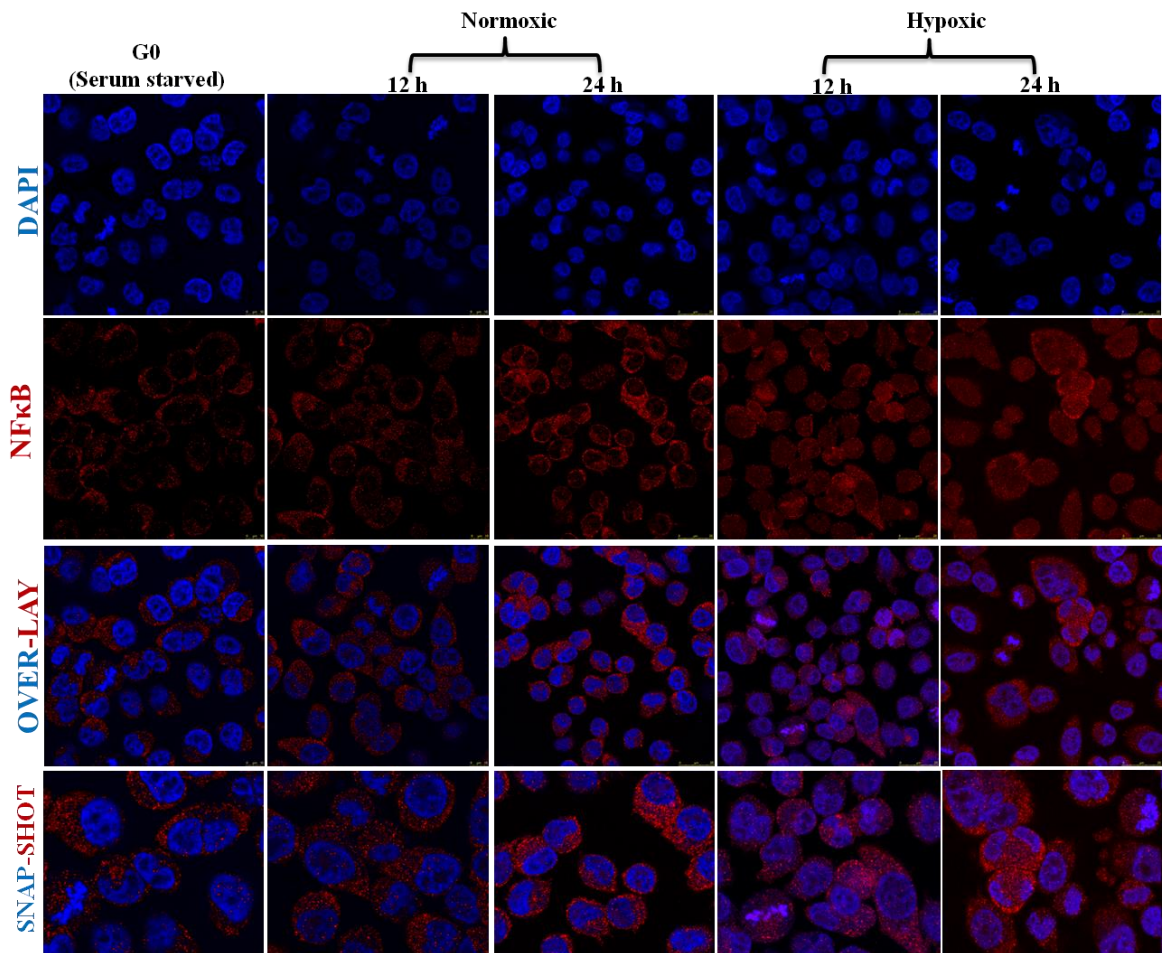


Figure 7-4: Sub-cellular localisation and expression of $\text{NF}\kappa\text{B}$ in human pancreatic adenocarcinoma cells.

PSN-1 cells were grown on glass cover slips in six well plates and fixed at various time points i.e. at G0 (Serum starvation), at normoxia 12 (N12) and 24 (N24) hours; at hypoxia 12 (H12) and 24 (H24) hours. Immunocytochemistry was performed using a specific antibody to $\text{NF}\kappa\text{B}$ and TRIC labelled secondary antibody was used. Coverslips with cells were mounted on glass slides with mounting medium containing DAPI which stains the nucleus of cells. Cells were analysed by confocal microscopy and images were captured at 65X magnification. Results are representative of three separate experiments and images were representative of six separate fields. $\text{NF}\kappa\text{B}$ localisation and expression; at G0: Cytoplasmic; at N12: Cytoplasmic and lower expression; at N24: Cytoplasmic; at H12: Cytoplasmic and low nuclear expression and at H24: Nuclear and cytoplasmic expression. Over-all $\text{NF}\kappa\text{B}$ was highly expressed in the cytoplasm; with very low expression under hypoxic conditions.

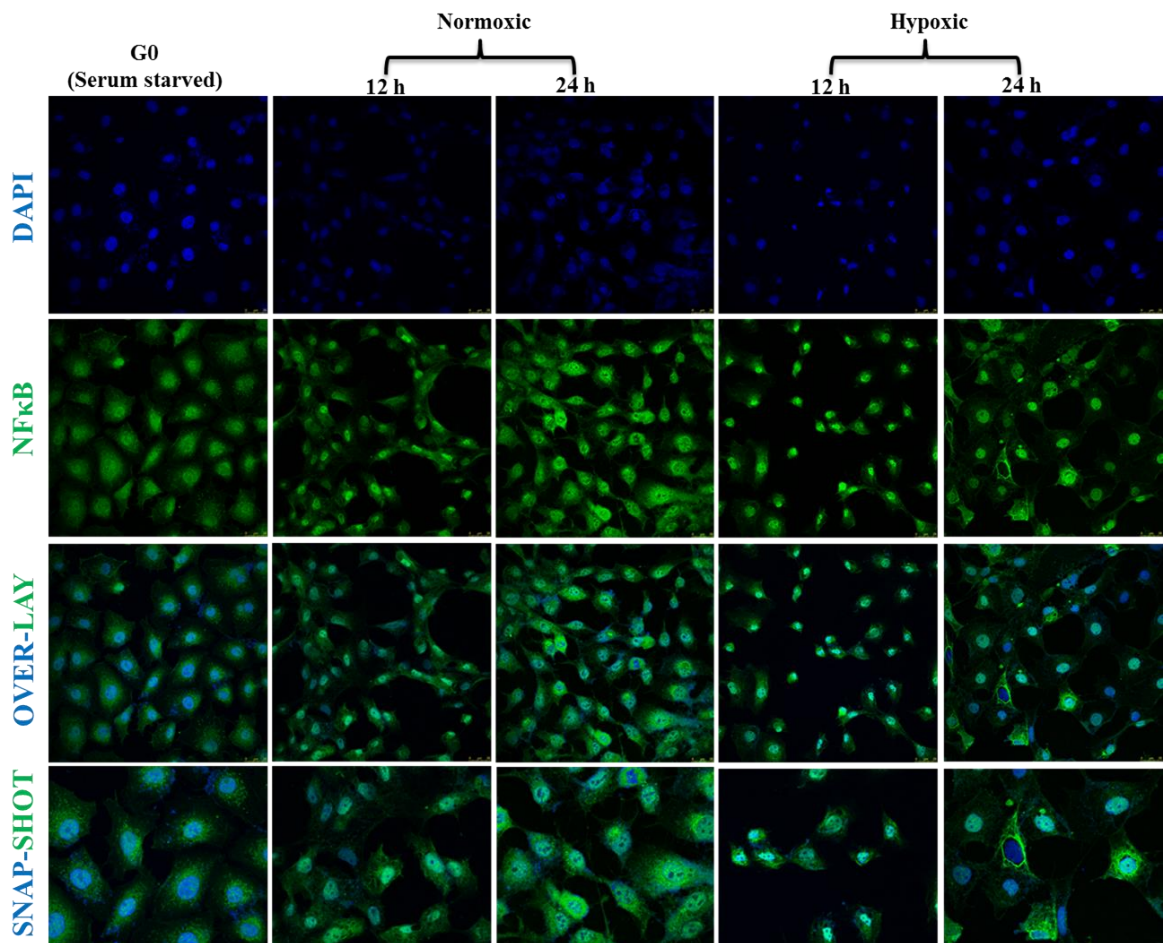


Figure 7-5: Sub-cellular localisation and expression of $\text{NF}\kappa\text{B}$ in pancreatic ductal cells.

ARIP cells were grown on glass cover slips in six well plates and fixed at various time points i.e. at G0 (Serum starvation), at normoxia 12 (N12) and 24 (N24) hours; at hypoxia 12 (H12) and 24 (H24) hours. Immunocytochemistry was performed using a specific antibody to $\text{NF}\kappa\text{B}$ and FITC labelled secondary antibody was used. Coverslips with cells were mounted on glass slides with mounting medium containing DAPI, which stains the nucleus of cells. Cells were analysed by confocal microscopy and images were captured at 65X magnification. Results are representative of three separate experiments and images were representative of six separate fields. $\text{NF}\kappa\text{B}$ was expressed in the nucleus as well cytoplasm at G0, N12 and N24. Under hypoxic conditions at H12 and H24, $\text{NF}\kappa\text{B}$ was highly expressed in the nucleus compared to the cytoplasm of cells.

7.2.2. NFκB expression and subcellular localisation in normal and adenocarcinoma pancreas tissue

In order to investigate the expression and subcellular localisation of NFκB in normal pancreas (mouse) and human pancreatic adenocarcinoma tissue sections, immunohistochemistry was performed. Formalin fixed paraffin embedded pancreas tissue blocks were sectioned (5µm) and mounted on glass slides. Tissue sections were deparaffinised by dipping sections in xylene and rehydrated using gradient ethanol. Immunohistochemistry was performed using a specific antibody to NFκB and HRP conjugated secondary was used. NFκB immuno-stained sections were counterstained with haematoxylin. Sections were mounted using DPX mounting medium and analysed by light microscopy; images were captured at 10X and 40X magnifications.

7.2.2.1. *NFκB in Mouse pancreas*

Immunohistochemistry was performed to reveal the expression and subcellular localisation of NFκB in mouse pancreas. Immunohistochemistry results are shown in Figure 7-6 (10X) and Figure 7-7 (40X). It is clear from these results that NFκB was highly expressed in normal pancreas; however, ductal epithelial cells, islets of Langerhans and blood vessels show high expression compared to acinar cells as shown in Figure 7-6. Further, in order to determine the subcellular localisation and expression of NFκB in normal mouse pancreas, sections were analysed under higher magnification. Images were captured at 40X magnification as shown in Figure 7-7 and it was clear that acinar cells showed positive cytoplasmic expression of NFκB as shown in Figure 7-7 (B). It was clear from Figure 7-7 (A, C & D) that intercalated ducts, islets of Langerhans, ductal epithelial cells and blood vessels shown positive nuclear and cytoplasmic expression of NFκB. These results suggest that NFκB was highly expressed in the cytoplasm and nucleus of normal mouse pancreas sections.

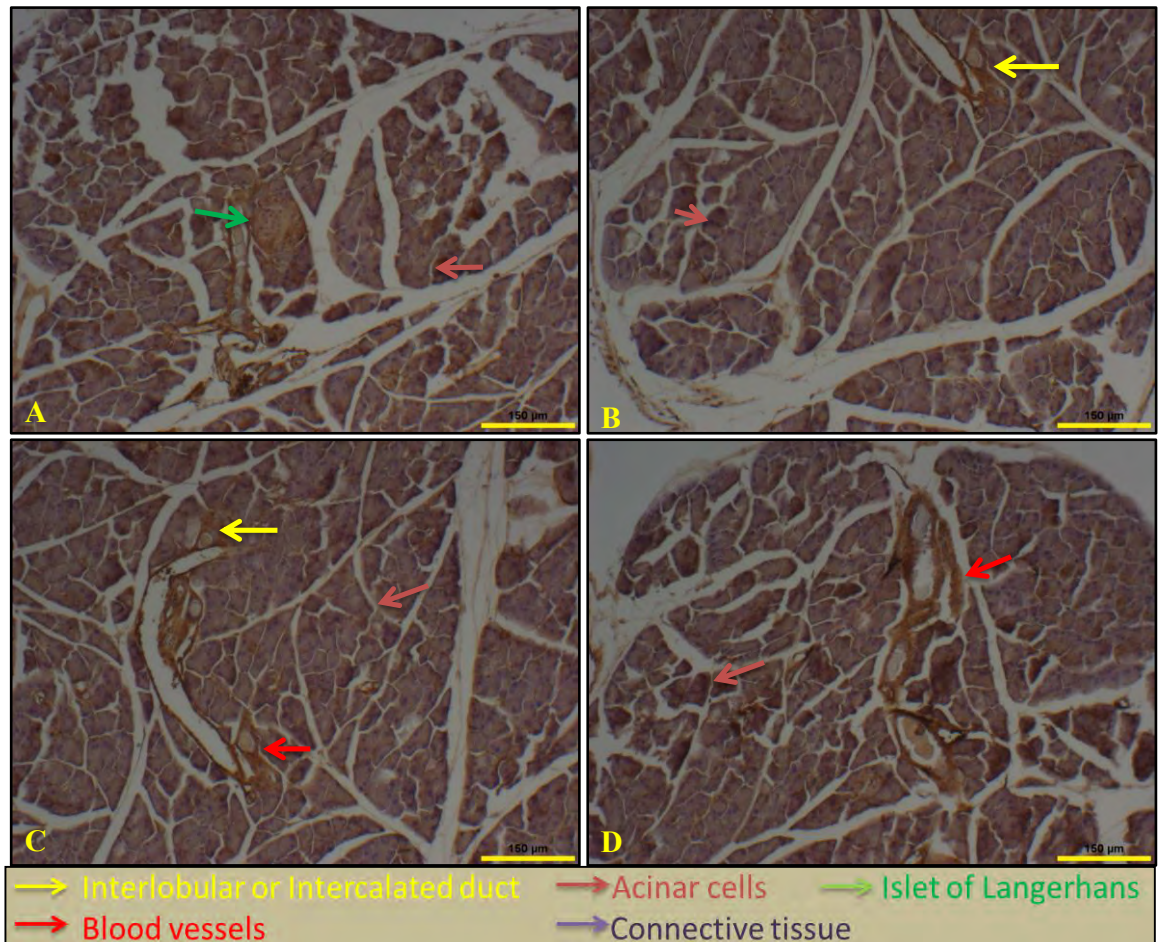


Figure 7-6: Immunohistochemical analysis of the expression of NFκB in mouse pancreas (10X magnification).

Formalin fixed, paraffin embedded mouse pancreas tissue blocks were sectioned (5μm) and mounted on glass slides. Immunohistochemistry was performed using a specific antibody to NFκB. NFκB immunostained sections were counter stained with haematoxylin and sections were mounted using mounting medium. Stained sections were analysed by light microscopy and images were captured at 10X magnification. Results are representative of three separate experiments and images were representative of six separate fields. All sections show positive expression of NFκB in **acinar cells**, **Islet of Langerhans**, **blood vessels** and **ductal epithelial cells**.

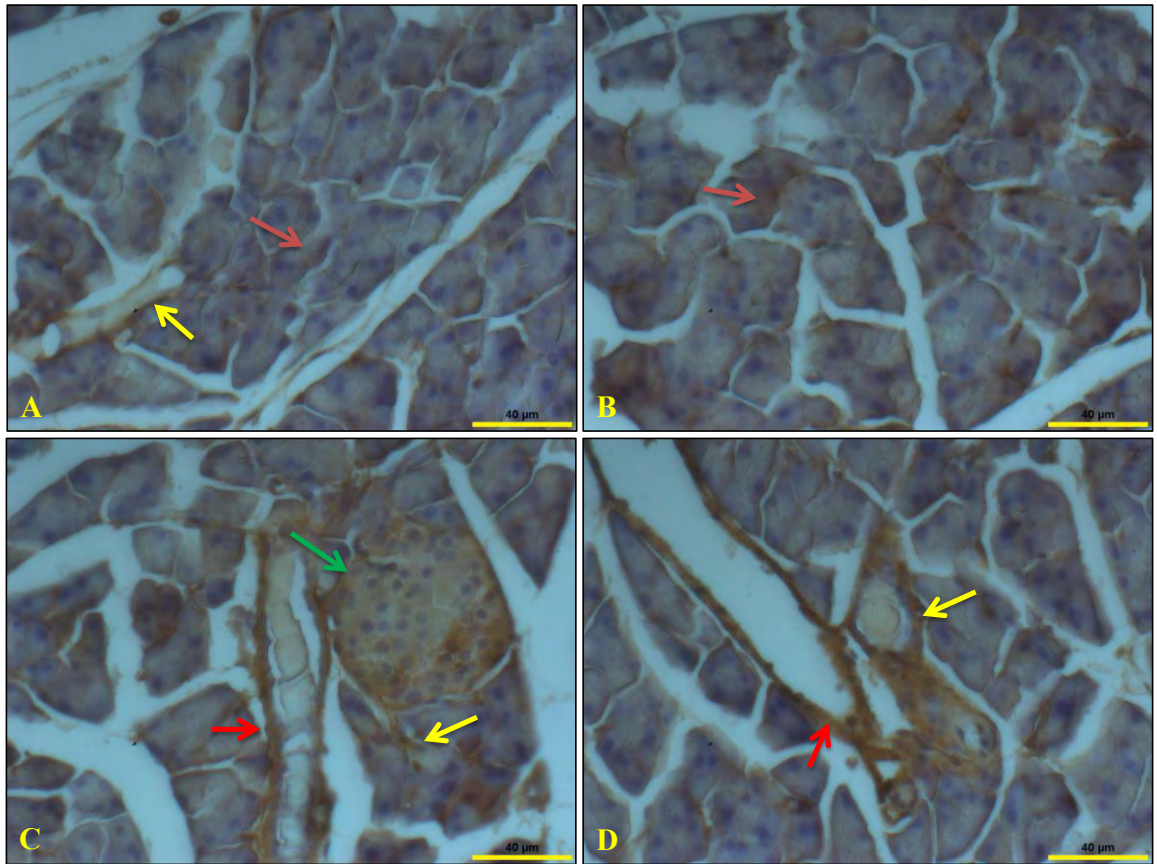


Figure 7-7: Immunohistochemical analysis of the expression of NFκB in mouse pancreas (40X magnification).

Formalin fixed, paraffin embedded mouse pancreas tissue blocks were sectioned (5μm) and mounted on glass slides. Immunohistochemistry was performed using a specific antibody to NFκB. NFκB immunostained sections were counter stained with haematoxylin and sections were mounted using mounting medium. Stained sections were analysed by light microscopy and images were captured at 40X magnification. Results are representative of three separate experiments and images were representative of six separate fields. NFκB expression was observed in the nucleus and cytoplasm of **intercalated ducts** (A) and in the cytoplasm of **acinar cells** (B). Cytoplasmic and nuclear expression of NFκB was observed in **islet of Langerhans** (C) and in **blood vessels** and **duct cells** (D).

7.2.2.2. *NFκB in human pancreatic adenocarcinoma tissues*

In order to investigate expression of NFκB in human pancreatic adenocarcinoma tissue sections immunohistochemistry was performed. In the present study, human pancreatic adenocarcinoma tissue sections from four patients were studied for the expression of NFκB by immunohistochemistry.

7.2.2.2.1. **Case study 1**

Immunohistochemistry was performed to reveal expression and subcellular localisation of NFκB in human pancreatic adenocarcinoma tissue (sample 1). Immunohistochemistry results are shown in Figure 7-8 (5X), Figure 7-9 (10X) and Figure 7-10 (40X). It is clear from immunohistochemistry analysis that NFκB was positively expressed throughout the tissue section. Additionally, very high expression was detected in acinar cells which were still intact in a lobule structure as shown in Figure 7-8. Analysing tissue sections on higher magnification it was clear that NFκB was positively expressed in ductal cells, rudimentary acinar cells, pleomorphic malignant epithelial cells and fibrous connective tissue as shown in Figure 7-9. In order to determine the subcellular expression of NFκB, stained tissue sections were analysed under higher magnification (40X) and it was clear that NFκB was expressed in the cytoplasm of ductal cells, acinar cells, fibrous connective tissues, pleomorphic malignant epithelial cells and islets of Langerhans. However, in rudimentary acinar cells NFκB was observed in the nucleus and cytoplasm as shown in Figure 7-10.

These results suggest that NFκB was positively expressed and localized inside the cytoplasm of ductal cells, acinar cells, fibrous connective tissue and pleomorphic malignant epithelial cells and rudimentary acinar cells in this tissue sample.

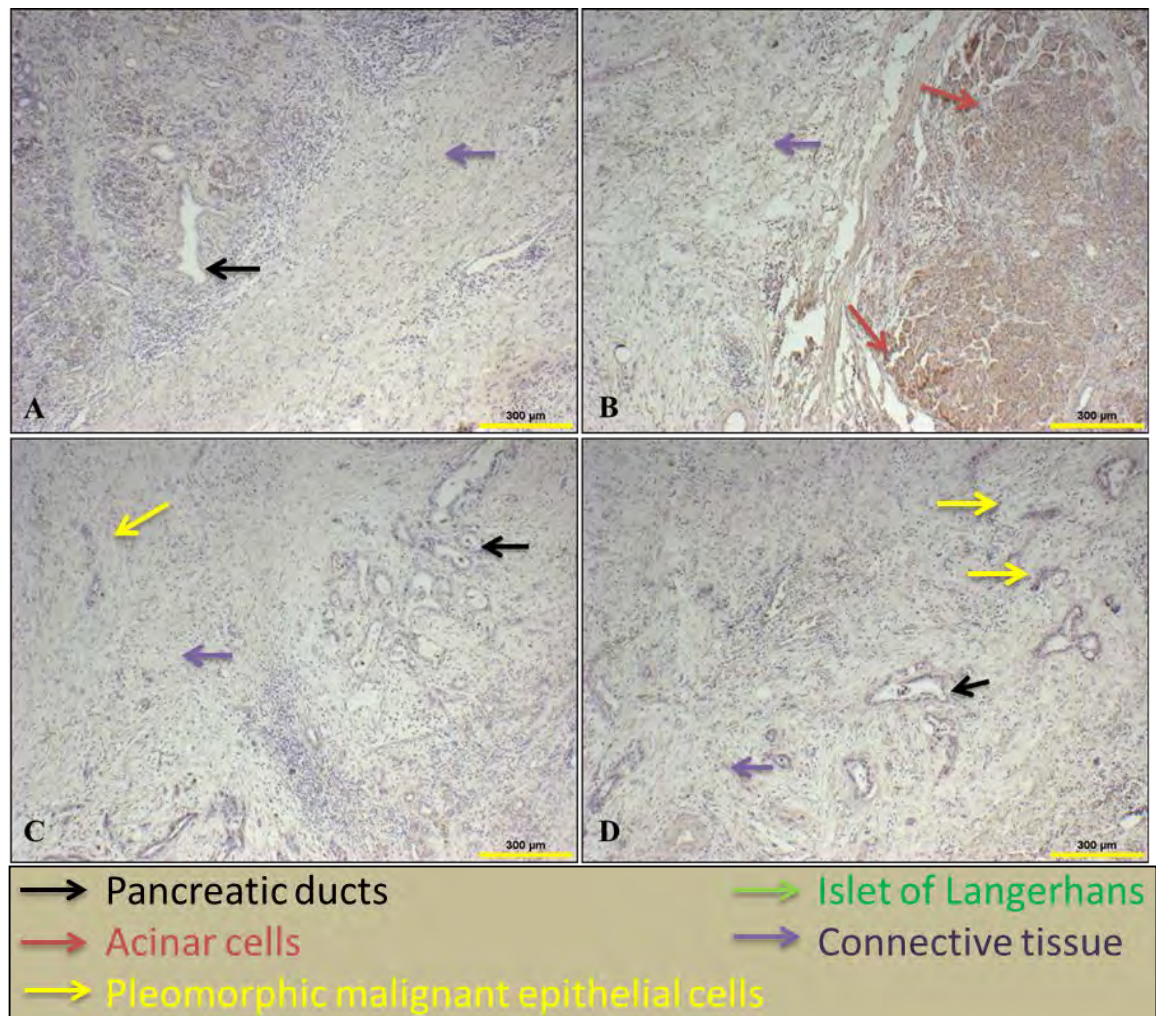


Figure 7-8: Immunohistochemical analysis of the expression of NFκB in human pancreatic adenocarcinoma tissue case study 1 (5X magnification).

Formalin fixed, paraffin embedded pancreatic adenocarcinoma tissue blocks were sectioned (5μm) and mounted on glass slides. Immunohistochemistry was performed using a specific antibody to NFκB. NFκB immunostained sections were counter stained with haematoxylin and sections were mounted using mounting medium. Stained sections were analysed by light microscopy and images were captured at 5X magnification. (A, C & D) Positive expression of NFκB was detected in ductal cells, **rudimentary acinar cells** and **fibrous connective tissues** (B) **Acinar cells** which are still intact in lobular structure show very high expression of NFκB.

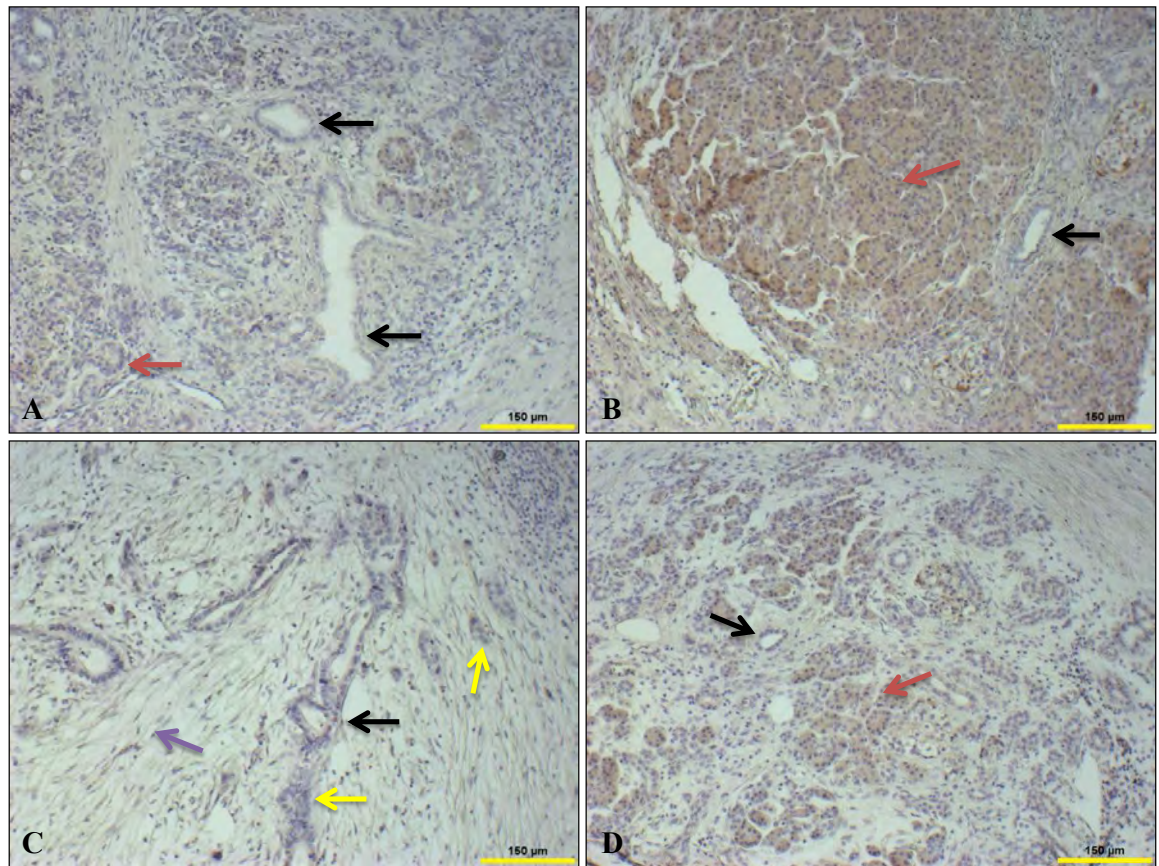


Figure 7-9: Immunohistochemical analysis of the expression of NFκB in human pancreatic adenocarcinoma tissue case study 1 (10X magnification).

Formalin fixed, paraffin embedded pancreatic adenocarcinoma tissue blocks were sectioned (5μm) and mounted on glass slides. Immunohistochemistry was performed using a specific antibody to NFκB. NFκB immunostained sections were counter stained with haematoxylin and sections were mounted using mounting medium. Stained sections were analysed by light microscopy and images were captured at 10X magnification. Expression of NFκB is as follows: (A & D) Positive expression of NFκB was observed in ductal and rudimentary acinar cells. (B) NFκB was highly expressed in the acinar cells which are still intact in lobular structure. (C) Cytoplasmic expression of NFκB in ductal epithelial cells, fibrous connective tissue and pleomorphic malignant ductal epithelial cells was observed.

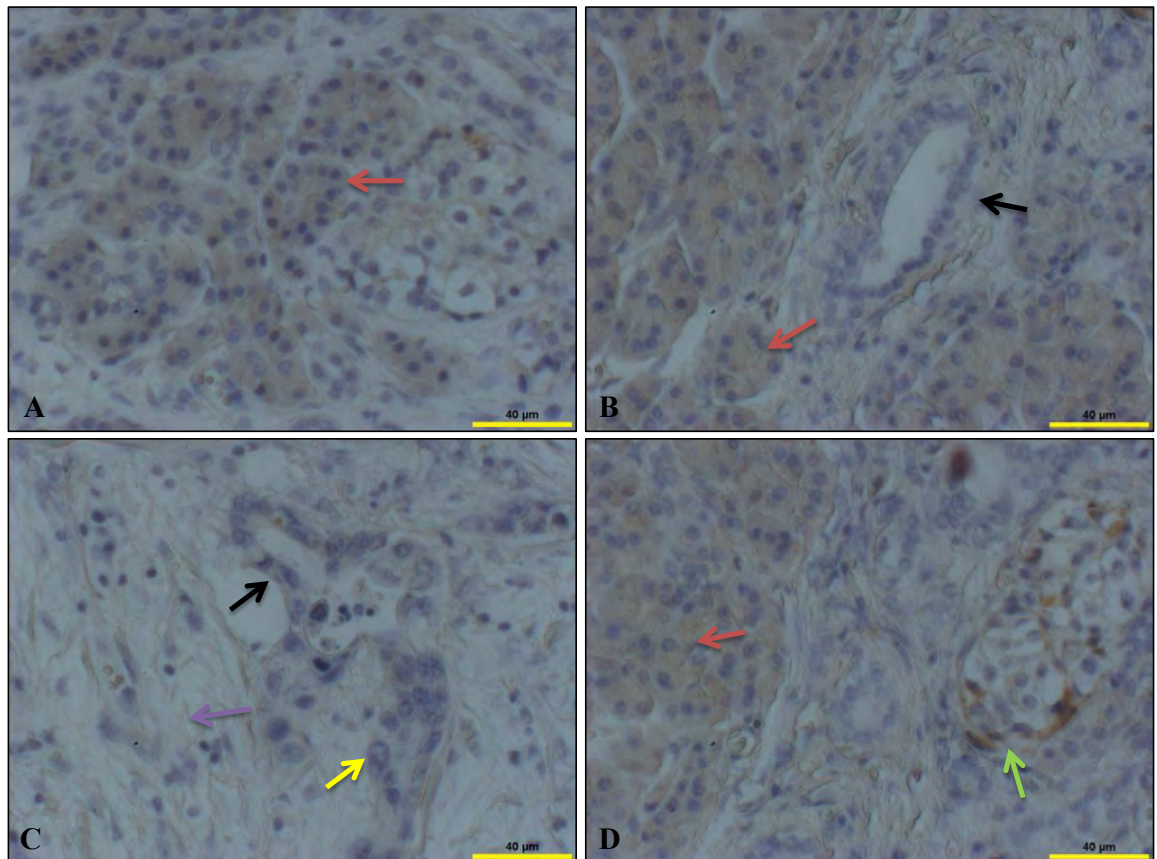


Figure 7-10: Immunohistochemical analysis of the expression of NFκB in human pancreatic adenocarcinoma tissue case study 1 (40X magnification).

Formalin fixed, paraffin embedded pancreatic adenocarcinoma tissue blocks were sectioned (5μm) and mounted on glass slides. Immunohistochemistry was performed using a specific antibody to NFκB. NFκB immunostained sections were counter stained with haematoxylin and sections were mounted using mounting medium. Stained sections were analysed by light microscopy and images were captured at 40X magnification. NFκB expression identified as follows: (A) Nuclear and cytoplasmic expression of NFκB in rudimentary acinar cells was identified. (B & C) Cytoplasmic expression of NFκB was observed in **acinar** cells, ductal cells, **fibrous connective tissue** and **pleomorphic malignant ductal epithelial cells**. (D) Cytoplasmic expression of NFκB was detected in acinar cells and **islets of Langerhans**.

7.2.2.2.2. Case study 2

In order to determine the expression and subcellular localisation of NFκB in human pancreatic adenocarcinoma tissue (sample 2), immunohistochemistry was performed. Immunohistochemistry results are shown in Figure 7-11 (5X), Figure 7-12 (10X) and Figure 7-13 (40X). It is clear from gross examination of sample 2 that NFκB was positively expressed in ductal cells, acinar cells and fibrous connective tissue, as shown in Figure 7-11. Analysing stained tissue sections under higher magnification at 10X it was clear that NFκB was positively expressed in rudimentary acinar cells and ductal cells. However, islets of Langerhans and fibrous connective tissue show very high expression of NFκB as shown in Figure 7-12. In order to determine the subcellular localisation of NFκB, samples were analysed under higher magnification (40X). It was clear from these results that NFκB was localised in the nucleus and cytoplasm of rudimentary acinar cells and cytoplasmic expression in fibrous connective tissue was observed as shown in Figure 7-13 (A). However, malignant ductal epithelial cells showed positive expression in cytoplasm as shown in Figure 7-13 (B&C). Islets of Langerhans showed exceptionally high expression of NFκB as shown in Figure 7-13(D). These results suggest that NFκB was positively expressed in the cytoplasm of malignant ductal epithelial cells in tissue sample 2.

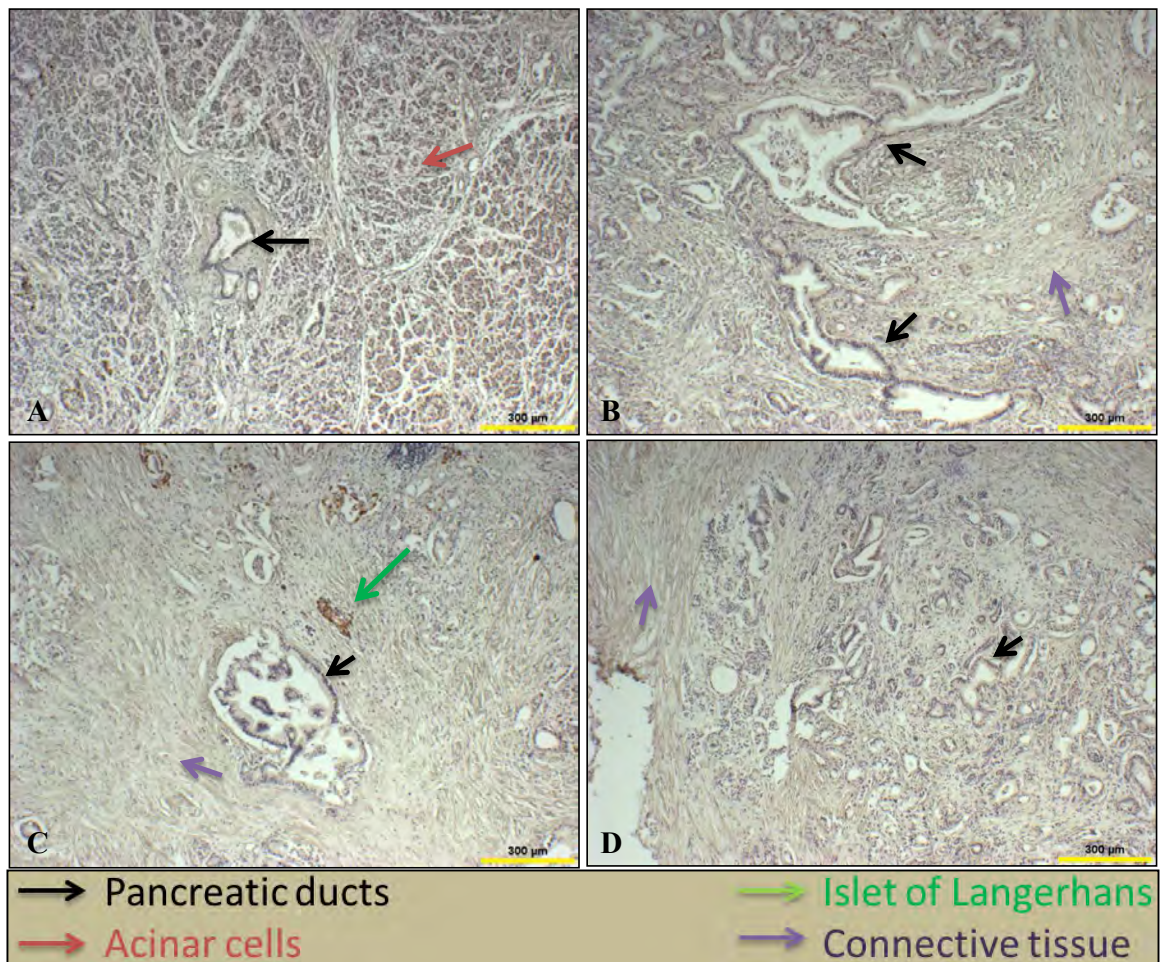


Figure 7-11: Immunohistochemical analysis of the expression of NFκB in human pancreatic adenocarcinoma tissue case study 2 (5X magnification).

Formalin fixed, paraffin embedded pancreatic adenocarcinoma tissue blocks were sectioned (5μm) and mounted on glass slides. Immunohistochemistry was performed using a specific antibody to NFκB. NFκB immunostained sections were counter stained with haematoxylin and sections were mounted using mounting medium. Stained sections were analysed by light microscopy and images were captured at 5X magnification. NFκB expression identified as follows: (A) Positive expression of NFκB was observed in ductal and **acinar** cells. (B, C & D) Ductal cells, **islets of Langerhans** and **fibrous connective tissue** show positive expression of NFκB.

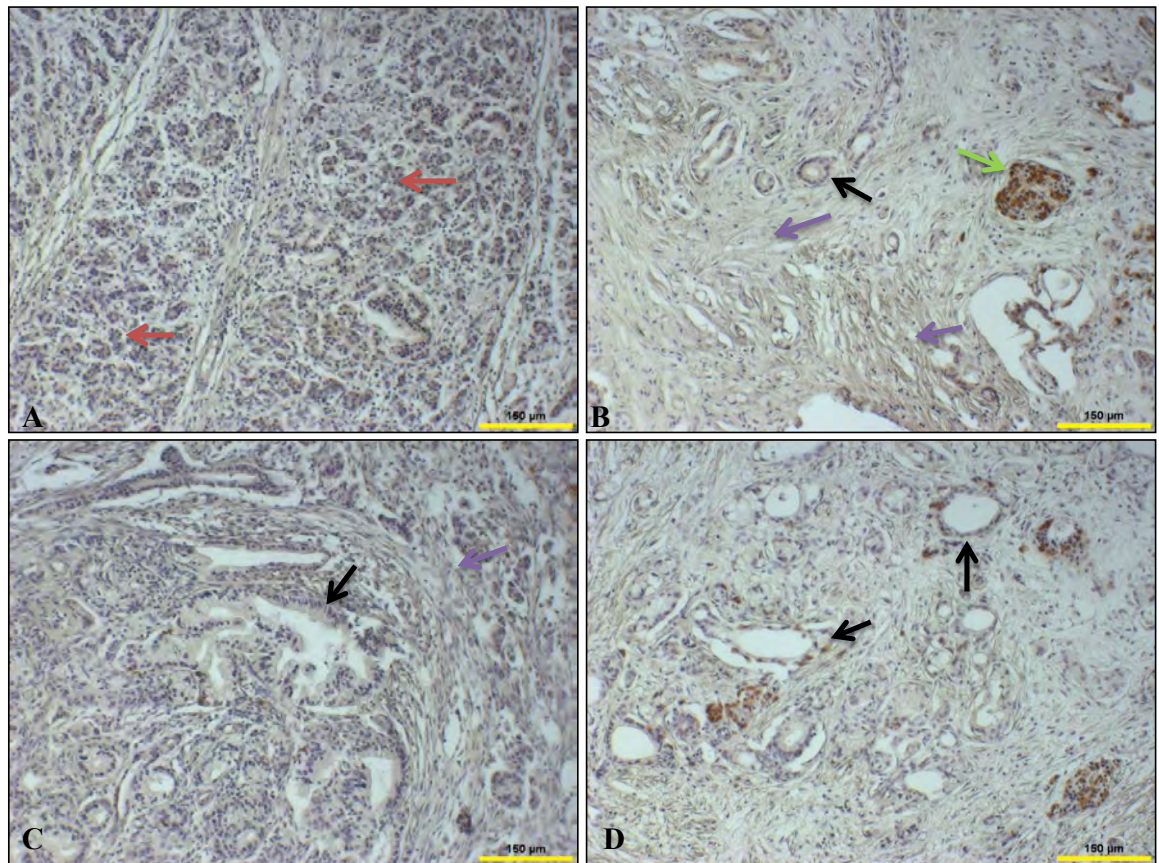


Figure 7-12: Immunohistochemical analysis of the expression of NFκB in human pancreatic adenocarcinoma tissue case study 2 (10X magnification).

Formalin fixed, paraffin embedded pancreatic adenocarcinoma tissue blocks were sectioned (5μm) and mounted on glass slides. Immunohistochemistry was performed using a specific antibody to NFκB. NFκB immunostained sections were counter stained with haematoxylin and sections were mounted using mounting medium. Stained sections were analysed by light microscopy and images were captured at 10X magnification. NFκB expression identified as follows: (A) Positive expression of NFκB in **acinar** cells was identified. (B & D) Ductal, **islets of Langerhans** and **fibrous connective tissue** show positive expression of NFκB. (C) Ductal epithelial and **fibrous connective tissue** show positive expression of NFκB.

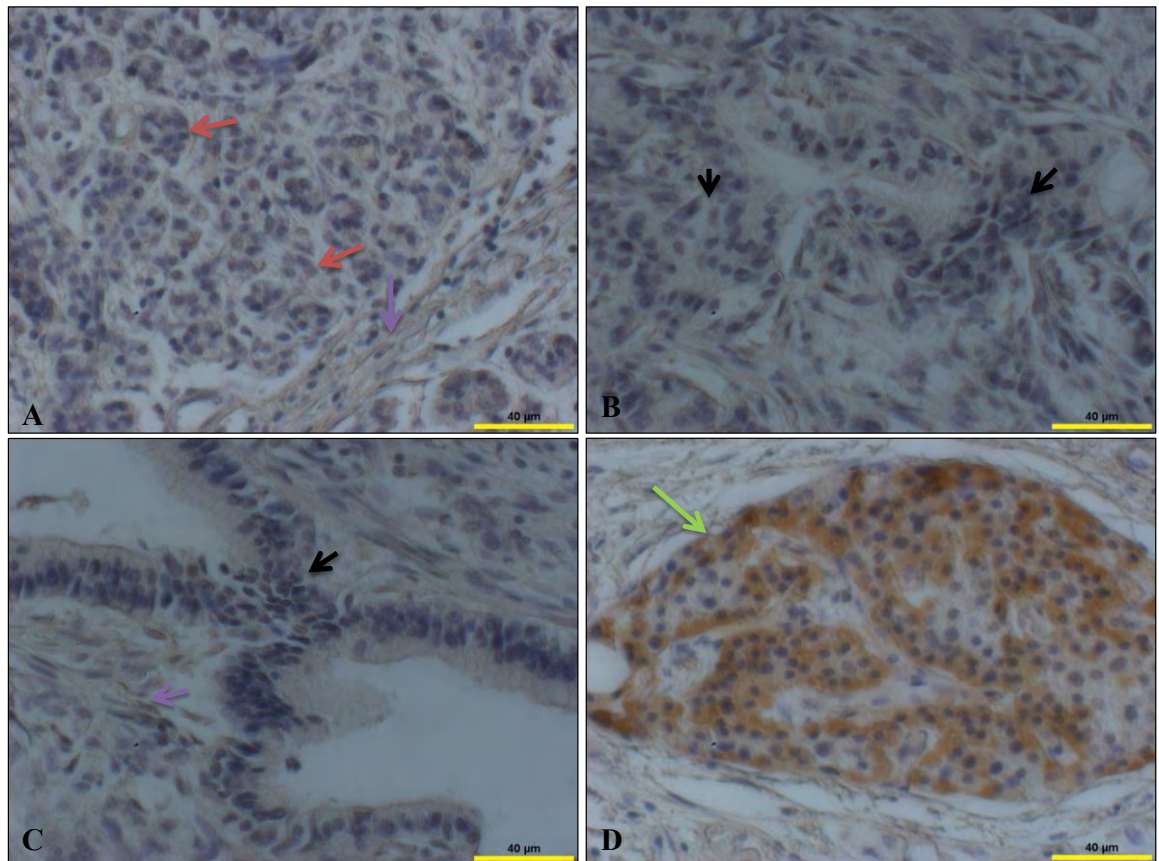


Figure 7-13: Immunohistochemical analysis of the expression of NFκB in human pancreatic adenocarcinoma tissue case study 2 (40X magnification).

Formalin fixed, paraffin embedded pancreatic adenocarcinoma tissue blocks were sectioned (5μm) and mounted on glass slides. Immunohistochemistry was performed using a specific antibody to NFκB. NFκB immunostained sections were counter stained with haematoxylin and sections were mounted using mounting medium. Stained sections were analysed by light microscopy and images were captured at 40X magnification. NFκB expression identified as follows: (A) Nuclear and cytoplasmic expression of NFκB was observed in rudimentary **acinar** cells and cytoplasmic expression in **fibrous connective tissue** (B & C) Cytoplasmic expression of NFκB in ductal and malignant ductal epithelial cells was detected. (D) Positive cytoplasmic expression NFκB in **islet of Langerhans** was observed.

7.2.2.2.3. Case study 3

Immunohistochemistry was performed to reveal expression and subcellular localisation of NFκB in human pancreatic adenocarcinoma tissue (sample 3). Immunohistochemistry results are shown in Figure 7-14 (5X), Figure 7-15 (10X) and Figure 7-16 (40X). It is clear from gross examination of sample 3 that NFκB was positively expressed throughout the tissue section as shown in Figure 7-14. On analysing at the higher magnification (10X) it is clear that NFκB was differentially expressed in ductal cells with positive nuclear and cytoplasmic expression identified in Figure 7-15 (A, B & C) and negative expression identified in Figure 7-15 (D). Also stromal cells show differential expression of NFκB as some parts of the tissue section were positive as shown in Figure 7-15 (B) and some part were negative for expression as shown in Figure 7-15 (C & D). NFκB was positively expressed in pleomorphic malignant cells as shown in Figure 7-15 (B, C & D). In order to determine the subcellular expression of NFκB we further analysed sample 3 under higher magnification at 40X. It was clear from these analyses that NFκB was positively expressed in the cytoplasm and nucleus of pleomorphic malignant cells and ductal cells as shown in Figure 7-16 (A, C & D). NFκB was also positively expressed in both the nucleus and the cytoplasm of stromal cells as shown in Figure 7-16.

These results suggest that NFκB was positively expressed in pleomorphic malignant cells, however, ductal and stromal cells shows differential expression of NFκB in tissue sample 3.

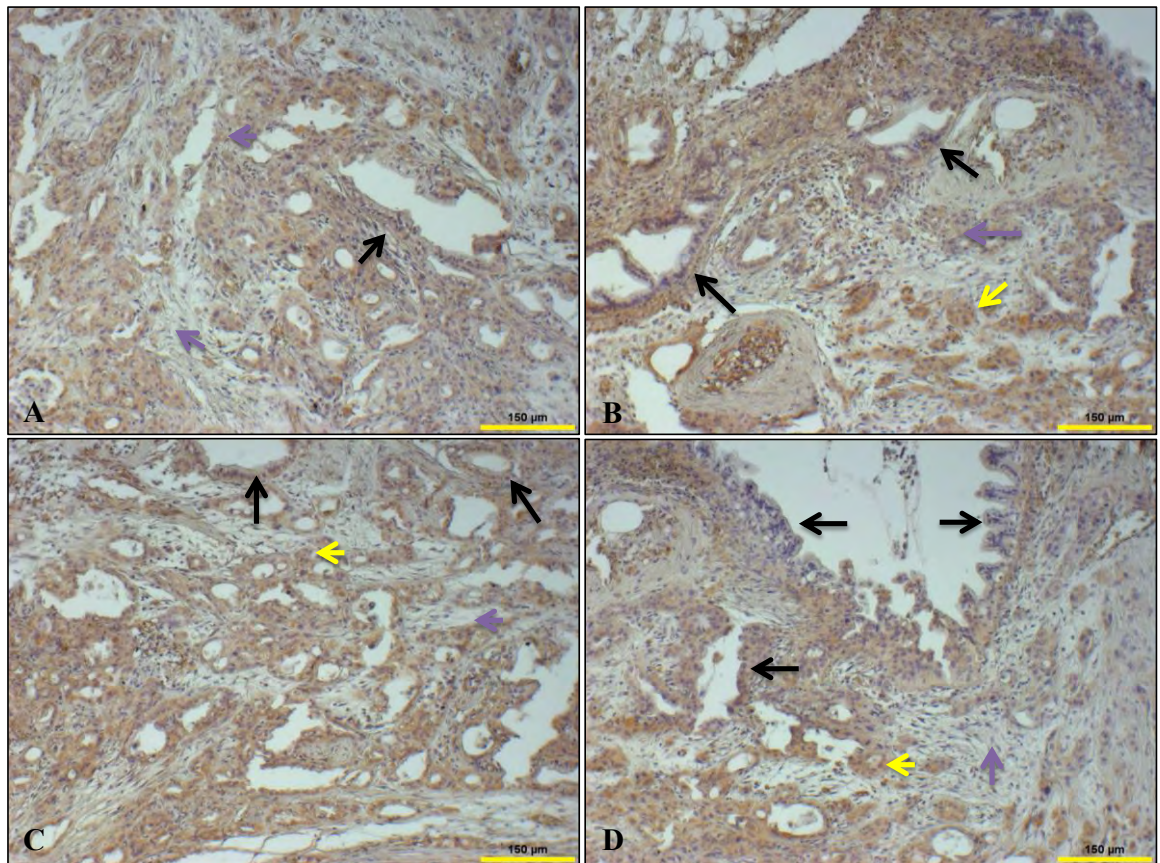


Figure 7-15: Immunohistochemical analysis of the expression of NFκB in human pancreatic adenocarcinoma tissue case study 3 (10X magnification).

Formalin fixed, paraffin embedded pancreatic adenocarcinoma tissue blocks were sectioned (5μm) and mounted on glass slides. Immunohistochemistry was performed using a specific antibody to NFκB. NFκB immunostained sections were counter stained with haematoxylin and sections were mounted using mounting medium. Stained sections were analysed by light microscopy and images were captured at 10X magnification. NFκB expression identified as follows: (A) Positive expression of NFκB in ductal and **stromal cells** (B & C) Positive expression of NFκB in ductal and **pleomorphic malignant cells**. (D) Differential (Positive and negative) expression of NFκB in ductal cells and low cytoplasmic expression in **stromal cells**.

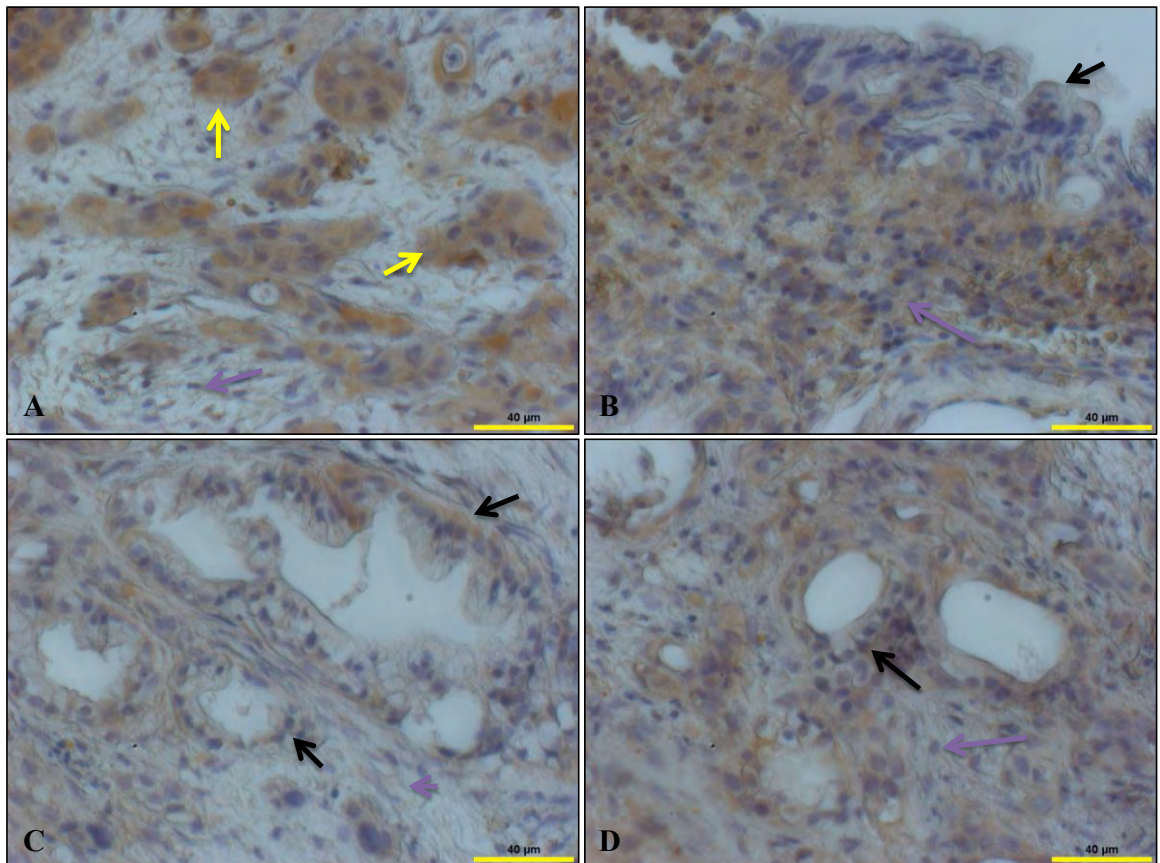


Figure 7-16: Immunohistochemical analysis of the expression of NFκB in human pancreatic adenocarcinoma tissue case study 3 (40X magnification).

Formalin fixed, paraffin embedded pancreatic adenocarcinoma tissue blocks were sectioned (5μm) and mounted on glass slides. Immunohistochemistry was performed using a specific antibody to NFκB. NFκB immunostained sections were counter stained with haematoxylin and sections were mounted using mounting medium. Stained sections were analysed by light microscopy and images were captured at 40X magnification. NFκB expression identified as follows: (A) Positive expression of NFκB in **pleomorphic malignant cells** and very low expression in **stromal cells** (B &C) Positive expression of NFκB in **stromal cells** (B) Negative expression of NFκB in ductal epithelial cells (C) Nuclear and cytoplasmic expression of NFκB in ductal cells (C) Nuclear and cytoplasmic expression of NFκB in ductal cells.

7.2.2.2.4. Case study 4

In order to determine the expression and subcellular localisation of NFκB in human pancreatic adenocarcinoma tissue (sample 4), immunohistochemistry was performed and results are shown in Figure 7-17 (5X), Figure 7-18 (10X) and Figure 7-19 (40X). It is clear from gross examination of sample 4 that NFκB was highly expressed throughout the tissue sections, whether they had normal or adenocarcinoma morphology (Figure 7-17). On analysing at higher magnification at 10X it was clear that NFκB was highly expressed in islets of Langerhans, pleomorphic malignant epithelial cells and fibrous connective tissue as shown in Figure 7-18. In order to determine the subcellular expression of NFκB we further analysed sample 4 under higher magnification at 40X. It was clear from these analyses that NFκB was differentially expressed in islets of Langerhans; the outer cells of the islets showed higher expression compared to the cells in the centre of islets. NFκB was localised in the nucleus of islets of Langerhans cells as shown in Figure 7-19 (A). It was clear from Figure 7-19 (B) that nerve cells bundle showed low cytoplasmic expression of NFκB. NFκB was highly expressed in the nucleus as well as the cytoplasm of pleomorphic malignant epithelial cells as shown in Figure 7-19(C). Ductal cells showed positive nuclear and cytoplasmic expression of NFκB as shown in Figure 7-19 (D).

In summary, immunohistochemistry analyses of sample 4 suggested that, NFκB was positively expressed in the nucleus and the cytoplasm of cells.

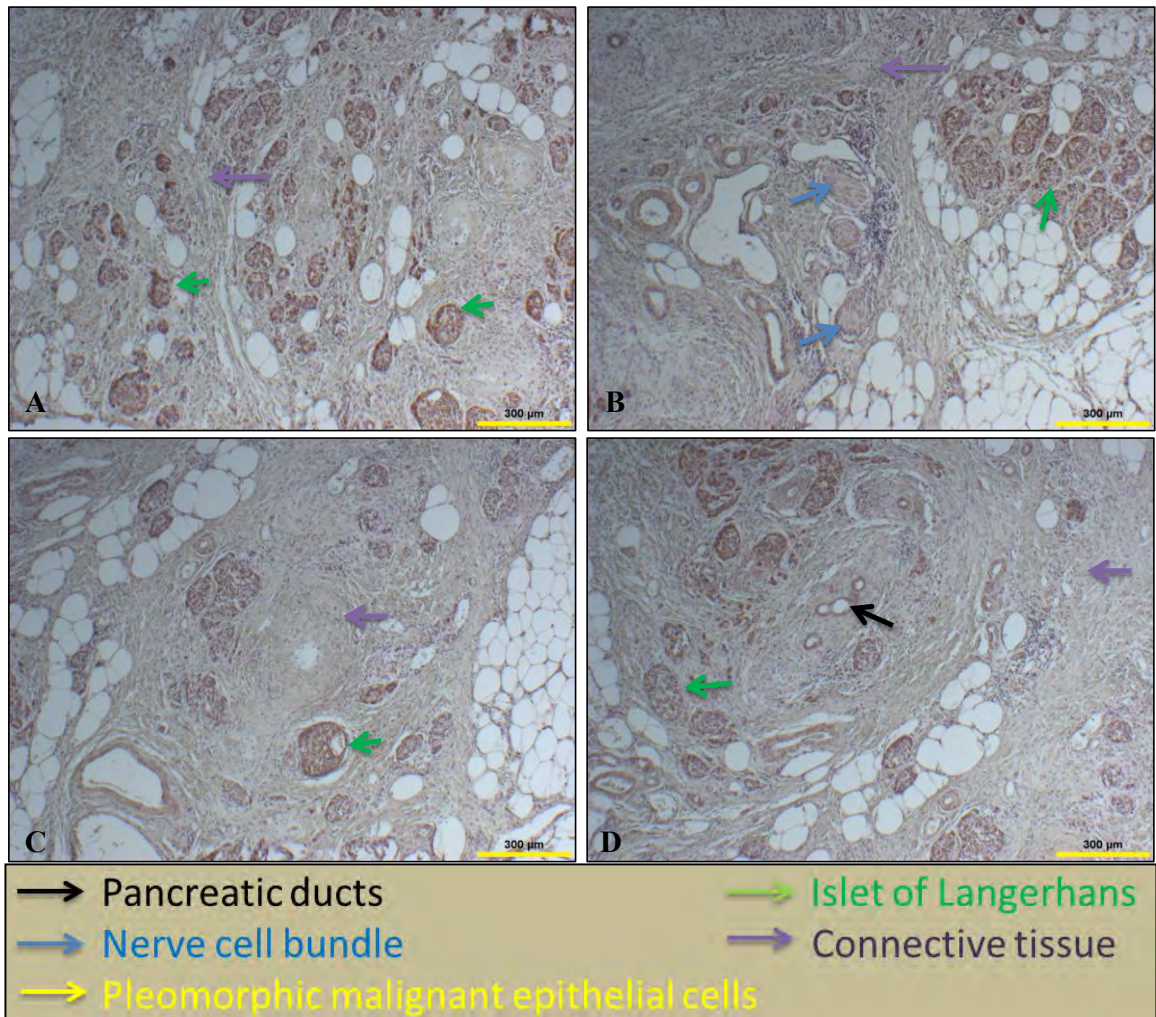


Figure 7-17: Immunohistochemical analysis of the expression of NFκB in human pancreatic adenocarcinoma tissue case study 4 (5X magnification).

Formalin fixed, paraffin embedded pancreatic adenocarcinoma tissue blocks were sectioned (5μm) and mounted on glass slides. Immunohistochemistry was performed using a specific antibody to NFκB. NFκB immunostained sections were counter stained with haematoxylin and sections were mounted using mounting medium. Stained sections were analysed by light microscopy and images were captured at 5X magnification. NFκB was positively expressed in **islets of Langerhans**, ductal cells, **nerve cell bundle** and **fibrous connective tissue**.

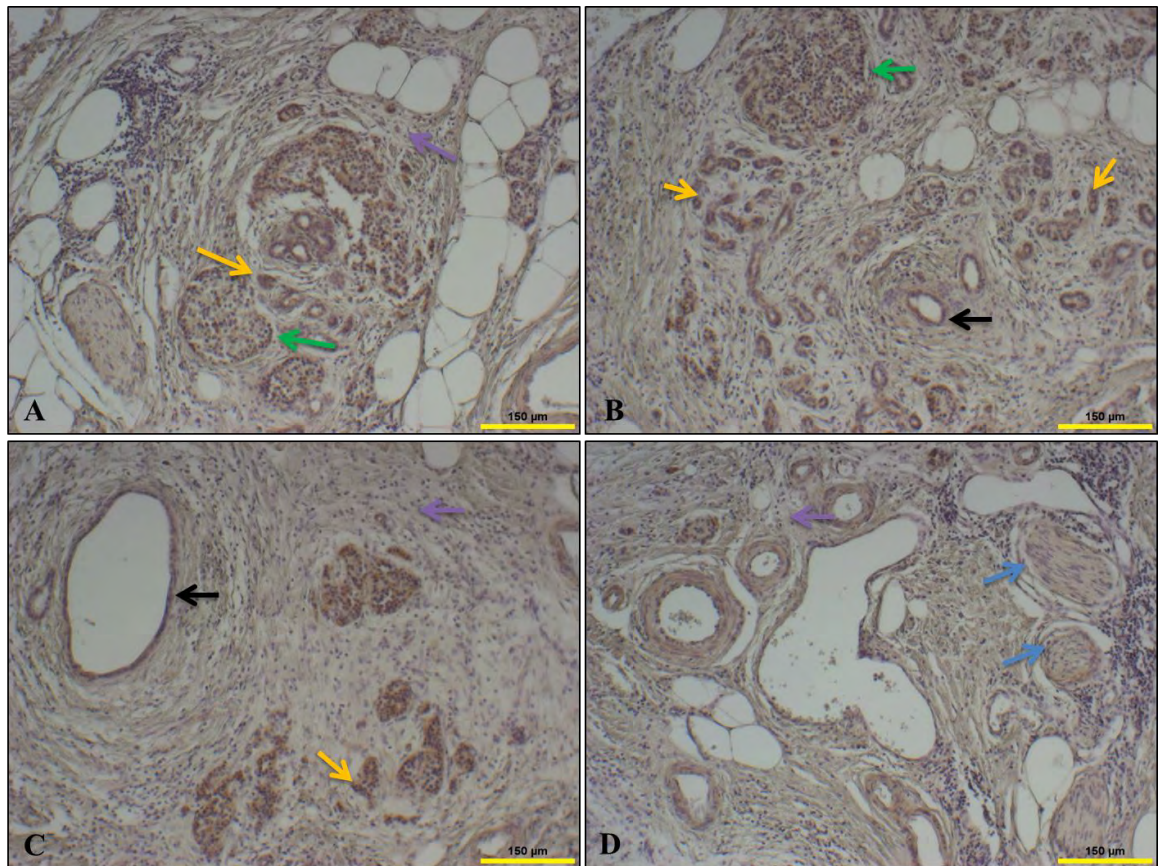


Figure 7-18: Immunohistochemical analysis of the expression of NFκB in human pancreatic adenocarcinoma tissue case study 4 (10X magnification).

Formalin fixed, paraffin embedded pancreatic adenocarcinoma tissue blocks were sectioned (5μm) and mounted on glass slides. Immunohistochemistry was performed using a specific antibody to NFκB. NFκB immunostained sections were counter stained with haematoxylin and sections were mounted using mounting medium. Stained sections were analysed by light microscopy and images were captured at 10X magnification. NFκB was positively expressed in **Pleomorphic malignant epithelial cells**, **islets of Langerhans** ductal cells, **nerve cell bundle** and **fibrous connective tissue**.

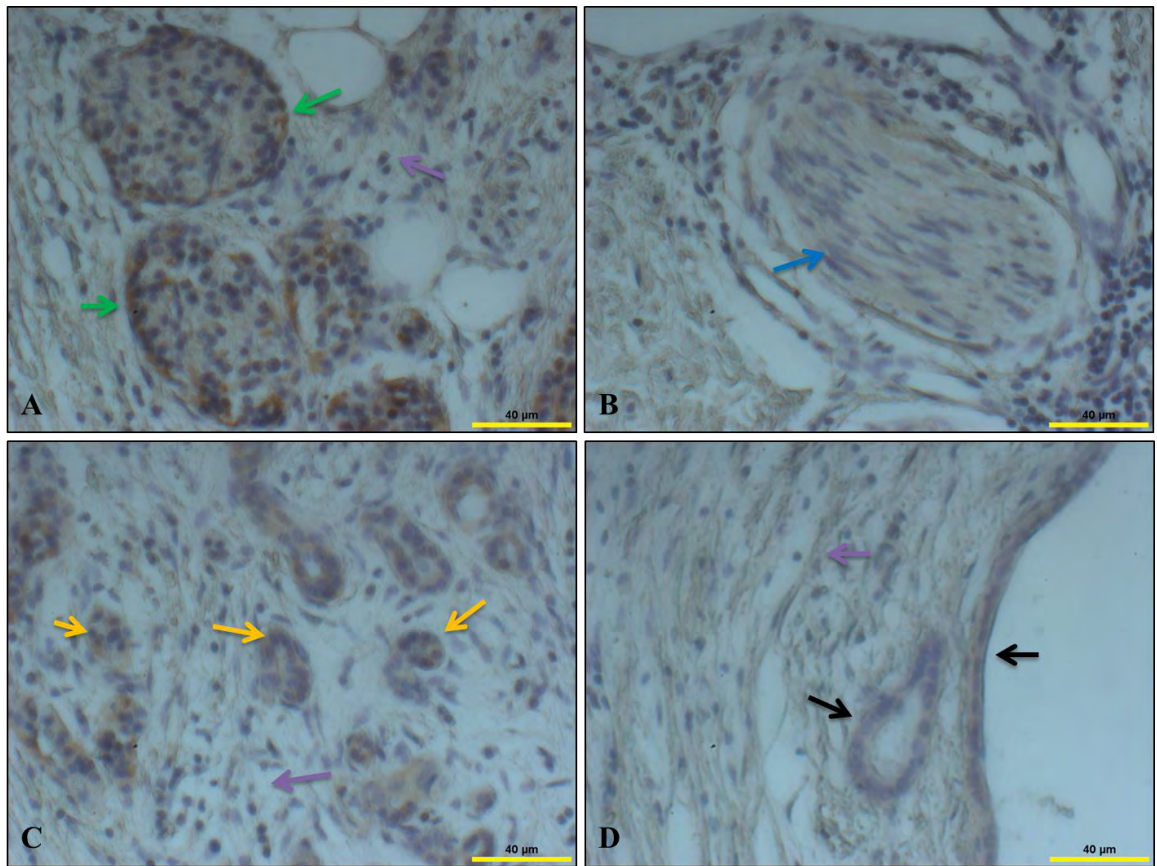


Figure 7-19: Immunohistochemical analysis of the expression of NFκB in human pancreatic adenocarcinoma tissue case study 4 (40X magnification).

Formalin fixed, paraffin embedded pancreatic adenocarcinoma tissue blocks were sectioned (5μm) and mounted on glass slides. Immunohistochemistry was performed using a specific antibody to NFκB. NFκB immunostained sections were counter stained with haematoxylin and sections were mounted using mounting medium. Stained sections were analysed by light microscopy and images were captured at 40X magnification. NFκB expression identified as follows. (A) Nuclear localisation of NFκB in **islets of Langerhans**. (B) Cytoplasmic expression of NFκB in **nerve cell bundle**. (C) Nuclear and cytoplasmic localisation of NFκB in **fibrous connective tissue** and **Pleomorphic malignant epithelial cells**. (D) Nuclear and cytoplasmic localisation of NFκB in ductal epithelial cells.

7.3. Discussion

Nuclear factor kappa B (NFκB) plays a crucial role in tumorigenesis and tumour progression in various types of cancer. NFκB is sequestered in the cytoplasm by binding to inhibitor of kappa B (IκB) protein and upon stimulation by a variety of signals IκB undergoes proteasomal degradation; ultimately results in translocation of NFκB to the nucleus and induce gene expression [406]. Over-expression of NFκB has been observed previously in other cancer such as gastric [407], oral [408], hepatocellular [409], cervical [410] and prostate [411, 412] carcinoma. Constitutive activation of NFκB has been observed in most pancreatic cancer cells and human tumour samples but not in normal pancreatic cell lines or normal pancreatic tissues [262, 391, 400]. Hypoxia leads to activation of NFκB by phosphorylation of IκB [413] and activation of NFκB is a critical transcriptional response to hypoxia. Reports on NFκB (p65 or RelA) expression in pancreatic cancer especially, under the influence of hypoxia are sparse.

We started our investigation in human pancreatic adenocarcinoma cells (PSN-1) and ductal cells (ARIP) under real tumour micro-environmental conditions (hypoxic) and normal (normoxic) conditions. In PSN-1 cells we observed that NFκB was highly expressed in the cytoplasm under normoxic and hypoxic conditions, except H24 where nuclear NFκB expression was observed as shown in Figure 7-2 (Western blotting) and Figure 7-4 (Immunocytochemistry). These results suggest that hypoxia may trigger nuclear localisation or activation of NFκB in pancreatic adenocarcinoma cells (PSN-1) but very low compared to expression in the cytoplasm which might be the reason behind survival of PSN-1 cells under hypoxic conditions. In order to further evaluate the role of NFκB, we examined localisation and expression in normal pancreatic ductal cells. Western blotting analysis showed that in ARIP cells NFκB was localised in the cytoplasm and the nucleus under normoxic and hypoxic conditions. No significant difference in localisation and expression of NFκB was found under normoxic and

hypoxic conditions in ARIP cell as shown in Figure 7-3. These findings were further evaluated by immunocytochemistry and we found that NF κ B was highly expressed in the cytoplasm and the nucleus of ARIP cells. However, on careful examination it was clear that the cytoplasmic NF κ B was mostly localised near to the nuclear membrane, especially under hypoxic conditions in ARIP cells. NF κ B was highly expressed in the nucleus and highly concentrated on the nuclear membrane of ARIP cells as shown in Figure 7-5. These results suggest hypoxia does activate NF κ B and may be involved in the shuttling of NF κ B from the cytoplasm to nucleus in ARIP ductal cells; this may be responsible for triggering apoptosis in ARIP cells under hypoxic conditions as shown in Figure 3-5. In PSN-1 cells hypoxia induced a slight accumulation of NF κ B in the nucleus, but this was not enough to induce apoptosis. Recently, it has been reported that hypoxia can trigger activation of NF κ B in pancreatic cancer cells [279]. Previous reports suggest that hypoxia mediates phosphorylation of I κ B which ultimately leads to activation and nuclear expression of NF κ B [413]. It has been reported in several studies that NF κ B has an effect on apoptosis during the process of tumour progression and development by regulating several genes [414] but conflicting results have been reported regarding the exact role of NF κ B in apoptosis [415]. NF κ B can act in an anti- or pro- apoptotic manner, [416] but how it mediates apoptosis is unclear. Further investigation is needed before concluding the specific role of NF κ B in pancreatic adenocarcinomas and normal ductal cells.

Further NF κ B localisation and expression was evaluated in normal mouse pancreatic tissue and human pancreatic adenocarcinoma tissue sections by immunohistochemistry. We started our investigation in normal pancreas tissue and found that NF κ B was positively expressed throughout the tissue section as shown in Figure 7-6. Higher magnification analysis revealed cytoplasmic localisation of NF κ B in acinar cells as shown in Figure 7-7 (A, B & C), however, blood vessels, islets of Langerhans,

intercalated ducts and interlobular ductal cells showed positive expression in the nucleus and the cytoplasm as shown in Figure 7-7 (A & D). From these findings we can conclude that NFκB is positively expressed in normal pancreatic tissue sections and localised in the cytoplasm and nucleus of ductal cells which complements results obtained from western blotting and immunocytochemistry analysis of ARIP cells. Wang *et. al.*, (1999) were the first who reported constitutive dysregulation of NFκB (p65 subunit) in human pancreatic cancer cells, 9 out of 11 pancreatic cancer cell lines analysed showed high expression of NFκB. This report also showed high expression of NFκB (p65 subunit) in pancreatic adenocarcinoma tissues in compared to normal pancreatic tissues [262]. So in order to determine the expression and localisation of NFκB in pancreatic adenocarcinoma tissues, we further evaluated four case studies of human pancreatic adenocarcinoma tissue sections by immunohistochemistry. Case study 1 immunohistochemistry results (Figure 7-8, Figure 7-9 and Figure 7-10) showed that NFκB was expressed in human pancreatic adenocarcinoma tissue but expression and localisation varied between different types of pancreatic cell within same tissue section. Cytoplasmic expression of NFκB was observed in ductal cells, fibrous connective tissue and pleomorphic malignant ductal epithelial cells in sample 1 as shown in Figure 7-10. These results complement results from PSN-1 cells where it was found that NFκB was highly expressed in the cytoplasm of cells. We continued our investigation and analysed NFκB expression and localisation in human pancreatic adenocarcinoma sample 2 (Figure 7-11, Figure 7-12 and Figure 7-13) by immunohistochemistry. Immunohistochemistry staining for NFκB showed that NFκB was positively expressed throughout the tissue section, in well and moderate and poorly differentiated adenocarcinoma, as shown in Figure 7-12. NFκB was localised in the cytoplasm of malignant ductal epithelial cells and stromal cells as shown in Figure 7-13. In case study 3 (Figure 7-14, Figure 7-15 and Figure 7-16), we found that NFκB was

highly expressed in pleomorphic malignant epithelial cells however, ductal and stromal cells showed differential expression of NFκB as shown in Figure 7-15 and Figure 7-16. We further analysed NFκB expression and localisation in human pancreatic adenocarcinoma sample 4 (Figure 7-17, Figure 7-18 and Figure 7-19), which showed a pronounced amount of autolysis throughout the tissue sections. We found that NFκB was positively expressed throughout the tissue section as shown in Figure 7-17 and Figure 7-18. NFκB was positively expressed in the cytoplasm as well as the nucleus of pleomorphic malignant epithelial cells, ductal cells, islets of Langerhans and stromal cells as shown in Figure 7-19.

Immunohistochemistry evaluation of NFκB in all four samples from human pancreatic adenocarcinoma tissue sections showed positive expression of NFκB. However, ductal cells, fibrous connective tissue or stromal cells and pleomorphic malignant epithelial cells which account for adenocarcinoma of the pancreas showed cytoplasmic expression of NFκB in two samples out of four, a similar expression pattern of NFκB was observed in PSN-1 cells. Tissue sections from mouse pancreas, case study 3 and case study 4 showed nuclear and cytoplasmic expression ductal cells, pleomorphic malignant epithelial cells and stromal cells; a similar expression pattern of NFκB was observed in ARIP cells.

We observed cytoplasmic expression of NFκB in 2 case studies and in the other 2 case studies positive nuclear & cytoplasmic staining was identified. Thus cytoplasmic expression of NFκB was observed in 100% and nuclear expression in 50% of the four case studies. Due to limitations of the immunohistochemistry method we could not see any translocation of NFκB from cytoplasm to nucleus of cells but we did observe nuclear translocation of NFκB in PSN-1 cells and ARIP cells (under hypoxic conditions). From these results it can be hypothesised that cytoplasmic expression of NFκB might be a better indirect marker to estimate nuclear expression of NFκB, which

itself difficult to study from primary human pancreatic adenocarcinoma tissue. Translocation of NFκB into the nucleus is required for its activation. Activation of NFκB has been observed previously in pancreatic adenocarcinoma tissues [233, 260, 262]. It has been reported that *K-Ras* mutation (which are found in 100% pancreatic adenocarcinoma cases [92-94]) and *EGFR* mutation (which are found in 30-50% of human pancreatic cancer [417]) lead to an activation of NFκB in pancreatic cancer [418, 419]. Many studies have reported that hypoxia lead to NFκB activation in pancreatic cancer [279] as our data suggest hypoxia triggered the activation or translocation of NFκB to the nucleus in human pancreatic adenocarcinoma and rat pancreatic ductal cells. The commonly accepted view is activation of NFκB leads to resistance to chemotherapy resistance in pancreatic cancer [271, 384, 385, 420].

An unavoidable limitation of our present study is the relatively small number of human pancreatic adenocarcinoma case studies available. Therefore, these results need to be confirmed in a larger study of human pancreatic adenocarcinoma tissue to draw any firm conclusions.

Chapter 8. General discussion

With one of the highest mortality to incident ratios, pancreatic ductal adenocarcinoma (PDAC), commonly referred to as pancreatic cancer, is the fifth most common cause of cancer death. The 5 year survival rate is only 4% and this figure has not changed in over 40 years [34, 35]. Three key features of pancreatic cancer are multiple molecular aberrations, intense desmoplastic stroma and hypoxic conditions resulting in a cancer which is biologically and clinically aggressive. This leads to short overall survival, no early detection, early metastasis, and resistance to chemotherapy and radiotherapy [421]. The reasons and mechanisms behind the late presentation, malignancy, and resistance to chemotherapy and radiotherapy are not well known. However, it has been proposed that the microenvironment of extreme hypoxia found inside the solid tumours of the pancreas may contribute [297]. The role of tumour hypoxia has become a major focus in cancer research as it can trigger the invasive and metastatic nature of cancer, a phenomenon noted in pancreatic cancer in particular [281]. Therefore it is of great importance to investigate further the hypoxia and find new molecular targets to determine the behaviour of different pancreatic cell types under hypoxic conditions. A better understanding of the tumour suppressor PDCD4 and transcription factors HIF-1 α and NF κ B under hypoxic conditions may lead to novel therapeutic strategies for pancreatic cancer.

In the present investigation three mammalian cell lines; human pancreatic adenocarcinoma cell line (PSN-1), rat pancreatic ductal epithelial cell line (ARIP) and mouse pancreatic beta cell line (MIN6) were studied under hypoxic (1% oxygen) and normoxic (ambient 21% oxygen) conditions. Healthy mouse pancreas and human pancreatic adenocarcinoma tissue sections (from four patients) were investigated for expression of PDCD4, HIF-1 α and NF κ B.

8.1. Cell Viability in Hypoxia

We began our study by confirming cell viability of all three lines (PSN-1, ARIP and MIN6) under normoxic and hypoxic conditions. Hypoxic microenvironment leads to coordinated biochemical responses in tumour cells that ultimately decide the fate of cells; either cell death or adaptation [300]. It is evident that many cancer cells under hypoxic conditions develop an efficient adaptive metabolic response to ensure their survival and proliferation [171, 306, 307] whereas, normal cells under hypoxic conditions undergo cell cycle arrest [311]. Our data from viability studies indicated that PSN-1 cells were well adapted to survive under hypoxic conditions. Hypoxia did trigger apoptosis but not necrosis in ARIP cells however, in beta-cells (MIN6) hypoxia triggered both necrosis and apoptosis. Therefore it could be said that pancreatic ductal cells were able to adapt to hypoxic conditions more effectively than pancreatic beta-cells. Particularly in MIN6 cells, hypoxia had a catastrophic effect (viability reduced by 70%) on the viability at 24 hours. These results indicate the great importance of oxygen for normal cell survival and function. In order to secrete insulin in response to blood glucose, pancreatic beta cells require a large amount of oxygen [216]. Low oxygen conditions damage beta-cells and alter beta cell function in diabetes [313]. MIN6 viability results may have great relevance to the procedure of islet transplantation as a therapy for type 1 diabetes [314, 315]. Revascularization and supply of sufficient oxygen to pancreatic islets can provide protection against hypoxia and ultimately increase beta-cell survival [323]. Our beta cell viability results support this need to restore oxygen supply as soon as possible following islet transplantation.

8.2. Cell Morphology

Data from PSN-1 cell morphology studies indicated that PSN-1 cells have characteristics of cancer cells as defined in section 4.2.1.1. Cell surfaces were fully

covered with filopodia and cells were connected to each with other lamellipodia. Filopodia and lamellipodia distinguish cancer cells from normal cells. These extensions help cancer cells to invade adjacent tissue, migrate into the blood stream and to spread to other organs by metastasis [332]. Accordingly, increased filopodia formation has been associated with cancer cell migration [333] and invasion [334] and plays an important role in the process of EMT (Epithelial-mesenchymal transition) [335]. Data from viability and morphology analyses further confirmed that PSN-1 cells are truly representative of pancreatic cancer.

We investigated the morphology of ARIP cells; results indicated that ARIP cells under normoxic conditions had characteristics of non-cancerous cells as defined in section 4.2.1.2. However, under hypoxic conditions a change in morphology was observed. Cell surfaces were covered with filopodia, resembling cancerous PSN-1 cells. It is generally believed that pancreatic duct cells are the progenitor of pancreatic adenocarcinoma [422, 423]. Our data from viability and morphology analysis (under hypoxia) of ARIP cells further suggest that pancreatic ductal cells may serve as the progenitor of pancreatic adenocarcinoma [69, 70].

Morphology analysis of MIN6 cells indicated that MIN6 cells under hypoxic conditions have characteristics of normal beta-cells as defined in section 4.2.1.3. Hypoxia triggered a change in the morphology, as the membrane showed blebbing (apoptosis) and pores (characteristic of necrosis). Our data from viability and morphology studies of MIN6 under hypoxic conditions further confirmed that an adequate oxygen supply is necessary for beta-cell survival and function. This finding supports the need for improving oxygen supply post islet transplantation as quickly as possible.

The mature pancreas has morphologically and functionally distinct endocrine (comprises islet of Langerhans, accounts for 2%) and exocrine (comprises acinar and ductal cells, accounts for 85%) structures. The majority of pancreatic cancers arise in

the exocrine part of the pancreas especially adenocarcinoma (ductal epithelial cell lining), accounting for ~90% of all pancreatic cancer [69, 70]. Most pancreatic cancers are well to moderately differentiated, however, variation of differentiation within the same neoplasm is quite common [80, 338, 350]. Histological evaluation remains a vital tool for diagnosis of any cancer. In the present study human pancreatic adenocarcinoma tissue biopsies (paraffin embedded) from patients diagnosed with pancreatic adenocarcinoma were evaluated to define their histopathology.

We began our investigation by defining the normal morphology of the pancreas and our data demonstrated that the normal pancreas was divided into lobules and these lobules were composed of numerous acini. These numerous acini were connected to intercalated ducts which further open into intralobular ducts. Islets of Langerhans (clusters of cells) are surrounded by numerous acini and scattered in a random pattern mostly next to interlobular ducts.

Histopathology analysis of four human pancreatic adenocarcinoma tissues suggested that sample 1 and 2 were well to moderately differentiated but in some parts poorly differentiated (with a total loss of pancreas integrity). Sample 3 was moderately to poorly differentiated and sample 4 was well differentiated. Three samples (1, 2 and 4) were highly infiltrated with desmoplastic fibrous connective tissue and small gland-like pleomorphic malignant epithelial cell structures. Grading of human pancreatic adenocarcinoma tissue samples was determined by semi-quantitative method as shown in Table 8-1. We have established that hypoxia triggers a change in the morphology and viability of pancreatic beta-cells and ductal cells. No effect was found on the morphology or viability of pancreatic ductal adenocarcinoma cells in hypoxia. It is essential to understand what molecular pathways pancreatic cancer cells adapt in order to survive under hypoxic conditions and to investigate the genes which play a role in apoptosis or necrosis in pancreatic beta- and ductal cells.

Table 8-1: Semi-quantitative method for grading of human pancreatic adenocarcinoma tissue samples.

	Case study 1	Case study 2	Case study 3	Case study 4
Rudimentary acinar cells	***	**	-	***
Normal acinar cells	*	**	-	-
Islets of Langerhans	-	*	-	**
Normal lobular morphology	*	**	-	-
Loss of lobular morphology	***	**	***	***
Desmoplastic stroma	***	**	***	***
Pleomorphic malignant epithelial cells	***	***	***	***
Pleomorphic nucleus	***	***	***	***
Large duct like structures	**	***	-	**
Lymphocyte infiltration	***	-	***	***
Nerve cell bundle invasion	***	***	-	***

Abundant or high number observed denoted as ***, Medium number observed denoted as **, low number observed denoted as * and negative denoted as -.

8.3. Role of PDCD4 in pancreatic cancer

PDCD4 is a novel tumour suppressor gene which is up-regulated during apoptosis. Loss of *PDCD4* expression has been reported in several type of cancer [136-141]. *PDCD4* has recently been linked with type 1 diabetes [370] and pancreatic cancer [372] but the role has not been definitively defined especially under the influence of the hypoxic microenvironment in human pancreatic adenocarcinoma. In the present study, our data revealed that *PDCD4* expression decreased significantly under hypoxic conditions in PSN-1 cells *PDCD4* expression has not previously been studied under the influence of hypoxia however, we reveal that *PDCD4* expression decreased under the influence of hypoxia. Studies have reported loss of *PDCD4* expression in several types of cancer, but the reason behind this loss of expression has not yet been elucidated. Results from this study suggest that hypoxia may be a factor behind the loss or reduced expression of *PDCD4*, which ultimately contributes to cancer invasion and migration. The present study has revealed that loss or reduced expression of *PDCD4* may play an important role in pancreatic cancer cells survival under hypoxic conditions as observed in PSN-1 cell viability studies. Further investigation revealed that *PDCD4* was highly expressed in ARIP and MIN6 cells under hypoxic conditions. Cell viability analysis of ARIP and MIN6 cells showed that hypoxia triggered apoptosis or necrosis. The importance of *PDCD4* in cell cycle control of pancreatic cells has been illustrated in a previous study demonstrating up-regulation of *PDCD4* during the process of islet neogenesis [280].

How *PDCD4* exerts its effects it is still not clear, but it has been reported that inside the cytoplasm *PDCD4* inhibits helicase activity of eIF4a as well as interfering in the interaction of eIF4a with eIF4G, ultimately resulting in an inhibitory effect on protein translation [107, 113]. Subcellular localisation of *PDCD4* is still a topic of some controversy; some studies have reported *PDCD4* localized in the nucleus of normal cells and in the cytoplasm of cancer cells [123, 124] whilst others reported vice versa

[125]. Our data from subcellular localization studies as detailed in section 5.2.1.2 revealed that PDCD4 was expressed in the cytoplasm of pancreatic (PSN-1, ARIP and MIN6) cells and does not translocate from the cytoplasm to the nucleus, however, weak diffuse expression of PDCD4 was observed in the nucleus under normoxic conditions at 24 hours in PSN-1 cells as well as ARIP cells.

The exact role of PDCD4 during the process of apoptosis remains to be defined, as some studies have identified it as up-regulated [104] and others as down-regulated during the process of apoptosis [424]. Studies into the cell type specific role of PDCD4 in apoptosis have also given inconsistent findings; PDCD4 has role in apoptosis in the case of lung [425] and breast cancer [426] however, no apoptotic effect has been found in other tissues [382, 387]. In some studies even overexpression of PDCD4 in ovarian cancer did not induce apoptosis [379].

Expression and subcellular localisation studies here clearly demonstrate a high expression of PDCD4 may have link with apoptosis in normal pancreatic (ARIP and MIN6) cells under the influence of hypoxia. Loss or low expression of PDCD4 may result in cancer cell survival or no apoptosis even under hypoxia.

After elucidating a novel response of PDCD4 in pancreatic cell lines, we further investigated the expression and subcellular localisation of PDCD4 in pancreatic tissue (normal and adenocarcinoma tissue samples) as detailed in section 5.2.2. Differential PDCD4 expression was identified in ARIP and MIN6 cells. PDCD4 was mostly localized in the cytoplasm; however, expression increased or decreased depended upon the type of cells or environment.

Data for PDCD4 expression and subcellular localisation from human pancreatic adenocarcinoma tissue samples (four case studies) suggested that the expression of PDCD4 was reduced with progression of malignancy and has an inverse correlation

with the advance stage of malignancy. PDCD4 shows differential expression and localisation in normal tissue but highly malignant pancreatic tissue showed weak cytoplasmic expression or localisation.

Overall data from pancreatic cell lines (cancerous and normal) and tissue (normal and adenocarcinoma) have identified PDCD4 as a target with great potential to fight notorious diseases of pancreas i.e. pancreatic cancer. There is potential for PDCD4 to be used as an additional diagnostic tool to discriminate between normal tissues, benign and malignant pancreatic cancer tissues. Especially in the people on high risk of pancreatic adenocarcinoma can be screened for PDCD4 expression.

Increased expression of PDCD4 may induce apoptosis while decreased or lost expression of PDCD4 may inhibit apoptosis in normal and pancreatic cancer cells under hypoxic conditions. The role of PDCD4 under hypoxic conditions might be decided by the master regulator of oxygen homeostasis i.e. HIF-1 α . In order to determine the upstream regulation of PDCD4 in the pancreas under hypoxic conditions we investigated HIF-1 α .

8.4. Role of HIF-1 α in pancreatic cancer

We began our investigation of the role of HIF-1 α in pancreatic cell lines (PSN-1 and ARIP cells) under hypoxic and normoxic conditions as detailed in section 6.2.1 Our data from HIF-1 α expression analysis revealed that no significant difference was found in PSN-1 cells between hypoxic and normoxic conditions. In ARIP cells significantly high expression of HIF-1 α was observed under hypoxic conditions compared to normoxic conditions. Our data from subcellular localisation analysis showed that HIF-1 α was exclusively localized to the nucleus of pancreatic cells (PSN-1 and ARIP cells) under hypoxic and normoxic conditions. Normal as well as adenocarcinoma cells of the pancreas showed expression of HIF-1 α under normoxic conditions. This is in keeping

with results of Akakura *et al*, (2001) which suggested that several human pancreatic cancer cell lines express HIF-1 α under normoxic conditions [215].

Significantly higher expression of HIF-1 α and PDCD4 under hypoxic conditions compared to normoxic conditions together with viability findings of ARIP cells, suggest both HIF-1 α and PDCD4 may play role in apoptosis induction in normal pancreatic cells under hypoxic conditions. Loss or reduced expression of PDCD4 with no significantly higher expression of HIF-1 α , and evidence of cell survival under hypoxic conditions, suggest that PDCD4 and HIF-1 α may facilitate PSN-1 cell survival under hypoxia. However, it is too early to conclude the role of PDCD4 in conjunction with HIF-1 α in pancreatic cells; more investigations are required in order to draw any firm conclusions.

After determining expression and localization of HIF-1 α in pancreatic cell lines, we continued our investigation in pancreatic tissue samples (normal and adenocarcinoma tissue samples) as detailed in section 6.2.2. Data from normal tissue samples revealed that HIF-1 α was expressed in normal pancreatic tissue samples as observed in ARIP cells. Nuclear and cytoplasmic expression of HIF-1 α was observed in normal pancreatic tissue samples. Data from adenocarcinoma tissue samples revealed that HIF-1 α was highly expressed in all pancreatic adenocarcinoma tissue samples (1, 2 and 4) except sample 3 (moderate expression was observed). High expression of HIF-1 α observed in these analyses further revealed nuclear localization of HIF-1 α especially in ductal cells as observed in PSN-1 and ARIP cells.

Hypoxia regulates the activation of NF κ B [391, 400] and overexpression of HIF-1 α induces epithelial to mesenchymal transition (EMT) in pancreatic cancer in an NF κ B dependent manner [279]. NF κ B has been linked to unique regulation of *PDCD4* in pancreatic beta cells through the miRNA-21 axis [370]. NF κ B (p65 or RelA) expression in pancreatic cancer has been studied extensively in particular under the influence of

hypoxia. NF κ B may play a crucial role in the regulation of PDCD4 in pancreatic adenocarcinoma.

8.5. Role of NF κ B in pancreatic cancer

We began our investigation by analysis of expression and subcellular localization of NF κ B in pancreatic cell lines (ARIP and PSN-1 cells) under hypoxic and normoxic conditions as detailed in section 7.2.1. Our data suggested that hypoxia may trigger the nuclear localization or activation of NF κ B in PSN-1 cells under hypoxic conditions but expression was very low compared to that in the cytoplasm. Further analysis of ARIP cells revealed that hypoxia triggered the nuclear localisation or activation of NF κ B. NF κ B was highly expressed in the nucleus and highly concentrated on the nuclear membrane of ARIP cells under hypoxic conditions. These findings suggest that hypoxia does activate NF κ B and may be involved in the shuttling of NF κ B from the cytoplasm to nucleus in ARIP ductal cells. This may be responsible for triggering apoptosis in ARIP cells under hypoxic conditions whereas in PSN-1 cells hypoxia induced a slight accumulation of NF κ B in the nucleus, but cells did not undergo apoptosis. Previous reports suggest that hypoxia mediates phosphorylation of I κ B which ultimately leads to activation and nuclear expression of NF κ B [413]. Several studies have reported that NF κ B has an effect on apoptosis during the process of tumour progression and development by regulating several genes [414] but conflicting results have been reported regarding the exact role of NF κ B in apoptosis [415]. NF κ B can act in an anti- or pro- apoptotic manner, [416] but how it mediates apoptosis is unclear. Further investigation is needed before concluding the specific role of NF κ B in pancreatic adenocarcinomas and normal ductal cells. However, our data suggest that hypoxia does trigger the activation of NF κ B, which ultimately may link with pancreatic cancer cell survival.

After evaluating expression and localization of NFκB in pancreatic cell lines, we continued our investigation in pancreatic tissue samples (normal and adenocarcinoma tissue samples) as detailed in section 7.2.2. Data from normal tissue samples revealed that NFκB was positively expressed in the cytoplasm and nuclei of normal pancreatic tissue sample, as we had observed in the ARIP cell line.

We observed cytoplasmic expression of NFκB in 2 case studies (a similar expression pattern of NFκB was observed in PSN-1 cells) and in the other 2 case studies positive nuclear & cytoplasmic staining was identified. Thus cytoplasmic expression of NFκB was observed in 100% and nuclear expression in 50% of the four case studies. Due to limitations of the immunohistochemistry method we could not see any translocation of NFκB from cytoplasm to nucleus of cells but we did observe nuclear translocation of NFκB in PSN-1 cells and ARIP cells (under hypoxic conditions). From these results it can be hypothesised that cytoplasmic expression of NFκB might be a better indirect marker to estimate nuclear expression of NFκB, which is itself difficult to study from primary human pancreatic adenocarcinoma tissue. Translocation of NFκB into the nucleus is required for its activation. Activation of NFκB has been observed previously in pancreatic adenocarcinoma tissues [233, 260, 262]. Many studies have reported that hypoxia leads to NFκB activation in pancreatic cancer [279] our data also suggests hypoxia triggered the activation or translocation of NFκB to the nucleus in human pancreatic adenocarcinoma and rat pancreatic ductal cells. The commonly accepted view is activation of NFκB leads to resistance to chemotherapy in pancreatic cancer [271, 384, 385, 420].

8.6. Overview of hypothesis

On the bases of cell viability, morphology, and PDCD4, HIF-1α and NFκB expression data schematic diagrams are shown in Figure 8-1 and Figure 8-2. These illustrate the

proposed role of PDCD4, HIF-1 α and NF κ B in hypoxic conditions in normal (Figure 8-1) and cancerous (Figure 8-2) pancreatic cells. Drawing on H&E staining and PDCD4, HIF-1 α and NF κ B expression studies in human adenocarcinoma tissue samples, a suggested role played by PDCD4, HIF-1 α and NF κ B is illustrated in Figure 8-3.

Loss of PDCD4 expression correlating with an increase in severity of disease was observed by IHC in human pancreatic adenocarcinoma tissue samples. The potential for PDCD4 to be used as an additional diagnostic tool to discriminate between normal tissues, benign and malignant pancreatic cancer tissues is demonstrated in Figure 8-4.

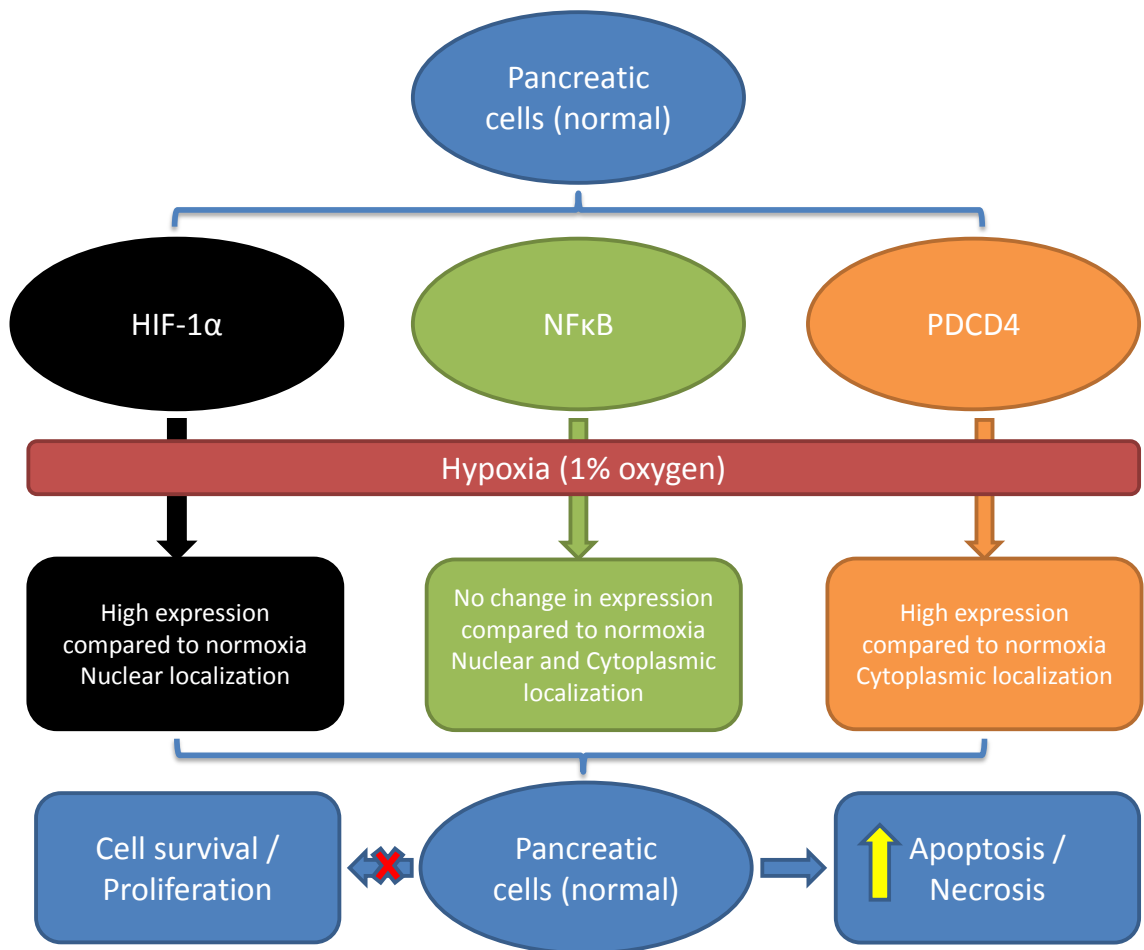


Figure 8-1: Schematic representation of the proposed effect of HIF-1 α , NF κ B and PDCD4 expression on normal pancreatic cell survival under hypoxic conditions. High expression of PDCD4, high expression of HIF-1 α (nuclear localization) and activation of NF κ B (Nuclear and Cytoplasmic localization) may result in low proliferation and the triggering of apoptosis or necrosis in normal pancreatic cells under hypoxic conditions.

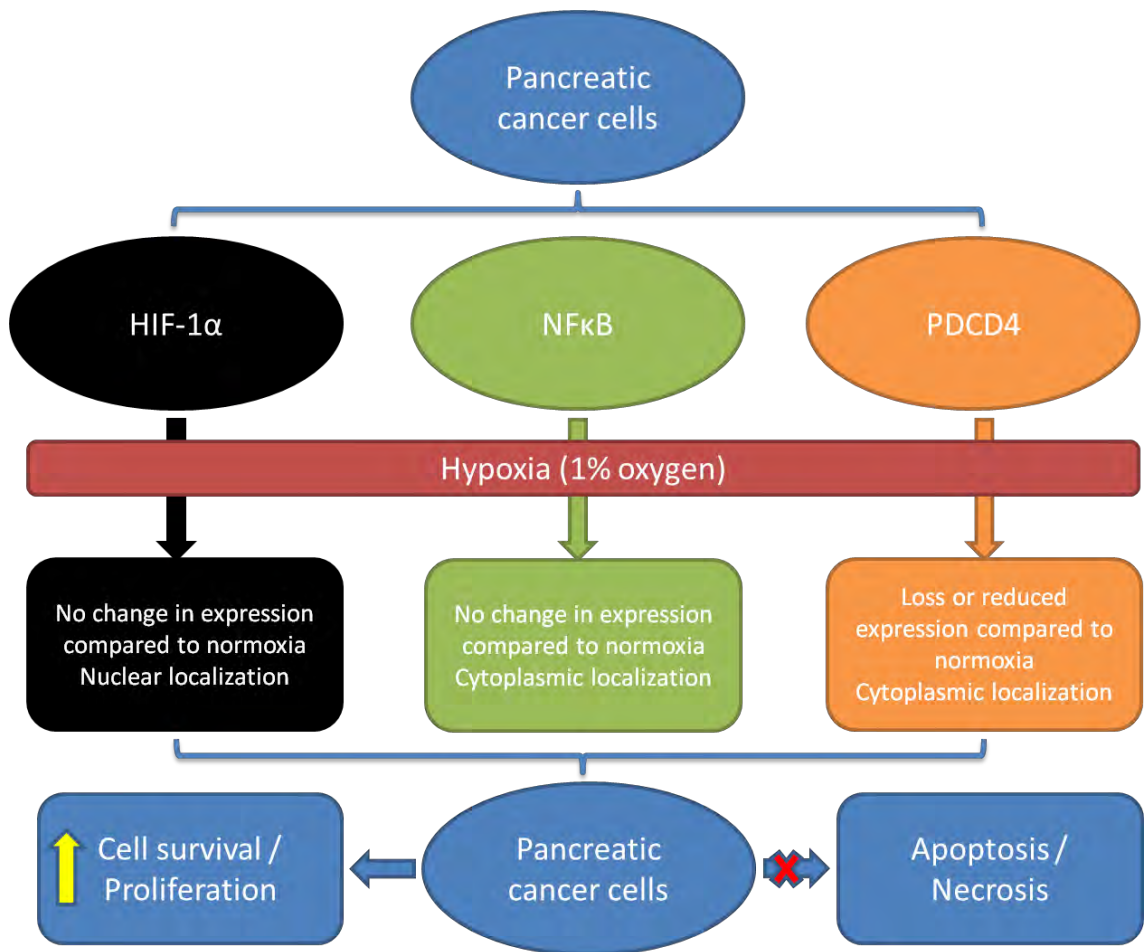


Figure 8-2: Schematic representation of the proposed effect of HIF-1 α , NF κ B and PDCD4 expression on pancreatic cancer cell (PSN-1) survival under hypoxic conditions.

Loss or reduced expression of PDCD4, activation of HIF-1 α (nuclear localisation) and inactive NF κ B (cytoplasmic localisation) may provide human pancreatic adenocarcinoma cells (PSN-1) escape from cell death (apoptosis or necrosis) and continued cells proliferation under hypoxic conditions.

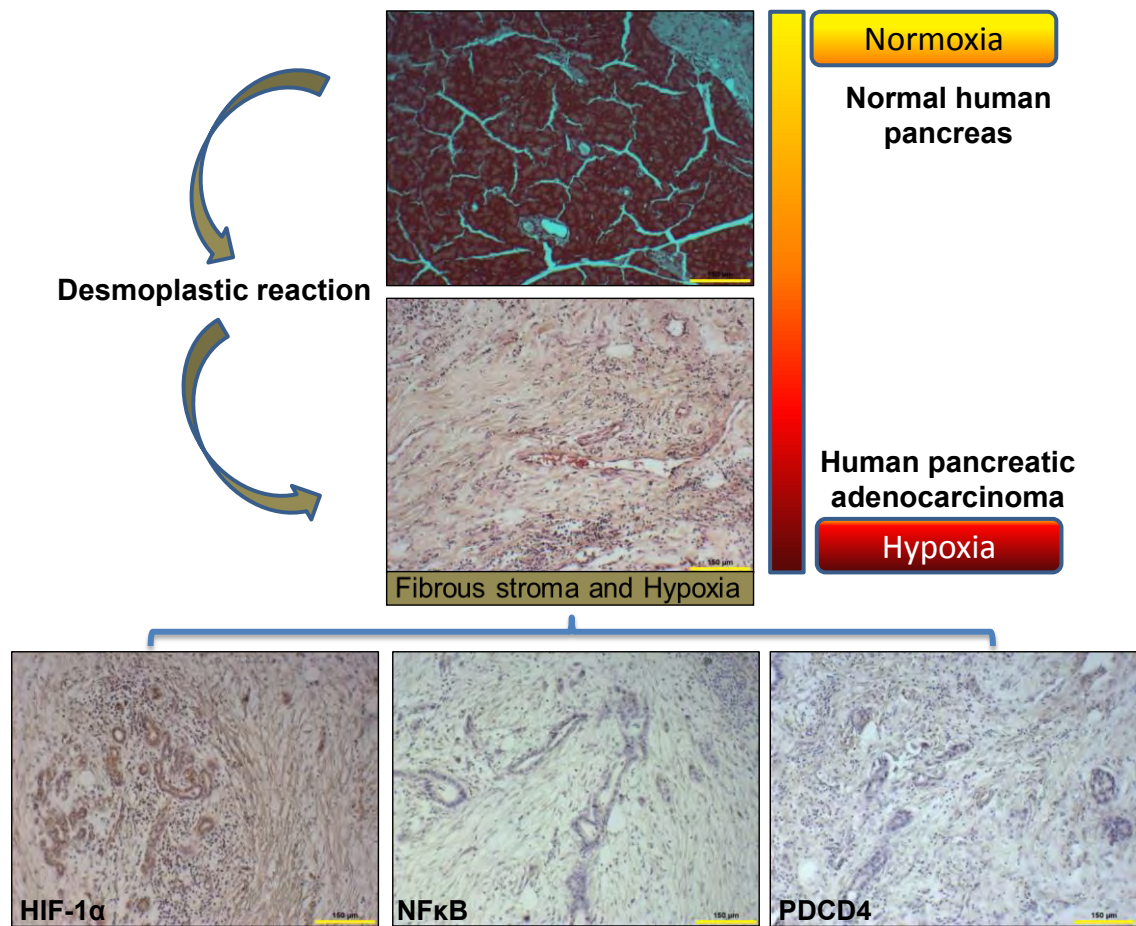


Figure 8-3: Proposed effect of desmoplastic reaction or fibrous stroma and hypoxia in human pancreatic adenocarcinoma tissue.

Extensive desmoplastic reaction in pancreatic cancer results in fibrosis which leads to tumour hypoxia, a major determinant of chemoresistance in pancreatic cancer. Activation or high expression of HIF-1 α , weak cytoplasmic expression of NF κ B and loss or reduced expression of PDCD4 in response to hypoxia in pancreatic cancer cells may play role in cells survival and adaptation.

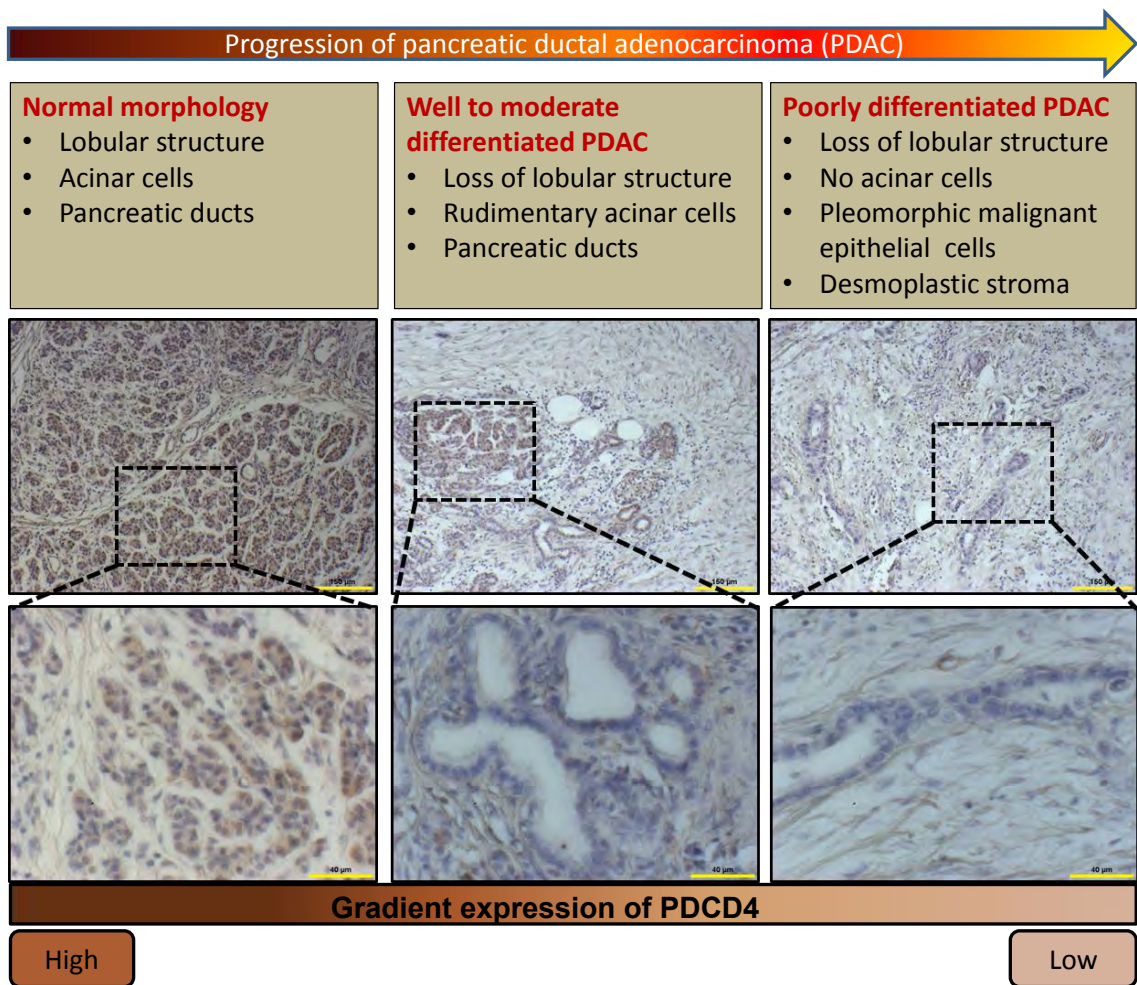


Figure 8-4: Gradient expression of PDCD4 in human pancreatic ductal adenocarcinoma tissue.

Immunohistochemistry analysis of PDCD4 in human pancreatic ductal adenocarcinoma tissue samples revealed that expression of PDCD4 was reduced with progression of malignancy and has an inverse correlation with the advanced stage of malignancy. PDCD4 can be used as an additional diagnostic tool to discriminate between normal tissues, benign and malignant pancreatic cancer tissues.

Chapter 9. Conclusions and Future Work

9.1. Aims, main findings and conclusion

➤ Effect of hypoxia on cell viability of PSN-1, ARIP and MIN6 cells.

- a) PSN-1 cells were well adapted to hypoxic conditions and hypoxia did not have an effect on the viability and growth of cells compared to normoxic conditions.
- b) Hypoxia did not trigger apoptosis or necrosis within 12 hours of exposure, however, 24 hours exposure did trigger apoptosis in ARIP cells.
- c) Hypoxia had a detrimental effect on MIN6 cell viability and induced both apoptosis and necrosis.

Conclusion: Pancreatic cancer cells are well adapted and survive under hypoxic conditions, whereas normal pancreatic ductal and beta-cells are reliant on sufficient oxygen for cell survival and function.

➤ Effect of hypoxia on morphology of PSN-1, ARIP and MIN6 cells.

- a) PSN-1 cells have characteristics of cancer cells and hypoxia did not have any effect on the morphology of PSN-1 cells.
- b) ARIP cells have characteristics of normal cells. Hypoxia induced morphological changes in ARIP cells towards a PSN-1 cell phenotype.
- c) MIN6 cells have characteristics of normal beta-cells. Hypoxia triggered morphological changes in MIN6 cells such as membrane blebbing (apoptosis) and pores (characteristic of necrosis).

Conclusion: Morphology characterisation confirmed that PSN-1, ARIP and MIN6 cells are truly representative of pancreatic cancer, pancreatic ductal cells and pancreatic beta-cells respectively. Hypoxia does not have any effect on the change in morphology of

pancreatic cancer cells, but does trigger a change in morphology of ARIP and MIN6 cells.

➤ **Investigate histology and histopathology of pancreatic tissue samples (Normal mouse pancreas and four samples of human pancreatic adenocarcinoma tissue).**

- a) The mouse pancreas was divided into lobules and has morphologically distinct endocrine (comprises islet of Langerhans) and exocrine (comprises acinar and ductal cells) pancreas. The mouse pancreas shared mostly similar morphological features on comparing with already published data on normal human pancreas.
- b) Histopathology of human pancreatic adenocarcinoma tissue samples
 - ◆ Case study 1: Well to moderately differentiated adenocarcinoma but some parts poorly differentiated.
 - ◆ Case study 2: Well to moderately differentiated adenocarcinoma but some parts poorly differentiated.
 - ◆ Case study 3: Moderate to poorly differentiated adenocarcinoma
 - ◆ Case study 4: Well differentiated adenocarcinoma

Conclusion: Human pancreatic adenocarcinoma samples show huge variability in the severity of disease within the same tissue sample from normal morphology features to total loss of tissue integrity. Tissue samples were highly infiltrated with desmoplastic fibrous connective tissue and pleomorphic malignant epithelial cells.

➤ **Investigate the expression, subcellular localisation and regulation of PDCD4 in human adenocarcinoma of pancreatic cancer cells line (PSN-1), mouse beta-cell (MIN6) and rat pancreas ductal cell line (ARIP) under normoxic (21% oxygen) and hypoxic (1% oxygen) conditions.**

- a) Significantly low expression of PDCD4 under hypoxic conditions compared to normoxic conditions in PSN-1 cells. PDCD4 localised to the cytoplasm of PSN-1 cells in normoxia with no observed changes under hypoxic conditions.
- b) Significantly high expression of PDCD4 under hypoxic conditions compared to normoxic conditions in ARIP cells. PDCD4 localised to the cytoplasm of ARIP cells in normoxia with no observed changed under hypoxic conditions.
- c) Significantly high expression of PDCD4 under hypoxic conditions compared to normoxic conditions in MIN6 cells. PDCD4 localised to the cytoplasm of MIN6 cells in normoxia with no observed changed under hypoxic conditions.

Conclusion: Loss or reduced expression of PDCD4 in pancreatic adenocarcinoma cells may correlate with cancer cell survival under hypoxic conditions. Induced or high expression of PDCD4 under the influence of hypoxia in pancreatic ductal and beta-cells may have role in apoptosis or necrosis induction in normal cells.

➤ **Investigate the expression, subcellular localisation and regulation of HIF-1 α in human adenocarcinoma of pancreatic cancer cells line (PSN-1) and rat pancreas ductal cell line (ARIP) under normoxic (21% oxygen) and hypoxic (1% oxygen) conditions.**

- a) HIF-1 α was exclusively localised to the nucleus and hypoxia did not trigger the expression of HIF-1 α in PSN-1 cells. HIF-1 α was highly expressed in PSN-1 cells under hypoxic and normoxic conditions.
- b) HIF-1 α was exclusively localised to the nucleus and significantly high expression of HIF-1 α was observed in ARIP cells under hypoxic conditions compared to normoxia.

Conclusion: HIF-1 α was expressed under normoxic conditions in both ARIP and PSN-1 cells. Induced or high expression of HIF-1 α together with PDCD4 under the influence of hypoxia may have a role in apoptosis induction in pancreatic ductal cells. Significantly higher expression of HIF-1 α together with reduced or loss of expression of PDCD4 may help pancreatic cancer cells to survive and proliferate under hypoxic conditions.

➤ **Investigate the expression, subcellular localisation and regulation of NF κ B in human adenocarcinoma pancreatic cancer cells line (PSN-1) and rat pancreas ductal cell line (ARIP) under normoxic (21% oxygen) and hypoxic (1% oxygen) conditions.**

a) NF κ B was highly expressed in the cytoplasm of PSN-1 cells under hypoxic and normoxic conditions. Hypoxia triggers the nuclear translocation of NF κ B in PSN-1 cells.

b) NF κ B was highly expressed in the nucleus and the cytoplasm of ARIP cells under hypoxic and normoxic conditions. Hypoxia triggers nuclear translocation of NF κ B, which was highly expressed and localised around the nuclear membrane and inside the nucleus of ARIP cells in hypoxia.

Conclusion: Hypoxia activates and translocates NF κ B to the nucleus in normal pancreatic ductal cells and plays a role as an apoptosis inducer in normal pancreatic cells. In pancreatic cancer cells, NF κ B was highly expressed in the cytoplasm under hypoxic and normoxic conditions. Hypoxia does trigger nuclear localisation or activation of NF κ B, but this was not enough to induce apoptosis in pancreatic cancer cells.

➤ **Investigate subcellular localisation and expression of PDCD4 in primary human pancreatic adenocarcinoma tissue and normal mouse pancreatic tissue sections.**

- a) PDCD4 is expressed in normal pancreatic cells, expression differs by cell-type; acinar cells have weak cytoplasmic expression and ductal and islet cells show both nuclear and cytoplasmic expression.
- b) Differential expression of PDCD4 was observed in all human pancreatic adenocarcinoma tissue samples (1 to 4 case studies). Expression of PDCD4 was reduced with progression of malignancy and had an inverse correlation with the advanced stage of malignancy (from well to poorly differentiated). Highly malignant pancreatic tissue showed cytoplasmic expression or localisation of PDCD4.

Conclusion: Loss or reduced expression of PDCD4 with progression of malignancy and high expression in sample 4 with pronounced autolysis further confirmed the importance of PDCD4 expression as indicated in pancreatic cell line studies. Also PDCD4 can be used as an additional diagnostic tool to discriminate between normal tissues, benign and malignant pancreatic cancer tissues.

➤ **Investigate subcellular localisation and expression of HIF-1 α in primary human pancreatic adenocarcinoma tissue and normal mouse pancreatic tissue sections.**

- a) HIF-1 α was expressed in normal pancreatic tissue samples, however, differential expression was observed; ductal and islet cells showed positive expression whereas acinar cells showed weak cytoplasmic expression of HIF-1 α .
- b) HIF-1 α was highly expressed in pancreatic adenocarcinoma tissue samples (1, 2 and 4) and mostly localised inside the nucleus of cells.

Conclusion: Desmoplastic fibrous connective tissue may result in tumour hypoxia, which might be a reason for high expression of HIF-1 α , ultimately resulting in pancreatic cancer cell survival and adaptation.

➤ **Investigate subcellular localisation and expression of NFκB in primary human pancreatic adenocarcinoma tissue and normal mouse pancreatic tissue sections.**

- a) NFκB was positively expressed in the cytoplasm and nuclei of normal pancreatic tissue samples.
- b) Cytoplasmic expression of NFκB was identified in 2 human case pancreatic cancer studies and in the other 2 case studies positive nuclear and cytoplasmic staining was identified. Thus cytoplasmic expression of NFκB was observed in 100% and nuclear expression in 50% of the four case studies.

Conclusion: Cytoplasmic expression of NFκB might be a better indirect marker to estimate nuclear expression of NFκB, which in itself is difficult to study from primary human pancreatic adenocarcinoma tissue.

9.2. Future work

Cell viability investigations revealed that pancreatic cancer (PSN-1) cells were well adapted to hypoxic conditions, whereas reduced viability was observed in normal pancreatic (ARIP and MIN6) cells in response to hypoxia. Morphological examination of pancreatic cancer (PSN-1) cells revealed the presence of filopodia and lamellipodia on the surface of cells, which play important roles in cell to cell contact, adhesion, migration and angiogenesis [332]. Increased filopodia formation has been associated with cancer cell migration [333] and invasion [334] and plays an important role in the process of EMT (Epithelial-mesenchymal transition) [335]. ARIP cell morphology analysis revealed filopodia formation under hypoxia, which might be an adaptation or resistance response to the hypoxia. Although most of the ARIP cells under hypoxic conditions undergo apoptosis, some are adapted to survive, potentially via filopodia formation. This situation could lead to clonal expansion of mutated cells and could

progress to pancreatic ductal adenocarcinoma. It would be interesting to analyse filopodia formation by analysing expression and regulation of Fascin, a filopodia actin bundling protein. Recently, it has been reported that in pancreatic ductal adenocarcinoma, the hypoxic microenvironment up-regulates fascin expression [425]. Our data suggested that hypoxia triggered filopodia formation in normal pancreatic ductal cells, which has never been reported before and needs more investigation. Initiation of filopodia formation could be targeted for anticancer therapy to stop invasion and migration of PDAC and is therefore a valuable area to study.

1. Analyse expression and regulation of filopodia actin bundling protein Fascin in normal pancreatic ductal cells and pancreatic ductal adenocarcinoma cells under the influence of hypoxia.

Induced expression of PDCD4 in normal pancreatic (ARIP and MIN6) cells and loss or reduced expression of PDCD4 in pancreatic ductal adenocarcinoma cells under hypoxic conditions suggest the great importance of PDCD4 expression in deciding pancreatic cell fate. Our data suggest PDCD4 as a promising target for pancreatic cancer. Further work needs to be done to investigate if restoration of normal PDCD4 expression levels in pancreatic cancer cells under hypoxia induces cell death or senescence. Understanding how PDCD4 expression can be manipulated in pancreatic cancer as well as normal cells, may well arm us with a new weapon in our fight for more effective therapeutic interventions in the treatment and prevention of this disease.

2. Analyse the effect of knock-down and over-expression of PDCD4 on proliferation of pancreatic cells (cancerous and normal) under the influence of hypoxia.

Immunohistochemistry and western blotting analysis revealed the comparative PDCD4, HIF-1 α and NF κ B protein expression in pancreatic cancer as well as normal cells. Future work should confirm whether PDCD4, HIF-1 α and NF κ B protein expression

correlate with a specific down-regulation or up-regulation of *PDCD4*, *HIF-1 α* and *NF κ B* gene expression.

3. **Analyse comparative *PDCD4*, *HIF-1 α* and *NF κ B* mRNA levels by *in situ* hybridization and qRT-PCR, in pancreatic cancer as well as normal cells and tissue.**
4. **Analyse expression of proliferative marker Ki67 to determine whether loss or high expression of *PDCD4* correlates with changes in proliferation status of pancreatic cells.**

Immunohistochemistry data from four human pancreatic ductal adenocarcinoma tissues revealed loss or reduced expression of *PDCD4* with progression of malignancy, high expression of *HIF-1 α* and weak cytoplasmic/nuclear expression of *NF κ B*. Although these results are quite promising, an unavoidable limitation of our present study is the relatively small number of human pancreatic adenocarcinoma case studies available. Therefore, these results need to be confirmed in a larger study of human pancreatic adenocarcinoma tissue to draw any firm conclusions. Gene expression could be studied on fresh or frozen pancreatic adenocarcinoma tissue samples by qRT-PCR and *in situ* hybridization.

5. **Analyse gene expression and protein expression of *PDCD4*, *HIF-1 α* and *NF κ B* by immunohistochemistry, *in situ* hybridization and RT-PCR.**

Together, these analyses will provide important new information on the role of *PDCD4* in the development and progression of pancreatic cancer. Could restoration of normal *PDCD4* expression levels in pancreatic cancer cells restore normal control of proliferation? Although our present data revealed *PDCD4* as a novel molecular target in pancreatic cancer these additional analyses may well arm us with a new weapon in our fight for more effective therapeutic interventions in the treatment and prevention of this disease.

References

1. Bardeesy, N. and R.A. DePinho, *Pancreatic cancer biology and genetics*. Nat Rev Cancer, 2002. **2**(12): p. 897-909.
2. F. Charles Brunicaardi, D.K.A., Timothy R. Billiar, David L. Dunn, John G. Hunter, Jeffrey B. Matthews, Raphael E. Pollock, *Schwartz's Principles of Surgery: Chapter 33- Pancreas* 9ed. Pancreas, ed. F.C. Brunicaardi. 2010, United States of America: The McGraw-Hill Companies, Inc.
3. Fisher, W.E., et al., eds. *Schwartz's Principles of Surgery, Ninth Edition*. 9th ed. 2009, Mc Graw Hill.
4. Kim, S.K. and R.J. MacDonald, *Signaling and transcriptional control of pancreatic organogenesis*. Curr Opin Genet Dev, 2002. **12**(5): p. 540-7.
5. Schwitzgebel, V.M., *Programming of the pancreas*. Mol Cell Endocrinol, 2001. **185**(1-2): p. 99-108.
6. Wierup, N., et al., *The ghrelin cell: a novel developmentally regulated islet cell in the human pancreas*. Regul Pept, 2002. **107**(1-3): p. 63-9.
7. Rorsman, P. and E. Renstrom, *Insulin granule dynamics in pancreatic beta cells*. Diabetologia, 2003. **46**(8): p. 1029-45.
8. Dunning, B.E., J.E. Foley, and B. Ahren, *Alpha cell function in health and disease: influence of glucagon-like peptide-1*. Diabetologia, 2005. **48**(9): p. 1700-13.
9. Portela-Gomes, G.M., et al., *Expression of the five different somatostatin receptor subtypes in endocrine cells of the pancreas*. Appl Immunohistochem Mol Morphol, 2000. **8**(2): p. 126-32.
10. Adrian, T.E., *Pancreatic polypeptide*. J Clin Pathol Suppl (Assoc Clin Pathol), 1978. **8**: p. 43-50.
11. Park, H.J., Y.L. Lee, and H.Y. Kwon, *Effects of pancreatic polypeptide on insulin action in exocrine secretion of isolated rat pancreas*. J Physiol, 1993. **463**: p. 421-9.
12. Westermark, P., A. Andersson, and G.T. Westermark, *Islet amyloid polypeptide, islet amyloid, and diabetes mellitus*. Physiol Rev, 2011. **91**(3): p. 795-826.
13. Ahren, B., et al., *Pancreastatin inhibits insulin secretion and stimulates glucagon secretion in mice*. Diabetes, 1988. **37**(3): p. 281-5.
14. Egido, E.M., et al., *Inhibitory effect of ghrelin on insulin and pancreatic somatostatin secretion*. Eur J Endocrinol, 2002. **146**(2): p. 241-4.
15. Slack, J.M., *Developmental biology of the pancreas*. Development, 1995. **121**(6): p. 1569-80.
16. Kim, S.K. and M. Hebrok, *Intercellular signals regulating pancreas development and function*. Genes Dev, 2001. **15**(2): p. 111-27.
17. Edlund, H., *Pancreatic organogenesis--developmental mechanisms and implications for therapy*. Nat Rev Genet, 2002. **3**(7): p. 524-32.

18. Pawlina, M.H.R.a.W., *Histology: A text and Atlas: with correlated cell and molecular biology.* , ed. S. Edition. 2011, Philadelphia: Wolters Kluwer, Lippincott Williams & Wilkins.
19. Pandol, S.J., in *The Exocrine Pancreas*. 2010: San Rafael (CA).
20. Havel, P.J. and G.J. Taborsky, Jr., *The contribution of the autonomic nervous system to changes of glucagon and insulin secretion during hypoglycemic stress.* *Endocr Rev*, 1989. **10**(3): p. 332-50.
21. Parsons, D.W., et al., *An integrated genomic analysis of human glioblastoma multiforme.* *Science*, 2008. **321**(5897): p. 1807-12.
22. Duffy, J.P., et al., *Influence of hypoxia and neoangiogenesis on the growth of pancreatic cancer.* *Mol Cancer*, 2003. **2**: p. 12.
23. Real, F.X., *A "catastrophic hypothesis" for pancreas cancer progression.* *Gastroenterology*, 2003. **124**(7): p. 1958-64.
24. Harnack, L.J., et al., *Smoking, alcohol, coffee, and tea intake and incidence of cancer of the exocrine pancreas: the Iowa Women's Health Study.* *Cancer Epidemiol Biomarkers Prev*, 1997. **6**(12): p. 1081-6.
25. Dusek, L., et al., *Cancer incidence and mortality in the Czech Republic.* *Klin Onkol*, 2010. **23**(5): p. 311-24.
26. Tilyou, S.M., *BEIR V report. Experts urge cautious interpretation of higher risk estimates.* *J Nucl Med*, 1990. **31**(4): p. 13A-19A.
27. Larsson, S.C. and A. Wolk, *Red and processed meat consumption and risk of pancreatic cancer: meta-analysis of prospective studies.* *Br J Cancer*, 2012. **106**(3): p. 603-7.
28. Li, D., et al., *Body mass index and risk, age of onset, and survival in patients with pancreatic cancer.* *JAMA*, 2009. **301**(24): p. 2553-62.
29. Pickartz, T., et al., *[Chronic pancreatitis as a risk factor for the development of pancreatic cancer--diagnostic challenges].* *Med Klin (Munich)*, 2010. **105**(4): p. 281-5.
30. Grote, V.A., et al., *Diabetes mellitus, glycated haemoglobin and C-peptide levels in relation to pancreatic cancer risk: a study within the European Prospective Investigation into Cancer and Nutrition (EPIC) cohort.* *Diabetologia*, 2011. **54**(12): p. 3037-46.
31. Elena, J.W., et al., *Diabetes and risk of pancreatic cancer: a pooled analysis from the pancreatic cancer cohort consortium.* *Cancer Causes Control*, 2013. **24**(1): p. 13-25.
32. Li, D., et al., *Diabetes and risk of pancreatic cancer: a pooled analysis of three large case-control studies.* *Cancer Causes Control*, 2011. **22**(2): p. 189-97.
33. Pezzilli, R., et al., *Obesity and the risk of pancreatic cancer: an italian multicenter study.* *Pancreas*, 2005. **31**(3): p. 221-4.
34. Chu, D., W. Kohlmann, and D.G. Adler, *Identification and screening of individuals at increased risk for pancreatic cancer with emphasis on known environmental and genetic factors and hereditary syndromes.* *JOP*, 2010. **11**(3): p. 203-12.
35. Males, S., *Pancreatic cancer.* cancer, 2014.

36. Society, A.C., *Cancer Facts & Figures 2013*. 2013.
37. McSweeney, S.E., P.M. O'Donoghue, and K. Jhaveri, *Current and emerging techniques in gastrointestinal imaging*. J Postgrad Med, 2010. **56**(2): p. 109-16.
38. Galasso, D., A. Carnuccio, and A. Larghi, *Pancreatic cancer: diagnosis and endoscopic staging*. Eur Rev Med Pharmacol Sci, 2010. **14**(4): p. 375-85.
39. Jiang, J.T., et al., *Serum level of TSGF, CA242 and CA19-9 in pancreatic cancer*. World J Gastroenterol, 2004. **10**(11): p. 1675-7.
40. Koopmann, J., et al., *Evaluation of osteopontin as biomarker for pancreatic adenocarcinoma*. Cancer Epidemiol Biomarkers Prev, 2004. **13**(3): p. 487-91.
41. Yiannakou, J.Y., et al., *Prospective study of CAM 17.1/WGA mucin assay for serological diagnosis of pancreatic cancer*. Lancet, 1997. **349**(9049): p. 389-92.
42. Takayama, R., et al., *Serum tumor antigen REG4 as a diagnostic biomarker in pancreatic ductal adenocarcinoma*. J Gastroenterol, 2010. **45**(1): p. 52-9.
43. Simeone, D.M., et al., *CEACAM1, a novel serum biomarker for pancreatic cancer*. Pancreas, 2007. **34**(4): p. 436-43.
44. Fong, D., et al., *TROP2: a novel prognostic marker in squamous cell carcinoma of the oral cavity*. Mod Pathol, 2008. **21**(2): p. 186-91.
45. Varga, M., et al., *Overexpression of epithelial cell adhesion molecule antigen in gallbladder carcinoma is an independent marker for poor survival*. Clin Cancer Res, 2004. **10**(9): p. 3131-6.
46. Bausch, D., et al., *Plectin-1 as a novel biomarker for pancreatic cancer*. Clin Cancer Res, 2011. **17**(2): p. 302-9.
47. Jemal, A., et al., *Cancer statistics, 2009*. CA Cancer J Clin, 2009. **59**(4): p. 225-49.
48. Bilimoria, K.Y., et al., *National failure to operate on early stage pancreatic cancer*. Ann Surg, 2007. **246**(2): p. 173-80.
49. Shrikhande, S.V., et al., *Pancreatic resection for MI pancreatic ductal adenocarcinoma*. Ann Surg Oncol, 2007. **14**(1): p. 118-27.
50. Loos, M., et al., *Surgical treatment of pancreatic cancer*. Ann N Y Acad Sci, 2008. **1138**: p. 169-80.
51. Kalser, M.H. and S.S. Ellenberg, *Pancreatic cancer. Adjuvant combined radiation and chemotherapy following curative resection*. Arch Surg, 1985. **120**(8): p. 899-903.
52. Burris, H.A., 3rd, et al., *Improvements in survival and clinical benefit with gemcitabine as first-line therapy for patients with advanced pancreas cancer: a randomized trial*. J Clin Oncol, 1997. **15**(6): p. 2403-13.
53. Heinemann, V., et al., *Meta-analysis of randomized trials: evaluation of benefit from gemcitabine-based combination chemotherapy applied in advanced pancreatic cancer*. BMC Cancer, 2008. **8**: p. 82.
54. Gourgou-Bourgade, S., et al., *Impact of FOLFIRINOX compared with gemcitabine on quality of life in patients with metastatic pancreatic cancer: results from the PRODIGE 4/ACCORD 11 randomized trial*. J Clin Oncol, 2013. **31**(1): p. 23-9.

55. Korc, M., et al., *Overexpression of the epidermal growth factor receptor in human pancreatic cancer is associated with concomitant increases in the levels of epidermal growth factor and transforming growth factor alpha*. J Clin Invest, 1992. **90**(4): p. 1352-60.
56. Safran, H., et al., *Overexpression of the HER-2/neu oncogene in pancreatic adenocarcinoma*. Am J Clin Oncol, 2001. **24**(5): p. 496-9.
57. Herreros-Villanueva, M., et al., *Adjuvant and neoadjuvant treatment in pancreatic cancer*. World J Gastroenterol, 2012. **18**(14): p. 1565-72.
58. Moertel, C.G., et al., *Therapy of locally unresectable pancreatic carcinoma: a randomized comparison of high dose (6000 rads) radiation alone, moderate dose radiation (4000 rads + 5-fluorouracil), and high dose radiation + 5-fluorouracil: The Gastrointestinal Tumor Study Group*. Cancer, 1981. **48**(8): p. 1705-10.
59. Maitra, A. and R.H. Hruban, *Pancreatic cancer*. Annu Rev Pathol, 2008. **3**: p. 157-88.
60. Hruban, R.H., et al., *Pancreatic intraepithelial neoplasia: a new nomenclature and classification system for pancreatic duct lesions*. Am J Surg Pathol, 2001. **25**(5): p. 579-86.
61. Hruban, R.H., et al., *An illustrated consensus on the classification of pancreatic intraepithelial neoplasia and intraductal papillary mucinous neoplasms*. Am J Surg Pathol, 2004. **28**(8): p. 977-87.
62. Maitra, A., et al., *Precursors to invasive pancreatic cancer*. Adv Anat Pathol, 2005. **12**(2): p. 81-91.
63. Hruban, R.H., A. Maitra, and M. Goggins, *Update on pancreatic intraepithelial neoplasia*. Int J Clin Exp Pathol, 2008. **1**(4): p. 306-16.
64. Brune, K., et al., *Multifocal neoplastic precursor lesions associated with lobular atrophy of the pancreas in patients having a strong family history of pancreatic cancer*. Am J Surg Pathol, 2006. **30**(9): p. 1067-76.
65. Rosty, C., et al., *p16 inactivation in pancreatic intraepithelial neoplasias (PanINs) arising in patients with chronic pancreatitis*. American Journal of Surgical Pathology, 2003. **27**(12): p. 1495-1501.
66. Moskaluk, C.A., R.H. Hruban, and S.E. Kern, *p16 and K-ras gene mutations in the intraductal precursors of human pancreatic adenocarcinoma*. Cancer Research, 1997. **57**(11): p. 2140-2143.
67. Brat, D.J., et al., *Progression of pancreatic intraductal neoplasias to infiltrating adenocarcinoma of the pancreas*. American Journal of Surgical Pathology, 1998. **22**(2): p. 163-169.
68. Wilentz, R.E., et al., *Loss of expression of Dpc4 in pancreatic intraepithelial neoplasia: Evidence that DPC4 inactivation occurs late in neoplastic progression*. Cancer Research, 2000. **60**(7): p. 2002-2006.
69. Cowgill, S.M. and P. Muscarella, *The genetics of pancreatic cancer*. Am J Surg, 2003. **186**(3): p. 279-86.
70. Li, D. and L. Jiao, *Molecular epidemiology of pancreatic cancer*. Int J Gastrointest Cancer, 2003. **33**(1): p. 3-14.

71. Lichtenstein, D.R. and D.L. Carr-Locke, *Mucin-secreting tumors of the pancreas*. *Gastrointest Endosc Clin N Am*, 1995. **5**(1): p. 237-58.
72. Mullan, M.H., P.G. Gauger, and N.W. Thompson, *Endocrine tumours of the pancreas: review and recent advances*. *ANZ J Surg*, 2001. **71**(8): p. 475-82.
73. Erkan, M., et al., *The role of stroma in pancreatic cancer: diagnostic and therapeutic implications*. *Nat Rev Gastroenterol Hepatol*, 2012. **9**(8): p. 454-67.
74. Olive, K.P., et al., *Inhibition of Hedgehog signaling enhances delivery of chemotherapy in a mouse model of pancreatic cancer*. *Science*, 2009. **324**(5933): p. 1457-61.
75. Duner, S., et al., *Pancreatic cancer: the role of pancreatic stellate cells in tumor progression*. *Pancreatology*, 2010. **10**(6): p. 673-81.
76. Krautz, C., et al., *An update on molecular research of pancreatic adenocarcinoma*. *Anticancer Agents Med Chem*, 2011. **11**(5): p. 411-7.
77. Klöppel, G., *Histological Typing of Tumours of the Exocrine Pancreas*. 1996: Springer Berlin Heidelberg.
78. Hyland, C., S.M. Kheir, and M.B. Kashlan, *Frozen Section Diagnosis of Pancreatic-Carcinoma - a Prospective-Study of 64 Biopsies*. *American Journal of Surgical Pathology*, 1981. **5**(2): p. 179-191.
79. Cioc, A.M., et al., *Frozen section diagnosis of pancreatic lesions*. *Archives of Pathology & Laboratory Medicine*, 2002. **126**(10): p. 1169-1173.
80. Klöppel, G., Hruban, R.H., Longnecker, D.S., G. Adler, S.E. Kern and T.J. Partanen, *Tumours of the Exocrine Pancreas*. *Pathology and Genetics of Tumours of the Digestive System*, ed. P.K.a.L.H. Sobin. 2000, Lyon, France: International Agency for Research on Cancer (IARC). 220-251.
81. Yen, T.W., et al., *Myofibroblasts are responsible for the desmoplastic reaction surrounding human pancreatic carcinomas*. *Surgery*, 2002. **131**(2): p. 129-34.
82. Hidalgo, M., *Pancreatic Cancer*. *New England Journal of Medicine*, 2010. **362**(17): p. 1605-1617.
83. Moore, P.S., et al., *Pancreatic tumours: molecular pathways implicated in ductal cancer are involved in ampullary but not in exocrine nonductal or endocrine tumorigenesis*. *Br J Cancer*, 2001. **84**(2): p. 253-62.
84. Rozenblum, E., et al., *Tumor-suppressive pathways in pancreatic carcinoma*. *Cancer Res*, 1997. **57**(9): p. 1731-4.
85. Levine, A.J. and M. Oren, *The first 30 years of p53: growing ever more complex*. *Nat Rev Cancer*, 2009. **9**(10): p. 749-58.
86. Redston MS, C.C., Seymour AB et al., *p53 mutations in pancreatic carcinoma and evidence of common involvement of homocopolymer tracts in DNA microdeletions*. *Cancer Res*, 1994. **54**(11): p. 3025-3033.
87. Ohtsubo, K., et al., *Abnormalities of tumor suppressor gene p16 in pancreatic carcinoma: immunohistochemical and genetic findings compared with clinicopathological parameters*. *J Gastroenterol*, 2003. **38**(7): p. 663-71.
88. Gerdes, B., et al., *p16INK4a is a prognostic marker in resected ductal pancreatic cancer: an analysis of p16INK4a, p53, MDM2, an Rb*. *Ann Surg*, 2002. **235**(1): p. 51-9.

89. Hu, Y.X., et al., *Frequent loss of p16 expression and its correlation with clinicopathological parameters in pancreatic carcinoma*. Clin Cancer Res, 1997. **3**(9): p. 1473-7.
90. Naka, T., et al., *Aberrant p16INK4 expression related to clinical stage and prognosis in patients with pancreatic cancer*. Int J Oncol, 1998. **12**(5): p. 1111-6.
91. Malumbres, M. and M. Barbacid, *RAS oncogenes: the first 30 years*. Nat Rev Cancer, 2003. **3**(6): p. 459-65.
92. Grunewald, K., et al., *High frequency of Ki-ras codon 12 mutations in pancreatic adenocarcinomas*. Int J Cancer, 1989. **43**(6): p. 1037-41.
93. Smit, V.T.H.B.M., et al., *Kras Codon-12 Mutations Occur Very Frequently in Pancreatic Adenocarcinomas*. Nucleic Acids Research, 1988. **16**(16): p. 7773-7782.
94. Rozenblum, E., et al., *Tumor-suppressive pathways in pancreatic carcinoma*. Cancer Research, 1997. **57**(9): p. 1731-1734.
95. Moskaluk, C.A., R.H. Hruban, and S.E. Kern, *p16 and K-ras gene mutations in the intraductal precursors of human pancreatic adenocarcinoma*. Cancer Res, 1997. **57**(11): p. 2140-3.
96. Venkitaraman, A.R., *Cancer susceptibility and the functions of BRCA1 and BRCA2*. Cell, 2002. **108**(2): p. 171-82.
97. Murphy, K.M., et al., *Evaluation of candidate genes MAP2K4, MADH4, ACVR1B, and BRCA2 in familial pancreatic cancer: deleterious BRCA2 mutations in 17%*. Cancer Res, 2002. **62**(13): p. 3789-93.
98. Jones, S., et al., *Exomic Sequencing Identifies PALB2 as a Pancreatic Cancer Susceptibility Gene*. Science, 2009. **324**(5924): p. 217-217.
99. Tischkowitz, M.D., et al., *Analysis of the Gene Coding for the BRCA2-Interacting Protein PALB2 in Familial and Sporadic Pancreatic Cancer*. Gastroenterology, 2009. **137**(3): p. 1183-1186.
100. Ashkenazi, A. and V.M. Dixit, *Death receptors: signaling and modulation*. Science, 1998. **281**(5381): p. 1305-8.
101. Evan, G. and T. Littlewood, *A matter of life and cell death*. Science, 1998. **281**(5381): p. 1317-22.
102. Green, D.R. and J.C. Reed, *Mitochondria and apoptosis*. Science, 1998. **281**(5381): p. 1309-12.
103. Hetts, S.W., *To die or not to die: an overview of apoptosis and its role in disease*. JAMA, 1998. **279**(4): p. 300-7.
104. Shibahara, K., et al., *Isolation of a novel mouse gene MA-3 that is induced upon programmed cell death*. Gene, 1995. **166**(2): p. 297-301.
105. Matsushashi, S., Yoshinaga, H., Yatsuki, H., Tsugita, A., Hori, K., *Isolation of a novel gene from a human cell line with Pr-28 mAb which recognizes a nuclear antigen involved in the cell cycle*. Res. Commun. Biochem. Cell Mol. Biol., 1997. **1**: p. 109-120.
106. Azzoni, L., et al., *Differential transcriptional regulation of CD161 and a novel gene, 197/15a, by IL-2, IL-15, and IL-12 in NK and T cells*. J Immunol, 1998. **161**(7): p. 3493-500.

107. Goke, A., et al., *DUG is a novel homologue of translation initiation factor 4G that binds eIF4A*. Biochemical and Biophysical Research Communications, 2002. **297**(1): p. 78-82.
108. Wagner, C., et al., *Apoptosis in marine sponges: a biomarker for environmental stress (cadmium and bacteria)*. Marine Biology, 1998. **131**(3): p. 411-421.
109. Kang, M.J., et al., *Up-regulation of PDCD4 in senescent human diploid fibroblasts*. Biochemical and Biophysical Research Communications, 2002. **293**(1): p. 617-621.
110. Soejima, H., et al., *Assignment of the programmed cell death 4 gene (PDCD4) to human chromosome band 10q24 by in situ hybridization*. Cytogenet Cell Genet, 1999. **87**(1-2): p. 113-4.
111. Lankat-Buttgereit, B. and R. Goke, *The tumour suppressor Pdc4: recent advances in the elucidation of function and regulation*. Biol Cell, 2009. **101**(6): p. 309-17.
112. Ponting, C.P., *Novel eIF4G domain homologues linking mRNA translation with nonsense-mediated mRNA decay*. Trends Biochem Sci, 2000. **25**(9): p. 423-6.
113. Yang, H.S., et al., *The transformation suppressor Pdc4 is a novel eukaryotic translation initiation factor 4A binding protein that inhibits translation*. Molecular and Cellular Biology, 2003. **23**(1): p. 26-37.
114. Suzuki, C., et al., *PDCD4 inhibits translation initiation by binding to eIF4A using both its MA3 domains*. Proceedings of the National Academy of Sciences of the United States of America, 2008. **105**(9): p. 3274-3279.
115. Bohm, M., et al., *The transformation suppressor protein Pdc4 shuttles between nucleus and cytoplasm and binds RNA*. Oncogene, 2003. **22**(31): p. 4905-4910.
116. Palamarchuk, A., et al., *Akt phosphorylates and regulates Pdc4 tumor suppressor protein*. Cancer Res, 2005. **65**(24): p. 11282-6.
117. Waters, L.C., et al., *Structure of the tandem MA-3 region of Pdc4 protein and characterization of its interactions with eIF4A and eIF4G: molecular mechanisms of a tumor suppressor*. J Biol Chem, 2011. **286**(19): p. 17270-80.
118. Morino, S., et al., *Eukaryotic translation initiation factor 4E (eIF4E) binding site and the middle one-third of eIF4GI constitute the core domain for cap-dependent translation, and the C-terminal one-third functions as a modulatory region*. Molecular and Cellular Biology, 2000. **20**(2): p. 468-477.
119. Matsubishi, S., T. Watanabe, and K. Hori, *An Antigen Expressed in Proliferating Cells at Late G1-S Phase*. Experimental Cell Research, 1987. **170**(2): p. 351-362.
120. Yoshinaga H, M.S., Ahaneku J, Masaki Z and Hori K. , *Expression and identification of H731 gene product in HeLa cells*. Res. Commun. Biochem. Cell Mol. Biol. **1**, 121–131. Res. Commun. Biochem. Cell Mol. Biol. , 1997. **1**: p. 121–131.
121. K., M.S.H., *Pr-28 antigen is localized in proliferating cell nuclei but absent from S phase nuclei*. Res. Commun. Biochem. Cell. Mol. Biol., 1998. **2**: p. 19-26.
122. Schlichter, U., et al., *The chicken Pdc4 gene is regulated by v-Myb*. Oncogene, 2001. **20**(2): p. 231-239.

123. Matsushashi, S., et al., *Expression patterns of programmed cell death 4 protein in normal human skin and some representative skin lesions*. *Experimental Dermatology*, 2007. **16**(3): p. 179-184.
124. Mudduluru, G., et al., *Loss of programmed cell death 4 expression marks adenoma-carcinoma transition, correlates inversely with phosphorylated protein kinase B, and is an independent prognostic factor in resected colorectal cancer*. *Cancer*, 2007. **110**(8): p. 1697-1707.
125. Wen, Y.H., et al., *Alterations in the expression of PDCD4 in ductal carcinoma of the breast*. *Oncology Reports*, 2007. **18**(6): p. 1387-1393.
126. Lankat-Buttgereit, B., et al., *The action of Pcd4 may be cell type specific: evidence that reduction of dUTPase levels might contribute to its tumor suppressor activity in Bon-1 cells*. *Apoptosis*, 2008. **13**(1): p. 157-164.
127. Dorrello, N.V., et al., *S6K1- and betaTRCP-mediated degradation of PDCD4 promotes protein translation and cell growth*. *Science*, 2006. **314**(5798): p. 467-71.
128. Onishi, Y., S. Hashimoto, and H. Kizaki, *Cloning of the TIS gene suppressed by topoisomerase inhibitors*. *Gene*, 1998. **215**(2): p. 453-9.
129. Onishi, Y. and H. Kizaki, *Molecular cloning of the genes suppressed in RVC lymphoma cells by topoisomerase inhibitors*. *Biochemical and Biophysical Research Communications*, 1996. **228**(1): p. 7-13.
130. Vikhrev, P.N. and I.V. Korobko, *Expression of Pcd4 tumor suppressor in human melanoma cells*. *Anticancer Res*, 2014. **34**(5): p. 2315-8.
131. Wei, Z.T., et al., *PDCD4 inhibits the malignant phenotype of ovarian cancer cells*. *Cancer Sci*, 2009. **100**(8): p. 1408-13.
132. Afonja, O., et al., *Induction of PDCD4 tumor suppressor gene expression by RAR agonists, antiestrogen and HER-2/neu antagonist in breast cancer cells. Evidence for a role in apoptosis*. *Oncogene*, 2004. **23**(49): p. 8135-45.
133. Zhang, H., et al., *Involvement of programmed cell death 4 in transforming growth factor-beta1-induced apoptosis in human hepatocellular carcinoma*. *Oncogene*, 2006. **25**(45): p. 6101-12.
134. Yang, H.S., et al., *Tumorigenesis suppressor Pcd4 down-regulates mitogen-activated protein kinase kinase kinase 1 expression to suppress colon carcinoma cell invasion*. *Mol Cell Biol*, 2006. **26**(4): p. 1297-306.
135. Chen, Y., et al., *Loss of PDCD4 expression in human lung cancer correlates with tumour progression and prognosis*. *J Pathol*, 2003. **200**(5): p. 640-6.
136. Carinci, F., et al., *Potential markers of tongue tumor progression selected by cDNA microarray*. *Int J Immunopathol Pharmacol*, 2005. **18**(3): p. 513-24.
137. Wen, Y.H., et al., *Alterations in the expression of PDCD4 in ductal carcinoma of the breast*. *Oncology Reports*, 2007. **18**(6): p. 1387-93.
138. Gao, F., et al., *Frequent loss of PDCD4 expression in human glioma: possible role in the tumorigenesis of glioma*. *Oncology Reports*, 2007. **17**(1): p. 123-8.
139. Fang, W., et al., *Transcriptional patterns, biomarkers and pathways characterizing nasopharyngeal carcinoma of Southern China*. *J Transl Med*, 2008. **6**: p. 32.

140. Guo, P.T., et al., *PDCD4 functions as a suppressor for pT2a and pT2b stage gastric cancer*. *Oncology Reports*, 2013. **29**(3): p. 1007-12.
141. Fassan, M., et al., *PDCD4 nuclear loss inversely correlates with miR-21 levels in colon carcinogenesis*. *Virchows Arch*, 2011. **458**(4): p. 413-9.
142. Wei, N.A., et al., *Loss of Programmed cell death 4 (Pdc4) associates with the progression of ovarian cancer*. *Mol Cancer*, 2009. **8**: p. 70.
143. Zhang, Z. and R.N. DuBois, *Detection of differentially expressed genes in human colon carcinoma cells treated with a selective COX-2 inhibitor*. *Oncogene*, 2001. **20**(33): p. 4450-6.
144. Davis, B.N., et al., *SMAD proteins control DROSHA-mediated microRNA maturation*. *Nature*, 2008. **454**(7200): p. 56-61.
145. Asangani, I.A., et al., *MicroRNA-21 (miR-21) post-transcriptionally downregulates tumor suppressor Pdc4 and stimulates invasion, intravasation and metastasis in colorectal cancer*. *Oncogene*, 2008. **27**(15): p. 2128-2136.
146. Frankel, L.B., et al., *Programmed cell death 4 (PDCD4) is an important functional target of the microRNA miR-21 in breast cancer cells*. *Journal of Biological Chemistry*, 2008. **283**(2): p. 1026-1033.
147. Lu, Z., et al., *MicroRNA-21 promotes cell transformation by targeting the programmed cell death 4 gene*. *Oncogene*, 2008. **27**(31): p. 4373-9.
148. Zhu, S., et al., *MicroRNA-21 targets tumor suppressor genes in invasion and metastasis*. *Cell Res*, 2008. **18**(3): p. 350-9.
149. Li, L., et al., *MicroRNA-21 stimulates gastric cancer growth and invasion by inhibiting the tumor suppressor effects of programmed cell death protein 4 and phosphatase and tensin homolog*. *J BUON*, 2014. **19**(1): p. 228-36.
150. Ren, W., et al., *miR-21 modulates chemosensitivity of tongue squamous cell carcinoma cells to cisplatin by targeting PDCD4*. *Mol Cell Biochem*, 2014. **390**(1-2): p. 253-62.
151. Chan, J.K., et al., *The inhibition of miR-21 promotes apoptosis and chemosensitivity in ovarian cancer*. *Gynecol Oncol*, 2014. **132**(3): p. 739-44.
152. Wang, Y.Q., et al., *MicroRNA-182 promotes cell growth, invasion and chemoresistance by targeting programmed cell death 4 (PDCD4) in human ovarian carcinomas*. *J Cell Biochem*, 2013.
153. Zhang, D., et al., *Hypoxia-induced miR-424 decreases tumor sensitivity to chemotherapy by inhibiting apoptosis*. *Cell Death Dis*, 2014. **5**: p. e1301.
154. Schmid, T., et al., *Translation inhibitor Pdc4 is targeted for degradation during tumor promotion*. *Cancer Research*, 2008. **68**(5): p. 1254-1260.
155. Woodard, J., et al., *Statin-dependent suppression of the Akt/mammalian target of rapamycin signaling cascade and programmed cell death 4 up-regulation in renal cell carcinoma*. *Clinical Cancer Research*, 2008. **14**(14): p. 4640-4649.
156. Schlichter, U., et al., *Identification of the myb-inducible promoter of the chicken Pdc4 gene*. *Biochim Biophys Acta*, 2001. **1520**(1): p. 99-104.
157. Appl, H. and K.H. Klempnauer, *Targeted disruption of c-myb in the chicken pre B-cell line DT40*. *Oncogene*, 2002. **21**(19): p. 3076-3081.

158. Fan, H., et al., *DNA methyltransferase 1 knockdown induces silenced CDH1 gene reexpression by demethylation of methylated CpG in hepatocellular carcinoma cell line SMMC-7721*. European Journal of Gastroenterology & Hepatology, 2007. **19**(11): p. 952-961.
159. Cmarik, J.L., et al., *Differentially expressed protein Pcd4 inhibits tumor promoter-induced neoplastic transformation*. Proc Natl Acad Sci U S A, 1999. **96**(24): p. 14037-42.
160. Yang, H.S., et al., *A novel transformation suppressor, Pcd4, inhibits AP-1 transactivation but not NF-kappa B or ODC transactivation*. Oncogene, 2001. **20**(6): p. 669-676.
161. Yang, H.S., et al., *Pcd4 suppresses tumor phenotype in JB6 cells by inhibiting AP-1 transactivation*. Oncogene, 2003. **22**(24): p. 3712-3720.
162. Bitomsky, N., M. Bohm, and K.H. Klempnauer, *Transformation suppressor protein Pcd4 interferes with JNK-mediated phosphorylation of c-Jun and recruitment of the coactivator p300 by c-Jun*. Oncogene, 2004. **23**(45): p. 7484-7493.
163. Yang, H.S., et al., *Tumorigenesis suppressor Pcd4 down-regulates mitogen-activated protein kinase kinase kinase 1 expression to suppress colon carcinoma cell invasion*. Molecular and Cellular Biology, 2006. **26**(4): p. 1297-306.
164. Bekku, S., et al., *Expression of carbonic anhydrase I or II and correlation to clinical aspects of colorectal cancer*. Hepatogastroenterology, 2000. **47**(34): p. 998-1001.
165. Lankat-Buttgereit, B., et al., *Pcd4 inhibits growth of tumor cells by suppression of carbonic anhydrase type II*. Mol Cell Endocrinol, 2004. **214**(1-2): p. 149-53.
166. Jansen, A.P., C.E. Camalier, and N.H. Colburn, *Epidermal expression of the translation inhibitor programmed cell death 4 suppresses tumorigenesis*. Cancer Res, 2005. **65**(14): p. 6034-41.
167. Hilliard, A., et al., *Translational regulation of autoimmune inflammation and lymphoma genesis by programmed cell death 4*. J Immunol, 2006. **177**(11): p. 8095-102.
168. Hufbauer, M., et al., *Skin tumor formation in human papillomavirus 8 transgenic mice is associated with a deregulation of oncogenic miRNAs and their tumor suppressive targets*. Journal of Dermatological Science, 2011. **64**(1): p. 7-15.
169. Wang, Q., et al., *Down-regulation of programmed cell death 4 leads to epithelial to mesenchymal transition and promotes metastasis in mice*. Eur J Cancer, 2013.
170. White, K., et al., *Endothelial apoptosis in pulmonary hypertension is controlled by a microRNA/programmed cell death 4/caspase-3 axis*. Hypertension, 2014. **64**(1): p. 185-94.
171. Bertout, J.A., S.A. Patel, and M.C. Simon, *The impact of O2 availability on human cancer*. Nat Rev Cancer, 2008. **8**(12): p. 967-75.
172. Murdoch, C., M. Muthana, and C.E. Lewis, *Hypoxia regulates macrophage functions in inflammation*. J Immunol, 2005. **175**(10): p. 6257-63.

173. Semenza, G.L., *Targeting HIF-1 for cancer therapy*. Nat Rev Cancer, 2003. **3**(10): p. 721-32.
174. Semenza, G.L., *Hypoxia-inducible factors in physiology and medicine*. Cell, 2012. **148**(3): p. 399-408.
175. Xia, Y., H.K. Choi, and K. Lee, *Recent advances in hypoxia-inducible factor (HIF)-1 inhibitors*. Eur J Med Chem, 2012. **49**: p. 24-40.
176. Jiang, B.H., et al., *Dimerization, DNA binding, and transactivation properties of hypoxia-inducible factor 1*. Journal of Biological Chemistry, 1996. **271**(30): p. 17771-8.
177. Ema, M., et al., *A novel bHLH-PAS factor with close sequence similarity to hypoxia-inducible factor 1alpha regulates the VEGF expression and is potentially involved in lung and vascular development*. Proc Natl Acad Sci U S A, 1997. **94**(9): p. 4273-8.
178. Tian, H., S.L. McKnight, and D.W. Russell, *Endothelial PAS domain protein 1 (EPAS1), a transcription factor selectively expressed in endothelial cells*. Genes Dev, 1997. **11**(1): p. 72-82.
179. Gu, Y.Z., et al., *Molecular characterization and chromosomal localization of a third alpha-class hypoxia inducible factor subunit, HIF3alpha*. Gene Expr, 1998. **7**(3): p. 205-13.
180. Verheul, H.M.W., et al., *Combination strategy targeting the hypoxia inducible factor-1 alpha with mammalian target of rapamycin and histone deacetylase inhibitors*. Clinical Cancer Research, 2008. **14**(11): p. 3589-3597.
181. Wang, G.L., et al., *Hypoxia-Inducible Factor-1 Is a Basic-Helix-Loop-Helix-Pas Heterodimer Regulated by Cellular O₂ Tension*. Proceedings of the National Academy of Sciences of the United States of America, 1995. **92**(12): p. 5510-5514.
182. Hu, Y., J. Liu, and H. Huang, *Recent agents targeting HIF-1alpha for cancer therapy*. J Cell Biochem, 2013. **114**(3): p. 498-509.
183. Kallio, P.J., et al., *Activation of hypoxia-inducible factor 1alpha: posttranscriptional regulation and conformational change by recruitment of the Arnt transcription factor*. Proc Natl Acad Sci U S A, 1997. **94**(11): p. 5667-72.
184. Salceda, S. and J. Caro, *Hypoxia-inducible factor 1alpha (HIF-1alpha) protein is rapidly degraded by the ubiquitin-proteasome system under normoxic conditions. Its stabilization by hypoxia depends on redox-induced changes*. J Biol Chem, 1997. **272**(36): p. 22642-7.
185. Wiesener, M.S., et al., *Induction of endothelial PAS domain protein-1 by hypoxia: characterization and comparison with hypoxia-inducible factor-1alpha*. Blood, 1998. **92**(7): p. 2260-8.
186. Wang, G.L., et al., *Hypoxia-inducible factor 1 is a basic-helix-loop-helix-PAS heterodimer regulated by cellular O₂ tension*. Proc Natl Acad Sci U S A, 1995. **92**(12): p. 5510-4.
187. Brahimi-Horn, C., N. Mazure, and J. Pouyssegur, *Signalling via the hypoxia-inducible factor-1alpha requires multiple posttranslational modifications*. Cell Signal, 2005. **17**(1): p. 1-9.

188. Srinivas, V., et al., *Characterization of an oxygen/redox-dependent degradation domain of hypoxia-inducible factor alpha (HIF-alpha) proteins*. *Biochem Biophys Res Commun*, 1999. **260**(2): p. 557-61.
189. Masson, N., et al., *Independent function of two destruction domains in hypoxia-inducible factor-alpha chains activated by prolyl hydroxylation*. *EMBO J*, 2001. **20**(18): p. 5197-206.
190. Lando, D., et al., *FIH-1 is an asparaginyl hydroxylase enzyme that regulates the transcriptional activity of hypoxia-inducible factor*. *Genes Dev*, 2002. **16**(12): p. 1466-71.
191. Huang, L.E., et al., *Activation of hypoxia-inducible transcription factor depends primarily upon redox-sensitive stabilization of its alpha subunit*. *J Biol Chem*, 1996. **271**(50): p. 32253-9.
192. Lando, D., et al., *Asparagine hydroxylation of the HIF transactivation domain a hypoxic switch*. *Science*, 2002. **295**(5556): p. 858-61.
193. Harris, A.L., *Hypoxia--a key regulatory factor in tumour growth*. *Nat Rev Cancer*, 2002. **2**(1): p. 38-47.
194. Maxwell, P.H., C.W. Pugh, and P.J. Ratcliffe, *Activation of the HIF pathway in cancer*. *Current Opinion in Genetics & Development*, 2001. **11**(3): p. 293-9.
195. Giaccia, A., B.G. Siim, and R.S. Johnson, *HIF-1 as a target for drug development*. *Nature Reviews Drug Discovery*, 2003. **2**(10): p. 803-811.
196. Koong, A.C., et al., *Pancreatic tumors show high levels of hypoxia*. *Int J Radiat Oncol Biol Phys*, 2000. **48**(4): p. 919-22.
197. Schwartz, D.L., et al., *Radiosensitization and stromal imaging response correlates for the HIF-1 inhibitor PX-478 given with or without chemotherapy in pancreatic cancer*. *Mol Cancer Ther*, 2010. **9**(7): p. 2057-67.
198. Ruan, K., G. Song, and G. Ouyang, *Role of hypoxia in the hallmarks of human cancer*. *J Cell Biochem*, 2009. **107**(6): p. 1053-62.
199. Zhong, H., et al., *Overexpression of hypoxia-inducible factor 1alpha in common human cancers and their metastases*. *Cancer Res*, 1999. **59**(22): p. 5830-5.
200. Schindl, M., et al., *Overexpression of hypoxia-inducible factor 1alpha is associated with an unfavorable prognosis in lymph node-positive breast cancer*. *Clinical Cancer Research*, 2002. **8**(6): p. 1831-7.
201. Birner, P., et al., *Overexpression of hypoxia-inducible factor 1alpha is a marker for an unfavorable prognosis in early-stage invasive cervical cancer*. *Cancer Res*, 2000. **60**(17): p. 4693-6.
202. Birner, P., et al., *Expression of hypoxia-inducible factor 1alpha in epithelial ovarian tumors: its impact on prognosis and on response to chemotherapy*. *Clinical Cancer Research*, 2001. **7**(6): p. 1661-8.
203. Sivridis, E., et al., *Association of hypoxia-inducible factors 1alpha and 2alpha with activated angiogenic pathways and prognosis in patients with endometrial carcinoma*. *Cancer*, 2002. **95**(5): p. 1055-63.
204. Birner, P., et al., *Expression of hypoxia-inducible factor-1 alpha in oligodendrogliomas: its impact on prognosis and on neoangiogenesis*. *Cancer*, 2001. **92**(1): p. 165-71.

205. Aebersold, D.M., et al., *Expression of hypoxia-inducible factor-1alpha: a novel predictive and prognostic parameter in the radiotherapy of oropharyngeal cancer*. *Cancer Res*, 2001. **61**(7): p. 2911-6.
206. Iliopoulos, O., M. Ohh, and W.G. Kaelin, *pVHL(19) is a biologically active product of the von Hippel-Lindau gene arising from internal translation initiation*. *Proceedings of the National Academy of Sciences of the United States of America*, 1998. **95**(20): p. 11661-11666.
207. Ravi, R., et al., *Regulation of tumor angiogenesis by p53-induced degradation of hypoxia-inducible factor 1alpha*. *Genes Dev*, 2000. **14**(1): p. 34-44.
208. Zundel, W., et al., *Loss of PTEN facilitates HIF-1-mediated gene expression*. *Genes Dev*, 2000. **14**(4): p. 391-6.
209. Koong, A.C., et al., *Pancreatic tumors show high levels of hypoxia*. *International Journal of Radiation Oncology Biology Physics*, 2000. **48**(4): p. 919-922.
210. Buchler, P., et al., *Hypoxia-inducible factor 1 regulates vascular endothelial growth factor expression in human pancreatic cancer*. *Pancreas*, 2003. **26**(1): p. 56-64.
211. Layer, P. and J. Keller, *Lipase supplementation therapy: standards, alternatives, and perspectives*. *Pancreas*, 2003. **26**(1): p. 1-7.
212. Vukovic, V., et al., *Hypoxia-inducible factor-1alpha is an intrinsic marker for hypoxia in cervical cancer xenografts*. *Cancer Res*, 2001. **61**(20): p. 7394-8.
213. Nakayama, K., et al., *Hypoxia-inducible factor 1 alpha (HIF-1 alpha) gene expression in human ovarian carcinoma*. *Cancer Lett*, 2002. **176**(2): p. 215-23.
214. Ide, T., et al., *Tumor-stromal cell interaction under hypoxia increases the invasiveness of pancreatic cancer cells through the hepatocyte growth factor/c-Met pathway*. *Int J Cancer*, 2006. **119**(12): p. 2750-9.
215. Akakura, N., et al., *Constitutive expression of hypoxia-inducible factor-1alpha renders pancreatic cancer cells resistant to apoptosis induced by hypoxia and nutrient deprivation*. *Cancer Res*, 2001. **61**(17): p. 6548-54.
216. Sato, Y., et al., *Cellular Hypoxia of Pancreatic beta-Cells Due to High Levels of Oxygen Consumption for Insulin Secretion in Vitro*. *Journal of Biological Chemistry*, 2011. **286**(14).
217. Oettle, H., et al., *Adjuvant chemotherapy with gemcitabine vs observation in patients undergoing curative-intent resection of pancreatic cancer: a randomized controlled trial*. *JAMA*, 2007. **297**(3): p. 267-77.
218. Hu, H., et al., *DNA-PKcs is important for Akt activation and gemcitabine resistance in PANC-1 pancreatic cancer cells*. *Biochem Biophys Res Commun*, 2014.
219. Boisserie-Lacroix, M., *Radio-histological correlations in breast imaging: understanding for providing better care*. *Diagn Interv Imaging*, 2014. **95**(2): p. 123.
220. Chen, J., et al., *Dominant-negative hypoxia-inducible factor-1 alpha reduces tumorigenicity of pancreatic cancer cells through the suppression of glucose metabolism*. *Am J Pathol*, 2003. **162**(4): p. 1283-91.
221. Kung, A.L., et al., *Suppression of tumor growth through disruption of hypoxia-inducible transcription*. *Nat Med*, 2000. **6**(12): p. 1335-40.

222. He, G., et al., *The effect of HIF-1alpha on glucose metabolism, growth and apoptosis of pancreatic cancerous cells*. Asia Pac J Clin Nutr, 2014. **23**(1): p. 174-80.
223. Sen, R. and D. Baltimore, *Inducibility of kappa immunoglobulin enhancer-binding protein Nf-kappa B by a posttranslational mechanism*. Cell, 1986. **47**(6): p. 921-8.
224. DiDonato, J.A., F. Mercurio, and M. Karin, *NF-kappaB and the link between inflammation and cancer*. Immunol Rev, 2012. **246**(1): p. 379-400.
225. Perkins, N.D., *The diverse and complex roles of NF-kappaB subunits in cancer*. Nat Rev Cancer, 2012. **12**(2): p. 121-32.
226. Novack, D.V., *Role of NF-kappaB in the skeleton*. Cell Res, 2011. **21**(1): p. 169-82.
227. Hayden, M.S. and S. Ghosh, *NF-kappaB in immunobiology*. Cell Res, 2011. **21**(2): p. 223-44.
228. Wullaert, A., M.C. Bonnet, and M. Pasparakis, *NF-kappaB in the regulation of epithelial homeostasis and inflammation*. Cell Res, 2011. **21**(1): p. 146-58.
229. Joyce, D., et al., *NF-kappaB and cell-cycle regulation: the cyclin connection*. Cytokine Growth Factor Rev, 2001. **12**(1): p. 73-90.
230. Van Antwerp, D.J., et al., *Suppression of TNF-alpha-induced apoptosis by NF-kappaB*. Science, 1996. **274**(5288): p. 787-9.
231. Beg, A.A. and D. Baltimore, *An essential role for NF-kappaB in preventing TNF-alpha-induced cell death*. Science, 1996. **274**(5288): p. 782-4.
232. Huang, S., et al., *Blockade of NF-kappaB activity in human prostate cancer cells is associated with suppression of angiogenesis, invasion, and metastasis*. Oncogene, 2001. **20**(31): p. 4188-97.
233. Weichert, W., et al., *High expression of RelA/p65 is associated with activation of nuclear factor-kappaB-dependent signaling in pancreatic cancer and marks a patient population with poor prognosis*. Br J Cancer, 2007. **97**(4): p. 523-30.
234. Wang, W., et al., *The nuclear factor-kappa B RelA transcription factor is constitutively activated in human pancreatic adenocarcinoma cells*. Clin Cancer Res, 1999. **5**(1): p. 119-27.
235. Sclabas, G.M., et al., *NF-kappaB in pancreatic cancer*. Int J Gastrointest Cancer, 2003. **33**(1): p. 15-26.
236. Chua, H.L., et al., *NF-kappaB represses E-cadherin expression and enhances epithelial to mesenchymal transition of mammary epithelial cells: potential involvement of ZEB-1 and ZEB-2*. Oncogene, 2007. **26**(5): p. 711-24.
237. Yang, J., et al., *Systemic targeting inhibitor of kappaB kinase inhibits melanoma tumor growth*. Cancer Res, 2007. **67**(7): p. 3127-34.
238. Tew, G.W., et al., *SmgGDS regulates cell proliferation, migration, and NF-kappaB transcriptional activity in non-small cell lung carcinoma*. J Biol Chem, 2008. **283**(2): p. 963-76.
239. Scartozzi, M., et al., *Nuclear factor-kB tumor expression predicts response and survival in irinotecan-refractory metastatic colorectal cancer treated with cetuximab-irinotecan therapy*. J Clin Oncol, 2007. **25**(25): p. 3930-5.

240. Keats, J.J., et al., *Promiscuous mutations activate the noncanonical NF-kappaB pathway in multiple myeloma*. *Cancer Cell*, 2007. **12**(2): p. 131-44.
241. Vilimas, T., et al., *Targeting the NF-kappaB signaling pathway in Notch1-induced T-cell leukemia*. *Nat Med*, 2007. **13**(1): p. 70-7.
242. Zhang, B., et al., *NF-kappaB2 mutation targets TRAF1 to induce lymphomagenesis*. *Blood*, 2007. **110**(2): p. 743-51.
243. Wan, F. and M.J. Lenardo, *The nuclear signaling of NF-kappaB: current knowledge, new insights, and future perspectives*. *Cell Res*, 2010. **20**(1): p. 24-33.
244. O'Shea, J.M. and N.D. Perkins, *Regulation of the RelA (p65) transactivation domain*. *Biochem Soc Trans*, 2008. **36**(Pt 4): p. 603-8.
245. Hayden, M.S. and S. Ghosh, *NF-kappaB, the first quarter-century: remarkable progress and outstanding questions*. *Genes Dev*, 2012. **26**(3): p. 203-34.
246. Sun, S.C. and Z.G. Liu, *A special issue on NF-kappaB signaling and function*. *Cell Res*, 2011. **21**(1): p. 1-2.
247. Hoesel, B. and J.A. Schmid, *The complexity of NF-kappaB signaling in inflammation and cancer*. *Mol Cancer*, 2013. **12**: p. 86.
248. Kanarek, N., et al., *Ubiquitination and degradation of the inhibitors of NF-kappaB*. *Cold Spring Harb Perspect Biol*, 2010. **2**(2): p. a000166.
249. Orłowski, R.Z. and A.S. Baldwin, Jr., *NF-kappaB as a therapeutic target in cancer*. *Trends Mol Med*, 2002. **8**(8): p. 385-9.
250. Courtois, G. and T.D. Gilmore, *Mutations in the NF-kappaB signaling pathway: implications for human disease*. *Oncogene*, 2006. **25**(51): p. 6831-43.
251. Kim, H.J., N. Hawke, and A.S. Baldwin, *NF-kappaB and IKK as therapeutic targets in cancer*. *Cell Death Differ*, 2006. **13**(5): p. 738-47.
252. Kumar, A., et al., *Nuclear factor-kappaB: its role in health and disease*. *J Mol Med (Berl)*, 2004. **82**(7): p. 434-48.
253. Karin, M., *Nuclear factor-kappaB in cancer development and progression*. *Nature*, 2006. **441**(7092): p. 431-6.
254. Fan, Y., et al., *Regulation of programmed cell death by NF-kappaB and its role in tumorigenesis and therapy*. *Adv Exp Med Biol*, 2008. **615**: p. 223-50.
255. Johnson, R.F., Witzel, II, and N.D. Perkins, *p53-dependent regulation of mitochondrial energy production by the RelA subunit of NF-kappaB*. *Cancer Res*, 2011. **71**(16): p. 5588-97.
256. Ben-Neriah, Y. and M. Karin, *Inflammation meets cancer, with NF-kappaB as the matchmaker*. *Nat Immunol*, 2011. **12**(8): p. 715-23.
257. Greten, F.R., et al., *IKKbeta links inflammation and tumorigenesis in a mouse model of colitis-associated cancer*. *Cell*, 2004. **118**(3): p. 285-96.
258. Grivennikov, S.I. and M. Karin, *Inflammation and oncogenesis: a vicious connection*. *Current Opinion in Genetics & Development*, 2010. **20**(1): p. 65-71.
259. Baud, V. and M. Karin, *Is NF-kappaB a good target for cancer therapy? Hopes and pitfalls*. *Nature Reviews Drug Discovery*, 2009. **8**(1): p. 33-40.

260. Liptay, S., et al., *Mitogenic and antiapoptotic role of constitutive NF-kappaB/Rel activity in pancreatic cancer*. Int J Cancer, 2003. **105**(6): p. 735-46.
261. Garcea, G., et al., *Role of inflammation in pancreatic carcinogenesis and the implications for future therapy*. Pancreatology, 2005. **5**(6): p. 514-29.
262. Wang, W.X., et al., *The nuclear factor-kappa B RelA transcription factor is constitutively activated in human pancreatic adenocarcinoma cells*. Clinical Cancer Research, 1999. **5**(1): p. 119-127.
263. Fujioka, S., et al., *Function of nuclear factor kappaB in pancreatic cancer metastasis*. Clinical Cancer Research, 2003. **9**(1): p. 346-54.
264. Ougolkov, A.V., et al., *Glycogen synthase kinase-3beta participates in nuclear factor kappaB-mediated gene transcription and cell survival in pancreatic cancer cells*. Cancer Res, 2005. **65**(6): p. 2076-81.
265. Fernandez-Zapico, M.E., et al., *Ectopic expression of VAV1 reveals an unexpected role in pancreatic cancer tumorigenesis*. Cancer Cell, 2005. **7**(1): p. 39-49.
266. Asano, T., et al., *The PI 3-kinase/Akt signaling pathway is activated due to aberrant Pten expression and targets transcription factors NF-kappaB and c-Myc in pancreatic cancer cells*. Oncogene, 2004. **23**(53): p. 8571-80.
267. Niu, J., et al., *Identification of an autoregulatory feedback pathway involving interleukin-1alpha in induction of constitutive NF-kappaB activation in pancreatic cancer cells*. Journal of Biological Chemistry, 2004. **279**(16): p. 16452-62.
268. Melisi, D., et al., *Secreted interleukin-1alpha induces a metastatic phenotype in pancreatic cancer by sustaining a constitutive activation of nuclear factor-kappaB*. Mol Cancer Res, 2009. **7**(5): p. 624-33.
269. Wang, Z., et al., *Down-regulation of notch-1 inhibits invasion by inactivation of nuclear factor-kappaB, vascular endothelial growth factor, and matrix metalloproteinase-9 in pancreatic cancer cells*. Cancer Res, 2006. **66**(5): p. 2778-84.
270. Burris, H.A., et al., *Improvements in survival and clinical benefit with gemcitabine as first-line therapy for patients with advanced pancreas cancer: A randomized trial*. Journal of Clinical Oncology, 1997. **15**(6): p. 2403-2413.
271. Chandel, N.S., et al., *Role of oxidants in NF-kappa B activation and TNF-alpha gene transcription induced by hypoxia and endotoxin*. J Immunol, 2000. **165**(2): p. 1013-21.
272. Yokoi, K. and I.J. Fidler, *Hypoxia increases resistance of human pancreatic cancer cells to apoptosis induced by gemcitabine*. Clinical Cancer Research, 2004. **10**(7): p. 2299-306.
273. Wang, S.J., et al., *Dihydroartemisinin inactivates NF-kappa B and potentiates the anti-tumor effect of gemcitabine on pancreatic cancer both in vitro and in vivo*. Cancer Letters, 2010. **293**(1): p. 99-108.
274. Kong, R., et al., *Downregulation of nuclear factor-kappaB p65 subunit by small interfering RNA synergizes with gemcitabine to inhibit the growth of pancreatic cancer*. Cancer Lett, 2010. **291**(1): p. 90-8.

275. Huber, M.A., N. Kraut, and H. Beug, *Molecular requirements for epithelial-mesenchymal transition during tumor progression*. *Curr Opin Cell Biol*, 2005. **17**(5): p. 548-58.
276. Cannito, S., et al., *Redox mechanisms switch on hypoxia-dependent epithelial-mesenchymal transition in cancer cells*. *Carcinogenesis*, 2008. **29**(12): p. 2267-78.
277. Shin, S.R., et al., *7,12-dimethylbenz(a)anthracene treatment of a c-rel mouse mammary tumor cell line induces epithelial to mesenchymal transition via activation of nuclear factor-kappaB*. *Cancer Res*, 2006. **66**(5): p. 2570-5.
278. Arumugam, T., et al., *Epithelial to mesenchymal transition contributes to drug resistance in pancreatic cancer*. *Cancer Res*, 2009. **69**(14): p. 5820-8.
279. Cheng, Z.X., et al., *Nuclear factor-kappaB-dependent epithelial to mesenchymal transition induced by HIF-1alpha activation in pancreatic cancer cells under hypoxic conditions*. *PLoS One*, 2011. **6**(8): p. e23752.
280. Ferris, W.F., et al., *Tumor Suppressor Pcd4 Is a Major Transcript That Is Upregulated During In Vivo Pancreatic Islet Neogenesis and Is Expressed in Both Beta-Cell and Ductal Cell Lines*. *Pancreas*, 2011. **40**(1): p. 61-66.
281. Vaupel, P., O. Thews, and D.K. Kelleher, *Pancreatic tumors show high levels of hypoxia: regarding Koong et al. IJROBP 2000;48:919-922*. *Int J Radiat Oncol Biol Phys*, 2001. **50**(4): p. 1099-100.
282. Rollins, B.J. and C.D. Stiles, *Serum-inducible genes*. *Adv Cancer Res*, 1989. **53**: p. 1-32.
283. Pardee, A.B., *GI events and regulation of cell proliferation*. *Science*, 1989. **246**(4930): p. 603-8.
284. Yamada, H., et al., *Establishment of a human pancreatic adenocarcinoma cell line (PSN-1) with amplifications of both c-myc and activated c-Ki-ras by a point mutation*. *Biochem Biophys Res Commun*, 1986. **140**(1): p. 167-73.
285. Ishihara, H., et al., *Pancreatic beta cell line MIN6 exhibits characteristics of glucose metabolism and glucose-stimulated insulin secretion similar to those of normal islets*. *Diabetologia*, 1993. **36**(11): p. 1139-45.
286. Mossman, T., *Rapid calorimetric assay for cellular growth and survival: application to proliferation and cytotoxic assays*. *Journal of Immunological Methods*, 1983. **65**: p. 55-63.
287. Latt, S.A. and G. Stetten, *Spectral studies on 33258 Hoechst and related bisbenzimidazole dyes useful for fluorescent detection of deoxyribonucleic acid synthesis*. *J Histochem Cytochem*, 1976. **24**(1): p. 24-33.
288. Latt, S.A. and J.C. Wohlleb, *Optical studies of the interaction of 33258 Hoechst with DNA, chromatin, and metaphase chromosomes*. *Chromosoma*, 1975. **52**(4): p. 297-316.
289. Edwards, B.S., et al., *High-throughput cytotoxicity screening by propidium iodide staining*. *Curr Protoc Cytom*, 2007. **Chapter 9**: p. Unit9 24.
290. Riccardi, C. and I. Nicoletti, *Analysis of apoptosis by propidium iodide staining and flow cytometry*. *Nat Protoc*, 2006. **1**(3): p. 1458-61.
291. Brunk, U., V.P. Collins, and E. Arro, *The fixation, dehydration, drying and coating of cultured cells of SEM*. *J Microsc*, 1981. **123**(Pt 2): p. 121-31.

292. Bradford, M.M., *A rapid and sensitive method for the quantitation of microgram quantities of protein utilizing the principle of protein-dye binding*. Anal Biochem, 1976. **72**: p. 248-54.
293. Junqueira, L.C.U., J. Caneiro, and R.O. Kelly, *Basic Histology*. 1992: Appleton & Lange.
294. Jamur, M.C. and C. Oliver, *Permeabilization of cell membranes*. Methods Mol Biol, 2010. **588**: p. 63-6.
295. *Cancer Statistics Report: Cancer incidence and mortality in the UK (incidence 2011, mortality 2011)*. January 2014.: UK. p. 1-2.
296. Ko, A.H. and M.A. Tempero, *Current and future strategies for combined-modality therapy in pancreatic cancer*. Curr Oncol Rep, 2002. **4**(3): p. 202-12.
297. Semenza, G.L., *Hypoxia-inducible factors: mediators of cancer progression and targets for cancer therapy*. Trends Pharmacol Sci, 2012. **33**(4): p. 207-14.
298. DiMagno, E.P., H.A. Reber, and M.A. Tempero, *AGA technical review on the epidemiology, diagnosis, and treatment of pancreatic ductal adenocarcinoma*. Gastroenterology, 1999. **117**(6): p. 1464-1484.
299. Jung, F., et al., *Hypoxic regulation of inducible nitric oxide synthase via hypoxia inducible factor-1 in cardiac myocytes*. Circulation Research, 2000. **86**(3): p. 319-325.
300. Covello, K.L. and M.C. Simon, *HIFs, hypoxia, and vascular development*. Developmental Vascular Biology, 2004. **62**: p. 37-+.
301. Jacobson, M.D., M. Weil, and M.C. Raff, *Programmed cell death in animal development*. Cell, 1997. **88**(3): p. 347-54.
302. Evan, G.I. and K.H. Vousden, *Proliferation, cell cycle and apoptosis in cancer*. Nature, 2001. **411**(6835): p. 342-8.
303. Donath, M.Y. and P.A. Halban, *Decreased beta-cell mass in diabetes: significance, mechanisms and therapeutic implications*. Diabetologia, 2004. **47**(3): p. 581-9.
304. Oleinick, N.L., R.L. Morris, and I. Belichenko, *The role of apoptosis in response to photodynamic therapy: what, where, why, and how*. Photochem Photobiol Sci, 2002. **1**(1): p. 1-21.
305. Hans-Jürgen Rode, P.D., Doris Eisel, Inge Frost, *Apoptosis, Cell Death and Cell Proliferation Manual*, ed. r. edition. Germany. 174.
306. Guillaumond, F., et al., *Strengthened glycolysis under hypoxia supports tumor symbiosis and hexosamine biosynthesis in pancreatic adenocarcinoma*. Proc Natl Acad Sci U S A, 2013. **110**(10): p. 3919-24.
307. Denko, N.C., *Hypoxia, HIF1 and glucose metabolism in the solid tumour*. Nat Rev Cancer, 2008. **8**(9): p. 705-13.
308. Chiche, J., M.C. Brahimi-Horn, and J. Pouyssegur, *Tumour hypoxia induces a metabolic shift causing acidosis: a common feature in cancer*. J Cell Mol Med, 2010. **14**(4): p. 771-94.
309. Le, A., et al., *Glucose-independent glutamine metabolism via TCA cycling for proliferation and survival in B cells*. Cell Metab, 2012. **15**(1): p. 110-21.

310. Zhou, W., et al., *Proteomic analysis reveals Warburg effect and anomalous metabolism of glutamine in pancreatic cancer cells*. J Proteome Res, 2012. **11**(2): p. 554-63.
311. Gardner, L.B., et al., *Hypoxia inhibits G1/S transition through regulation of p27 expression*. J Biol Chem, 2001. **276**(11): p. 7919-26.
312. Hanahan, D. and R.A. Weinberg, *The hallmarks of cancer*. Cell, 2000. **100**(1): p. 57-70.
313. Pallayova, M., I. Lazurova, and V. Donic, *Hypoxic damage to pancreatic beta cells--the hidden link between sleep apnea and diabetes*. Med Hypotheses, 2011. **77**(5): p. 930-4.
314. Hering, B.J., et al., *Transplantation of cultured islets from two-layer preserved pancreases in type 1 diabetes with anti-CD3 antibody*. Am J Transplant, 2004. **4**(3): p. 390-401.
315. Zhang, N., et al., *Elevated vascular endothelial growth factor production in islets improves islet graft vascularization*. Diabetes, 2004. **53**(4): p. 963-70.
316. Robertson, R.P., et al., *Pancreas and islet transplantation for patients with diabetes*. Diabetes Care, 2000. **23**(1): p. 112-6.
317. Pipeleers, D., et al., *Physiologic relevance of heterogeneity in the pancreatic beta-cell population*. Diabetologia, 1994. **37 Suppl 2**: p. S57-64.
318. Kin, T., et al., *Risk factors for islet loss during culture prior to transplantation*. Transpl Int, 2008. **21**(11): p. 1029-35.
319. Toso, C., et al., *Factors affecting human islet of Langerhans isolation yields*. Transplant Proc, 2002. **34**(3): p. 826-7.
320. Carlsson, P.O., F. Palm, and G. Mattsson, *Low revascularization of experimentally transplanted human pancreatic islets*. J Clin Endocrinol Metab, 2002. **87**(12): p. 5418-23.
321. Brissova, M. and A.C. Powers, *Revascularization of transplanted islets - Can it be improved?* Diabetes, 2008. **57**(9): p. 2269-2271.
322. Wang, N., et al., *Impairment of pancreatic beta-cell function by chronic intermittent hypoxia*. Exp Physiol, 2013. **98**(9): p. 1376-85.
323. Lazard, D., P. Vardi, and K. Bloch, *Induction of beta-cell resistance to hypoxia and technologies for oxygen delivery to transplanted pancreatic islets*. Diabetes Metab Res Rev, 2012. **28**(6): p. 475-84.
324. Carthew, R.W., *Adhesion proteins and the control of cell shape*. Curr Opin Genet Dev, 2005. **15**(4): p. 358-63.
325. Ding, M., W.M. Woo, and A.D. Chisholm, *The cytoskeleton and epidermal morphogenesis in C. elegans*. Exp Cell Res, 2004. **301**(1): p. 84-90.
326. Schock, F. and N. Perrimon, *Molecular mechanisms of epithelial morphogenesis*. Annu Rev Cell Dev Biol, 2002. **18**: p. 463-93.
327. Huang, S. and D.E. Ingber, *Shape-dependent control of cell growth, differentiation, and apoptosis: switching between attractors in cell regulatory networks*. Exp Cell Res, 2000. **261**(1): p. 91-103.
328. Wenger, J.B., et al., *Combination therapy targeting cancer metabolism*. Med Hypotheses, 2011. **76**(2): p. 169-72.

329. Vardaxis, N.J., *A Textbook of Pathology*. 2010, New York, USA: Elsevier.
330. Gonda, M.A., et al., *Ultrastructural studies of surface features of human normal and tumor cells in tissue culture by scanning and transmission electron microscopy*. J Natl Cancer Inst, 1976. **56**(2): p. 245-63.
331. Passey, S., S. Pellegrin, and H. Mellor, *Scanning electron microscopy of cell surface morphology*. Curr Protoc Cell Biol, 2007. **Chapter 4**: p. Unit4 17.
332. Arjonen, A., R. Kaukonen, and J. Ivaska, *Filopodia and adhesion in cancer cell motility*. Cell Adh Migr, 2011. **5**(5): p. 421-30.
333. Zhang, H.Q., et al., *Myosin-X provides a motor-based link between integrins and the cytoskeleton*. Nature Cell Biology, 2004. **6**(6): p. 523-531.
334. Clevers, H., *Wnt/beta-catenin signaling in development and disease*. Cell, 2006. **127**(3): p. 469-80.
335. Weinberg, R.A., *The Biology of Cancer*. 2007, New York, NY, USA.: Garland Science.
336. Motta, P.M., et al., *Histology of the exocrine pancreas*. Microsc Res Tech, 1997. **37**(5-6): p. 384-98.
337. Fesinmeyer, M.D., et al., *Differences in survival by histologic type of pancreatic cancer*. Cancer Epidemiol Biomarkers Prev, 2005. **14**(7): p. 1766-73.
338. Capella, C., et al., *[Carcinoma of the exocrine pancreas: histology report]*. Pathologica, 2013. **105**(1): p. 28-38.
339. Koestner, A., *Prognostic role of cell morphology of animal tumors*. Toxicol Pathol, 1985. **13**(2): p. 90-4.
340. Hauge-Evans, A.C., et al., *Pancreatic beta-cell-to-beta-cell interactions are required for integrated responses to nutrient stimuli: enhanced Ca²⁺ and insulin secretory responses of MIN6 pseudoislets*. Diabetes, 1999. **48**(7): p. 1402-8.
341. Benavides, F. and J.L. Guenet, *[Murine models for human diseases]*. Medicina (B Aires), 2001. **61**(2): p. 215-31.
342. Chu, G.C., et al., *Stromal biology of pancreatic cancer*. J Cell Biochem, 2007. **101**(4): p. 887-907.
343. Arias, A.E. and M. Bendayan, *Differentiation of Pancreatic Acinar-Cells into Duct-Like Cell in-Vitro*. Laboratory Investigation, 1993. **69**(5): p. 518-530.
344. Wessells, N.K. and J.H. Cohen, *Early Pancreas Organogenesis: Morphogenesis, Tissue Interactions, and Mass Effects*. Dev Biol, 1967. **15**(3): p. 237-70.
345. Bhonde, R., et al., *Isolated islets in diabetes research*. Indian J Med Res, 2007. **125**(3): p. 425-40.
346. Butler, A.E., et al., *Beta-cell deficit and increased beta-cell apoptosis in humans with type 2 diabetes*. Diabetes, 2003. **52**(1): p. 102-10.
347. Zehetner, J., et al., *PVHL is a regulator of glucose metabolism and insulin secretion in pancreatic beta cells*. Genes Dev, 2008. **22**(22): p. 3135-46.
348. Bastidas JA, P.J., Niederhuber JE, *Pancreas*. 2000, New York: Churchill Livingstone: Clinical oncology

349. Rindi, G. and C. Bordi, *Highlights of the biology of endocrine tumours of the gut and pancreas*. *Endocr Relat Cancer*, 2003. **10**(4): p. 427-36.
350. Kloppel, G., *Classification and pathology of gastroenteropancreatic neuroendocrine neoplasms*. *Endocr Relat Cancer*, 2011. **18 Suppl 1**: p. S1-16.
351. Guturu, P., V. Shah, and R. Urrutia, *Interplay of tumor microenvironment cell types with parenchymal cells in pancreatic cancer development and therapeutic implications*. *J Gastrointest Cancer*, 2009. **40**(1-2): p. 1-9.
352. Hwang, R.F., et al., *Cancer-associated stromal fibroblasts promote pancreatic tumor progression*. *Cancer Res*, 2008. **68**(3): p. 918-26.
353. Mahadevan, D. and D.D. Von Hoff, *Tumor-stroma interactions in pancreatic ductal adenocarcinoma*. *Mol Cancer Ther*, 2007. **6**(4): p. 1186-97.
354. Bachem, M.G., et al., *Pancreatic stellate cells--role in pancreas cancer*. *Langenbecks Arch Surg*, 2008. **393**(6): p. 891-900.
355. Lowenfels, A.B., et al., *Pancreatitis and the risk of pancreatic cancer. International Pancreatitis Study Group*. *N Engl J Med*, 1993. **328**(20): p. 1433-7.
356. Dangi-Garimella, S., et al., *Three-dimensional collagen I promotes gemcitabine resistance in pancreatic cancer through MT1-MMP-mediated expression of HMGA2*. *Cancer Res*, 2011. **71**(3): p. 1019-28.
357. Hidalgo, M., *Pancreatic cancer*. *N Engl J Med*, 2010. **362**(17): p. 1605-17.
358. Vincent, A., et al., *Pancreatic cancer*. *Lancet*, 2011. **378**(9791): p. 607-20.
359. Hruban RH, K.D., Pitman MB., *Tumors of the Pancreas*. Pathology. 2006, Washington, DC: Armed Forces Inst. .
360. J.Crocker, R.C.C.a., *Curran's Atlas of Histopathology*, ed. Four. 2005, England: Oxford university Press.
361. Mohazzab, K.M. and M.S. Wolin, *Oxidant signalling and vascular oxygen sensing. Role of H2O2 in responses of the bovine pulmonary artery to changes in PO2*. *Adv Exp Med Biol*, 2000. **475**: p. 249-58.
362. Lu, X. and Y. Kang, *Hypoxia and hypoxia-inducible factors: master regulators of metastasis*. *Clin Cancer Res*, 2010. **16**(24): p. 5928-35.
363. Wu, X.Z., G.R. Xie, and D. Chen, *Hypoxia and hepatocellular carcinoma: The therapeutic target for hepatocellular carcinoma*. *J Gastroenterol Hepatol*, 2007. **22**(8): p. 1178-82.
364. Yoon, D.Y., et al., *Identification of genes differentially induced by hypoxia in pancreatic cancer cells*. *Biochem Biophys Res Commun*, 2001. **288**(4): p. 882-6.
365. Bluestone, J.A., K. Herold, and G. Eisenbarth, *Genetics, pathogenesis and clinical interventions in type 1 diabetes*. *Nature*, 2010. **464**(7293): p. 1293-300.
366. Prentki, M. and C.J. Nolan, *Islet beta cell failure in type 2 diabetes*. *J Clin Invest*, 2006. **116**(7): p. 1802-12.
367. Johnson, J.D. and D.S. Luciani, *Mechanisms of pancreatic beta-cell apoptosis in diabetes and its therapies*. *Adv Exp Med Biol*, 2010. **654**: p. 447-62.
368. Cnop, M., et al., *Mechanisms of pancreatic beta-cell death in type 1 and type 2 diabetes: many differences, few similarities*. *Diabetes*, 2005. **54 Suppl 2**: p. S97-107.

369. Stokes, R.A., et al., *Hypoxia-inducible factor-1alpha (HIF-1alpha) potentiates beta-cell survival after islet transplantation of human and mouse islets*. Cell Transplant, 2013. **22**(2): p. 253-66.
370. Ruan, Q., et al., *The microRNA-21-PDCD4 axis prevents type 1 diabetes by blocking pancreatic beta cell death*. Proc Natl Acad Sci U S A, 2011. **108**(29): p. 12030-5.
371. Wang, Q., et al., *Programmed cell death-4 deficiency prevents diet-induced obesity, adipose tissue inflammation, and insulin resistance*. Diabetes, 2013. **62**(12): p. 4132-43.
372. Nagao, Y., et al., *Association of microRNA-21 expression with its targets, PDCD4 and TIMP3, in pancreatic ductal adenocarcinoma*. Mod Pathol, 2012. **25**(1): p. 112-21.
373. Moritz, W., et al., *Apoptosis in hypoxic human pancreatic islets correlates with HIF-1alpha expression*. FASEB J, 2002. **16**(7): p. 745-7.
374. Herget, J., et al., *A possible role of the oxidant tissue injury in the development of hypoxic pulmonary hypertension*. Physiol Res, 2000. **49**(5): p. 493-501.
375. Calabrese, V., T.E. Bates, and A.M. Stella, *NO synthase and NO-dependent signal pathways in brain aging and neurodegenerative disorders: the role of oxidant/antioxidant balance*. Neurochem Res, 2000. **25**(9-10): p. 1315-41.
376. Min, S.K., et al., *Role of lipid peroxidation and poly(ADP-ribose) polymerase activation in oxidant-induced membrane transport dysfunction in opossum kidney cells*. Toxicol Appl Pharmacol, 2000. **166**(3): p. 196-202.
377. Varin, R., et al., *Improvement of endothelial function by chronic angiotensin-converting enzyme inhibition in heart failure : role of nitric oxide, prostanoids, oxidant stress, and bradykinin*. Circulation, 2000. **102**(3): p. 351-6.
378. Said, S.I., et al., *NMDA receptor activation: critical role in oxidant tissue injury*. Free Radic Biol Med, 2000. **28**(8): p. 1300-2.
379. Banan, A., et al., *Oxidant-induced intestinal barrier disruption and its prevention by growth factors in a human colonic cell line: role of the microtubule cytoskeleton*. Free Radic Biol Med, 2000. **28**(5): p. 727-38.
380. Rao, G.N., *Oxidant stress stimulates phosphorylation of eIF4E without an effect on global protein synthesis in smooth muscle cells. Lack of evidence for a role of H2O2 in angiotensin II-induced hypertrophy*. J Biol Chem, 2000. **275**(22): p. 16993-9.
381. Tan, X.D., et al., *Prostanoids mediate the protective effect of trefoil factor 3 in oxidant-induced intestinal epithelial cell injury: role of cyclooxygenase-2*. J Cell Sci, 2000. **113** (Pt 12): p. 2149-55.
382. Zhang, C., L.M. Walker, and P.R. Mayeux, *Role of nitric oxide in lipopolysaccharide-induced oxidant stress in the rat kidney*. Biochem Pharmacol, 2000. **59**(2): p. 203-9.
383. Fujioka, S., et al., *Function of nuclear factor kappaB in pancreatic cancer metastasis*. Clin Cancer Res, 2003. **9**(1): p. 346-54.
384. Lluís, J.M., et al., *Dual role of mitochondrial reactive oxygen species in hypoxia signaling: activation of nuclear factor- κ B via c-SRC and oxidant-dependent cell death*. Cancer Res, 2007. **67**(15): p. 7368-77.

385. Yokoi, K. and I.J. Fidler, *Hypoxia increases resistance of human pancreatic cancer cells to apoptosis induced by gemcitabine*. Clin Cancer Res, 2004. **10**(7): p. 2299-306.
386. Delpu, Y., et al., *Genetic and epigenetic alterations in pancreatic carcinogenesis*. Curr Genomics, 2011. **12**(1): p. 15-24.
387. Vasseur, S., et al., *Hypoxia induced tumor metabolic switch contributes to pancreatic cancer aggressiveness*. Cancers (Basel), 2010. **2**(4): p. 2138-52.
388. Hoffmann, A. and D. Baltimore, *Circuitry of nuclear factor kappaB signaling*. Immunol Rev, 2006. **210**: p. 171-86.
389. Qing, G. and G. Xiao, *Essential role of IkappaB kinase alpha in the constitutive processing of NF-kappaB2 p100*. J Biol Chem, 2005. **280**(11): p. 9765-8.
390. Yang, G., et al., *Identification of the distinct promoters for the two transcripts of apoptosis related protein 3 and their transcriptional regulation by NFAT and NFkappaB*. Mol Cell Biochem, 2007. **302**(1-2): p. 187-94.
391. Algul, H., G. Adler, and R.M. Schmid, *NF-kappaB/Rel transcriptional pathway: implications in pancreatic cancer*. Int J Gastrointest Cancer, 2002. **31**(1-3): p. 71-8.
392. Kizaka-Kondoh, S., et al., *Selective killing of hypoxia-inducible factor-1-active cells improves survival in a mouse model of invasive and metastatic pancreatic cancer*. Clin Cancer Res, 2009. **15**(10): p. 3433-41.
393. Carmeliet, P., et al., *Role of HIF-1alpha in hypoxia-mediated apoptosis, cell proliferation and tumour angiogenesis*. Nature, 1998. **394**(6692): p. 485-90.
394. Graeber, T.G., et al., *Hypoxia-mediated selection of cells with diminished apoptotic potential in solid tumours*. Nature, 1996. **379**(6560): p. 88-91.
395. Huang, L.E., et al., *Regulation of hypoxia-inducible factor 1alpha is mediated by an O2-dependent degradation domain via the ubiquitin-proteasome pathway*. Proc Natl Acad Sci U S A, 1998. **95**(14): p. 7987-92.
396. Maxwell, P.H., et al., *The tumour suppressor protein VHL targets hypoxia-inducible factors for oxygen-dependent proteolysis*. Nature, 1999. **399**(6733): p. 271-275.
397. Saikumar, P., et al., *Role of hypoxia-induced Bax translocation and cytochrome c release in reoxygenation injury*. Oncogene, 1998. **17**(26): p. 3401-3415.
398. Costa, A., et al., *Re: Levels of hypoxia-inducible factor-1 alpha during breast carcinogenesis*. Journal of the National Cancer Institute, 2001. **93**(15): p. 1175-1177.
399. Bos, R., P.J. van Diest, and E. van der Wall, *Re: Levels of hypoxia-inducible factor-1 alpha during breast carcinogenesis - Response*. Journal of the National Cancer Institute, 2001. **93**(15): p. 1177-1177.
400. Chandler, N.M., J.J. Canete, and M.P. Callery, *Increased expression of NF-kappa B subunits in human pancreatic cancer cells*. J Surg Res, 2004. **118**(1): p. 9-14.
401. Belair, C., F. Darfeuille, and C. Staedel, *Helicobacter pylori and gastric cancer: possible role of microRNAs in this intimate relationship*. Clin Microbiol Infect, 2009. **15**(9): p. 806-12.

402. Selcuklu, S.D., M.T.A. Donoghue, and C. Spillane, *miR-21 as a key regulator of oncogenic processes*. Biochemical Society Transactions, 2009. **37**: p. 918-925.
403. Wang, Y. and C.G.L. Lee, *MicroRNA and cancer - focus on apoptosis*. Journal of Cellular and Molecular Medicine, 2009. **13**(1): p. 12-23.
404. Young, M.R., et al., *Have tumor suppressor PDCD4 and its counteragent oncogenic miR-21 gone rogue?* Mol Interv, 2010. **10**(2): p. 76-9.
405. du Rieu, M.C., et al., *MicroRNA-21 Is Induced Early in Pancreatic Ductal Adenocarcinoma Precursor Lesions*. Clinical Chemistry, 2010. **56**(4): p. 603-612.
406. Karin, M., Y. Yamamoto, and Q.M. Wang, *The IKK NF-kappa B system: a treasure trove for drug development*. Nat Rev Drug Discov, 2004. **3**(1): p. 17-26.
407. Yamanaka, N., et al., *Nuclear factor-kappaB p65 is a prognostic indicator in gastric carcinoma*. Anticancer Res, 2004. **24**(2C): p. 1071-5.
408. Nakayama, H., et al., *High expression levels of nuclear factor kappaB, IkappaB kinase alpha and Akt kinase in squamous cell carcinoma of the oral cavity*. Cancer, 2001. **92**(12): p. 3037-44.
409. Tai, D.I., et al., *Constitutive activation of nuclear factor kappaB in hepatocellular carcinoma*. Cancer, 2000. **89**(11): p. 2274-81.
410. Nair, A., et al., *NF-kappaB is constitutively activated in high-grade squamous intraepithelial lesions and squamous cell carcinomas of the human uterine cervix*. Oncogene, 2003. **22**(1): p. 50-8.
411. Ismail, H.A., et al., *Expression of NF-kappaB in prostate cancer lymph node metastases*. Prostate, 2004. **58**(3): p. 308-13.
412. Shukla, S., et al., *Nuclear factor-kappaB/p65 (Rel A) is constitutively activated in human prostate adenocarcinoma and correlates with disease progression*. Neoplasia, 2004. **6**(4): p. 390-400.
413. Koong, A.C., E.Y. Chen, and A.J. Giaccia, *Hypoxia Causes the Activation of Nuclear Factor Kappa-B through the Phosphorylation of I-Kappa-B-Alpha on Tyrosine Residues*. Cancer Research, 1994. **54**(6): p. 1425-1430.
414. Kucharczak, J., et al., *To be, or not to be: NF-kappaB is the answer--role of Rel/NF-kappaB in the regulation of apoptosis*. Oncogene, 2003. **22**(56): p. 8961-82.
415. Dolcet, X., et al., *NF-kB in development and progression of human cancer*. Virchows Arch, 2005. **446**(5): p. 475-82.
416. Nakai, M., et al., *Kainic acid-induced apoptosis in rat striatum is associated with nuclear factor-kappa B activation*. Journal of Neurochemistry, 2000. **74**(2): p. 647-658.
417. Korc, M., P. Meltzer, and J. Trent, *Enhanced expression of epidermal growth factor receptor correlates with alterations of chromosome 7 in human pancreatic cancer*. Proc Natl Acad Sci U S A, 1986. **83**(14): p. 5141-4.
418. Finco, T.S., et al., *Oncogenic Ha-Ras-induced signaling activates NF-kappaB transcriptional activity, which is required for cellular transformation*. J Biol Chem, 1997. **272**(39): p. 24113-6.

419. Habib, A.A., et al., *The epidermal growth factor receptor engages receptor interacting protein and nuclear factor-kappa B (NF-kappa B)-inducing kinase to activate NF-kappa B. Identification of a novel receptor-tyrosine kinase signalosome.* J Biol Chem, 2001. **276**(12): p. 8865-74.
420. Arora, S., et al., *An undesired effect of chemotherapy: gemcitabine promotes pancreatic cancer cell invasiveness through reactive oxygen species-dependent, nuclear factor kappaB- and hypoxia-inducible factor 1alpha-mediated up-regulation of CXCR4.* J Biol Chem, 2013. **288**(29): p. 21197-207.
421. Tempero, M.A., et al., *Pancreatic cancer treatment and research: an international expert panel discussion.* Ann Oncol, 2011. **22**(7): p. 1500-6.
422. Aichler, M., et al., *Origin of pancreatic ductal adenocarcinoma from atypical flat lesions: a comparative study in transgenic mice and human tissues.* Journal of Pathology, 2012. **226**(5): p. 723-734.
423. Hruban, R.H. and N. Fukushima, *Pancreatic adenocarcinoma: update on the surgical pathology of carcinomas of ductal origin and PanINs.* Modern Pathology, 2007. **20**: p. S61-S70.
424. Gisselbrecht, C., et al., *Phase-Ii Trial of Fap (5-Fluorouracil, Adriamycin, and Cisdiammedichloroplatinum) Chemotherapy for Advanced Measurable Pancreatic-Cancer (Pc) and Adenocarcinoma of Unknown Primary Origin (Auo).* Proceedings of the American Association for Cancer Research, 1981. **22**(Mar): p. 454-454.
425. Zhao, X., et al., *Hypoxia-inducible factor-1 promotes pancreatic ductal adenocarcinoma invasion and metastasis by activating transcription of the actin-bundling protein fascin.* Cancer Res, 2014. **74**(9): p. 2455-64.
426. Bockman, D.E., et al., *Origin of Tubular Complexes Developing during Induction of Pancreatic Adenocarcinoma by 7,12-Dimethylbenz(a)Anthracene.* American Journal of Pathology, 1978. **90**(3): p. 645-658.

Publications

Kumar S., Alhasawi A., Marriott C.E., Bone A.J., Macfarlane W.M. Differential expression of programmed cell death gene 4 (Pcd4) and hypoxia- inducible factor 1 alpha (HIF-1alpha) in isolated human pancreatic cancer tissue, as well as in pancreatic cells in culture. *Diabetic Medicine, Volume 31(1)*, P24, ISSN 1464-5491, March 2014.

Kumar S., Marriott C.E., Bone A.J., Macfarlane W.M. Expression and sub-cellular localization of nuclear factor kappa B (NF-κB), hypoxia- inducible factor 1 alpha (HIF-1alpha) and program cells death gene 4 (Pcd4) in pancreatic cells in response to hypoxia. *Diabetic Medicine, Volume 30(1)*, P20, ISSN 1464-5491, March 2013.

Kumar S., Marriott C.E., Bone A.J., Macfarlane W.M. Cell type specific regulation of program cell death protein PDCD4 in pancreas. *Diabetic Medicine, Volume 29(1)*, 30-177, March 2012.

Appendix



Service Level Agreement to supply human tissue to the School of Pharmacy and Biomolecular Sciences at the University of Brighton for generic academic use including teaching, training and ethics-approved research projects, subject to the restrictions of the PABS Human Tissue Licence (No 12583) and compliance with the Human Tissues Act (2004) and HTA Codes of Practice.

I (clinician/sender name and title) Sergii V. Zemskov, MD

confirm that the human tissue sample(s) (to be) provided to the School of Pharmacy and Biomolecular Sciences, University of Brighton), and described in the attached Schedule A, was (were/will be) obtained in accordance with the requirements of the HTA Act (2004), as amended from time to time, and the HTA Code of Practice relating to the seeking and acquisition of the appropriate consent.

HTA licence number of Sender's Institute (if applicable) _____

NHS REC number and short title (if applicable) _____

_____ Start date _____
Finish date _____

PABS REC number and short title (if applicable) _____

_____ Start date _____
Finish date _____

Signature

Authorised to sign for and on behalf of [Institute name]
Zemskov Centre for Hepatopancreatobiliary Surgery

Print Name: S. Zemskov

Title: MD

Date 04.10.2013



Schedule A

This Service Level Agreement is made on the [insert date]

BETWEEN *Zemskov Centre for Hepatopancreatobiliary Surgery,
Goloseievsky Ave 59b, Kyiv, 03039, Ukraine*

(1) [suppliers address]; and

(2) The University of Brighton ("the Recipient") whose principal place of business is at
Mithras House, Lewes Road, Brighton, East Sussex BN2 4AT

Please specify the type and quantity (if known) of Materials that are to be supplied by [name].

Tissue details:

Paraffin embedded pancreatic tissues
Paraffin embedded pancreatic cancer tissues
Pancreatic fresh tissue

Additional information to be complete (if appropriate) by supplying unit:

Is consent granted for the donated sample to be

- used for genetic research YES/NO
- stored for future unspecified (but ethics approved) use YES/NO

Any further restriction on use? YES/NO
If yes, please specify

Should be used in University of Brighton only and not for other
Universities or Institutes

Any storage requirements to protect integrity of tissue sample? YES/NO
If yes, please specify

Store at room temp for Paraffin embaded and -80 C for fresh tissue
samples

Any specific instructions regarding the disposal of any unused sample? YES/NO
If yes, please specify

Dispos as clinical waste

Signature 
Authorised to sign for and on behalf of [Institute name] *Zemskov Centre for Hepatopancreato-
biliary Surgery*